N° d'ordre : 804

THÈSE

présentée à

L'UNIVERSITÉ DES SCIENCES et TECHNOLOGIES DE LILLE

pour obtenir

le grade de Docteur ès Sciences Physiques

par

Michel LE BRAS
Docteur de Troisième Cycle

ETUDE DU PROCESSUS RETARDATEUR DE FLAMME INDUIT PAR LA CARBONISATION ABLATIVE DE MATERIAUX POLYMERES APPLICATION AUX MATÉRIAUX INTUMESCENTS

oOo

***TOME 1** - MODELISATION*

Soutenue le 08 Octobre 1997 devant la Commission d'Examen

Président	J.-M. LEROY	Professeur
Rapporteurs	J.-C. BROSSE	Professeur
	G. CAMINO	Professeur
Examinateurs	J. VERDU	Professeur
	H. BAUSSART	Professeur
	G. ANTONINI	Professeur

A Michèle,

pour sa patience.

Les Travaux qui ont fait l'objet de ce Mémoire ont été effectués au Laboratoire de Chimie Analytique et de Physico-Chimie des Solides de l'Ecole Nationale Supérieure de Chimie de Lille sous la direction de Monsieur le Professeur J.-M. Leroy.

Je voudrais lui exprimer ma très vive reconnaissance, non seulement pour ses nombreux conseils, mais, bien plus pour m'avoir «supporté» pendant plus d'un quart de siècle.

Monsieur J. C. Brosse, Professeur à l'Université du Maine, m'a fait l'honneur de bien vouloir examiner mes Travaux et faire partie du Jury de cette Thèse. Qu'il soit assuré de ma déférente gratitude.

Monsieur G. Camino, Professeur à l'Université de Turin, me fait plus qu'un honneur d'avoir accepté de rapporter la présente thèse. En effet, plus qu'un correcteur, il est le Chercheur dont les Travaux ont permis le développement de mon sujet. Je le prie d'accepter l'expression de ma respectueuse reconnaissance.

Mes remerciements vont également à Monsieur G. Antonini, Professeur à l'Université de Technologie de Compiègne, et Monsieur J. Verdu, Professeur à l'Ecole Nationale Supérieure des Arts et Métiers de Paris, qui me font l'honneur d'être membres du Jury de ma Thèse. Nous espérons qu'ils accepteront, au-delà de leurs présentes corrections, de bien vouloir continuer à m'aider de leur savoir, respectivement en Génie des Procédés et en Science des Polymères, lors de la poursuite de mes Recherches.

Je tiens à personnaliser mes remerciements au Professeur Hervé Baussart, Vice-Président de l'Université des Sciences et Technologies de Lille. Sa participation à l'examen de mes Travaux va de soi. En effet, il m'a encadré à mon arrivée dans le Laboratoire, m'a appris le «boulot», a su me persuader de l'humilité nécessaire au Chercheur pour l'examen et la critique de tout résultat et de tout protocole opératoire. Qu'il accepte l'expression de ma reconnaissance pour m'avoir transmis sa passion pour la Recherche.

Je tiens à associer également à ces remerciements le Professeur R. Delobel, avec qui, en 1981, nous avons créé une Equipe «ignifugation» au sein du Laboratoire, et le Docteur S. Bourbigot, Maître de Conférence à l'E.N.S.C.L., pour leur participation à ce travail.

Que mes camarades du Laboratoire : chercheurs, techniciens et Isabelle trouvent ici mention du plaisir que nous avons à travailler avec eux.

Les différentes approches de l'objectif du sujet ont nécessité une collaboration avec de nombreux Collègues qui ont accepté de me faire profiter de leurs compétences. Que le Professeur J. P. Amoureux, les Docteurs R. Descressain, L. Gengembre, J. Laureyns, B. Mouchel et M. Traisnel et Messieurs D. Normand et B. Revel trouvent ici l'expression de mes remerciements pour leur aide et leur contribution.

Finalement, je remercie le personnel administratif et technique de notre établissement et, tout particulièrement, Monsieur P. Lambour qui a participé à l'impression de ce mémoire avec diligence et minutie.

SOMMAIRE

TOME I

GLOSSAIRE

Termes génériques

CA	additif agent de carbonisation
CP	additif précurseur d'espèces catalytiques
FR	retardateur de la flamme
FRS	systèmes d'adjuvants retardateurs de la flamme
SA	adjuvant agent de synergie

Termes généraux

at.	mole d'atome
HTT, T_{tr}	plus haute température du traitement thermique (°C)
F	indice statistique de Fisher
mol.	mole de molécule
P	pression (Pa)
PI	indice de plasticité
r	coefficient de régression
R	constante de Boltzmann
W	masse (kg, g)
t	temps (s, min., h)
T	température (°C ou K)
T_g	température de la transition vitreuse (°C, K)
X	teneur en additif (% pondéral)
λ	conductibilité thermique

Produits et matériaux

APB	pentaborate d'ammonium
APP, PPA	polyphosphate d'ammonium
BCOH, βcD	β-cyclodextrine
BZN	borate de zinc
DDA	dicyandiamine
DDS	diamino 4, 4' diphényle sulfone
EVA28	éthylène (72%) - acétate de vinyle (28%)
EVAx	copolymère éthylène (100-x%) - acétate de vinyle (x %)
FEABu5	éthylène (95 %) - acrylate de butyle (5%)
FEABu13	éthylène (87%) - acrylate de butyle (13%)
HDPE	polyéthylène haute densité
LDPE	polyéthylène basse densité
LN	éthylène
LQVA5	éthylène (95%) - acétate de vinyle (5%)
LQVA15	éthylène (85%) - acétate de vinyle (15%)
LRAM2,8	éthylène (92,2%) - acrylate de butyle (5%) - anhydride maléique (2,8%),
LRAM 3.5	éthylène (91,5%) - acrylate de butyle (5%) - anhydride maléique (3,5%)
LYABu30	éthylène (70%)- acrylate de butyle (30%)
LYAMe30	éthylène (70%) - acrylate de méthyle (30%)
MOH	mannitol
NK	argile naturelle de structure kaolinite
PA	polyamide

PA-6	polyamide-6
PE	polyéthylène (lactène Elf Atochem, melt index : 20 g/10 min à 190°C)
PER	pentaérythritol
PP	polypropylène isotactique
PY	pyrophosphate (diphosphate) diammonique
PS	polystyrène
SK	kaolinite de synthèse
SOH	d-sorbitol
TGMDA (TGDDM)	tétraglycidyle-méthylène-dianiline
TMS	tétraméthyle silane
TXXXX	argile réfractaire du lot XXXX
XOH	xylitol
YZSM-5	zéolithe de type ZSM-5
Y	zéolithe de type Y
3A	zéolithe de type KA (3A)
4A	zéolithe de type 4A (cocation Na)
5A	zéolithe de type CaA (5A)
10X	zéolithe de type CaX (10X)
13X	zéolithe de type NaX (13X)

Abréviations techniques

LOI	indice (index) limite d'oxygène (% volumique)
UL-94	test ANSI/ASTM D635-77 (classement V0, V1 ou V2)

<u>calorimètre à cône</u>

ehc	chaleur effective de combustion (kJ/kg)
m, m'	flux de matière (massique) (kg/m^2)
P	puissance calorifique volumique
q, q'	flux de chaleur, irradiance (kW/m^2)
rhr	flux calorimétrique (rate of heat release) (kW/m^2)
t.h.e.	chaleur émise (kJ)
t_i	temps pour atteindre l'ignition (s)

<u>modèle du front de dégradation</u>

T_d	température du front de dégradation
$T_{tc}, T_s, T_{éch}$	température au sein de l'échantillon
$x(\alpha,t)$	distance du front de dégradation au support

Analyses thermiques

<u>ATG</u>	analyse thermogravimétrique
DTG	thermogravimétrie différentielle
TG	thermogravimétrie
<u>DSC</u>	calorimétrie différentielle
W, M	masse résiduelle (kg %)
ΔH	enthalpie de la réaction, de la transformation
$\Delta W, \Delta M, \Delta T$	différence de masse calculée
α	degré (taux) de conversion (kg/kg ou kg %)

IKP	paramètres cinétiques invariants
A_{jv}, A_{inv}	facteurs pré-exponentiel apparent, invariant (s^{-1})
B_v, I_v	paramètres déduits de l'effet de compensation
E_{jv}, E_{inv}	énergie d'activation apparente et invariante (kJ/mole)
dW/dt	vitesse de la perte de masse (kg/s)
$(d\alpha/dT)_{iv}$	valeur de la courbe dérivée au point α_{iv}
$f_j(\alpha)$, Sj	$j^{ème}$ fonction de dégradation
k_v	constante de vitesse invariante (s^{-1})
n	ordre de réaction
P_j	probabilité associée à la fonction $f_j(\alpha)$
$q(F_j)$	distribution F
T_v	température déduite de l'effet de compensation (K)
β_v	vitesse de chauffe (K/min)
Γ	fonction Gamma

Spectroscopies

IR, FT-IR	absorption dans l'infra-rouge, id. à transformées de Fourrier
ν	nombre d'onde (cm^{-1})
RMN (NMR)	résonance magnétique nucléaire
CP	en polarisation croisée
DD	avec découplage dipolaire
J	constante du couplage
MAS	avec rotation à l'angle magique
T_1 ET T_2	temps de relaxation
δ	glissement chimique (ppm)
FWHM	largeur à demi hauteur (ppm)
RPE (ESR ou EPR)	résonance paramagnétique électronique
C*	concentration en complexes radicalaires
g	facteur spectroscopique (de Landé)
K = B/A	facteur de forme
H	valeur du champ magnétique (T)
n, nsp, N_{sp}	nombre de spins (spin/kg)
bande X (X band)	à une fréquence d'environ $9,5 \times 10^9$ Hz
XPS (ESCA)	spectroscopie de photoélectrons X
E	énergie de la liaison (eV)
FWHM	largeur du signal à la demi-intensité (eV)
XRD	diffraction des rayons X
d	distance interréticulaire (Å ou nm)
$\beta_{½}$	largeur à mi-hauteur (radians)
θ	angle de diffraction (de Bragg)(°)
λ	longueur d'onde des rayons X incidents (nm)

Les statistiques récentes sur les « dégâts » provoqués par le feu en Europe ou en France sont difficiles à obtenir, voire inexistantes. Un rapport récent de l'ASTM (American Society for Testing and Materials) signale qu'aux Etats-Unis, 3 millions de feux annuels provoquent 29 000 handicaps et 4 500 décès [1]. Les dégâts sur les propriétés et les biens excèdent 8 milliards de US$, alors que le coût pour la Société est estimé à environ 100 milliards US$ [2]. Les pertes personnelles concernent les résidences dans lesquelles le combustible est le mobilier, les vêtements et les tissus d'ameublement et parfois les combustibles de chauffage. Cependant, les pertes financières les plus importantes concernent les immeubles officiels ou à vocation commerciale et les entrepôts. Les moyens de transports (avion, train, autobus et métro) viennent en second dans l'ordre des pertes.

Une autre évaluation de l'importance des dégâts causés par les incendies est apportée par les statistiques concernant la construction dans les pays industrialisés [3]. En 1993 la construction de nouveaux immeubles a représenté un investissement de 470 milliards de US$ (7,9 % des produits nationaux bruts cumulés). Le coût cumulé annuel de la sécurité au feu et des pertes relatives à l'incendie dans le bâtiment s'élève à plus de 128 milliards de US$, alors que celui relatif aux catastrophes naturelles est comparativement faible, de l'ordre de quelques milliards de US$. Une critique des Normes et des matériaux utilisés est toujours nécessaire. La recherche de stratégies pour combattre ou éviter l'inflammation des matériaux est donc toujours d'actualité.

Le processus de la naissance et du développement d'un feu est connu depuis le XIX^{éme} siècle. Le feu survient lorsqu'une source d'ignition (à titre d'exemples : une allumette, une cigarette, un réchaud ou un calorifère) est mise en présence d'un

produit inflammable tel un siège, un mur ou une feuille de papier. La chaleur fournie par la source est alors susceptible de briser des liaisons chimiques dans le matériau, générant (via un processus généralement endothermique) de petits fragments qui se vaporisent. Si la température est suffisamment élevée, ces fragments réagissent avec l'oxygène de l'air pour produire plus de chaleur. Une partie de cette chaleur est rétrocédée par des processus radiatifs ou convectifs à la source de combustible, y maintenant le processus de fragmentation et de dégrafage de chaînes et contribuant ainsi à alimenter la flamme. Les menaces à la vie et aux biens proviennent donc d'un processus pour lequel le flux de chaleur provenant du matériau combustible est supérieur à la somme de la chaleur dissipée dans l'environnement de la combustion et de l'enthalpie marginale nécessaire pour maintenir l'écoulement stationnaire en phase gaz des pyrolysats.

Historiquement, la synthèse de matériaux « ignifuges » a précédé la compréhension du mécanisme du feu. Elle date du XVII^{ème} siècle en Europe avec le traitement des tentures des théâtres parisiens en 1638 et le tissage de matériaux textiles pour vêtements « incombustibles » à Oxford en 1684. Les travaux de Gay Lussac réalisés au début du XIX^{ème} siècle sur la carbonisation non naturelle de la cellulose en présence de l'acide orthophosphorique relèvent de cette approche[4].

Le présent mémoire traite de la formulation de matériaux possédant la propriété de retarder leur dégradation thermique et, en conséquence, leur inflammation, matériaux désignés par le sigle FR dans ce texte.

Actuellement, la tenue au feu des matériaux est optimisée :

- en augmentant leur résistance à l'ignition,
- en réduisant la propagation de la flamme par une dilution des gaz combustibles et/ou du comburant. Cette réduction est obtenue par émission d'un inerte et/ou par modification du régime de la flamme. Le dernier processus est obtenu par émission d'espèces gazeuses radicalaires qui agissent comme des agents de terminaison pour les réactions radicalaires en chaîne responsables de la flamme,

- ou en diminuant le flux de chaleur émis lors de la combustion par abaissement du taux de « fuels » libérés dans la phase gaz et/ou en modifiant leur composition et donc leur pouvoir calorifique.

Dans la construction, l'ameublement, les transports, les applications électriques et électroniques, les polymères de synthèse (résines plastiques, thermoplastiques et (thermo -) durcissables) sont d'un emploi généralisé en raison de la facilité de leur mise en œuvre et de leurs prix de vente faibles. Leur marché aux Etats-Unis était supérieur à 50 000 t en 1995 et a présenté entre 1986 et 1995 une progression approximative annuelle de 9 % pondéral [5] . Ces matériaux, en particulier les polymères de grande consommation (polyéthylènes (PE, prix : 6 à 8,50 FF/kg), polypropylènes (PP, prix : 5,20 à 7,20 FF/kg), polyamides (PA, prix : 15 à 70,20 FF/kg) et polystyrène (PS, prix : 5,80 à 10 FF/kg) [6]) et leurs alliages ou mélanges sont facilement inflammables. La généralisation de leur utilisation nécessite donc l'obtention de la propriété FR. La formulation de matériaux polymères FR doit prendre en compte leur faible prix, les conditions de leur mise en œuvre et la préservation de leurs propriétés intrinsèques (propriétés rhéologiques, mécaniques et résistances au vieillissement, aux rayons ultra-violets et aux intempéries).

Plusieurs voies sont proposées à l'homme de l'art pour le choix ou la formulation du matériau polymère FR. Elles consistent

- en l'utilisation de polymères, tels certaines résines thermodurcissables (résine phénol/formaldéhyde) ou certains thermoplastiques (polyphénylène sulfone, polyamides aromatiques (aramides), poly(bis-maléimides), intrinsèquement résistants à la chaleur et/ou FR,

- en l'ajout de monomères fonctionnalisés aux monomères lors de la réticulation du polymère. Les matières premières sont généralement d'un prix élevé et cette application reste comparativement confidentielle,

- en l'ajout d'adjuvants (« additifs ») FR lors de la synthèse ou de la mise en forme du polymère.

Une grande classe d'adjuvants FR est constituée de l'hydroxyde d'aluminium (55% pondéral du marché US en 1986 ; 6 % pondéral de croissance annuelle au US, 5 % des Brevets d'Invention mondiaux des FR en 1995-1996) et de l'hydroxyde

de Magnésium (3 % des Brevets en 1995-1996). Ces adjuvants présentent, dans les conditions d'un feu, une dégradation endothermique avec dégagement d'eau. Cette dégradation conduit à un retard à l'inflammation et à la dilution des gaz constituants de la flamme. La propriété FR est généralement obtenue pour des taux de charges élevés, compris entre 50 et 70 % pondéral, qui interdisent leur utilisation dans les polymères à propriété, en particulier par perte des propriétés mécaniques.

La seconde grande famille d'adjuvants regroupe les substances bromées (9% pondéral du marché US en 1986, 17 % des Brevets en 1995-1996) ou contenant un(des) halogène(s) (13% pondéral du marché US 1986, 16 % des Brevets 1995-1996) éventuellement en association avec des composés de l'antimoine (9 % pondéral du marché US 1986, 14 % des Brevets en 1995-1996). Le mécanisme de protection est un mécanisme en phase gaz mettant en jeu un processus radicalaire.

Les adjuvants contenant des phosphates et des composés du bore sont actuellement au stade de la recherche et des développements (37 % des Brevets mondiaux en 1995-1996).

Le choix d'une formulation FR doit prendre en compte :

- l'émission de fumées (suies, substances polyaromatiques en suspension, autres particules éventuellement minérales en suspension) dont l'opacité réduit le travail des combattants du feu. elle est, en outre, responsable du refus de fuir des victimes lié à une panique provenant de l'instabilité émotionnelle humaine en présence de la fumée [7, 8] et donc de la mortalité,

- l'émission de produits toxiques responsables de la mortalité directe ou des intoxications lors d'un incendie. La plupart des gaz produits par combustion sont classés en deux catégories principales : les asphyxiants (tels le monoxyde de carbone CO, le dioxyde de carbone CO_2 et l'acide cyanhydrique HCN) et les irritants (l'acroléine et divers autres aldéhydes, l'ammoniac NH_3, le chlorure et les autres halogénures d'hydrogène, l'anhydride sulfureux SO_2, et les oxydes d'azote NO_x. Le ***tableau 1*** rassemble, à titre d'exemples, les effets physiologiques [9, 10] de CO, NO_2, HCN et NH_3,

- l'émission de narcotiques,

- la diminution de la teneur en oxygène qui est, elle aussi, responsable de la mortalité (par hypoxie : diminution de l'apport d'oxygène à l'organisme).

Ces effets sont des préoccupations constantes de notre Groupe lors de l'évaluation de nouvelles formulations. Ils ne sont néanmoins pas directement rapportés ou discutés dans le présent mémoire.

EFFETS	Concentrations (p.p.m.)			
	CO	**HCN**	**NO_2**	**NH_3**
Sans danger pendant plusieurs heures	100	20	10-40	100
Sans danger pendant 1 heure	400-500	50-60	-	1000
Dangereux au bout de 1/2 ou 1 heure	1500-2000	100-240	100-150	2500-4500
Mortel en 1/2 heure	4000	200-450	-	-
Rapidement mortel	-	3000	200-270	5000-10000
Concentration minimale provoquant une irritation de la gorge	-	-	62	408
Seuil de détection olfactive	-	-	-	53

Tableau1 : Effets physiologiques de certains gaz dégagés lors des incendies [11, 12].

Une dernière catégorie de produits de combustion regroupe les substances dont l'ingestion ou l'inhalation produisent des effets à long terme sur la santé. L'effet carcinogène de certaines de ces substances (oxydes d'antimoine, benzène, familles des dioxines et des benzofuranes) a été tout particulièrement considéré. Une conséquence réside dans la limitation de l'emploi de matériaux intrinsèquement FR contenant des produits halogénés (souvent associés à Sb_2O_3) dont la dégradation conduit au rejet de ces substances soupçonnées carcinogènes [13].

Les nations industrialisées conseillent, d'ailleurs, la recherche d'adjuvants FR substituts aux additifs contenant du brome [14] et, en particulier, aux composés de la famille des diphénylés polybromés [15]. En addition, des directives récentes des Organismes Internationaux conduisent à rechercher des formulations nouvelles de polymères exemptes de produits halogénés. Parmi les axes de recherches à considérer , nous avons traité la recherche de formulations de polymères FR dont la protection met en jeu un processus en phase condensée et, en particulier, une carbonisation non naturelle catalytique des adjuvants et/ou de la matrice polymère.

Ce processus en phase condensée implique une dégradation partielle de la matrice polymère. Un tel comportement sera, dans ce mémoire, décrit comme un comportement ablatif. « L'ablation » du matériau doit être ici considéré selon sa signification chirurgicale **(qui accepte de sacrifier une de ses parties pour se protéger)** plutôt que selon celle retenue en sciences des matériaux (sublimation fortement endothermique sous l'effet d'un flux de chaleur).

Une compilation des propriétés FR intrinsèques des polymères [16] en relation avec la quantité de résidu carboné obtenue lors de leur pyrolyse montre une relation linéaire entre leurs indices limites d'oxygène (L.O.I., % volumique [17]) et leur pourcentage pondéral résiduel (CR, kg. %) à 850°C :

$$LOI \times 100 = (0,4 \times CR) + 17,5$$

van Krevelen explique la formation du résidu carboné [16] :

- par la composition chimique du polymère, en particulier la présence de groupements chimiques actifs dans des réactions de déshydrogénation ou de « disproportionation » (hydroxyle , carbonyles ou halogénés),
- par une organisation initiale de la résine selon un réseau tridimensionnel qui donne une stabilité thermique relativement importante au matériau et favorise la formation d'un résidu stable [18].

Une classe de ces matériaux, les résines polyépoxydes, peut être mise en œuvre pour la fabrication de pièces structurales allégées utilisées dans l'industrie aéronautique et spatiale. Ces résines, tel le système bisphénol-A/épichlorhydrine, sont généralement des combustibles à inflammation auto-supportée. Elles présentent une dégradation thermique qui peut être contrôlée et dirigée vers leur carbonisation.

Nous présentons l'étude de deux systèmes époxydes modèles :

- N, N', N', N' tétraglycidyle-méthylène-dianiline/diamino 4, 4' diphényle sulfone (TGMDA/DDS) (abréviation anglo-saxonne : TGDDM/DDS),
- N, N', N', N' tétraglycidyle-méthylène-dianiline/dicyandiamine (diamine aromatique) (TGMDA/DDA) (abréviation anglo-saxonne : TGDDM/DDA)

qui présentent des groupements chimiques hydroxyle et admettent des réticulations différentes selon leurs « stoechiométries » (les rapports résines/durcisseurs) initiales en matières premières [19] ou selon leurs structures [20, 21]. Ces matériaux sont auto-extinguibles et présentent une résistance au feu prouvée par les valeurs de leur LOI , respectivement 30 et 25 % à 25°C.

Nous décrivons dans la première partie de ce Mémoire les modifications chimiques qui prennent place lors de la dégradation thermique du premier système et présentons les techniques spectroscopiques, classiquement mises en œuvre pour l'étude des carbones de synthèse ou des charbons fossiles, utilisées par notre Groupe pour caractériser les matériaux protecteurs. Les données cinétiques de la dégradation thermo-oxydante des deux systèmes, en particulier les paramètres invariants, sont ensuite comparés. Ces paramètres cinétiques, associés aux données gravimétriques obtenues lors d'inflammations dans un calorimètre à cône, permettent finalement de proposer les étapes du processus ablatif, à savoir la destruction contrôlée des résines (réaction fortement endothermique) pour former un matériau superficiel qui limite les transferts de chaleur de la source vers le polymère résiduel. Cette dernière étude permettra, par ailleurs, de vérifier que le modèle du « Front de Dégradation » proposé par Bourbigot et al. [22, 23] (qui limite de manière simplificatrice [24] la zone de la réaction à une surface) est un outil qui permet la compréhension de la carbonisation et de la dégradation ultérieure des résines.

Les matériaux polymères thermoplastiques à chaînes linéaires enchevêtrées et non fonctionnalisées, tels PE, PP ou PS, ne présentent pas de performances FR intrinsèques, les valeurs de leur LOI sont proches de 17 % en accord avec van Krevelen. La formation d'un bouclier superficiel protecteur dans les conditions d'un feu peut être obtenue par l'ajout d'adjuvants au sein de ces résines. Les systèmes d'additifs généralement utilisés forment un matériau superficiel vitreux [25-27] ou expansé dit intumescent [28] lorsqu'ils sont soumis à un flux de chaleur ou aux conditions d'un feu.

Les systèmes d'adjuvants intumescents (dénomination proposée par Olsen et Bechle [29]) forment dans les conditions d'un feu un matériau carboné expansé protecteur (Planche 1). Ils sont développés depuis près de 60 ans [30] et appliqués

tout particulièrement dans la formulation de peintures pour matériaux coupe-feu [31, 32 et références citées en [32]].

Ces systèmes sont généralement composés d'un ou plusieurs agents de carbonisation (CA, polyols [32] ou polymères [33]), d'un ou plusieurs précurseurs d'espèces catalytiques acides (CP, tels les sels des acides phosphoriques [32], de l'acide sulfurique [29] ou des acides boriques [34]) stables aux températures élevées (280-550°C), d'un agent de gonflement (tels la mélamine [35], l'urée et leurs dérivés [32]) et d'agents de synergie (SA) [34, 36 et références citées par les Auteurs].

Les premiers adjuvants intumescents utilisés dans des polymères thermoplastiques sont le polyphosphate d'ammonium (APP) dans le PS [37] et le mélange APP - pentaérythritol (PER) dans le PP isotactique [38]. Notre Groupe a développé des formulations FR originales du PE basse densité (LDPE) [39] et de terpolymères de l'éthylène [23] contenant le mélange des adjuvants (APP/PER). Ces systèmes présentent tous des performances FR via un processus d'intumescence (Planche 1).

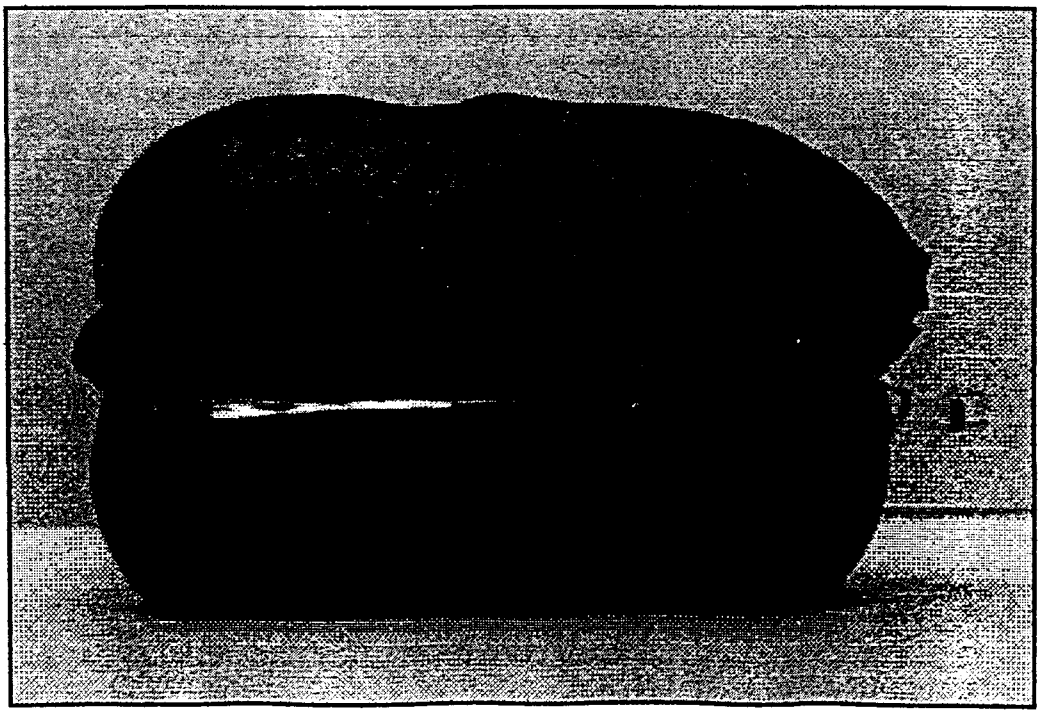

Planche 1. Matériau intumescent obtenu par carbonisation sous air à 280°C d'un système terpolymère éthylène - acrylate de butyle - anhydride maléique (LRAM 3.5)/APP/PER.

Dans les systèmes intumescents, Kishore et al. [37] et Camino et al. [40] proposent que l'étape déterminante pour la formation du matériau protecteur consiste en la formation d'esters de l'acide phosphorique. Ces esters sont formés par la réaction de l'acide avec les groupements hydroxyle créés dans la chaîne du PS lors d'un traitement thermo-oxydant ou les groupements hydroxyle du polyol. Un matériau carboné se forme ensuite par une séquence déshydratation de l'ester - carbonisation (APP/PS) ou par une séquence cyclisation des esters via des ions carboniums - condensation de type Diels Alder avec formation d'espèces aromatiques et polyaromatiques (APP/PER).

A ce jour, le système APP/PS reste un système modèle pour étudier en Laboratoire [41] des interactions entre un adjuvant du type CP et une matrice polymère, sans applications industrielles directes.

Le système APP/PER a été évalué par notre groupe comme adjuvant FR dans divers polymères. Deux paramètres tendent à limiter son utilisation, le coût cumulé des matières premières et de la mise en œuvre du mélange adjuvant - polymère est comparativement élevé (un PP FR apte au filage admet un prix équivalant à celui de fibres acryliques intrinsèquement FR [42]) et le vieillissement des formulations qui s'accompagne d'un phénomène d'exsudation des adjuvants (rejet des charges supposé lié à une augmentation de la cristallinité du matériau lors de la trempe ou dans le temps). Le système demeure néanmoins un étalon permettant un classement des performances feu des systèmes d'adjuvants dans diverses matrices. Il permet en outre l'étude des processus chimiques et physiques qui participent à la protection des matériaux [43-48].

L'étude du mélange modèle polyphosphate d'ammonium - pentaérythritol, adjuvant des formulations intumescentes de polymères thermoplastiques, présentée dans le Chapitre II de ce Mémoire représente une contribution à la compréhension du processus d'intumescence. Dans un premier paragraphe, l'étude physico-chimique de la dégradation thermo-oxydante du mélange des adjuvants est présentée. La participation des matrices polymères à la formation des matériaux carbonés protecteurs est discutée dans une deuxième partie qui vérifie le caractère ablatif de la formation des revêtements protecteurs intumescents. Finalement, l'étude thermogravimétrique, couplée à la calorimétrie par consommation d'oxygène,

de la dégradation de formulations intumescentes du polypropylène dans les conditions d'un incendie est présentée dans un troisième paragraphe. Elle permet de préciser les processus qui se produisent lors de la carbonisation des matériaux dans les conditions d'un incendie généralisé.

La formulation optimale des mélanges d'adjuvants intumescents se heurte souvent à des modifications des performances FR en fonction de la composition des mélanges. Trois types de variations sont présentés :

- un effet de type additivité : la propriété FR de la formulation est proche de celle calculée par combinaison linéaire des modifications de la propriété, induites par chaque adjuvant seul (exemple présenté Figure 1),
- un effet de type antagoniste : une diminution de la propriété est observée lors de l'ajout d'un des adjuvants (exemple présenté Figure 2)
- ou un effet de synergie : un maximum de la propriété est observé pour un rapport optimal des concentrations relatives des adjuvants (exemple présenté Figure 3).

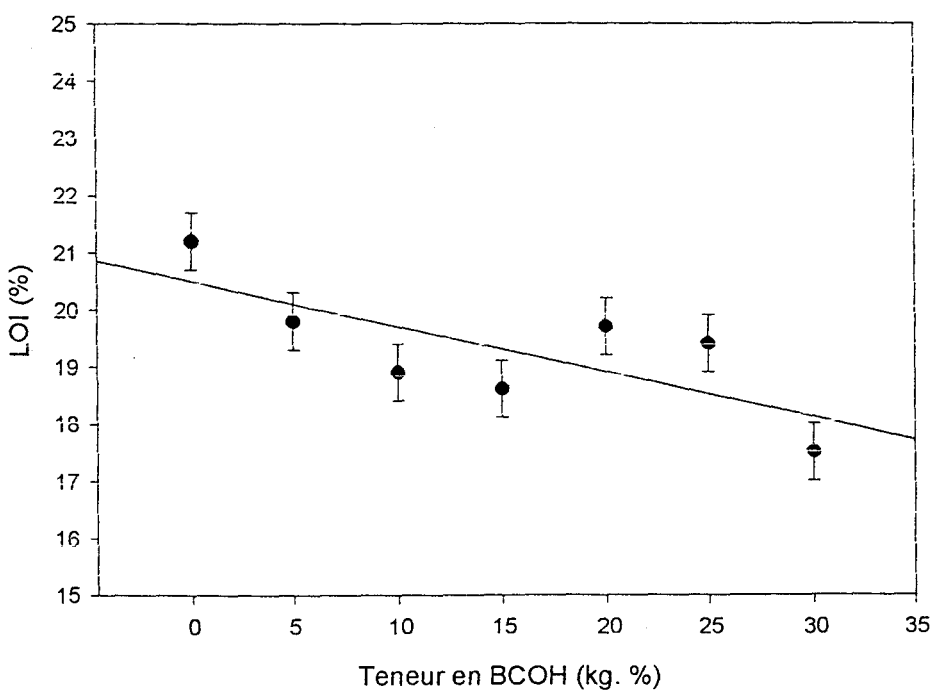

Figure 1. Exemple d'un effet du type additivité des propriétés FR - Résultat du test normalisé LOI fonction de la teneur pondérale en β-cyclodextrine (BCOH) dans la formulation PP-APP/BCOH (teneur pondérale en adjuvant: 30 kg. %) [33].

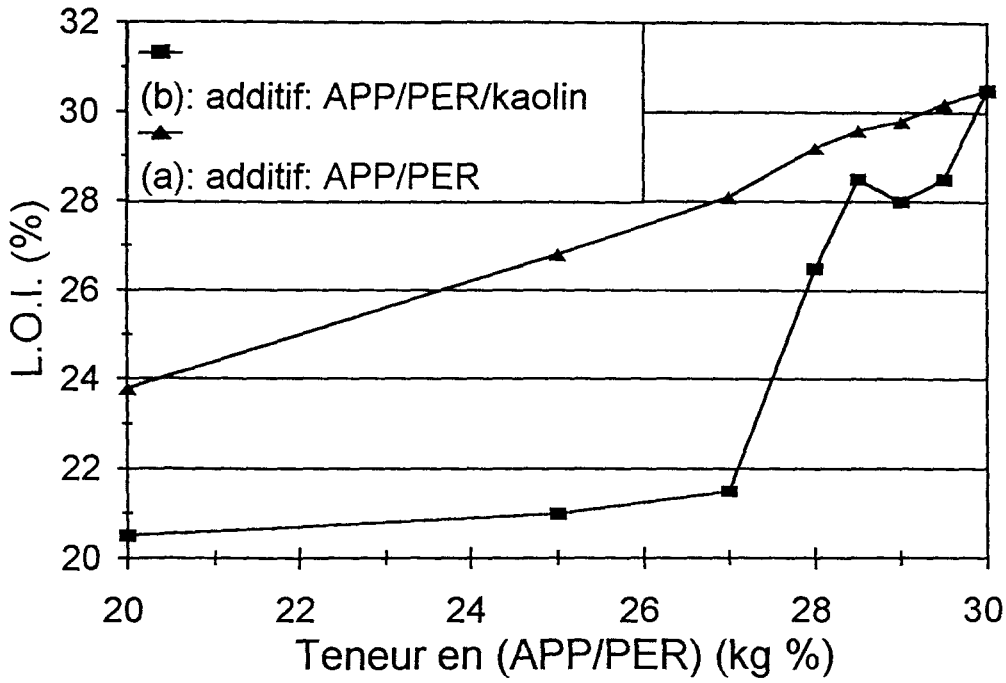

(erreur relative sur la mesure des LOI de l'ordre de 2 % (courbe a) et de 2,5 % (courbe b))

Figure 2. Exemple d'un effet du type antagoniste - Comparaison des résultats du test normalisé LOI fonction de la teneur pondérale en mélange APP/PER dans les formulations PP-APP/PER (APP : PER = 3 : 1) et PP-APP/PER/kaolin (APP : PER = 3 : 1 et teneur pondérale en APP/PER/kaolin : 30 kg. %) [49].

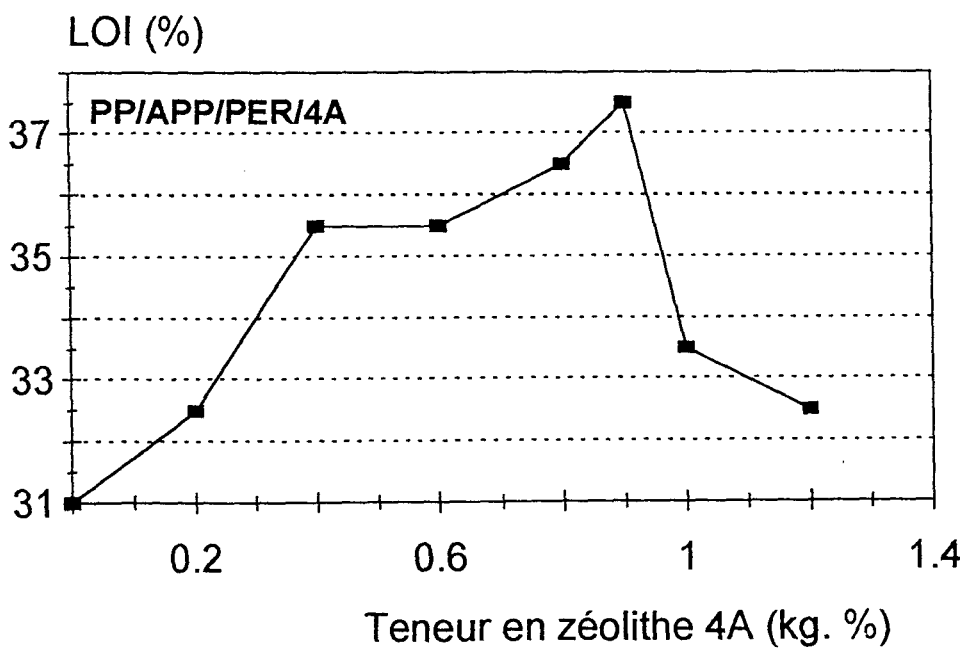

(erreur relative sur la mesure des LOI de l'ordre de 1,5 %)

Figure 3. Exemple typique d'un effet de type synergie - Résultat du test normalisé LOI fonction de la teneur pondérale en zéolithe 4A (4A) dans la formulation PP-APP/PER/4A (teneur pondérale en adjuvant (APP/PER/4A) : 30 kg %, rapport pondéral APP : PER = 3 : 1) [46].

L'effet de synergie est particulièrement intéressant puisque qu'il permet d'obtenir la performance souhaitée avec une teneur en adjuvants comparativement réduite. Il a été démontré dans de nombreuses formulations intumescentes. Les inventeurs étudient généralement les formulations optimales et attribuent par phénoménologie l'effet à un paramètre particulier du système. Citons à titre d'exemple, le cas particulier de l'adjuvant APP/PER pour lequel le rapport stoechiométrique, correspondant à la formation de l'ester de l'acide orthophosphorique de type « spiro » [50], a été tout particulièrement étudié [40].

L'objectif du présent travail consiste à proposer des règles « universelles » pour la formulation de polymères FR intumescents et donc à comprendre les mécanismes impliquant l'effet de synergie. Il implique de considérer divers paramètres propres aux adjuvants, au matériau et aux produits de leur dégradation :

- la structure et la morphologie des adjuvants dans la formulation polymère,
- la modification du polymère lors de sa mise en forme en présence de charges : modification de la longueur des chaînes et réticulation intramoléculaire dues à un effet thermo - mécano - radicalaire, la fonctionnalisation induite du polymère ou la modification de sa structure cristalline (teneur en phase amorphe, taille des domaines amorphes et cristallins, rigidité de l'amorphe),
- la structure et la morphologie des produits résultants des interactions entre les adjuvants et/ou entre les adjuvants et la matrice polymère lors d'une pyrolyse ou d'un traitement thermo-oxydant,
- la composition, la structure et, en conséquence, les propriétés physiques, en particulier dynamiques, du revêtement protecteur,
- les caractéristiques thermodynamiques des matériaux constituant ce bouclier (capacité calorifique, conductibilité thermique ...). Une étude en cours menées par des membres de notre Groupe concerne ces paramètres (Bourbigot S. et Morice L. [41]). Ces résultats ne seront pas rapportés dans le présent Mémoire.

L'approche présentée dans notre 3ème chapitre, regroupe l'étude de plus de 50 formulations différentes. Elle concerne, dans une première partie, l'évaluation dans le PP, le HDPE ou le LRAM 3.5:

•de nouveaux précurseurs d'espèces acides actives (CA) : pyrophosphate diammonique (PY) et pentaborate d'ammonium (APB),

•de nouvelles sources de matériau carboné (CP): polyols produits de l'industrie agro-alimentaire : xylitol (XOH), mannitol (MOH), d-sorbitol (SOH), dextrine de composition homologue de celle de la cellulose : β-cyclodextrine (BCOH ; $(-C_5H_5(OH)_2(CH_2OH)O\text{-}O\text{-})_7$) et des polymères thermoplastiques : polyamide-6 (PA), copolymère éthylène - acétate de vinyle (8 %) (EVA8) et leurs mélanges,

•et de nombreux agents de synergie (SA): 8 zéolithes et 16 argiles différentes (CP), et BCOH (CA).

Le mécanisme de la synergie est alors discuté en considérant le matériau carboné intumescent comme le résultat d'une réaction de polymérisation radicalaire. Un schéma simplifié décrivant une courbe de synergie comme la résultante de l'addition de plusieurs courbes : FR = fonction d'une propriété chimique et FR = fonction d'une propriété physique, est finalement proposé.

Une seconde partie concerne « l'effet de matrice » induit par la composition chimique des polymères et des copolymères, matrice hôtes des systèmes adjuvants. Les propriétés FR du système APP/PER/4A dans 14 matrices polymères fonctionnalisées y sont analysées par comparaison aux formulations du PE.

Finalement, une dernière partie présente différentes formulations intumescentes originales de polymères de commodité. Ces matériaux sont susceptibles d'être développés car il ne présentent plus de rejet des adjuvants lors de leur vieillissement et sont aptes à supporter divers modes de mises en œuvre (extrusion-moulage, calandrage ou assemblage par thermosoudage) ;

J'ai tenu à ce que l'ensemble des résultats fassent l'objet de publications dans des Journaux avec référés ou dans les Actes de Congrès Internationaux avant de les intégrer à cette dissertation. Notre Mémoire reprend de manière textuelle ces articles dans les chapitres du présent sommaire selon un ordre qui ne respecte pas nécessairement celui de leur parution.

CHAPITRE I : **LA PROTECTION AU FEU PAR UN PROCESSUS DE CARBONISATION ABLATIVE NATURELLE. ETUDE DE LA DEGRADATION THERMIQUE DES DEUX RESINES EPOXYDES MODELES TGMDA/DDA ET TGMDA/DDS.**

- Caractérisation chimique et spectrochimique des produits de la dégradation du système modèle TGMDA/DDS,

ROSE N., COSTES B., LE BRAS M. et DELOBEL R.

« Etude de la Thermodégradation de Résines TGMDA-DDS en fonction des Conditions de Polymérisation » dans les Actes du Colloque National du Groupe Français des Polymères **« Polymérisations - Mécanismes - Méthodes - Procédés »**, Bordeaux (18-20 novembre 1991), GFP, **CA27** (1991) pp ;73-74.

ROSE N., LE BRAS M., DELOBEL R., COSTES, B., et HENRY Y.

« Thermal Oxidative Degradation of an Epoxy Resin. », Polym. Deg. & Stab., **42** (1993) 307-316.

- Comparaison de la stabilité des deux résines modèles lors de leur dégradation thermo-oxydante

ROSE N., LE BRAS M., BOURBIGOT S., et DELOBEL R.

« Thermal Oxidative Degradation of Epoxy Resins : Evaluation of their Heat Resistance using Invariant Kinetic Parameters », Polym. Deg. & Stab., **45** (1994) 387-397.

- Discussion des propriétés retardatrices de la flamme des résines en relation avec leur mécanisme de dégradation - Définition et application du Modèle du front de dégradation.

LE BRAS M., ROSE N, BOURBIGOT S., HENRY Y. et DELOBEL R.

« The Degradation front model - A tool for the chemical study of the degradation of epoxy resins in fire. », J. Fire Sci., **14(5-6)** (1996) 199-233.

CHAPITRE II : **CONTRIBUTION A LA COMPREHENSION DU PROCESSUS D'INTUMESCENCE - ETUDE DU MELANGE MODELE (POLYPHOSPHATE D'AMMONIUM - PENTAERYTHRITOL), ADJUVANT DE FORMULATIONS INTUMESCENTES DES POLYMERES THERMOPLASTIQUES.**

- Etude de la dégradation thermo-oxydante du mélange des adjuvants,

DELOBEL R., BOURBIGOT S., LE BRAS M., LEROY J.-M. et KANOVNIK B.

« Amonij Polyfosfat - Pentaeritritol kao Dodatak za Smanjenje Gorenja : Strukturna Svojstva « Ugljika » u Nabubrenim Slojevima ; » dans **« Polimerni Materijali Smanjene Gorivosti »**, ed. JANOVIC, Z., Drustvo Plasticara i Gumaraca pub., Zagreb (1990), pp 08/01-08/04.

BOURBIGOT S., LE BRAS M. et DELOBEL R.

« Carbonization Mechanisms resulting from Intumescence Association with the Ammonium Polyphosphate - Pentaerythritol Fire Retardant System. », Carbon, **31(8)** (1993) 1219-1230.

BOURBIGOT S., LE BRAS M., GENGEMBRE L. et DELOBEL R.

« XPS study of an Intumescent coating - Application to the *Ammonium Polyphosphate - Pentaerythritol Fire-Retardant System »,* Applied Surface Sci. **81** (1994) 299-307.

- Mise en évidence de la participation des matrices polymères à la formation des matériaux carbonés protecteurs,

BOURBIGOT S., LE BRAS M. DELOBEL R. BREANT P. et TREMILLON J.-M.

« Carbonization Mechanisms resulting from Intumescence - Association with an Ethylene Terpolymer and the Ammonium Polyphosphate - Pentaerythritol Fire Retardant System. », Carbon, **33(3)** (1995) 283-294.

- Contribution à l'étude du mécanisme de protection au feu par un matériau intumescent.

BOURBIGOT S., DELOBEL R., LE BRAS M. et SCHMIDT Y.

*« Relation between limiting Oxygen Index and Invariant Activation Energy »,*J. Chim. Phys., **89** (1992) 1835-1852.

BOURBIGOT S., LE BRAS M., DELOBEL R. et NORMAND D.

« Comparative Study of the Integral TG Methods Used in the Invariant Kinetic Parameters Method. Application to Fire Retardant Polypropylene », J. Chim. Phys.,**90** (1993) 1909-1928.

BOURBIGOT S., LE BRAS M. et DELOBEL R.

« Fire Degradation of an Intumescent Flame Retardant Polypropylene using Cone Calorimeter », J. Fire Sci. **13(1-2)** (1995) 3-21.

MARCHAL A., DELOBEL R., LE BRAS M., LEROY J.-M. et PRICE D.

« Effect of Intumescence on Polymer Degradation », Polym. Deg. & Stab. **44** (1994) 263-272.

CHAPITRE III : **FORMULATION DE NOUVEAUX MATERIAUX THERMOPLASTIQUES RETARDATEURS DE FLAMME INTUMESCENTS - ETUDE PROSPECTIVE.**

- Evaluation de nouveaux adjuvants :

DELOBEL R., LE BRAS M., OUASSOU N. et ALISTIQSA.
« Thermal Behaviours of Ammonium Polyphosphate - Pentaerythritol and Ammonium Pyrophosphate - Pentaerythritol Intumescent Additives in Polypropylene Formulations. », J. Fire Sci., **8** (1990) 85-108.

LE BRAS M., BOURBIGOT S., DELPORTE C., SIAT C. et LE TALLEC Y.
« New Intumescent Formulations of Fire Retardant Polypropylene - Discussion about the Free Radicals Mechanism of the Formation of Carbonaceous Protective Materials during the Thermo-oxidative Treatment of the Additives. », Fire & Materials, **20** (1996) 191-203.

- Evaluation de nouveaux agents de synergie

LE BRAS M. et BOURBIGOT S.
« Mineral Fillers in Intumescent Fire Retardant Formulations - Criteria for the -Choice of a Natural Clay Filler for the Ammonium Polyphosphate/ Pentaerythritol/Polypropylene System. », Fire & Materials, **20** (1996) 39-49.

BOURBIGOT S., LE BRAS M., BREANT P., TREMILLON J.-M. et DELOBEL. R.
« Zeolites: new Synergistic Agents for Intumescent Fire Retardant Thermoplastic Formulations - Criteria for the Choice of the Zeolite. », Fire & Materials,20 (1996) 145-154.

BOURBIGOT S., LE BRAS M., DELOBEL R., DESCRESSAIN R. et AMOUREUX J.-P.
« Synergistic Effect of Zeolite in an Intumescence Process : Study of the Carbonaceous Structures using Solid State NMR. », J. Chem. Soc., Faraday Trans. **92(1)** (1996) 149-158.

BOURBIGOT S., LE BRAS M., DELOBEL R. et TREMILLON. J.-M.
« Synergistic Effect of Zeolite in an Intumescence Process - Part II - Study of the Interactions between the Polymer and the Additives. », J. Chem. Soc., Faraday Trans., **92(18)** (1996) 3435-3444.

LE BRAS M., BOURBIGOT S., LE TALLEC Y. et LAUREYNS J.
« Synergy in Intumescence - Application to β-cyclodextrin Carbonisation Agent in Intumescent Additives for Fire Retardant Polyethylene Formulations. », Polym. Deg. & Stab., **56(1)** (1997) 11-21,.

- Cas particulier des copolymères fonctionnalisés - La fonctionnalité des monomères constituants, un critère de choix du polymère dans les formulations intumescentes.

BOURBIGOT S., LE BRAS M., DELOBEL R., BREANT P. et. TREMILLON J-M.
« 4A Zeolite Synergistic Agent in New Flame Retardant Intumescent Formulations of Polyethylenic Polymers - Study of the Effect of the Constituent Monomers. », Polym. Deg. & Stab., 54 (1996) 275-287.

CHAPITRE IV : **FORMULATION DE NOUVEAUX MATERIAUX THERMOPLASTIQUES RETARDATEURS DE FLAMME INTUMESCENTS - PERSPECTIVE : LES MELANGES DE POLYMERES.**

Association du polyamide-6 et des phosphates d'ammonium dans des formulations et des mélanges maîtres FR - Un développement intéressant pour les matériaux FR intumescents

SIAT C., BOURBIGOT S. et LE BRAS M.

« Structural Study of the polymer phases in a PA6-EVA FR Additive Blend », The 7th Annual BCC Conference on Flame Retardancy - « *Recent Advances in Flame Retardancy of polymeric Materials* », Stamford (USA) (20-22 Mai 1996),

SIAT C., BOURBIGOT S. et LE BRAS M.

« Structural Study of the polymer phases in a PA6-EVA FR Additive Blend », « ***Recent Advances in FR of Polymeric Materials (Volume 7)*** », LEWIN M. ed., Business Communications Co Inc., Norwall (1997), 318-326,

performances des nouvelles formulations

Extraits de

BOURBIGOT S. et LE BRAS M., ***Enveloppe Soleau*** n° 36872 (17 juillet 1995).

LE BRAS M. et BOURBIGOT S., ***Enveloppe Soleau*** n° 59305 (30 mai 1996).

Ce Mémoire rapporte, outre des résultats personnels, ceux des étudiants et des stagiaires que j'ai dirigés ou que j'ai encadrés sous la direction du Professeur Jean-Marie Leroy et/ou en collaboration avec le Professeur René Delobel et Serge Bourbigot. Je tiens à remercier :

ROSE Nathalie, *« Etude de la Dégradation Thermique et du Comportement au Feu de Résines Epoxydes Utilisées dans l'Aéronautique »*, Thèse, Lille (France), 1995.

BOURBIGOT Serge, *« Les zéolithes, Nouveaux Agents de Synergie dans les Systèmes Intumescents - Compréhension des Mécanismes de Protection du Polyéthylène et de ses Dérivés »*, Thèse, Lille (1993).

ALISTIQSA Fathia, *« Mise au Point de Nouvelles Formulations Intumescentes Polyphosphate d'ammonium - Pentaérythritol ; Application à l'Ignifugation du Polypropylène. »*, Thèse, Lille (1993).

SCHMIDT-LE TALLEC Yannick, *« Valorisation de Différents Polyols dans des Systèmes Retardants de Flamme : Application au Polyéthylène »*, Thèse, Lille (1992).

SIAT Catherine, *« Les Polyamides, agents carbonisants de systèmes additifs intumescents »*, Thèse en cours.

DELPORTE Christelle, *« Etude du nouveau système intumescent retardateur de flamme pentaborate d'ammonium / pentaérythritol - Application au polypropylène »*,.Diplôme d'Etudes Approfondies « Spectroscopies », Lille (1995).

DUPOISSON Cécile, *« Optimisation de formulations intumescentes du polypropylène aptes au filage »*, Diplôme d'Etudes Approfondies « Spectroscopies », Lille(1993).

POUILLE Fabienne, « *Etude Spectroscopique de Formulations « Retard au Feu » à base de Polyamide. »*, Diplôme d'Etudes Approfondies « Spectroscopies », Lille (1995).

FELIX, Emmanuelle, *« Etude structurale par RMN du Solide de Formulations ignifugeantes à base de PA6. »*, Diplôme d'Etudes Approfondies « Spectroscopies », Lille (1995).

MORICE Ludovic, « *Etude et Modélisation des Transferts Thermiques dans un Bouclier Intumescent - Application au Polypropylène " Retard au Feu* », Diplôme d'Etudes Approfondies « Génie Chimique », Compiègne (1996).

pour l'excellence de leurs travaux et pour la qualité de nos discussions.

Je tiens également à associer à ce travail les Stagiaires du Laboratoire dont les résultats, rapportés dans le présent travail, se sont révélés précieux pour la progression de notre Groupe.

CHAPITRE I

PROTECTION AU FEU PAR UN PROCESSUS DE CARBONISATION ABLATIVE NATURELLE.

ETUDE DE LA DEGRADATION THERMIQUE DES DEUX RESINES EPOXYDES MODELES : TGMDA/DDA ET TGMDA/DDS

Lorsqu'un polymère est soumis à un flux de chaleur, sa participation à un incendie peut, en première approximation, se décrire par la formation de gaz combustibles volatils [52] produits par un ensemble de réactions chimiques endothermiques:

- scission de la chaîne principale de la macromolécule qui conduit à une diminution de la masse moléculaire et au départ de monomères ou d'oligomères (fragments de chaîne composés de moins de dix unités monomères),
- réactions affectant les extrémités de cette chaîne, en particulier élimination des groupements terminaux avec formation de monomères,
- élimination des groupements fixés sur cette chaîne avec insaturation de la chaîne.

Il est admis que le polymère ne réagit pas, à ce stade, avec l'oxygène moléculaire de l'environnement [53]. En effet, la consommation de l'oxygène dans la flamme et sa faible diffusion, à contre courant, dans le flux des produits de dégradation conduit à une concentration faible à l'interface solide/gaz. Par ailleurs, sa diffusion dans le matériau peut être négligée. Les produits de la dégradation thermique (pyrolyse) de la résine réagissent uniquement en phase gaz avec l'oxygène ou un autre comburant. Ils participent alors à la flamme via une réaction globalement exothermique. La dégradation du matériau est assurée par la rétro-donation de chaleur de la flamme vers le matériau.

Le mécanisme de décomposition peut, en fait, se révéler plus complexe. En effet, parallèlement à la formation des volatils, des réactions de réticulations inter et intramoléculaires peuvent se produire avec, éventuellement, une augmentation de la masse moléculaire du polymère et/ou une carbonisation « naturelle » du matériau avec formation de « carbone » ou de goudrons. La formation du « carbone » stable dans la phase condensée ou de « goudrons » a pour première conséquence la réduction du flux de combustibles volatils vers la flamme. Par ailleurs, la formation d'un matériau carboné superficiel de faible densité [51] entre la source de chaleur et le matériau polymère vierge réduit le flux de chaleur incident reçu par le polymère et, en conséquence, réduit la vitesse de la dégradation du matériau. Subséquemment, le flux de chaleur incident externe au matériau décroît lorsque l'apport de chaleur résulte uniquement de la combustion des volatils. Le matériau présente alors la

propriété « retard au feu » et peut, si les propriétés physiques du bouclier carboné sont adéquates, être autoextinguible.

Par malheur, la formation de « carbone » superficiel n'est pas toujours un processus avantageux. En effet, la combustion lente sans flamme, en phase condensée, de ce matériau est d'autant plus probable qu'il est abondant [52]. Elle conduit au maintien d'un processus d'incandescence ou de post incandescence (« point rouge ») qui correspond à la formation des oxydes de carbone via une réaction d'oxydation fortement exothermique. Il en découle que l'existence d'un processus de carbonisation naturelle affectant un matériau ne lui procure pas nécessairement la performance feu.

La carbonisation d'un polymère résulte d'un processus complexe de polymérisation avec formation d'hydrocarbures polynucléaires aromatiques ou de composés hétérocycliques dont les propriétés chimiques sont des fonctions de la composition du polymère et des conditions de sa dégradation [54]. L'étude du processus de carbonisation d'une résine devra nécessairement comprendre deux étapes : la caractérisation chimique du matériau carboné et la modélisation des mécanismes qui permettent la protection du polymère par le « carbone » superficiel.

Les méthodes généralement utilisées en transformation des matériaux plastiques pour accroître la température de fusion d'un polymère peuvent être mise en œuvre pour favoriser un processus type carbonisation lors de la dégradation. Elles consistent à augmenter sa réticulation. Typiquement, les résines thermodurcissables présentent des taux de réticulation importants nécessaires pour l'obtention des propriétés mécaniques. Elles peuvent donc servir de matériaux modèles pour tester les techniques analytiques susceptibles de caractériser les étapes de la formation de matériaux carbonés protecteurs. Elles peuvent, en outre, permettre l'évaluation de modèles qui permettent de lier la dégradation d'un matériau (sa carbonisation naturelle) à son comportement au feu.

Nous présentons ici l'étude de deux systèmes polyépoxydes modèles résultant de la réticulation de la résine TGMDA avec deux agents durcisseurs différents de type diamines DDS et DDA. Le premier agent présente un groupement

sulfone et deux noyaux aromatiques susceptibles de jouer un rôle dans la formation de structures polyaromatiques et/ou d'hétérocycles.

TGDDM

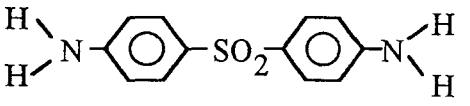

DDS

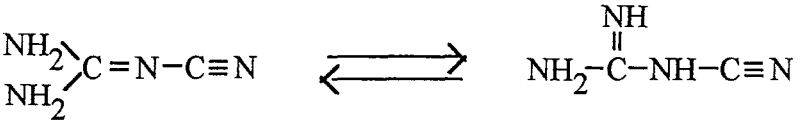

DDA

L'étude se divise en trois parties. Dans la première partie, l'apport de techniques physico-chimiques d'analyse à la compréhension du mécanisme de la dégradation thermo-oxydante des matériaux est présenté.

La seconde partie compare ensuite la stabilité des deux systèmes. Une méthode pour mesurer les paramètres cinétiques invariants (méthode IKP, « invariant kinetic parameters ») [55, 56] de la première étape de leur dégradation est rapportée. L'expression de la vitesse de dégradation, indépendante des conditions du traitement thermique, peut être utilisée pour la modélisation des transferts de matière ou de la température dans des conditions proches de celles d'une incendie.

Finalement, dans une troisième partie, la méthode IKP est appliquée à l'étude de l'étape de la dégradation des deux résines qui contribuent à la flamme par émission des combustibles volatils. Par ailleurs, le comportement de ces résines est simulé ,dans les conditions d'un incendie généralisé, en utilisant les résultats d'une étude au calorimètre à cône. Le calorimètre à cône est un appareil développé par le

NIST [57], qui permet l'analyse de données quantitatives relatives au phénomène de développement d'un feu (calorimétrie par consommation d'oxygène) et procure des informations sur la cinétique (analyse thermogravimétrique en temps réel) et les données thermodynamiques de la dégradation dans les conditions d'un feu [57-58]. Le modèle du « front de dégradation » est finalement appliqué pour comparer le mode de dégradation des deux résines, le caractère protecteur des résidus de leur dégradation et évaluer l'importance du processus de l'incandescence.

I-1. *Caractérisation chimique et spectrochimique des produits de la dégradation du système modèle TGMDA/DDS,*

Le système thermodurcissable modèle développé par la Société Aérospatiale [59] correspond à un mélange (effectué par la Société Structil) des monomères de la résine et de l'agent de réticulation (durcisseur) de compositions dites « stoechiométriques » ou non : les teneurs en fonctions époxydes de la résine et en protons primaires des groupements amines du durcisseur sont ou ne sont pas égales.

La réticulation correspond à la conversion des monomères liquides pour former un réseau tridimensionnel sous l'effet de la chaleur. Les réactions chimiques mises en jeu sont successivement une réaction entre une amine primaire et un groupement époxyde de bout de chaîne et des réactions de réticulation intra- et intermoléculaire [21]. La polymérisation est obtenue en respectant le protocole : traitement thermique 1 h à 135°C puis post-réticulation par un traitement 2h à 180°C. Le rendement de la réaction (degré de polymérisation évalué par mesure de la proportion de groupements époxydes consommés) est alors proche de 90% avec un mélange stoechiométrique [60]. Ce taux de réticulation est une fonction de la composition initiale de la résine ainsi que des conditions du traitement thermique de la résine (durée, température de traitement, post-réticulation éventuelle).

Les étapes successives : gélification (prise en masse) et vitrification (obtention du réseau tridimensionnel) ont été préalablement rapportées [20, 21]. L'étude du diagramme TTT (temps-température-transformation) des systèmes époxydes/diamine [60] montre une compétition entre la réticulation et la dégradation thermique aux températures élevées. La dégradation se produit en 2 étapes :

dévitrification (diminution de la température de transition vitreuse) et « revitrification » avec formation du structure carbonée de type « char ».

Des résines présentant des réticulations différentes sont susceptibles d'admettre des modes de dégradation et, en conséquence, des tenues au feu différents. La présente étude va concerner le système modèle TGMDA/DDS « stoechiométrique » ainsi que des systèmes admettant des degrés de polymérisation différents, obtenus en modifiant la composition du mélange initial et/ou en changeant le protocole du traitement thermique.

Dans ce paragraphe, les étapes de la dégradation de ces systèmes sont étudiées par analyse thermogravimétrique. Cette étude préalable permet de définir les domaines de températures dans lesquels des produits de dégradation solides et stables sont obtenus lors d'un traitement thermo-oxydant. Des analyses chimiques et spectroscopiques (absorption dans l'infrarouge, diffusion Raman, diffraction des rayons X, CP/DD-MAS RMN du ^{13}C et DD-MAS RMN du ^{31}P des solides) de ces produits permettent ensuite leur caractérisation. Elle permettra, par ailleurs, de définir les températures auxquelles le dégagement de produits combustibles se produit. En outre, le processus de dégradation par un mécanisme radicalaire sera discuté en considérant les teneurs en radicaux libres piégés dans les matériaux résiduels.

Finalement, le comportement au feu de ces systèmes est discuté en corrélant les résultats de l'étude à ceux d'une étude par calorimétrie de consommation d'oxygène conduite au calorimètre à cône.

I-1-a. Résultats

ETUDE DE LA THERMODEGRADATION DE RESINES TGMDA-DDS EN FONCTION DES CONDITIONS DE POLYMERISATION

Nathalie ROSE(*,**), Bruno COSTE**, Michel LE BRAS* et René DELOBEL*

* Laboratoire de Physicochimie des Solides, E.N.S.C.L. - U.S.T.L.F.A., B. P. 108, F-59652 VILLENEUVE d'ASCQ Cedex

** AEROSPATIALE, Centre Commun de Recherches Louis-Blériot - 12, rue Pasteur, B. P. 76, F-92152 SURESNES Cedex

La règlementation dans le secteur des transports de masse impose l'utilisation de matériaux présentant une bonne stabilité thermique et des propriétés "retard au feu" de plus en plus performantes. Cette exigence accrue vis-à-vis du feu interdit actuellement la plupart des matériaux utilisés dans l'aéronautique.

La dégradation thermique des résines époxydes, nécessaires à la fabrication de pièces structurales allégées utilisées dans l'industrie aéronautique et spatiale, peut être contrôlée et dirigée vers une carbonisation superficielle du matériau. Ce processus assure une "auto-protection" du matériau du fait qu'il se produit avec une absorption importante d'énergie et qu'il conduit à la formation d'un revêtement de surface susceptible de réduire notablement les transferts de chaleur vers le coeur du polymère.

L'optimisation de ce processus auto-protecteur nécessite de comprendre les phénomènes physico-chimiques associés à la thermo-dégradation des résines et, plus particulièrement, l'influence des conditions de leur polymérisation (cycles de cuisson et composition du mélange) **(1)**.

Deux systèmes époxydes du type N, N', N', N' tétraglycidyl-méthylène-dianiline/diamino 4, 4' diphénylsulfone (TGMDA/DDS) sont retenus pour cette étude :

- mélange stoéchiométrique (1 proton amine pour 1 fonction époxyde)
- mélange non stoéchiométrique (0,6 proton amine pour 1 fonction époxyde).

Les dégradations thermiques de ces deux systèmes, effectuées dans des conditions thermo-oxydantes, sont comparées pour différentes conditions de polymérisation.

Les courbes présentées sur la figure 2 sont obtenues par simple soustraction point par point entre les thermogrammes expérimentaux et calculés **(fig. 1)** à partir d'une combinaison linéaire de la perte de masse de chacun des additifs dégradé seul selon la formule (I) suivante :

$\Delta M(TGMDA/DDS)_T =$

$[x\Delta M(TGMDA)_T + y\Delta M(DDS)_T]/x+y$

(x et y : pourcentage massique en TGMDA et DDS).

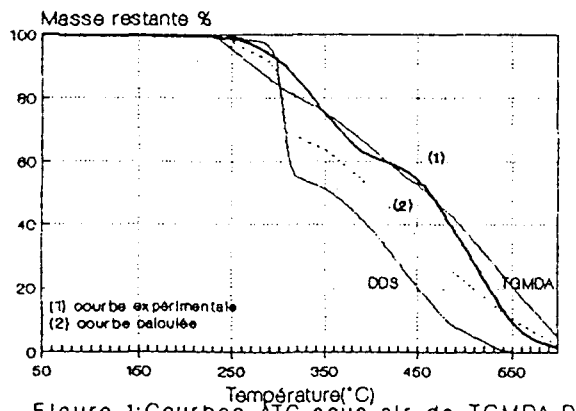

Figure 1:Courbes ATG sous air de TGMDA,DDS, TGMDA/DDS réticulé à 135°C 8h et la courbe calculée d'après la formule (I)

Pour une composition de mélange donnée, les quantités de résidus carbonés formées aux basses températures de traitement (T < 450°C) sont d'autant plus importantes que la température de polymérisation est élevée. Pour les plus hautes températures de traitement, cette caractéristique n'est plus vérifiée mais on observe qu'une post réticulation à 180°C améliore la stabilité thermique **(fig. 2)**.

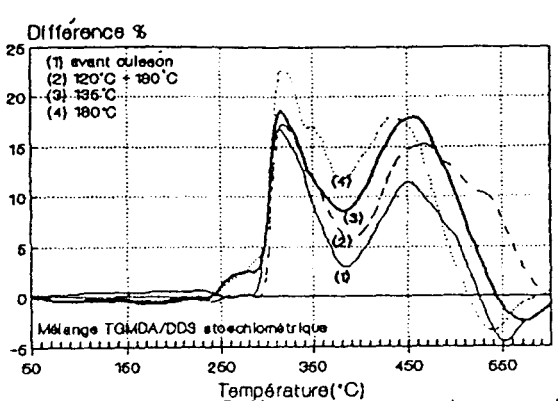

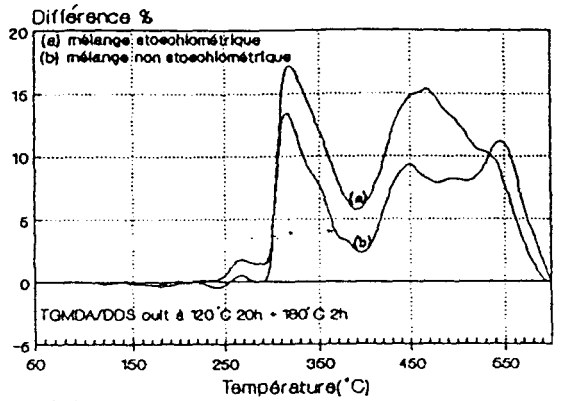

Figures 2 et 3:Différences entre les courbes expérimentales et calculées respectivement pour des températures de polymérisation et stoechiométries de mélange différentes.

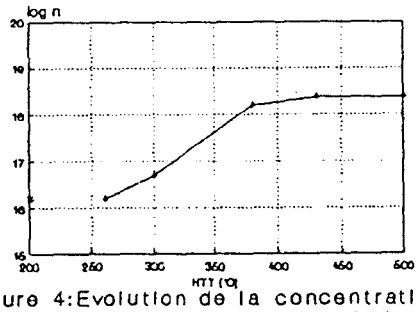

Figure 4:Evolution de la concentration en radicaux 'piégés' en fonction de la plus haute température de traitement (HTT).

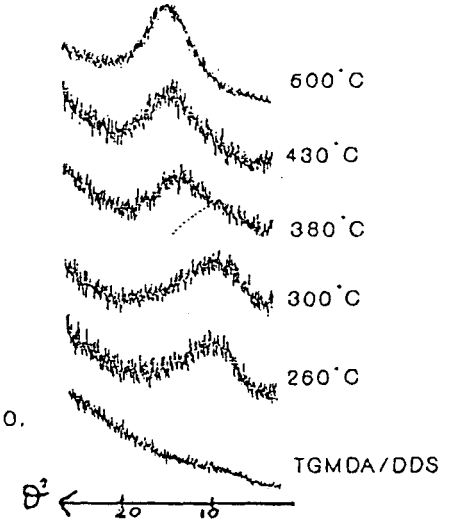

Figure 6:Diffractogramme RX du réticulat TGMDA/DDS et des résidus obtenus à 260, 300,380,430 et 600°C.

De plus, l'étude montre que les mélanges stoéchiométriques présentent une meilleure stabilité thermique que les mélanges non stoéchiométriques **(fig. 3)**.

Quel que soit le système époxyde, l'étude met, par ailleurs, en évidence :

a) aux basse température de dégradation (T < 380°C) :

- un phénomène de déshydratation conduisant à la formation d'une structure stable présentant une certaine orientation structurale **(fig. 5)**.

b) pour les hautes températures (T > 380°C) :

- un processus de carbonisation radicalaire, mis en évidence par R.P.E. **(fig.4)**. La structure carbonée est constituée de couches de polyaromatiques réparties de manière aléatoire dans une phase isotrope **(fig. 5)**.
- le rôle de l'oxygène moléculaire favorable à la stabilité thermique du matériau (2).

En conclusion, l'étude confirme que les conditions de polymérisation ainsi que la stoéchiométrie des mélanges joue un rôle important dans les comportements thermiques des résines.

(1) *B. COSTES - Thèse - Université du Maine.*
(2) *N. ROSE - D.E.A. - Lille I 1991.*

Polymer Degradation and Stability **42** (1993) 307–316

Thermal oxidative degradation of an epoxy resin

Nathalie Rose, Michel Le Bras, René Delobel

Laboratoire de Physiocochimie des Solides, ENSCL, Université des Sciences et Technologies de Lille, BP 108, F-59652 Villeneuve d'Ascq Cedex, France

&

Bruno Costes & Yves Henry

Aérospatiale 12, Rue Pasteur F-92152 Suresnes, France

(Received 2 March 1993; accepted 29 March 1993)

This study of the thermodegradation of the tetraglycidyl diamino diphenyl methane/diaminodiphenylsulfone system (TGDDM/DDS) defines the differents steps of the carbonization process. It characterizes, in particular, the domain of existence of an expanded carbonaceous structure which is constituted of small domains of turbostratic carbon. Moreover, this present work discusses the role of oxygen in the formation of this structure and shows that there is competition between the carbonization process and the oxidative degradation.

INTRODUCTION

Epoxy resins are widely used in the aeronautic industry. They constitute the organic matrix for high performances composite materials with reinforcement fibers, used for fabrication of light structural panels in the interior of aircraft. The analysis of several accidents[1] has shown the total implication of these materials in fire propagation and flash-over phenomena (total flare-up of gases). In all the cases, the concentration of gases and smoke generated involves, if not the death, a partial or total incapacity of occupants limiting their possibility to survive by a rapid evacuation.[2] Then, there is a considerable reinforcement of different regulations (FFA) and these new safety requirements seriously limit the number of materials used in habitable areas. It is necessary to improve the fire resistance of these materials and this requires a better understanding of their degradation.

Among the different epoxy resins, the tetraglycidyl diamino diphenyl methane/diaminodiphenylsulfone (TGDDM/DDS) system has been largely used. Its chemical properties and polymerization reactions are well known.[3]

The present work deals with the thermodegradation process of this epoxy resin TGDDM/DDS (*N*-glycidyle/aromatic amine). The thermal stability was studied by thermogravimetric (TG) analysis under air and inert gas (N_2) flow. The spectroscopic characterizations were carried out by IR, Raman, XRD, EPR, and ^{13}C solid-state NMR.

EXPERIMENTAL

Materials

The tetra epoxy prepolymer TGDDM is a commercial product (Lopox B3302) characterized by a functionality of 3·6 (theoretical 4). The formulation studied in this work contains 52·5 parts of curing agent per hundred parts of resin (phr) which corresponds to a stoichiometric ratio TGDDM/DDS with one epoxy group for each primary amino hydrogen on the DDS.

Polymer Degradation and Stability 0141-3910/93/$06.00

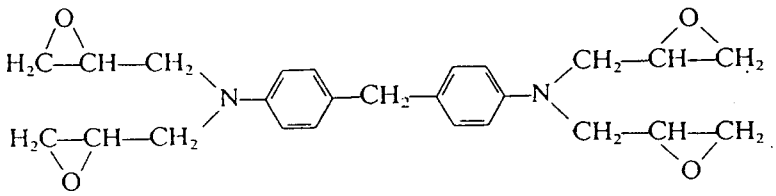

TGDDM (*N,N,N',N'* tetraglycidyl-4,4'diamino diphenyl methane)

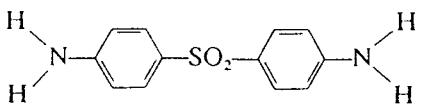

DDS (diamino 4,4' diphenylsulfone)

The TGDDM/DDS mixture was prepared by continuously stirring the curing agent into the resin heated at 100°C until a clear mixture was obtained. The homogeneous mixture was then out gassed at 100°C for 20 min, cooled to room temperature and stored at −20°C in a freezer until use.

Thermoset epoxy resins are processed by cure, i.e. conversion of liquid monomers into a three-dimensional thermoset network via chemical reactions.[3] The first reaction is the attack of a primary amine on an epoxy group on a side chain. This may be followed by two types of cross-linking reactions, intermolecular and intramolecular.

The resin was cured with the following procedure: 1 h at 135°C and a postcure at 180°C for 2 h. The epoxy consumed was around 90%.[3]

The spectroscopic characterizations were restricted to samples resulting from isothermal treatments (6 h under air) at temperatures deduced from TG analysis and noted HTT (higher treatment temperature).

Thermal analysis

Thermogravimetric analyses were carried out with temperature programming (heating rate: 3°C/min) under synthetic air (Air Liquid grade) or under inert gas (N_2, Air Liquid U grade) flows (5×10^{-7} m^3/s) using a Setaram MTB 10–8 microbalance. In each case, the mass was fixed at 20×10^{-6} kg and the samples were positioned in open vitreous silica pans. The precision on the temperature measurement was ±1·5°C in the range 50–650°C.

Spectroscopic analysis

Raman microprobe examination was performed with a Raman microspectrometer having spectrographic dispersion and multichannel detection (Microdil 28- Dilor). An optical beam produced by a continuous wave argon laser enters in a microscope and is directed on to an objective that focuses it to a one-micrometer spot on the sample surface. To avoid sample heating the power was kept below 4 mW. Subsequent visual examination of the surface was systematically made in order to check that no alteration had occurred around the focal point. In a typical experiment, the laser beam wavelength was fixed at 514·5 nm and the value of spectral slit width at 9 cm^{-1}.

^{13}C NMR measurements were performed on a Brucker CXP 100 weak field spectrometer at 25·2 MHz (2·35 T) with magic-angle spinning (MAS), high power ^{1}H decoupling and ^{1}H–^{13}C cross-polarization (CP). The Hartmann–Hahn matching condition was obtained by adjusting the power on the ^{1}H channel for a maximum ^{13}C FID signal of adamantane. All spectra were acquired with a single contact time of 5 ms. A repetition time of 10 s was used for all samples because the spin-lattice relaxation time (T_1) always stayed below 2 s at all temperatures (the repetition delay is chosen five times T_1). Typically 10 000 scans were necessary to obtain spectra with a good signal/noise ratio and the reference used was tetramethylsilane (TMS). All spectra of the solids were obtained at the spinning speed of 3 kHz.

EPR spectra were recorded at 25°C using a Varian 'E line' spectrophotometer. A frequency of $9{\cdot}5 \times 10^9$ Hz (X band), a Klystron modulation of 100 kHz, and a Varian 'strong pitch' standard were used. The scan was recorded on a scale of 40 G during 480 s with a time constant of 0·1 s and a peak-to-peak modulation amplitude fixed at 0·5 G. Saturation measurements were made by determining the peak-to-peak amplitude D of the

first derivative EPR curve as a function of microwave power (BPP plot).[4] The ratio $R_S = (D/P^{1/2})(D_u/P_u^{1/2})$ is equal to 1 in the absence of saturation. In this relation, P is the variable micropower, and P_u and D_u are respectively one power level in the unsaturated regime and the corresponding peak-to-peak amplitude. The concentration of the paramagnetic species was computed by using a method of integration of the signal previously described by Raymond.[5]

IR spectra were recorded in the range 4000–300 cm^{-1} using a Perkin–Elmer 683 instrument connected with a PE 3600 data station. The samples were obtained by powdering in KBr in adequate ratio to obtain transmission values above 15%.

RX patterns were recorded on a Siemens D500 diffractometer with powder patterns (40 KeV, 20 mA, $K\alpha_{1,2}$ of Cu,Ni monochromator).

RESULTS

The thermal stability of the cured epoxy resin TGDDM/DDS was evaluated by thermogravimetric analysis under air. The TG curve and the first derivative curve (DTG) are shown in Fig. 1. The thermal degradation starts from

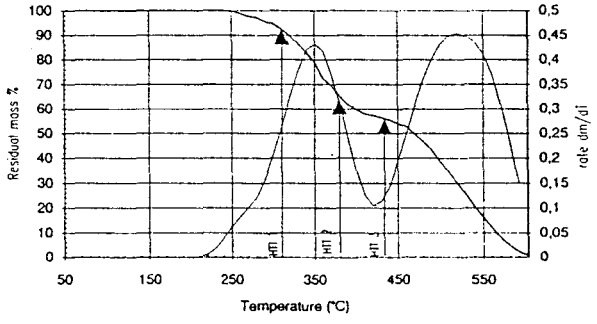

Fig. 1. TG and DTG curves in air of TGDDM/DDS 1/1 cured (arrows indicate the three characteristic temperatures discussed in text).

250°C and the rates of weight loss are maximal at 350 and 520°C. The last step leads to a complete degradation of the material.

To follow the evolution process, the authors have chosen some characteristic temperatures where it is interesting to study the residue formed after an isothermal treatment (6 h).

—310°C permits study of an intermediate product characterizing the first step;
—380°C is characteristic of the second step; and
—430°C represents the last step. This was chosen in order to recover enough solid residue; the residual mass after an isothermal treatment at 430°C, during 6 h, is low: 6% (Table 1).

Some characteristics of these residues are summarized in the Table 1. In particular, it is interesting to note that, for 380°C, there is formation of soot and a swelling and foaming of the material which corresponds to the formation of an intumescent structure.

The residues were first characterized by elemental analysis. Figure 2 presents the changes of the ratios of weight percentages H/C, N/C, O/C and S/C.

After a heat treatment at 310°C, the ratio O/C decreased strongly compared with its initial value. It may be assumed that a dehydratation reaction proposed by numerous authors[6,7] occurs with elimination of two alcohol functions to form an ether bond.

At higher temperatures, above 310°C, S/C and H/C decrease, which may be explained respectively by an evolution of SO_2 and a dehydrogenation process. This last phenomenon may correspond either to a dealkylation of hydrocarbon structures involving the formation of volatiles or to the development of a condensation process which would lead to the formation of polyaromatic structures.

From 310°C, we can also observe an enhancement of the N/C ratio. It may be

Table 1. Description of isothermally heat treated samples

HTT (°C)	Residual mass after isothermal treatment (%)	Soot	Aspect of residue	Swelling and foaming of the material surface
310	74·7	No	Tough and bright; brown powder	No
380	22	Yes	Crumbly; black powder	Yes
430	6·3	Yes	Crumbly; black powder	Yes

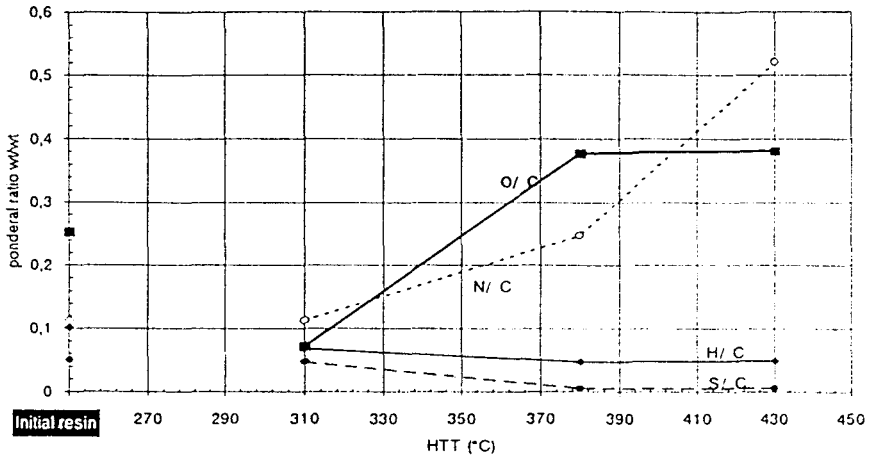

Fig. 2. H/C, O/C, N/C and S/C ratios versus HTT.

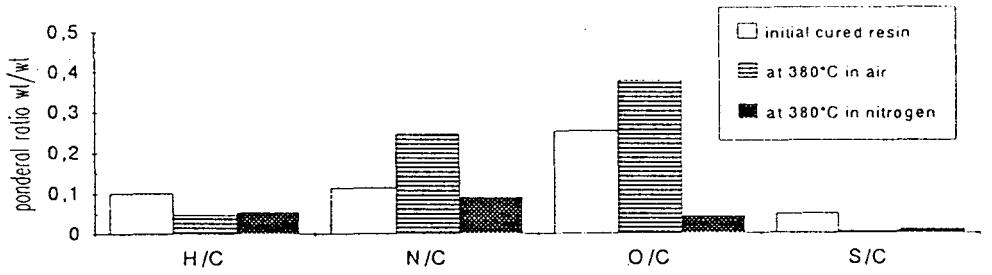

Fig. 3. Elemental analysis of solid residue obtained at 380°C in air and in N_2.

considered that the nitrogen may be implicated in heat resistant cyclized structures more stable than the carbonaceous structures.

The increase of the O/C ratio, above 310°C, may be related to an oxidation process of the polymer chains by molecular oxygen. This result is confirmed by treatment at 380°C in nitrogen atmosphere which leads to a decrease of the ratio O/C (Fig. 3).

For a better understanding of the oxidation phenomenon, we can compare the TG curve of the cured resin obtained under an inert gas (N_2) flow and in air (Fig. 4). The amount of residue between 250 and 520°C is higher in thermo-

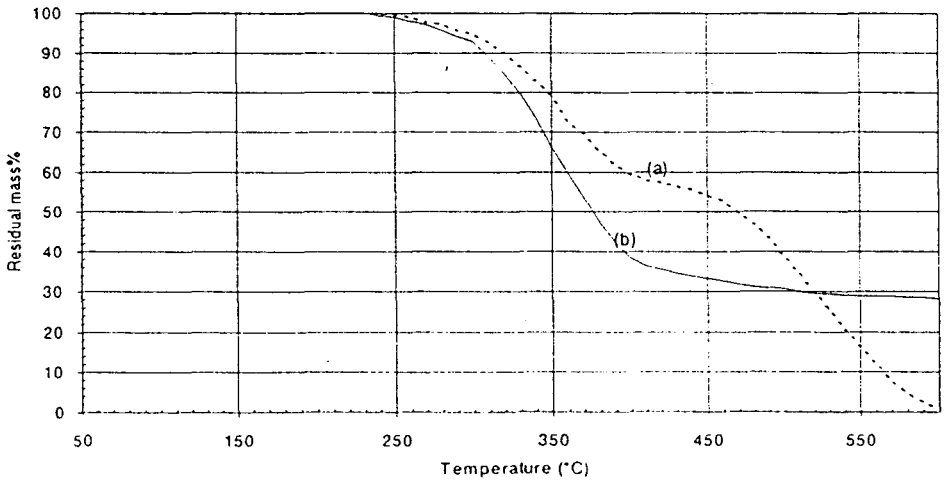

Fig. 4. TG curves of TGDDM/DDS 1/1 in air (a) and in N_2(b).

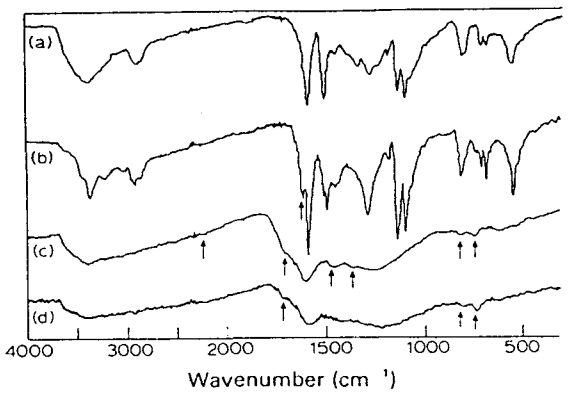

Fig. 5. IR spectra of TGDDM/DDS 1/1 cured (a) and after thermal treatment at 310°C (b), 380°C (c) and 430°C (d).

oxidative conditions than under inert gas. However, at higher temperatures, in air a complete degradation of material occurs, whereas in nitrogen atmosphere the amount of residue remains constant (about 30%).

Thus, it seems that the oxygen permits retention of good thermal properties during the degradation process, but up to 460°C the rate of weight loss increases and the degradation becomes complete.

In order to understand the degradation process, spectroscopic studies have been carried out with samples treated at temperatures previously defined.

Figure 5 compares IR spectra obtained after thermal treatment. The spectrum of the residue obtained at 310°C is unchanged compared with the initial sample, for which the assignments have been previously proposed by Costes.[3] However, between 310 and 380°C significant change is observed and spectra at 380 and 430°C show large absorptions which make the assignments difficult.

Nevertheless, the presence of hydrocarbonaceous species is characterized by absorption bands at 1370 and 1470 cm^{-1} assigned respectively to the deformation mode, symmetric and antisymmetric, of alkyl groups bonded to aromatic cycles.[8,9] Moreover, the presence of polyaromatic species is proved by the absorptions at 830 and 759 cm^{-1} assigned to the deformation mode of the aromatic CH.[10–12] The presence of a band at 1720 cm^{-1} may be assigned to C=O species, and the band at 2240 cm^{-1} indicates the presence of CO_2 adsorbed. Thus, from 380°C there is formation of oxidized products probably formed by a reaction with molecular oxygen.

In conclusion, IR spectroscopy permits us to observe from 380°C both oxidation and the formation of polyaromatic species in the residue.

Raman microspectroscopy has been used to specify the nature of polyaromatic species. The Raman spectrum of a sample treated at 380°C (Fig. 6) exhibits two broad bands around 1580 and 1350 cm^{-1}, which are generally assigned to carbon or carbon precursors. The diffuse band at 1580 cm^{-1} corresponds to the E_{2g} vibrational mode (C—C vibration in the aromatic layers). The band at 1350 cm^{-1} is assigned to A_{1g} vibrational mode and may be related to the structural organization of the carbonaceous material.[13,14]

Lespade *et al.* have studied the Raman spectra of a tar pitch versus their graphitization ratios and proposed the reactional scheme described in Fig. 7.[15,16] We can conclude, in the authors' case, that the residue obtained at 380°C corresponds either to phase I, or to phase II, or to a mixture of these two phases.

These results confirm the beginning of development of a structured carbonaceous material at this temperature.

X-ray diffraction allows us to specify the nature and the size of the carbonaceous structure and to evaluate its structural state. Figure 8 represents diffraction spectra of samples treated respectively at 310, 380 and 430°C. The initial resin shows a broad band at 0–9° that implies a low order in the network. This order is preserved after a treatment at 310°C. For samples treated at 380 430°C, a new broad band appears at around 12° which is assigned to (002) scatterings of turbostratic carbons.[17,18] This structure is made up of polyaromatic species which grow by arranging in parallel layers.[19,20]

Interlayer spacings and crystal sizes of turbostratic carbons are obtained respectively by application of the Bragg and Scherrer equations to the experimental X-ray scattering profile.[20,21] The results are in Table 2.

The interlayer spacing d decreases slightly with temperature which implies a beginning of structural ordering. Moreover, the development of crystal size remains low.

In conclusion, the X-ray diffraction study indicates the formation of small domains of turbostratic carbon in the high temperature residues ($T > 310$°C). This expanded carbonaceous structure is very interesting. Indeed, it could limit the transfer to heat in the material.

To obtain more information about the

Fig. 6. Raman spectrum of resin treated at 380°C in air.

formation of these carbonaceous structures, an electron paramagnetic resonance (EPR) spectroscopic study on the samples has been carried out.

The resonance spectra are characterized by: the spectroscopic splitting factor g, the resonance line shape factor $K = B/A$ (estimated using the slope method[22]) and the free radical concentration n (Fig. 9).

Figures 10–12 present the changes in these parameters with the higher treatment temperature (HTT). The presence of paramagnetic species may be assigned, according to Singer *et al.*,[4] to trapped free radicals, which may result from a charring process of the material.

The value of the splitting factor g for residues obtained is around 2.004 (Fig. 11), which corresponds to the value for a pitch, so this agrees with the hypothesis of such material. Figure 12 shows that the free radical concentration increases until 380°C (about 10^{18} spins g^{-1}).

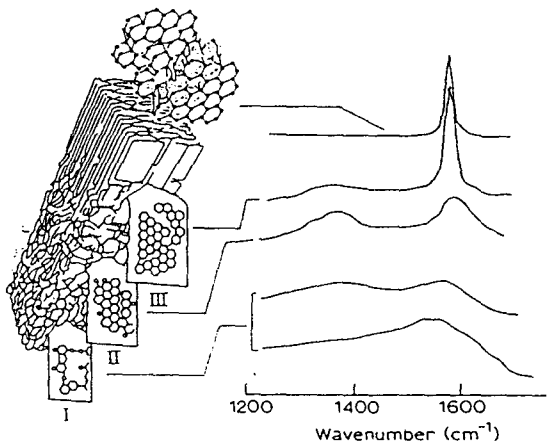

Fig. 7. Change of the Raman spectrum of a tar pitch with graphitization ratio.[15]

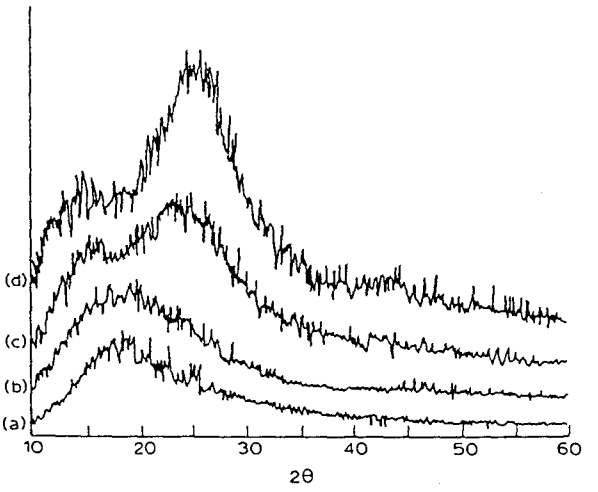

Fig. 8. X-ray diffraction profiles of TGDDM/DDS 1/1 cured (a) and after thermal treatment at 310°C (b), 380°C (c) and 430°C (d).

Table 2. Characteristics of the X-ray diffraction profiles of TGDDM/DDS 1/1 as function of the high temperature of treatment (HTT)

HTT (°C)	Bragg angles θ (°)	Interlayer spacings d002 (Å)	Full at half maximum $\beta_{1/2}$ (in 2θ radians)	Crystal size t (nm)
Initial cured resin	9	4·9	—	—
310	9	4·9	—	—
380	12	3·7	8	1·26
430	13	3·4	6	1·67

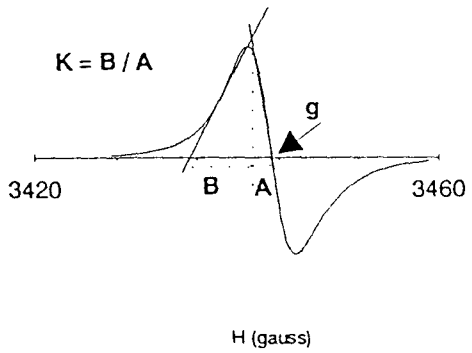

Fig. 9. Schematic of EPR spectra.

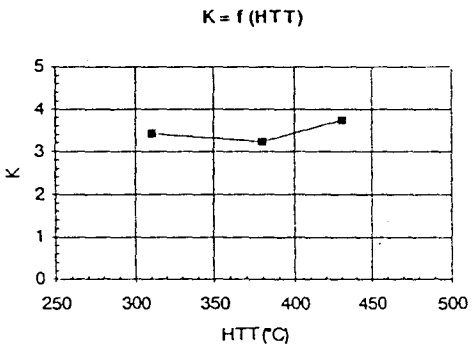

Fig. 10. Variation of the resonance line shape factor K versus HTT.

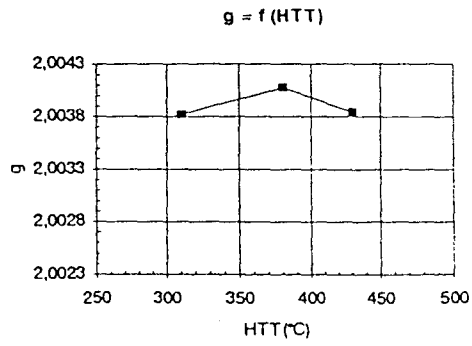

Fig. 11. Variation of the spectroscopic splitting factor g versus HTT.

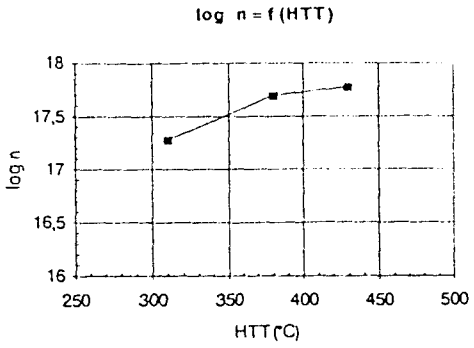

Fig. 12. Variation of the paramagnetic species concentrations versus HTT.

These radicals may be created by the formation of polyaromatic structures or may be associated to the formation of oxidized species. Between 380 and 430°C the concentration of free radicals remains relatively constant, which may imply a competition between the development of a condensation process of polyaromatic species and chain breaking.

Line shapes give information about the types of interactions between a spin system and its environment (Fig. 13).[4] In a simple homogeneous system, the relaxation process is controlled by spin–lattice interactions and the energy absorbed from the radiation field is distributed so that the spin system maintains thermal equilibrium throughout the resonance process. In this case, theory predicts that the line shape should be Lorentzian. On the other hand, in an inhomogeneous spin system, the individual electrons find themselves in different local fields so that resonance does not occur for all the spins simultaneously. The individual relaxations of all these spin systems add up to form a Gaussian signal. For distinguishing Lorentzian or Gaussian shapes, the slope method illustrated in Fig. 9 was used. The ratio of slopes B/A is 4 for a Lorentzian curve and 2 for a Gaussian one (Fig. 13).[4]

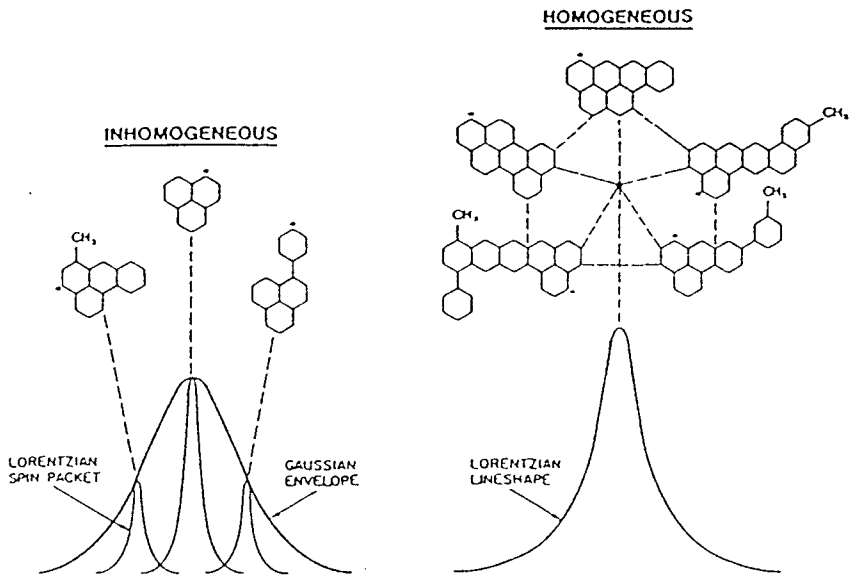

Fig. 13. Depiction of the relationship between molecular structure, molecular interactions, EPR line shapes, and spin relaxation mechanisms.[4]

The observed signals for each heat treated samples are Lorentzian lines characterized by a value of K around 4 (Fig. 10).

This result indicates a mechanism of homogeneous relaxation, so that the spins have identical interactions. It may be proposed that the mechanism of carbonization involves only one main radical species, probably a polyaromatic macromolecule which has trapped a free radical.

This technique allows us to confirm the condensation of polyaromatic structures above 310°C by a carbonization free radical process.

A study by ^{13}C solid-state NMR nuclear magnetic resonance spectroscopy CP/MAS (cross polarization/magic-angle spinning) has been carried out to characterize the chemical groups of the carbonaceous species obtained during the degradation. Figure 14 shows the spectra of the cured resin TGDDM/DDS obtained at the different temperatures. Two ranges are defined: the first between 100 and 150 ppm (characteristic of aromatic carbons) and the other between 30 and 80 ppm (characteristic of mobile side chains of the backbone). The values and the assignments of chemical shifts are listed in Table 3.

The interpretation of the spectra of the initial cured resin (Fig. 14(a)) was made from the literature.[1,23,24] The band at 150 ppm is characteristic of aromatic carbons in amines. The bands at 130 and 114 ppm are respectively assigned to the C3, C4 and C2 aromatic carbons drawn in formula at the top of the figure. The assignments of the large band between 30 and 80 ppm was made by Grenier–Loustalot and Grenier in comparison with the chemical shifts of model compounds[23,24] (Table 3).

When the sample is heat treated at 310°C, the corresponding NMR spectrum changes (Fig. 14(b)). Indeed, a broadening of the band, characteristic of the aromatic carbons, between 150 and 100 ppm is observed. Its maximum is noted at 130 ppm. Moreover, new lines are observed at 20 and 14 ppm which may be assigned to alkyl groups bonded to aromatic rings. This result shows that there is a destruction of the initial network and some breakdown reactions.

For the residues obtained at 380 and 430°C, the spectra present no characteristic bands of aliphatic carbons. The broadness of the 128 ppm line reflects the condensation of the polyaromatic structures. Moreover, a new band at 156 ppm shows the presence of oxygenated aromatic structures, which become more important at 430°C compared with the polyaromatic structures.

In conclusion, this method confirms the degradation mode of the resins. From 310°C, there are scission reactions along the macromolecule chain which lead to the formation of polyaromatic structures and, concurrently, an oxidation process which leads to the formation of

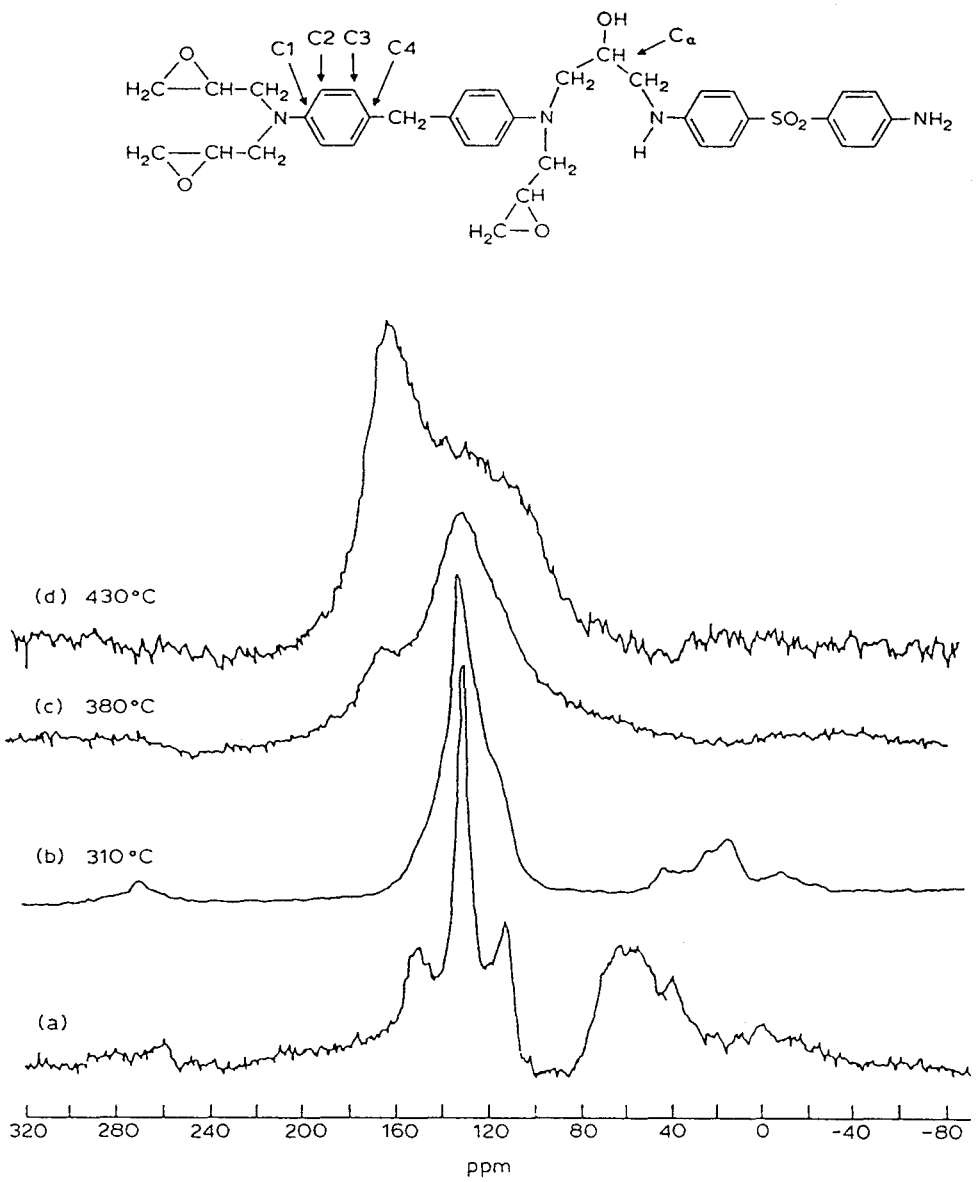

Fig. 14. Characteristics of the ^{13}C MAS.N.M.R. spectra of TGDDM/DDS 1/1 cured (a) and after thermal treatment at 310°C (b), 380°C (c) and 430°C (d).

oxygenated aromatic structures. These last structures are favored when the temperature increases. We can conclude that there is a competition between the carbonization process and the oxidative degradation.

CONCLUSION

Thermal analysis of an epoxy resin TGDDM/DDS shows that, at low treatment temperatures ($T < 310°C$), the mechanism of degradation is identical in air or under inert atmosphere; it corresponds principally to a dehydration reaction.

At higher temperatures ($T > 310°C$), an evolution of SO_2 can be suspected which is a problem in view of toxicology and environmental safety.

Spectroscopic characterization of the residue shows that there is formation of small domains of turbostratic carbon above 310°C. This structure is

Table 3. Assignments of the chemical shifts of ^{13}CCP/MAS NMR spectra of the initial epoxy resin and the residue obtained at 310, 380 and 430°C

HTT (°C)	Chemical shifts (ppm)	Assignments	Refs
Initial cured resin TGDDM/DDS 1/1	150	Aromatic carbon C_1—N	1, 23, 24
	130	Aromatic carbons C_3 and C_4	1, 23, 24
	114	Aromatic carbon C_2	1, 23, 24
	Large band	Methylene between aromatic rings	23, 24
		Alcohol	23, 24
		Ether bonds	23, 24
310°C	129	Aromatic carbons C_3 and C_4	25
	112 (shoulder)	Aromatic carbon C_2	25
	40	Methylene between the aromatic rings	23, 24
	20	Methyl on aromatic rings	26
	14	Alkyl groups	26
380°C	156	Aromatic oxygenated carbon	25
	122	Aromatic carbons C_3 and C_4 and/or polyaromatic	25
430°C	157·7	Aromatic oxygenated carbon	25
	Broad shoulder between 140 and 110	Polyaromatic carbon	25

made up of polyaromatic species lightly organized in parallel layers. There is a beginning of structural ordering.

The results in thermo-oxidative atmosphere show that the oxygen takes part in the degradation and leads to the formation of a material with good thermal properties until 460°C.

REFERENCES

1. Costes, B., Bodu, J. J. & Henry, Y., *Charges Minérales et Organiques fonctionnelles dans les Polymère*. Moffis, Le Mans, France (1992).
2. Kourtides, D. A., Parker, J. A. & Gilwee, W. J., *J. Fire & Flammability*, **6** (1975) 373.
3. Costes, B., Etude structurale du réticulat tetraglycidyl diaminodiphenylmethane (TGMDA) diaminodiphenylsulfone (DDS). Thèse, Le Mans, 1989.
4. Singer, L. S., Lewis, I. C. & Riffle, D. M., *J. Phys. Chem.*, **91** (1987) 2408–2415.
5. Raymond, S. A., *Electron Paramagnetic Resonance*. Wiley–Interscience, New York, 1974, p. 353.
6. Morgan, R. J. & Mones, E. T., *J. Appl. Polym. Sci.*, **33** (1987) 999.
7. Grayson, M. A. & Wolf, C. J., *J. Polym. Sci., Polym. Phys. Ed.*, **22** (8) (1984) 1897.
8. Ouassou, N., Etude d'un nouveau système intumescent 'retard au feu' pyrophosphate diammonique-pentaérythritol. Application au polypropylène. Thèse, Lille, 1991.
9. Camino, G., Martinasso, G., Costa, L. & Gobetto, R., *Poly. Deg. & Stab.*, **28** (1990) 24.
10. Low, M. J. D. & Morterra, C., *Structure and Reactivity of Surface*, ed. C. Morterra, A. Zecchina & G. Costa. Elsevier Science Publishers, Amsterdam, 1989, p. 607.
11. Morterra, G. & Low, M. D., *Carbon*, **21** (3) (1983) 286.
12. Wolf, E. E. & Alfani, F., *Catal. Rev. Sci. Eng.*, **24** (3) (1982) 339.
13. Lespade, P., Sishe, A. L. & Dresselhaus, M. S., *Carbon*, **20** (5) (1982).
14. Nakamizo, N., *Carbon*, **29**(6) (1988) 339.
15. Cottinet, D., Couderc, P., Saint Romain, J. L. & Dhamelincourt, P., *Carbon*, **26**(3) (1988) 339–44.
16. Lespade, P., Marchal, A., Couzi, M. & Cruege, F., *Carbon*, **22**(4/5) (1984) 375.
17. Singer, L.S. Lewis, I. C. & Greinke, R. A., *Mol. Cryst. Liq. Cryst.*, **132** (1986) 65.
18. Tse-Haoko & Ping-Chein Chen, *J. Mater. Sci. Lett.*, **10** (1991) 301.
19. Lausevic, Z. & Marinkovic, S., *Carbon*, **24**(5) (1986) 575.
20. Short, M. A. & Walker, P. L., *Carbon*, **1** (1963) 3.
21. Lemaitre, J. L., Goving-Menon, P. & Delannay, F., *Heterogeneous catalyst, Vol.* 15, ed. F. Delannay., Marcel Dekker, New York, 1984, p. 229.
22. Lewis, I. C. & Singer, S., *Chemistry and Physics of Carbon, 17* ed. P. L. Wather & P. P. Thrower. Marcel Dekker, New York, 1984, pp. 1–88.
23. Grenier-Loustalot, M. F. & Grenier, P., *British Polym. J.*, **22** (1990) 303.
24. Grenier-Loustalot, M. F. & Grenier, P., *Polymer*, **33**(6) (1992).
25. Duncan, T. M. & Douglass, D. C., *Chem. Phys.*, **87** (1984) 339.

I-1-b Discussion du comportement thermique et au feu du système TGMDA/DDS en fonction de sa réticulation initiale

Les comportements au feu sont, dans une norme ISO, directement liés aux données thermogravimétriques des matériaux [62]. Lors de la dégradation sous inerte des résines, la compétition entre deux réactions radicalaires : coupure des macromolécules avec départ de « petites » molécules et cyclisation, conduit à la formation d'un « carbone » stable aux hautes températures en une seule étape entre 230 et 380°C.

La dégradation sous air est très différente. Elle s'effectue en 3 étapes :

- entre 225 et 275°C, les réactions de dégradation concernant les monomères résiduels et le système réticulé (principalement une réaction de déshydratation) se produisent en parallèle. Les courbes de différence de perte de masse montrent que la stabilité du système (la conservation d'un résidu solide), est optimale lorsque le mélange initial des constituants est stoechiométrique et/ou lorsque la réticulation est conduite en une seule étape entre 135 et 180°C sans post-réticulation,
- entre 275 et 400°C, la dégradation conduit à l'émission de dioxyde de soufre et à la formation de «carbone » turbostratique (polyaromatiques organisés en couches parallèles) stable jusque 460°C. Ce carbone superficiel peut induire une protection du matériau dans les conditions d'un incendie. Cette étape est peu affectée par le degré de la réticulation.
- aux températures supérieures, la dégradation oxydante du « carbone » se produit. La stabilité thermique de ce matériau est classiquement optimale lorsque le rendement de réticulation est maximal suite à la procédure de réticulation de la résine. Elle est aussi liée aux faibles teneurs en DDS des mélanges TGMDA/DDS initiaux. Ce dernier résultat peut être expliqué par le caractère fortement exothermique de la dégradation de l'agent durcisseur aux températures supérieures à 330°C [59, 61].

Le matériau carboné est formé par une réaction radicalaire mise en évidence par la présence de radicaux libres piégés dans des structures carbonées [63,64], en fait des radicaux π dans lesquels l'électron célibataire est délocalisé dans

l'ensemble des noyaux des structures polyaromatiques [65]. Ces radicaux peuvent participer à la stabilité du matériau au feu, leur rôle sera discuté dans le chapitre III de ce Mémoire.

L'oxygène moléculaire participe, par ailleurs, à la formation du matériau carboné expansé en favorisant la conservation de l'«hétéro»élément N et en permettant l'élimination des groupements sulfone dans la structure polyaromatique, stable jusque 460°C. Un effet de cette participation est l'augmentation de la stabilité pondérale jusque environ 500°C.

Les données obtenues en étudiant le comportement des résines sous un flux de chaleur (au calorimètre à cône) en utilisant la calorimétrie par consommation d'oxygène permet une première approche qualitative et quantitative des phénomènes liés au feu (dégradation, inflammation, combustion, fumée...). La simple connaissance de la déplétion en oxygène provoquée par la combustion des matériaux permet de calculer le débit calorifique q' (flux de chaleur relâchée) et le flux calorifique rhr (« rate of heat release »). En effet, pour la plupart des matériaux combustibles, la quantité de chaleur libérée rapportée à la masse d'oxygène est une constante [66].

Le rhr s'exprime : $$rhr = \frac{E(m'^{\circ}_{O_2} - m'_{O_2})}{S}$$

avec $q' = E(m'^{\circ}_{O_2} - m'_{O_2})$ ($m'^{\circ}_{O_2}$ = flux massique d'oxygène dans les conditions ambiantes et m'_{O_2} = flux massique d'oxygène dans les produits de combustion)

S : surface totale de la face exposée de l'échantillon

et $E = \frac{\Delta H_c}{r_o} = 13{,}1 \times 10^3 \text{ kJ/kg}$ (r_o = masse oxygène / masse combustible et ΔH_C la chaleur de combustion) [67].

Les valeurs du rhr permettent d'estimer l'importance du feu, la vitesse de son développement et le temps nécessaire à son extinction [68]. Les courbes des valeurs du rhr en fonction du temps permettent d'accéder à la chaleur totale émise

pendant un temps donné t.h.e. (« total heat evolved ») :

$$t.h.e.(t) = \int_0^t r.h.r.(t)dt\ .$$

paramètre particulièrement intéressant pris en compte dans la norme aéronautique de la FAA [69].

Le calorimètre à cône a l'avantage de pouvoir simuler le comportement d'un matériau dans les conditions "quasi réelles" d'un incendie et permet d'obtenir différentes variables physico-chimiques déterminantes dans la compréhension des mécanismes de propagation de flamme. Nous rapportons les résultats d'une étude effectuée sous une irradiance de 50 kW/m2 qui simule un incendie dans un local ventilé dans un mode d'auto-inflammation (alors que des irradiances supérieures simulent une ignition dans un « flash over », embrasement généralisé impliquant la totalité de la charge combustible du local [57]).

Les figures I-1 et I-2 présentent les courbes du rhr et du t.h.e. de TGMDA/DDS « stoechiométrique » en fonction du cycle de cuisson des réticulats. Les courbes du rhr présentent deux augmentations successives qui conduisent au maximum. Les recuits conduisent à des valeurs du maximum de rhr plus faibles (respectivement 1400 kW x m^2 et environ 900kW x m^2 sans et avec recuit), induisent un retard (environ 20 s) pour l'émission de chaleur. En outre, le recuit à 180°C conduit à des valeurs optimales du t.h.e au bout de 150 s.

Les courbes du rhr et du t.h.e. des réticulats (réticulés selon la procédure standard) en fonction de leurs compositions (figures I-3 et I-4) montrent qu'un excès de TGMDA entraîne une diminution du temps nécessaire pour l'émission de chaleur et des valeurs optimales du rhr alors qu'un mélange stoechiométrique conduit au t.h.e. maximum.

Cette étude permet de proposer une formulation des résines TGMDA/DDS FR avec un excès de durcisseur et avec une post réticulation à T ≥ 185°C. Par contre, une corrélation phénoménologique entre les courbes TG et les données calorimétriques est, dans cette étape de la discussion, difficile. A titre d'exemples, les relations observées : stabilité optimale du matériau carboné - teneur faible en

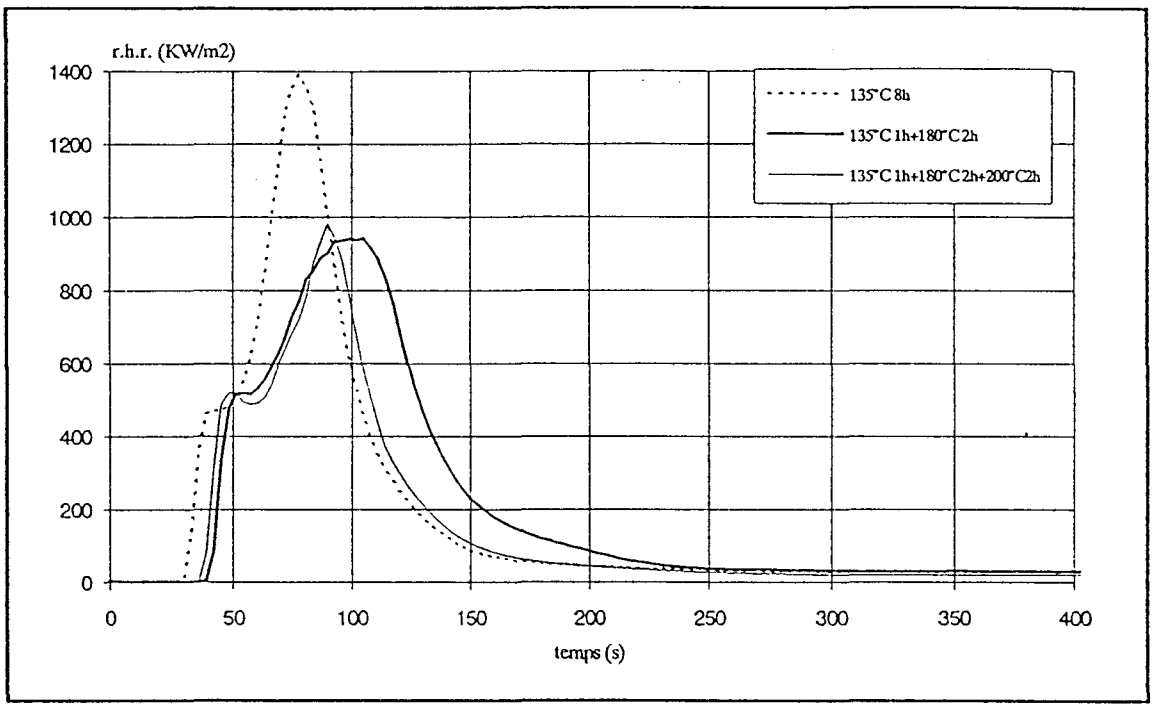

Figure I-1 rhr des réticulats TGMDA/DDS (TGMDA : DDS = 1) fonction du cycle de cuisson.

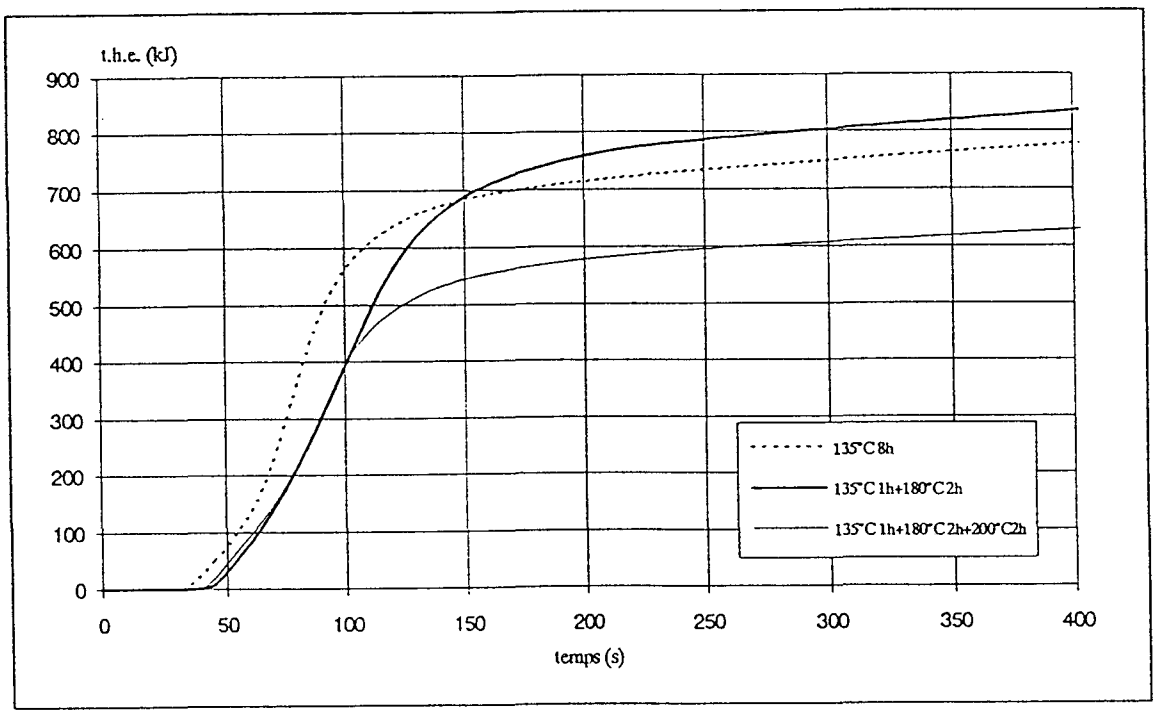

Figure I-2 t.h.e. des réticulats TGMDA/DDS (TGMDA : DDS = 1) fonction du cycle de cuisson.

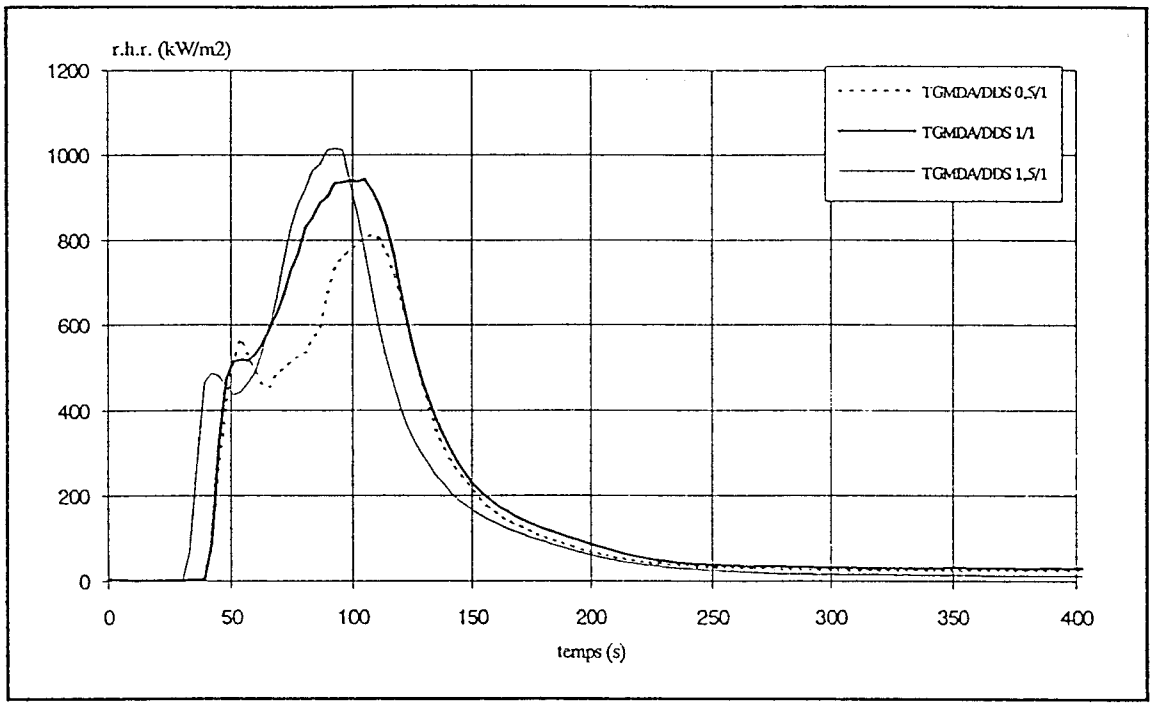

Figure I-3 rhr des réticulats TGMDA/DDS (après recuit à 185°C) fonction de leur composition.

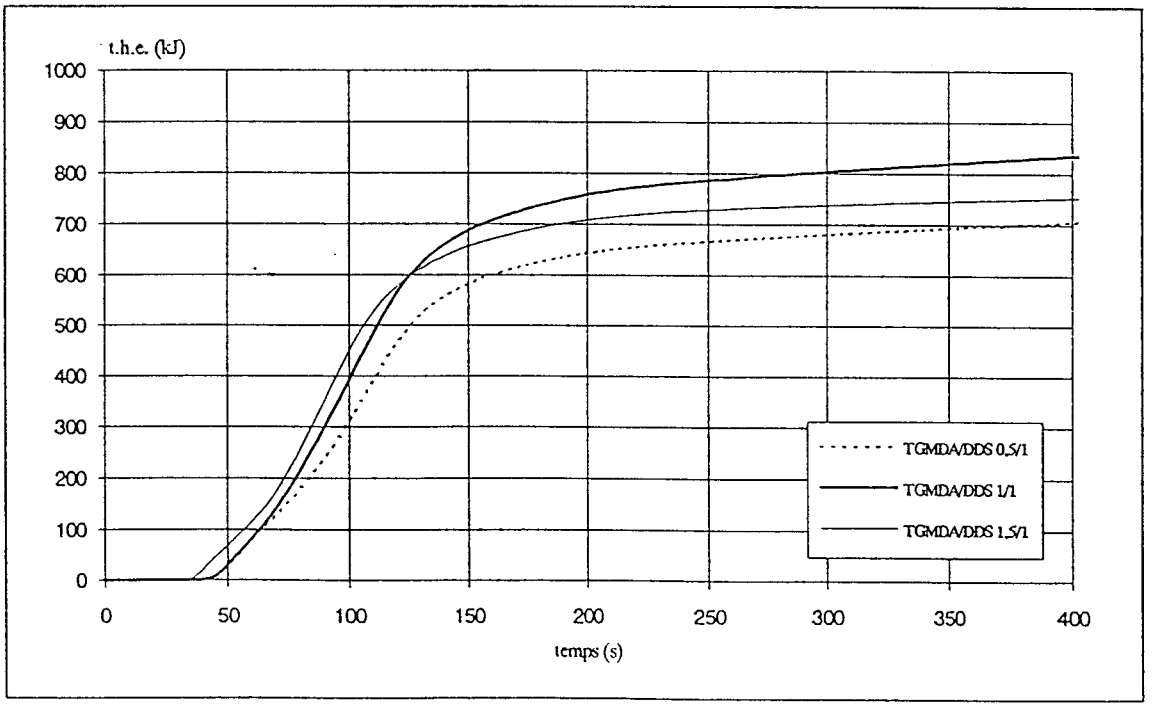

Figure I-4 t.h.e. des réticulats TGMDA/DDS (après recuit à 185°C) fonction de leur composition.

DDS et valeur maximale du rhr - excès de TGMDA, semblent contradictoires. Il est donc nécessaire de compléter l'étude en considérant la contribution au feu des formulations (compositions des volatils combustibles et inertes, incandescence, opacité des fumées).

Le calorimètre à cône permet de suivre en temps réel la perte de masse des échantillons avant l'inflammation, pendant la combustion et après l'extinction. Les données cinétiques de la dégradation sont donc disponibles. Pour obtenir des informations supplémentaires, il s'avère nécessaire de modéliser la relation vitesse de dégradation - température dans les conditions de l'incendie.

I-2 *Comparaison de la stabilité des deux résines modèles lors de leur dégradation thermo-oxydante*

La prédiction et la détermination de relations entre les propriétés FR et les données de l'analyse thermogravimétrique des résines paraissent complexes. Notre étude préalable du système TGMDA/DDS montre que l'étape de la dégradation qui conduit à la formation du « carbone » expansé protecteur et à la production des petites molécules susceptibles de participer à une flamme, provient en fait d'au moins deux processus parallèles.

Le premier processus correspond à la séquence dévitrification/ « revitrification », en fait à la déshydratation du maillon -NH-CH_2-CHOH- du réseau du polymère [70] avec formation de liaisons éthyléniques et réorganisation de la structure. Le second processus peut correspondre aux dégradations conjointes de la résine initiale résiduelle et de cette nouvelle résine. Il est probable que deux modes de dégradation (thermique et thermo-oxydante) se produisent parallèlement.

La dégradation thermique correspond à une rupture de la chaîne polymère [71, 72]. Elle se propage par formation de radicaux libres ou migration de l'hydrogène [73] avec formation de petites molécules et d'éthyléniques. Le mécanisme radicalaire, induit par cette étape, permet la carbonisation du matériau (formation d'espèces aromatiques puis polymérisation en structures

polyaromatiques), comme le prouve les teneurs en radicaux libres piégés (de l'ordre de 10^{22} spins/kg).

Le processus de la dégradation thermo-oxydante joue un rôle important dans la dégradation de la résine. Il est bien connu que les polymères absorbent l'oxygène de l'air. Une oxydation superficielle conduit alors une fissuration de la surface [74, 75]. L'effet combiné de la chaleur et de l'oxygène induit ensuite des réactions auto-oxydantes en chaînes dont le mécanisme implique la formation et la décomposition d'espèces hydroperoxydes. Ces réactions conduisent à la formation de produits oxydés gazeux combustibles (alcools, acides carboxyliques et esters).

Les matériaux auto-carbonisants peuvent présenter une dégradation plus complexe décrite par le modèle de Calcraft et Maries [76, 77]. Le matériau carbonisé superficiel conduit à des produits de dégradation très différents. La répartition de ces produits dépend en fait de la vitesse de diffusion de l'oxygène moléculaire dans le carbone superficiel [78].

La réaction de dégradation des résines est donc un phénomène complexe. Les données cinétiques relatives à ce phénomène ne permettent pas de rendre compte de la totalité de ces étapes et l'ordre des réactions n'est jamais parfaitement intégré. Elles permettent seulement une évaluation de l'aptitude à se dégrader et un classement en terme de stabilité thermique.

La dépendance d'une réaction avec la température est décrite par une loi d'Arrhénius et, de ce fait, l'énergie d'activation peut être utilisée comme un facteur de choix d'une résine. La difficulté pour déterminer les paramètres cinétiques à partir des données d'une analyse thermogravimétriques (ATG) non isotherme est discutée dans le présent paragraphe. La méthode IKP est utilisée pour calculer les paramètres cinétiques invariants (caractéristiques réelles du système, indépendantes des conditions expérimentales de la dégradation) et la répartition la plus probable des fonctions de dégradation. Cette méthode nous a préalablement permis de mettre en évidence une relation entre propriétés FR et vitesses de dégradation de systèmes intumescents [79] et de modéliser les dégradations thermiques de mélanges de fibres naturelles et synthétiques à usage textile [80, 81].

L'étude des systèmes DGMDA/DDS et DGMDA/DDA est conduite dans le domaine de température 250-350°C, où se produit le départ des gaz combustibles et où la dégradation du matériau carboné peut être négligée.

I-2-a. Résultats de l'étude cinétique

Polymer Degradation and Stability 45 (1994) 387–397

0141-3910/94/$07.00

Thermal oxidative degradation of epoxy resins: evaluation of their heat resistance using invariant kinetic parameters

Nathalie Rose,* Michel Le Bras, Serge Bourbigot & René Delobel

Laboratoire de physicochimie des Solides, E.N.S.C.L., Université des Sciences et Technologies de Lille, BP 108, F-59652 Villeneuve d'Ascq Cedex, France

(Received 13 April 1994; accepted 29 April 1994)

The thermal degradation of two epoxy resins was studied using a non-isothermal thermogravimetric technique. This work applies the invariant kinetic parameter (IKP) method in order to describe the degradation of the resins. The kinetic parameters (pre-exponential factor and activation energy) are independent of the experimental conditions and are computed without any hypothesis on the form of the kinetic degradation function. Moreover, the method allows us to compute the distribution of the probabilities associated to kinetic functions and to predict the degradation mode of the material.

The kinetic model which best describes the decomposition of epoxy resins is that corresponding to a diffusion mechanism. Invariant activation energies of the degradations of TGDDM/DDS and TGDDM/DDA systems allows the comparison of their heat resistances in air and shows that the resin cured using the aromatic diamine is the more stable.

NOTATION

A_{jv}	Apparent pre-exponential factor calculated with $f_j(\alpha)$ and with the TG curve plotted at β_v.
B_v & I_v	Parameter deduced of the linear relationship of the compensation effect at β_v.
$\left(\frac{d\alpha}{dT}\right)_{iv}$	Value of the derivative curve at the point α_{iv}.
E_{jv}	Apparent activation energy calculated with $f_j(\alpha)$ and with the TG curve plotted at β_v.
F_j	$F_j = \frac{\bar{S}_j^2}{\bar{S}_{j\,min}^2}$
$f_j(\alpha)$	jth kinetic function among the 18 functions used.
k_v & T_v	Invariant rate constant of the system at the temperature T_v (deduced from the compensation effect).
P_j	Probability associated with a given $f_j(\alpha)$.
p	Number of heating rates.
$q(F_j)$	F-distribution.
$\bar{S}_j^2$	Average on v of all S_{jv}^2.
$\bar{S}_{jmin}^2$	Minimum average of $\bar{S}_j^2$.
S_{jv}^2	Residual sum of squares for each $f_j(\alpha)$.
T_{iv}	Temperature associated at α_{iv}.
α_{iv}	Degree of conversion of the ith experimental point extracted of the thermogram plotted at β_v.
β_v	Heating rates.
Γ	Gamma function.
v	Degree of freedom.

INTRODUCTION

Epoxy resins are widely used in the aircraft industry. They constitute the organic matrix for high performance composite materials with reinforcement fibres used in fabrication of light structural panels in the interior of aircraft. The analysis of several accidents[1] has shown the total

implication of these materials in fire propagation and flash-over phenomenon (total flare-up of gases). Thus, there has been considerable reinforcement of different regulations (FAA) and these new safety requirements seriously limit the number of materials used in passenger areas. Thus, it is necessary to improve the fire resistance of these materials, which involves an understanding of their degradation, insofar as the flammability of polymers is the result of thermal degradation phenomena which take place when these materials are exposed to a heat flux.

A previous study[2] allowed us to define different chemical steps of the degradation process of an epoxy resin (TGDDM/DDS; *N*-glycidyl/aromatic amine). The first step, assigned to a dehydration process,[2,3] leads to the formation of a carbonaceous material which is the result of the chemical change of the resin network.[2,4] This carbonaceous material is the precursor for the formation of a polyaromatic structure.[2] The study characterizes, in particular, the existence of a domain of an expanded carbonaceous structure. This structure, formed of polyaromatic species lightly organized in parallel layers, may be responsible for the eventual heat resistance of the material.

The first step of the thermo-oxidative degradation of the resins has been previously described by several different processes: a surface oxidation[5] with an eventual development of cracks,[6] an initial thermal deterioration via the exothermic reaction of residual epoxy groups[7] or an oxidative breakdown in the polymer network at the amino alcohol portion of the cured resin backbone (dehydration process dependent on the nature of the curing agent).[8]

Kinetic data obtained from TG analyses may be used as criteria for the choice of a resin. The determination of kinetic parameters from data from non-isothermal thermogravimetry is one of the most difficult kinetic problems. The diversity of the calculation methods does not allow us to give preference to any one of them. Nevertheless, different methods of calculation of the kinetic parameters may lead to different results. As a typical example, the activation energy for a diglycidyl ether of bisphenol A (DGEBA)-type polymer cured with polyamine has been quoted in the literature in the 43–138 kJ mol^{-1} range.[9,10]

The present work uses a method developed by Lesnikovich *et al.*[11] to compute invariant kinetic parameters. These latters are independent of the experimental conditions and they are computed without making any hypothesis on the form of the kinetic degradation function. So, the values obtained are no longer apparent but real characteristics of the system studied. Moreover, the present method allows us to compute the distribution of probabilities associated to kinetic functions and then to obtain the degradation mode of the material[12] (the IKP method is reported in an Appendix to this paper).

There are several different types of epoxy resins which may be cured with a variety of hardeners such as aliphatic and aromatic diamines, acid anhydrides, and dicarboxylic acids. It is therefore possible to formulate a very large number of resin structures with thermal stabilities which depend on the particular epoxide/hardener combinations. The present work compares the thermodegradation of two epoxy resins TGDDM/DDS (*N*-glycidyl/aromatic amine) and TGDDM/DDA (*N*-glycidyl/dicyandiamide). The IKP method is applied using TG data in the temperature range which corresponds to the first step of the degradation of the resins, assigned to the dehydration, which leads to the formation of a carbonaceous material. The aim of this paper is the study of the eventual influence of the composition of the hardener (curing agent) on the heat behaviour of the epoxy resins in air.

EXPERIMENTAL

Materials

The tetra-epoxy prepolymer TGDDM is a commercial product (Lopox B3302) characterized by a functionality of 3·6 (theoretically 4). Two hardeners were used: an aromatic diamine (DDS) and dicyandiamide (DDA).

The formulations studied in this work (TGDDM/DDS and TGDDM/DDA) contain a percentage of curing agent which corresponds to the stoichiometric ratio TGDDM/hardener, i.e. one epoxy group for each primary amino hydrogen of the hardener.

The mixture was prepared by continuously stirring the curing agent into the resin heated at 100°C until a clear mixture was obtained. The homogeneous mixture was then outgassed at 100°C for 20 min, cooled to room temperature and stored at −20°C in a freezer until use.

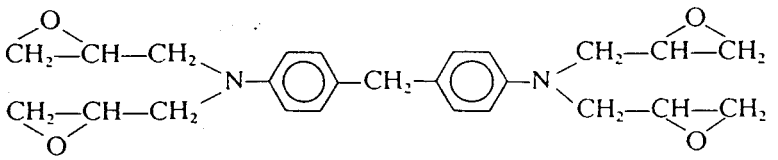

TGDDM(*N,N,N',N'* tetraglycidyl-4,4'diamino diphenyl methane)

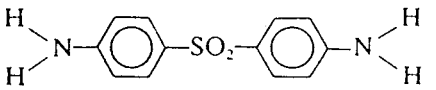

DDS (diamino 4,4' diphenylsulfone)

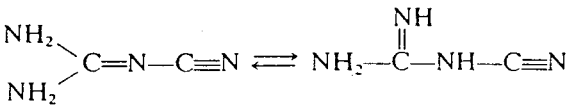

tautomeric forms
DDA (dicyandiamide)

Thermoset epoxy resins are then processed by cure, i.e. conversion of liquid monomers into a three-dimensional thermoset network via chemical reactions.[13,14]

For the TGDDM/DDS system, the first reaction is the attack of a primary amine on an epoxy group on a side chain leading to chain lengthening by successive polyaddition. This may be followed by two types of crosslinking reactions (intermolecular and intramolecular reactions). The resin TGDDM/DDS was cured with the following procedure: 1 h at 135°C and a postcure at 180°C for 2 h. The percentage epoxy group consumed is around 90%.[13]

For the TGDDM/DDA system, taking into account that dicyandiamide has two tautomers, the cure may involve several simultaneous reactions: NH/epoxy additions, cyano/epoxy addition and elimination/cyclisation reactions.[14,15] The resin TGDDM/DDA was cured for 8 h at 135°C; the postcure at 180°C for 2 h cannot be realized because of the exothermicity of this reaction.

Thermal analysis

Thermogravimetric analyses were carried out at several heating rates (β_v: 4·4, 7·7, 10·4 and 12·9°C/min) under synthetic air flow (Air Liquid grade; 5×10^{-7} Nm^3/s) using a Setaram MTB 10-8 microbalance. In each case, the mass of the pellet used was fixed at $15 \cdot 10^{-6}$ kg and the samples were positioned in open vitreous silica pans. The precision on the temperature measurement was ±1·5°C in the range 20–650°C.

The computation of the invariant kinetic parameters and of the probabilities for the degradation functions was carried out from TG curves using a software developed in this Laboratory.[16] In the IKP method, several functions given in the literature[17] (18 functions $f_j(\alpha)$ reported in Table 1) are used.

RESULTS AND DISCUSSION

The different thermograms are shown in Figs 1 and 2. The primary derivatives of TG curves show two significant changes in their slopes which may be assigned to two successive stages of the decomposition of the systems. A previous chemical study has shown that the first step (up to 400°C) mainly involves dehydration of the material and formation of a polyaromatic structure. This structure consists of small domains of turbostratic carbon weakly organized in parallel layers. The second stage corresponds to a thermo-oxidative reaction which leads to the complete degradation of the carbonaceous materials.

A classification of the resistance of the resins to heat and/or to oxidation using the experimental TG curves is quite difficult. Indeed, in all experimental conditions, the degradation of the resins seems to begin at the same temperature (about 240°C). Moreover, the chemical behaviour

Table 1. Kinetic models used in the IKP method

Kinetic models	$f_i(\alpha)$	$g_i(\alpha)$	
Nucleation and nucleus growing	$\frac{1}{n}(1-\alpha)(-\ln(1-\alpha))^{1-n}$	$(-\ln(1-\alpha))^n$	S1 – $n=\frac{1}{4}$ S2 – $n=\frac{1}{3}$ S3 – $n=\frac{1}{2}$ S4 – $n=\frac{2}{3}$ S5 – $n=1$
Phase boundary reaction	$(1-\alpha)^n$	$1-(1-\alpha)$ $1-(1-\alpha)^{1/2}$ $1-(1-\alpha)^{1/3}$	S6—Plane symmetry S7—Cylindrical symmetry S8—Spherical symmetry
Diffusion	α^{-1} $(-\ln(1-\alpha))^{-1}$ $((1-\alpha)^{-1/3}-1)^{-1}$	α^2 $(1-\alpha)\ln(1-\alpha)+\alpha$ $\frac{3}{2}(1-2/3\alpha-(1-\alpha)^{2/3})$	S9—Plane symmetry S10—Cylindrical symmetry S11—Spherical symmetry
Potential law	$\frac{1}{n}\alpha^{1-n}$	$\alpha^n(0<n<2)$	S12 – $n=\frac{1}{4}$ S13 – $n=\frac{1}{3}$ S14 – $n=\frac{1}{2}$ S17 – $n=\frac{2}{3}$ S18 – $n=\frac{3}{4}$
Reaction order	$\frac{1}{n}(1-\alpha)^{1-n}$	$-(1-\alpha)^2$ $-(1-\alpha)^3$	S15—order 2 S16—order 3

of the resins during the first stage of their degradation seems to be different depending on the curing agents and/or the heating rates. The first step of the degradation of the TGDDM/DDA system may be explained by one chemical reaction with only one maximum in the rate of weight loss (at about 350°C) which seems to be independent of the heating rate. On the other hand, the behaviour of the TGDDM/DDS system during the first stage of the degradation changes with the heating rate. Using low heating rates, a one-step process is observed with a maximum of the weight loss rate observed at about 370°C. In contrast, with comparatively high heating rates ($\beta_v > 7{\cdot}7$°C/mn), this degradation process seems to be more complex with at least

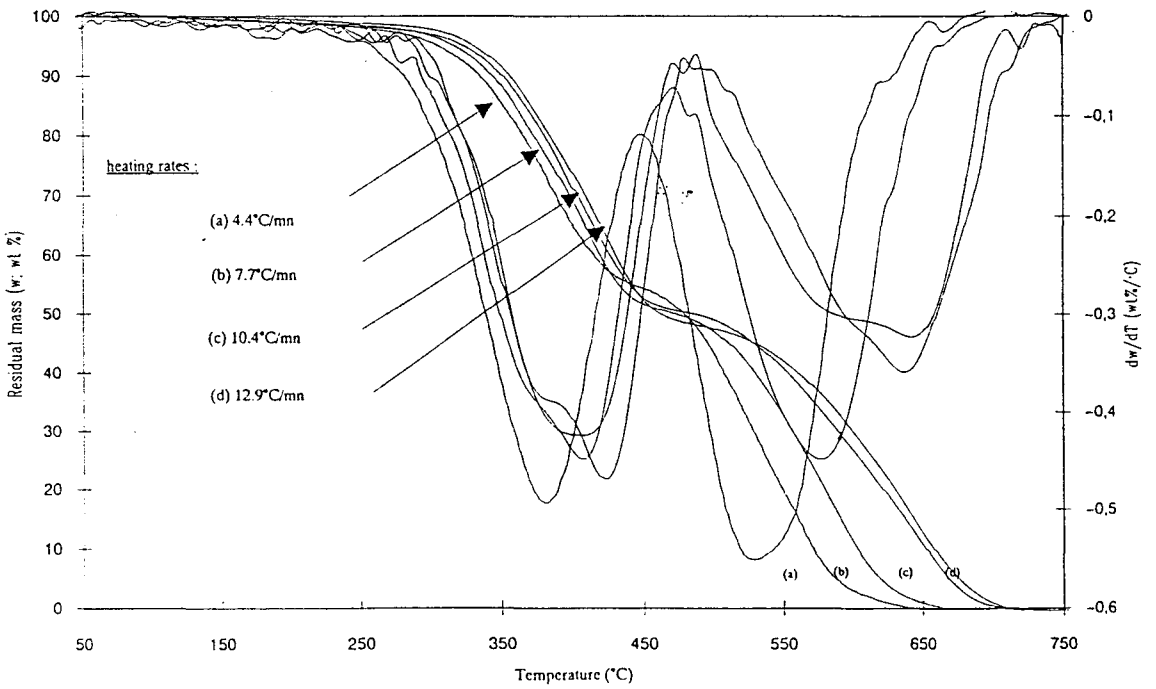

Fig. 1. TG and DTG curves of the TGDDM/DDS epoxy system versus heating rates.

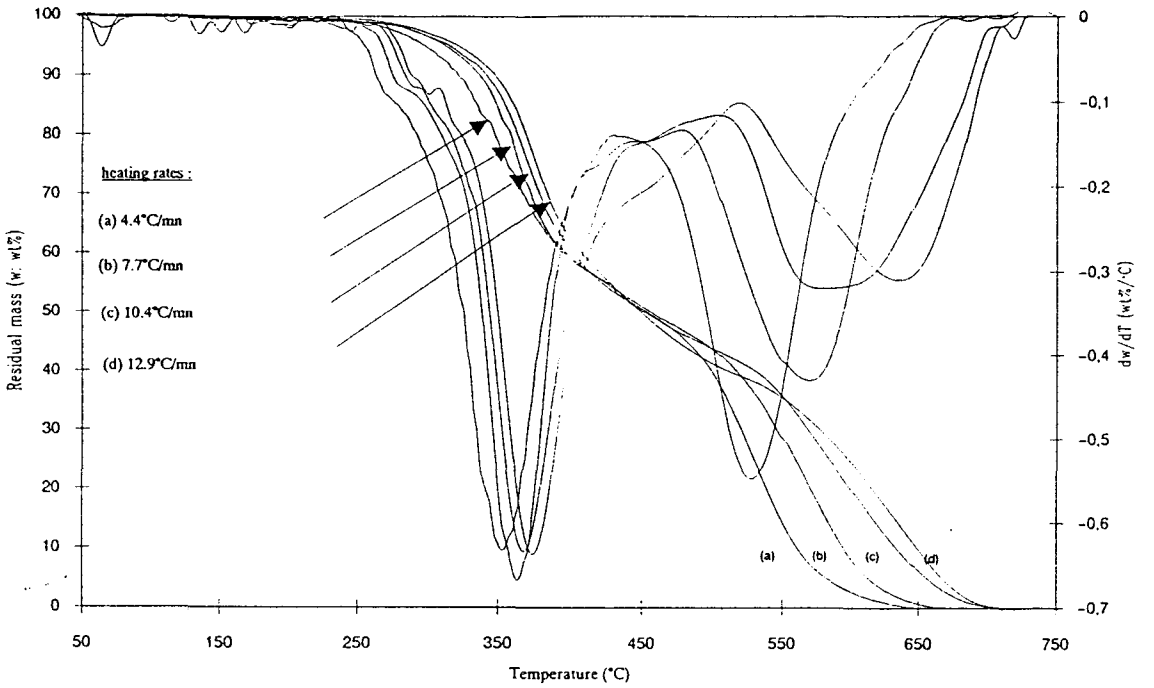

Fig. 2. TG and DTG curves of the TGDDM/DDA epoxy system versus heating rates.

two maxima of the rate of weight loss at about 375 and 420°C.

The thermal decomposition of a solid, in a heterogeneous process accompanied by release of gaseous products, is usually characterized by several mechanisms (nucleation, one- two- or three-dimensioned diffusion) and consequently by several forms of the function $f(\alpha)$. Thus it is helpful not to have to hypothesise one function $f(\alpha)$ rather than another one. The IKP method allows such a theoretical approach.

This method has been carried out for the two epoxy systems using TG data collected in the temperature range 200–400°C which corresponds to the first stage of the degradation of the materials. For each epoxy system, 18 couples (A_{jv}, E_{jv}) per heating rate βv are obtained, versus the kinetic functions $f_j(\alpha)$ used in the computation. These parameters (Tables 2 and 3) are only apparent data of the degradation process.

It is shown by plotting $\log A_j$ versus E_j that the compensation effect is observed for each heating rate (Figs 3 and 4). Indeed, the relation:

$$\log A_{jv} = B_v + l_v E_{jv}$$

with

$$B_v = \log(k_v)$$

and

$$l_v = \frac{1}{2{\cdot}3\,R\,T_v}$$

is always found. The values of B_v and l_v (Table 4) are then calculated from the slopes and the intercepts of the straight lines obtained. The curves $\log k_v = f(1/T_v)$ in Fig. 5 are straight lines, so the Arrhenius law

$$\log k_v = \log A_{inv} - \frac{E_{inv}}{2{\cdot}3\,R\,T_v}$$

is followed. Consequently, the values of the invariant activation and the invariant pre-exponential factor presented in Table 5 are calculated from the curves.

Moreover, Fig. 5 shows that, in the temperature range where the first step of the degradation of the epoxy resins occurs, the degradation rate of the TGDDM/DDA system is always higher than that of the TGDDM/DDS resin. In particular, this trend implies that the first step of the degradation of the resin cured with DDA takes place at a temperature lower than that of the degradation of the resin cured using DDS. The comparison of the values of the invariant activation energies leads us, in another sense, to

Table 2. Apparent kinetic parameters of the TGDDM/DDS system obtained for each kinetic function versus the heating rates

Heating rate	4·4°C/mn		7·7°C/mn		10·4°C/mn		12·9°C/mn	
Function	log A (A:s^{-1})	E (kJ/mol)	log A (A:s^{-1})	E (kJ/mol)	log A (A:s^{-1})	E (kJ/mol)	log A (A:s^{-1})	E (kJ/mol)
S1	−3·31	7·09	−2·70	10·01	−2·61	9·82	−2·20	12·62
S2	−2·62	12·69	−1·96	16·69	−1·88	16·47	−1·41	20·29
S3	−1·48	23·88	−0·68	30·05	−0·61	29·77	0·00	35·61
S4	−0·44	35·06	0·51	43·42	0·56	43·07	1·32	50·94
S5	1·51	57·44	2·78	70·15	2·80	69·66	3·86	81·59
S6	0·79	50·62	1·88	61·06	1·94	61·00	2·78	70·34
S7	−1·87	20·46	−1·17	25·51	−1·08	25·43	−0·58	29·99
S8	−2·93	10·41	−2·33	13·66	−2·23	13·58	−1·83	16·54
S9	5·67	110·94	7·55	132·16	7·56	132·12	9·10	151·04
S10	5·81	115·23	7·79	137·83	7·77	137·56	9·44	158·00
S11	−1·09	30·52	−0·26	37·36	−0·17	37·29	0·44	43·44
S12	−3·59	5·39	−3·02	7·73	−2·92	7·65	−2·56	9·81
S13	−2·93	10·41	−2·33	13·66	−2·23	13·58	−1·83	16·54
S14	−1·87	20·46	−1·17	25·51	−1·08	25·43	−0·58	29·99
S15	0·45	44·57	1·38	53·17	1·48	53·35	2·16	60·75
S16	0·05	39·24	0·86	46·37	0·98	46·67	1·54	52·66
S17	−0·94	30·52	−0·11	37·36	−0·03	37·29	0·58	43·44
S18	−0·50	35·54	0·39	43·28	0·47	43·21	1·14	50·16

conclude that the degradation of the epoxy resin hardened using the aromatic diamine needs, a higher heat transfer than a resin hardened using dicyadiamide.

This conclusion completes a previous stability classification[18] of the epoxy resins versus the chemical composition of the curing agent (this classification proposes that resins cured using aromatic diamine are more heat-resistant than resins cured using aliphatic diamines).

The apparent different behaviours of the TGDDM/DDS resin with the heating rates cannot be explained by these results. In an attempt to assign these differences, knowledge of the degradation modes of the resins is required.

In this purpose, the residual dispersions S^2_{jv} and the probabilities associated to each kinetic function are calculated using the experimental TG-curves. Their distributions are presented in Figs 6 and 7.

Table 3. Apparent kinetic parameters of the TGDDM/DDA system obtained for each kinetic function versus heating rates

Heating rate	4·4°C/mn		7·7°C/mn		10·4°C/mn		12·9°C/mn	
Function	log A (A:s^{-1})	E (kJ/mol)	log A (A:s^{-1})	E (kJ/mol)	log A (A:s^{-1})	E (kJ/mol)	log A (A:s^{-1})	E (kJ/mol)
S1	−2·64	11·93	−2·09	14·98	−2·36	11·64	−2·24	11·96
S2	−1·88	18·94	−1·26	23·12	−1·60	18·74	−1·48	19·19
S3	−0·51	32·95	0·26	39·41	−0·25	32·96	−0·12	33·64
S4	0·76	46·96	1·70	55·69	1·01	47·17	1·15	48·09
S5	3·21	74·99	4·47	88·27	3·43	75·60	3·58	77·00
S6	2·8[illegible]	71·35	4·06	84·29	2·89	70·26	3·07	71·92
S7	−0·7[illegible]	31·14	0·05	37·42	−0·54	30·29	−0·40	31·10
S8	−2·0[illegible]	17·73	−1·41	21·79	−1·81	16·96	−1·68	17·49
S9	9·52	151·79	11·72	178·03	9·34	150·20	9·60	153·56
S10	9·46	154·13	11·67	180·61	9·38	153·64	9·62	156·83
S11	0·35	44·54	1·28	53·04	0·50	43·61	0·65	44·70
S12	−2·77	11·03	−2·21	13·98	−2·54	10·30	−2·41	10·69
S13	−2·03	17·73	−1·41	21·79	−1·81	16·96	−1·68	17·49
S14	−0·72	31·14	0·05	37·42	−0·54	30·29	−0·40	31·10
S15	2·75	67·97	3·98	80·53	2·68	65·29	2·89	67·19
S16	2·58	64·81	3·79	77·00	2·38	60·68	2·62	62·79
S17	0·49	44·54	1·42	53·04	0·64	43·61	0·79	44·70
S18	1·08	51·25	2·09	60·85	1·21	50·27	1·37	51·51

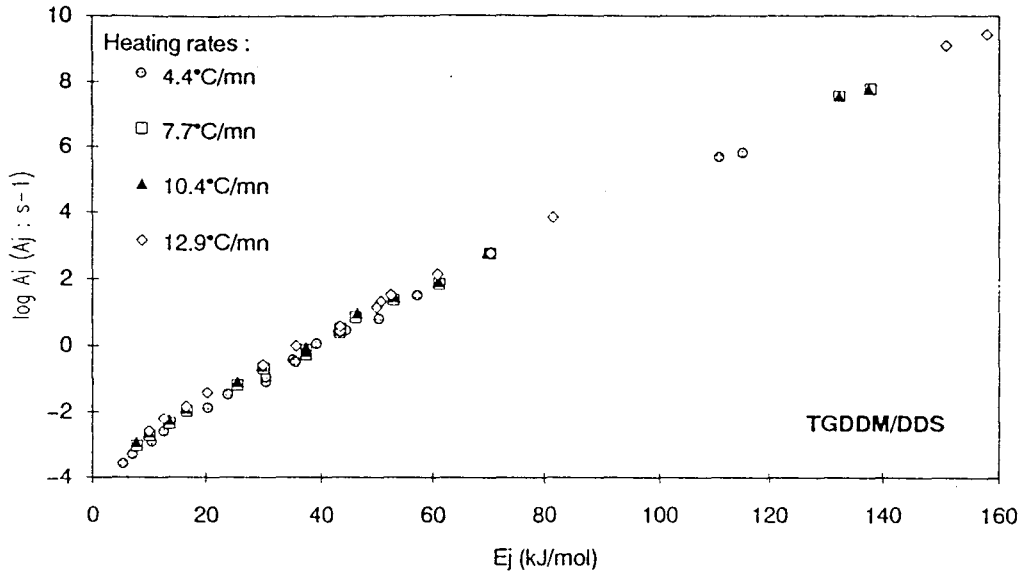

Fig. 3. Compensation effect for the TGDDM/DDS resin versus heating rates.

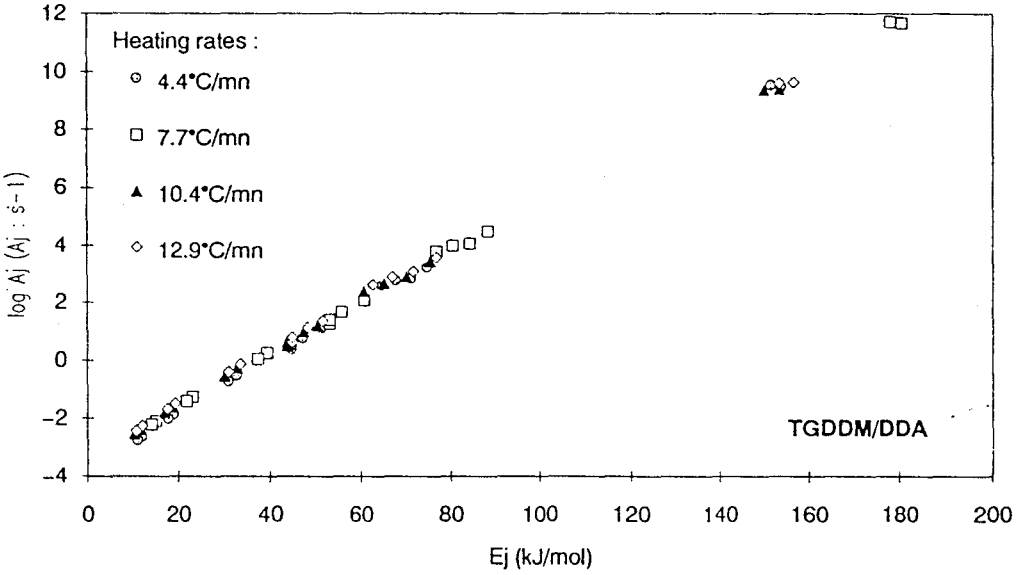

Fig. 4. Compensation effect of the TGDDM/DDA resin versus heating rates.

Table 4. k_v and T_v values of the epoxy resins versus the heating rates

β_v (°C/min)	TGDDM/DDS			TGDDM/DDA		
	$B_v = \log k_v$ (k_v: s^{-1})	I_v ($\times 10^{-5}$) (mol/J)	$1/T_v$ ($\times 10^{-5} K^{-1}$)	$B_v = \log k_v$ (k_v: s^{-1})	I_v ($\times 10^{-5}$) (mol/J)	$1/T_v$ ($\times 10^{-5} K^{-1}$)
4·4	−3·64	8·51	162·89	−3·41	8·59	164·32
7·7	−3·29	8·29	158·49	−3·10	8·38	160·33
10·4	−3·17	8·21	156·97	−3·08	8·34	159·56
12·9	−3·01	8·09	154·80	−2·98	8·26	158·13

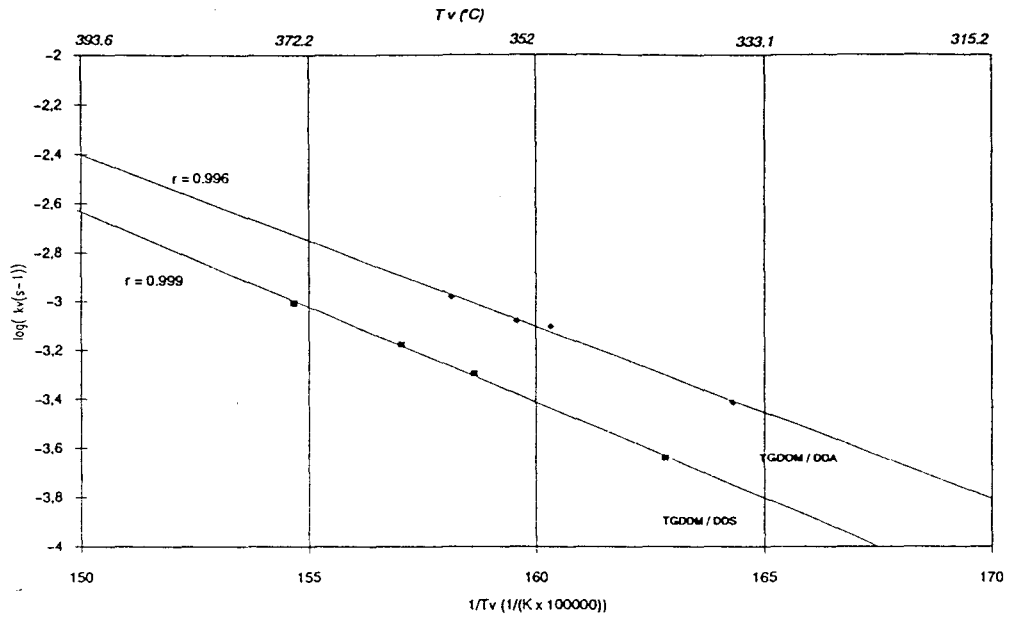

Fig. 5. $\log k_v = f(1/T_v)$ for two epoxy systems (r: regression factor of the linear relation).

Table 5. Invariant kinetic parameters of the TGDDM/DDS and the TGDDM/DDA systems

Invariant kinetic parameters	TGDDM/DDS	TGDDM/DDA
$\log(A_{inv})(A_{inv}: s^{-1})$	9·05 (±0·01)	8·13 (±0·02)
E_{inv} (kJ/mol)	149 (±4)	134 (±8)

The distribution of probabilities obtained with the two epoxy systems gives a good discrimination of the different kinetic functions. It shows that the two epoxy resins follow the same most probable degradation law S9 which corresponds to a diffusion model. This result is interesting because it shows that kinetic parameters obtained assuming a first-order reaction[9] have to be rejected.

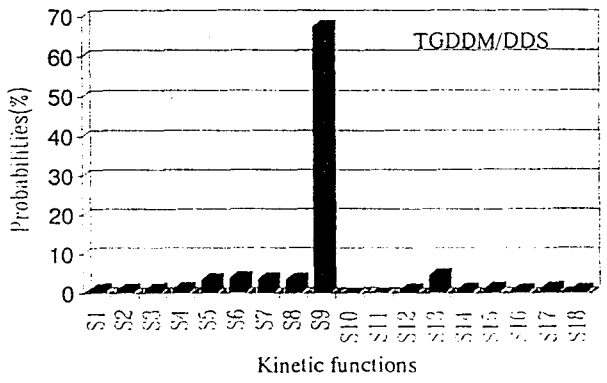

Fig. 6. Distribution of the probabilities of the TGDDM/DDS system.

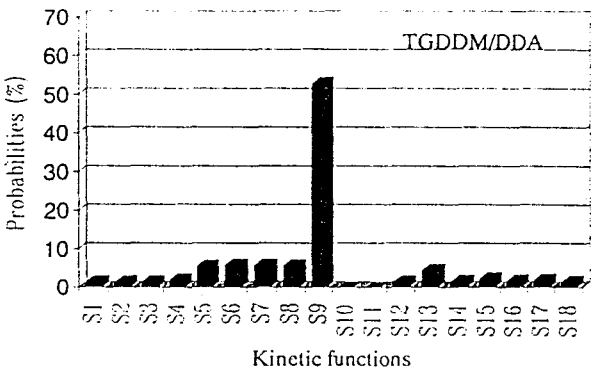

Fig. 7. Distribution of the probabilities of the TGDDM/DDA system.

The kinetic functions may then be subdivided into five classes of functions. The sum of probabilities calculated are presented in Table 6.

The table shows that the thermal oxidative degradation of the studied resins does not obey an order-reaction. The probable phase boundary reactions may be related to the existence of a surface oxidative process and the nucleation and nucleous growth reaction to the intramolecular elimination of water in the network of the resin

Table 6. Distribution of the kinetic functions following their different classes and sums of the probabilities P_j of kinetic degradation functions per class

Classes	1	2	3	4	5
Type of function	Nuncleation and nucleus growing S1 S2 S3 S4 S5	Phase boundary reaction S6 S7 S8	Diffusion S9 S10 S11	Potential law S12 S13 S14 S17 S18	Reaction order S15 S16
TGDDM/DDS P_j (%)	8·37	11·77	67·73	9·68	2·45
TGDDM/DDA P_j (%)	12·78	17·72	53·07	11·99	4·44

in which the nitrogen atom acts as a nucleophile.[3] The possible potential law-reactions present degradation functions which increase when α increases and may be related to the degradation of the carbonaceous material formed.

The most probable class of possible processes corresponds to the S9 kinetic model reaction. This process presents values of their kinetic functions $f_j(\alpha)$ which decrease when the degree of conversion α of the resins increases. Such behaviour is comparable to that of autoprotective ablative materials: in isothermal conditions, the rate of weight loss decreases when the degree of conversion increases.

From a chemical viewpoint, an expanded carbonaceous structure develops during ,the degradation, which lowers the rate of the degradation of the resins mainly via a diffusion process. It may be proposed that this coating protects the remaining undegraded material because it is not permeable to the degradation products.

Finally, the two successive apparent maxima of the rate of weight loss at about 375 and 420°C observed with the TGDDM/DDS system using comparatively high heating rates, may be explained by a competition between two degradation processes (respectively the formation of the carbonaceous material via elimination of water and the degradation of this protective material).

CONCLUSION

The IKP method allows us to obtain comparative kinetic data from TG curves of the two epoxy systems. The invariant activation energies of the thermo-oxidative degradation of the epoxy resin hardened with a aromatic diamine and with dicyandiamide are respectively 149 kJ/mol and 134 kJ/mol. Arrhenius plots shows that the polymer cured using the aromatic diamine is the more stable. Moreover, the study reveals that the chemical processes (intramolecular water elimination and/or surface oxidation) do not control the rates of weight loss of the resins and that their degradation takes place mainly via a diffusion-controlled process.

ACKNOWLEDGMENTS

The authors gratefully acknowledge support from Aérospatiale (12, rue Pasteur F-92152 Suresnes France). We also are indebted to Dr Yves Henry and Dr Bruno Costes for helpful discussions and comments.

REFERENCES

1. Costes, B., Bodu, J. J. & Henry, Y., "*Charges Minérales et Organiques Fonctionnelles dans les Polymères*". Moffis, Le Mans, 1992.
2. Rose, N., Le Bras, M., Delobel, R., Costes, B. & Henry, Y., *Polym. Deg. & Stab.*, **42** (1993) 307.
3. Paterson-Jones, J. C., *J. Appl. Polym. Sci.*, **19** (1975), 1539.
4. Paterson-Jones, J. C. & Smith, D. A., *J. Appl. Polym. Sci.*, **12** (1968) 1601.
5. Park, W. R. R. & Blount, J., *Ind. Eng. Chem.*, **49** (1957), 1897.
6. Bellenger, V. & Verdu, J., *J. Appl. Polym. Sci.*, **30** (1985) 363.
7. Lee, J. H., *J. Polym. Sci. (Part A)*, **3** (1965) 859.
8. Conley, R. T. & Dante, M. F., Stability of Plastics, *Tech. Conf. Soc. Plastics Eng.*, Washington, DC, June, 1964.
9. Patel, R. H., Patel, V. S. & Patel, R. G., *Thermochimica Acta*, **141** (1989) 77.
10. Barco, L., Belleri, G. & Beruto, D., *Materials Chem.*, **1** (1976), 243.
11. Levchik, S. V., Levchik, G. F. & Lesnikovich, A. J., *Thermochimica Acta*, **77** (1985) 157.
12. Bourbigot, S., Delobel, R., Le Bras, M. & Normand, D., *J. Chim. Phys.*, **90** (1993) 1909.
13. Costes, B., Etude structurale du réticulat tetraglycidyl diaminodiphenylmethane (TGMDA) diaminodiphenylsulfone (DDS). Doctoral Dissertation, Le Mans, 1989.
14. Bente, M. P., Réactivité à l'état fondu de systèmes

époxy/cyanamide–dicyanamide–mélamine. Doctoral Dissertation, Pau, 1993.
15. Guthner, T. & Hammer, B., *J. Appl. Polym. Sci.*, **50** (1993) 1453.
16. Bourbigot, S., Delobel, R., Le Bras, M. & Schmidt, Y., *J. Chim. Phys.*, **89** (1992) 1835.
17. Venger, A. E., Fraiman, Yu. E. & Yurevich, F. B., *J. Thermal Anal.*, **27** (1983) 325.
18. Bishop, D. P. & Smith, D. A., *Ind. Eng. Chem.*, **59**(8) (1967) 32.
19. Ozawa, T., *Bull. Chem. Soc. Jpn*, **38** (1965) 1881.
20. Flynn, J. H., *J. Thermal Anal.*, **27** (1983) 95.
21. Coats, A. W. & Redfern, J. P., *Nature*, **201** (1964) 68.
22. Nikoalev, A. V., Logvinenko, V. A. & Gorbarchev, V. M., *J. Thermal Anal.*, **27** (1983) 325.
23. Lesnikovich, A. I. & Lechchick, S. V. & Guslev, V. G., *Thermochimica Acta*, **77** (1984) 357.
24. Lesnikovich, A. I. & Levchick, S. V., *J. Thermal Anal.*, **27** (1983) 89.
25. Hoeel, P. G., *Statistique Mathématique*, Armand Colin, Paris, 1991.

APPENDIX: THE INVARIANT KINETIC PARAMETER METHOD (IKP)

In this method, we do not use just one assumed kinetic law but several functions given in the literature[17] (18 function $f_j(\alpha)$ previously indexed in Table 1) and different heating rates β_v are used. This method assumes only that the rate expression $d\alpha/dt$ only depends on α (as in isothermal conditions):

$$\frac{d\alpha}{dt} = kf(\alpha) \tag{1}$$

where α is the degree of conversion and $f(\alpha)$ a certain function of α.

When thermal oxidative degradation takes place under the conditions of thermogravimetric analysis, k cannot remain a constant and depends upon the temperature. The validity of the Arrhenius equation can be presumed for this dependance:

$$k_j = A_j \exp\left(\frac{-E_j}{R\,T}\right) \tag{2}$$

where A_j and E_j are respectively the pre-exponential factor and the activation energy.

In the case of a linear heating rate β_v, the combination of the above two equations gives the following relationship:

$$\frac{d\alpha}{f_j(\alpha)} = \frac{A_j}{\beta_v} \exp\left(\frac{-E_j}{R\,T}\right) dt \tag{3}$$

Different integration methods for eqn (3) may be used: the Ozawa method,[19] the Ozawa method corrected by the Flynn algorithm[20] and the Coats and Redfern method.[21] Bourbigot *et al.* have shown that IKP method is independent of the integral method used to compute the invariant activation energies and pre-exponential factors. But this method is sensitive to the integral methods used to calculate the probabilities associated with each kinetic function.[12] The Coats and Redfern method has been found to give the best discrimination of degradation process.

The integration of eqn (3) by Coats and Redfern method give the following relation (4):

$$\log\left(\frac{g_j(\alpha_{iv})}{T_{iv}^2}\right) = \log\left(\frac{A_{jv}R}{\beta_v E_{jv}}\right) - \frac{E_{jv}}{2{\cdot}3\,R\,T_{iv}} \tag{4}$$

with

$$g_j(\alpha) = \int_0^{\alpha} \frac{d\alpha}{f_j(\alpha)}$$

By plotting $\log(g_j(\alpha_{iv})/T_{iv}^2)$ versus $1/T_{iv}$, for a fixed heating rate β_v and a chosen degradation function $f_j(\alpha)$, the apparent activation energy E_{jv} and the apparent pre-exponential factor A_{jv} may be obtained.

The application of the method is based on the study of the compensation effect.[22] Indeed, the integration method applied to several functions $f_j(\alpha)$ implies significant changes of activation energies and pre-exponential factors. For each function $f_j(\alpha)$, $\log(A_j)$ versus E_j is plotted and, if a compensation effect is observed, a linear relation defined by the following equation is obtained for a given heating rate β_v ($1 < v < n$; with n the number of heating rates used):

$$\log A_{jv} = B_v + l_v E_{jv} \tag{5}$$

The significance of B_v and l_v has been discussed elsewhere[23] and it has been demonstrated that:

$$B_v = \log(k_v)$$

$$l_v = \frac{1}{2{\cdot}3\,R\,T_v}$$

where k_v represents the invariant rate constant of the system at the temperature T_v.

The essence of the method is to obtain a group of lines (determined by compensation effect) by varying the experimental conditions (heating rate β_v) and to find the coordinates of its centre, i.e. A_{inv} and E_{inv}. The coordinates are in an ellipsoidal domain that may be defined by a straight line.[24]

$$B_v = \log A_{inv} - E_{inv} l_v \tag{6}$$

To summarize, for p heating rates, p pairs of values (B_v, l_v) are obtained and by plotting $B_v = f(l_v)$ the compensation effect implies the linear relation $B_v = \log A_{inv} - E_{inv} l_v$ with the slope equal to $-E_{inv}$ gives invariant activation energy and an intercept equal to $\log A_{inv}$, the invariant pre-exponential factor of the system.

Calculation of probabilities associated with each kinetic degradation function

By using the E_{inv} and $\log A_{inv}$ values obtained, the kinetic functions $f_j(\alpha)$ may be discriminated. The residual sum of squares for each $f_j(\alpha)$ and for each heating rate β_v may be computed (7):

$$(n-1)S_{jv}^2 = \sum_{i=1}^{i=n} \left| \left(\frac{d\alpha}{dT}\right)_{iv} \frac{A_{inv}}{\beta_v} \exp\left(\frac{-E_{inv}}{R\,T_{iv}}\right) f_j(\alpha) \right|^2 \quad (7)$$

The most probable function is then chosen by the average minimum value of $\bar{S}_j$ defined by the relationship (8):

$$\bar{S}_j = \frac{1}{P} \sum_{v=1}^{v=p} S_{jv} \quad (8)$$

with p the number of heating rates used.

The probabilities associated with each function $f_j(\alpha)$ can be calculated by defining the ratio (9):

$$F_j = \frac{\bar{S}_j^2}{\bar{S}_{min}^2} \quad (9)$$

where $\bar{S}_j^2 = 1/p \sum_{v=1}^{v=p} S_{jv}^2$ and $\bar{S}_{min}^2 =$ the average minimum of residual dispersion. The ratio obeys the F-distribution law (10):

$$q(F_j) = \frac{\Gamma(v)}{\Gamma^2\left(\frac{v}{2}\right)} \times \frac{F_j^{v/2-1}}{(1+F_j)^v} \quad (10)$$

where v is the number of degrees of freedom equal for every dispersion and Γ the Gamma function.[25]

The probabilities of the jth function are computed on the assumption that the experimental data with L kinetic functions are described by a complete and independent events systems (11):

$$\sum_{j=1}^{j=L} P_j = 1 \quad (11)$$

Therefore, we obtain the probability of a kinetic function (12):

$$P_j = \frac{Z_j}{\sum_{j=1}^{j=L} Z_j} \quad (12)$$

with

$$Z_j = 1 - \frac{\Gamma(v)}{\Gamma^2\left(\frac{v}{2}\right)} \int_0^{F_j} x^{v/2-1}(1+x)^{-v}\,dx$$

I-2-b. Evaluation de la résistance à la chaleur des résines polyépoxydes

L'ATG des deux résines ne permet pas leur classement direct selon la résistance à la chaleur. En effet, leur dégradation commence dans le même domaine de température (environ 240°C). Elle montre, par ailleurs, que la dégradation des deux systèmes n'est pas identique. Celle de TGMDA/DDS s'effectue en deux étapes (maxima des vitesses à 375 et 425 °C) lorsque la vitesse de chauffe est importante, alors que celle de TGMDA/DDA s'effectue en une seule étape principale quelle que soit la vitesse de chauffe.

L'influence de la vitesse de chauffe sur le processus de carbonisation peut s'expliquer en terme de vitesse de transfert de chaleur. Le comportement de TGMDA/DDS (la teneur en résidu carboné diminue lorsque la vitesse de transfert de chaleur augmente) est comparable à celui de la cellulose dont la carbonisation est importante lorsque la vitesse de chauffe est faible et qui se dégrade sans résidu

solide lorsque la vitesse est importante. Un tel comportement implique une réaction hétérogène oxygène - solide dans le matériau carbonisé superficiel de TGMDA/DDS qui peut donc être déduite de l'étude ATG. La vitesse de la réaction hétérogène devient faible par comparaison à celle du transfert des hydrocarbures produit par la dégradation de la résine lorsque la vitesse du transfert de chaleur est élevée.

Une telle réaction peut être négligée dans TGMDA/DDA puisque les quantités de résidus à 400°C sont indépendantes de la vitesse de chauffe.

La méthode IKP est basée sur l'étude de l'effet de compensation (CE) [82, 83]. Pour chaque fonction $f_j(\alpha)$, les courbes de Log A_j en fonction de E_j sont des droites d'équation : Log $A_{jv} = B_v + I_v E_{jv}$ quelle que soit la vitesse de chauffe, lorsque l'effet de compensation existe. Un tel effet de compensation (faux ou superficiel [84]) provient d'une distorsion paramétrique attribuable à un modèle cinétique « non approprié » [85]. B_v et I_v sont néanmoins des paramètres significatifs [56] et le modèle isocinétique peut être présumé [86].

L'étude vérifie que la méthode IKP s'applique à la dégradation des deux résines dans les conditions opératoires choisies. Elle montre que la vitesse de dégradation de TGMDA/DDA est toujours supérieure à celle de TGMDA/DDS, en accord avec un classement préalable des polyépoxydes selon la nature des durcisseurs [87]. La stabilité optimale des résines réticulées avec des diamines aromatiques est confirmée.

La répartition des lois de dégradation des deux résines montre que le processus s'effectue par diffusion dans un plan (la vitesse à l'isotherme est une fonction linéaire de l'inverse du degré de conversion des matériaux). Une telle dégradation semble impliquer une protection par le produit résiduel de surface et, donc, un comportement ablatif protecteur. Ce résultat doit néanmoins être considéré avec précaution car la répartition obtenue en considérant 18 lois de dégradation peut provenir d'artefacts de calculs, permettant d'approcher au plus près les valeurs des vitesses de dégradation mais sans aucune réalité chimique. Nous observerons d'ailleurs au paragraphe suivant qu'une discrimination plus précise des domaines de température retenus pour le calcul conduit à une répartition différente des modèles cinétiques.

L'ATG reste un outil analytique controversé pour l'étude du comportement d'un matériau dans un incendie. En effet, les vitesses d'augmentation de température classiquement utilisée sont comparativement faibles à celles mesurées dans un incendie. La technique est donc suspectée de privilégier des dégradations à « basse température » qui sont négligeables dans les conditions d'un incendie. L'universalité des paramètres cinétiques invariants doit donc être vérifiée.

I-3. *Discussion des propriétés retardatrices de la flamme des résines en relation avec leur mécanisme de dégradation - Définition et application du Modèle du front de dégradation.*

L'existence d'une relation entre la cinétique de la dégradation thermique et la tenue au feu d'un matériau reste à vérifier. Les données cinétiques issues de la thermogravimétrie concernent l'effet ultime de la dégradation, à savoir la variation pondérale résultant d'un équilibre entre la perte de masse liée au transfert de matière dans la phase gaz et les gains de masse correspondant à des réactions chimiques du type oxydation partielle en phase condensée (formation de groupements lactones dans le matériau carboné et de groupements peroxydes, aldéhydes ou acides carboxyliques au sein de la résine). Par ailleurs, l'évaluation de la formation des espèces gazeuses est nécessairement erronée car elle ne permet pas la mesure de la quantité de gaz « encapsulés » dans un matériau carboné expansé (TGMDA/DDS à partir de 350°C et TGMDA/DDA à partir de 310°C). Finalement, l'étude TG ne permet pas de définir le lieu géométrique, où se produit le transfert de masse qui impose la cinétique mesurée.

Le comportement des matériaux carbonisants est extensivement traité dans la Littérature comme une problème de transferts de chaleur et de masse monodimensionnels [88] à travers un revêtement constitué d'une couche de carbone et d'une couche de matériau vierge, séparées par une fine zone de pyrolyse. La dynamique de l'effet de gonflement, la physique et la chimie du système sont alors négligés. Notre Groupe travaille actuellement à un modèle tridimensionnel prenant en compte ces paramètres. Les résultats partiels de cette étude ne sont pas rapportés.

Nous présentons ici un modèle monodimensionnel, où le lieu géométrique où se produit le dégagement gazeux est considéré comme caractéristique de la dégradation. C'est, en fait, l'endroit où les produits gazeux sont libérés par le matériau solide et/ou liquide (la phase condensée). La pression des gaz encapsulés y est suffisante pour assurer une fissuration du matériau et permettre leur passage en phase gaz avec perte de masse. Ce lieu est une fonction :

- du transfert thermique vers la zone de pyrolyse, fonction de l'irradiance externe, de l'épaisseur et de la conductibilité du revêtement carboné,
- de la cinétique de la pyrolyse
- et, finalement, des propriétés dynamiques du revêtement, fonctions de sa température et de sa composition.

Une solution consiste à considérer ce lieu comme une surface plane définie comme le front de dégradation (Figure I-5). Elle permet de proposer la représentation de la dégradation par un seul paramètre x(T, α). Le modèle du front de dégradation permet (en utilisant les données cinétiques calculées à l'aide de la méthode IKP) le calcul de la température T_d du lieu où se produit le départ de matière. Une comparaison de T_d avec des températures relevées au sein du matériau permet alors d'évaluer l'avancement de la dégradation.

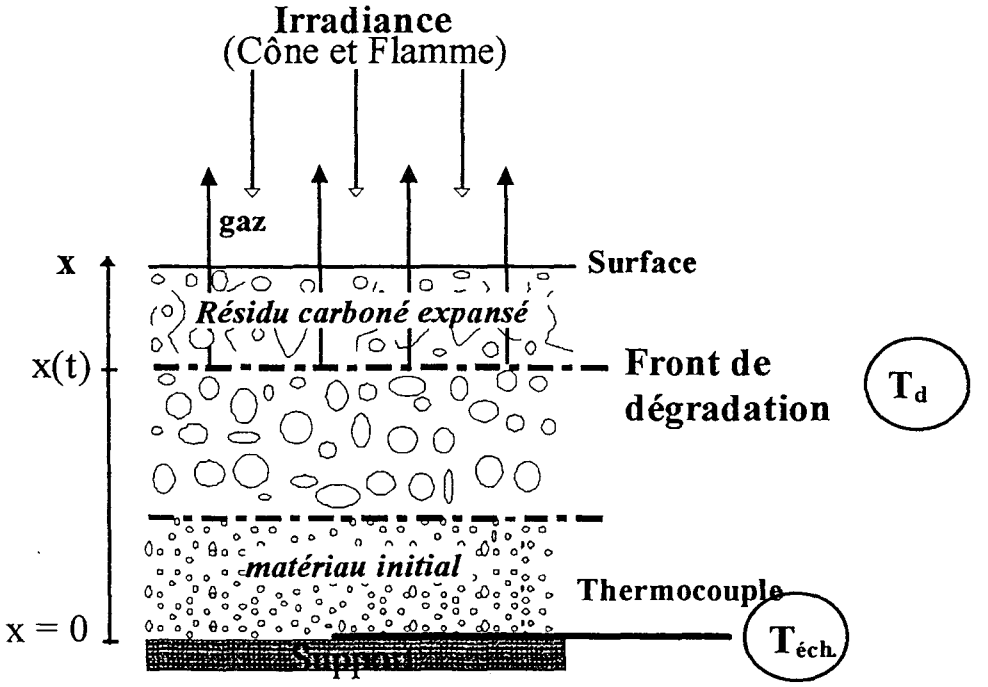

Figure I-5. Représentation modèle unidimensionnelle d'une carbonisation.

Le présent paragraphe rapporte le comportement au feu des 2 résines en terme de flux calorifique, de chaleur totale émise et de vitesse de dégradation évalués au calorimètre à cône dans les conditions d'un incendie dans un local ventilé. Les chaleurs effectives de combustion des deux systèmes sont déduites de l'ensemble de ces données et discutées en considérant différents modes d'oxydation ménagée du combustible.

Dans une seconde étape, une discussion préalable sur le rôle joué par l'oxygène dans le processus de dégradation est complétée en utilisant les résultats d'une ATG classique. Ces derniers permettent, par ailleurs, de connaître les paramètres cinétiques invariants et en conséquence, de comparer les vitesses de dégradation des deux résines. Les paramètres cinétiques permettent le calcul de la température des fronts de dégradation. Ces valeurs, calculées en fonction de la durée du processus :de l'avancement de la réaction, nous conduisent, finalement, à définir les étapes de l'inflammation des résines et à interpréter les profils des flux thermiques.

I-3-a. Résultats

JOURNAL OF FIRE SCIENCES, *VOL. 14–MAY/JUNE 1996*

0734-9041/96/03 0199–36 $10.00/0

The Degradation Front Model– A Tool for the Chemical Study of the Degradation of Epoxy Resins in Fire

(Received January 3, 1996)
(Revised April 13, 1996)

MICHEL LE BRAS, NATHALIE ROSE AND SERGE BOURBIGOT*
Laboratoire de Physico-Chimie de Solides, E. N. S. C. L.
Université des Sciences et Technologies de Lille
BP 108, F-59652
Villeneuve d'Ascq Cedex
France

YVES HENRY
Aérospatiale
12 Rue Pasteur, F-92152
Suresnes, France

RENÉ DELOBEL
Centre de Recherches et d'Etude sur les Procédés d'Ignifugation des Matériaux
(CREPIM) Zone Initia. F-62
Bruay la Bussière
France

ABSTRACT: This work studies two different epoxy resin systems using cone calorimeter data and the results of classical thermogravimetric analyses. It

presents a discussion of the chemical behavior of the resins using cone calorimeter results (mainly the rate of heat release). The thermogravimetric analyses give the invariant kinetic parameters (IKP) and a computation of the distribution of probabilities associated with the kinetic functions which allow a kinetic representation of the resins' degradations. Then, the study using the cone calorimeter allows to obtain kinetic data under the conditions of a fire and to compute the temperature of the degradation front (zone where the weight loss occurs). Comparison of the values of this temperature and of the temperature measured in the lowest volume of the sample allows the comparison of the protective character of the carbon-based shields which form in the first step of the resins' degradation.

KEY WORDS: epoxy resins TGDDM/DDA and TGDDM/DDS, rate of heat release, invariant kinetic parameters, degradation front.

INTRODUCTION

EPOXY RESINS ARE used extensively as protective coatings, adhesives, electrical laminates, reinforced plastics and flooring. They are characterized by the presence of one or more three-membered rings (known as the epoxy, epoxide, oxirane or ethoxyline group) and an aliphatic or aromatic backbone. Reaction of the functional epoxy group with a curing agent (or hardener) results in a thermoset polymer [1].

Epoxy resins constitute the organic matrix for high performance composite materials used in fabrication of light structural panels in the interior of an aircraft. The implication of these materials in fire propagation and flash-over phenomenon during aircraft crashes [as examples: DC9 Cincinnati (1983) and Boeing 737 Manchester (1985)] has led to reinforcement of the FFA regulations [2]. New safety requirements, such as low heat release and low level of smoke emission, limit the number of materials used in passenger areas.

New alternative halogen free thermoset polymers that meet processing, thermal, flammability and environmental requirements have been recently proposed. They use phosphorylated flame retardant curatives [3]. The selection of such resins for aircraft application requires evaluation methods allowing the knowledge of the behavior of these materials under the conditions of a fire and/or a classification of this behavior in terms of heat resistance. It needs parallel fundamental investigation on their degradation mechanisms.

The contribution of a material in a fire is a combustion process which may be assumed a chemical reaction in flows with heat and mass transfer. It involves chemical kinetics, thermodynamics, fluid mechanics and transport processes. In this work, chemical kinetics and thermodynamics and mass transfers are mainly studied.

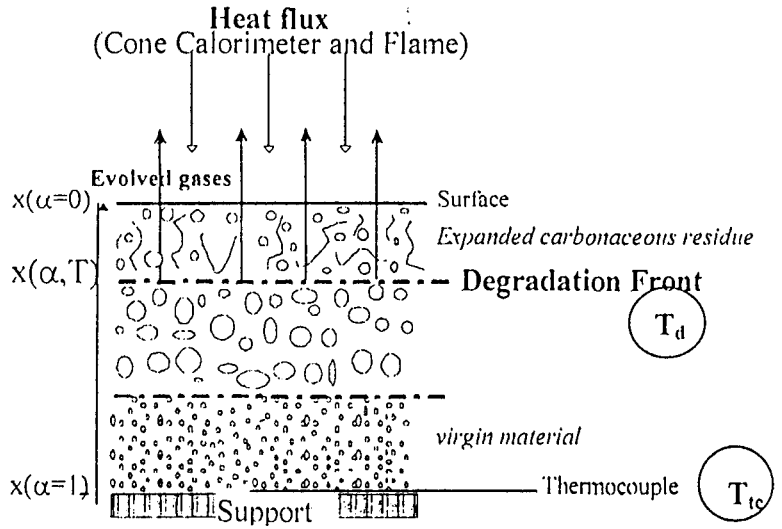

Figure 1. One-dimensional carbonization model.

Previous studies in this laboratory using thermogravimetric analysis (TG) allowed definition of the different steps of the thermal oxidative degradation of an epoxy resin [4], to appraise invariant kinetic parameters IKP and probabilities associated with kinetic functions and then to predict its degradation mode [5].

It is proposed that the degradation leads to the formation of a surface carbonaceous material which may take a part in the protection of the resin. Such a protective process has been described by a model which introduces the notion of degradation front [6] (hypothetical two-dimensional surface where the weight loss occurs) and assumes that the degradation progress is represented by an uni-dimensional model: $x(\alpha,T)$(α: conversion degree). The degradation front model (Figure 1) allows the computation of the temperature of the degradation zone (labeled T_d in this paper) using IKP data. A comparison between the value of this computed temperature and the value of the temperature in the bulk of the resin (labeled T_{tc} in this paper) is then possible.

The cone calorimeter is an apparatus developed by NIST in the eighties [7]. It allows the quantification of phenomena of fire development [8] and gives information on the kinetics and the thermodynamics of the chemical process under the conditions of a fire. Resins can be tested

under heat flux and their degradation followed dynamically by recording their rates of heat release (rhr) using oxygen consumption calorimetry, recording their weight losses using thermogravimetry and, computing their effective heat of combustion (ehc). Obtained data should allow a discussion of the successive chemical processes of the degradation.

This present study compares two "model" epoxy resins TGDDM/DDA and TGDDM/DDS (tetraepoxy prepolymer: *N,N,N′,N′* tetraglycidyl-4,4′ diamino diphenyl methane TGDDM; hardeners: dicyandiamide DDA and diamino 4,4′ diphenyl sulfone DDS). Fire retardancy properties of these two resins are proved by their limiting Oxygen Index (LOI) values [9], respectively 25 and 30%.

This work reports a method which provides information on the progress of the thermal degradation of a resin (versus time) under fire conditions and, as a consequence, on the heat release. The method uses data obtained using the cone calorimeter [weight loss (TG) and oxygen consumption calorimetry in fire] and classical thermogravimetry (TG).

EXPERIMENTAL

Materials

The tetra-epoxy prepolymer TGDDM is a commercial product (Lopox B3302) characterized by a functionality of 3.6 (theoretically 4). Two hardeners were used: an aromatic diamine (DDS) and dicyandiamide (DDA).

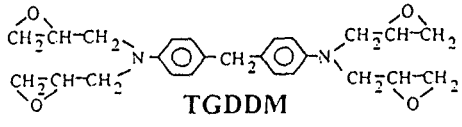

TGDDM

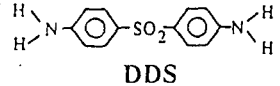

DDS

DDA

The formulations studied in this work contain a percentage of curative which corresponds to the stoichiometric ratio TGDDM/hardener, i.e., one epoxy group for each primary amino hydrogen of the hardener. The mode of preparation of the homogeneous mixtures has been previously given [5]. The TGDDM/DDA formulation was processed by cure, i.e., conversion of liquid monomers into a three-dimensional thermoset network via chemical reactions (8 hours at 135°C, no postcure because of the exothermicity of the reaction) and TGDDM/DDS by cure (1 hour at 135°C and postcure: 2 hours at 180°C) under conditions previously reported [5,10,11].

With the TGDDM/DDA system, taking into account that dicyandiamide presents two tautomers, the cure may involve several simultaneous reactions: NH/epoxy additions leading to

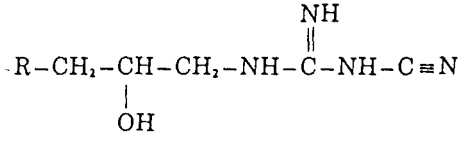

cyano/epoxy addition and elimination/cyclisation reactions [10,12]. For the TGDDM/DDS system, the first reaction is an attack of a primary amine on an epoxy group on a side chain leading to chain lengthening by successive polyaddition:

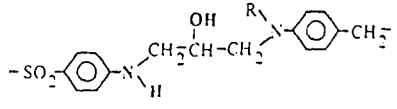

This may be followed by two types of crosslinking reactions (intermolecular and intramolecular).

Cone Calorimeter

Cone calorimeter experiments were carried out on sheets (100 × 100 × 5 mm³) exposed to a Stanton Redcroft apparatus according to ASTM 1356-90 under a heat flux of 50 kW/m². This heat flux corresponds to the evolved heat during a fire [13]. Acquisition of conventional data [rhr, effective heat of combustion (ehc), weight loss, weight loss rate (dW/dt)] and resulting computations have been previously stated [6 and references therein]. A thermocouple (Ni-Cr/Ni-Al; diameter: 0.5 mm) put into the sheet as presented in Figure 1, allowed ob-

Table 1. *Kinetic models used.*

Kinetic Models	$f_i(\alpha)$	$g_i(\alpha)$	
Nucleation and nucleus growing	$\frac{1}{n}(1-\alpha)(-\ln(1-\alpha))^{1-n}$	$(-\ln(1-\alpha))^n$	S1 – n = 1/4
			S2 – n = 1/3
			S3 – n = 1/2
			S4 – n = 2/3
			S5 – n = 1
Phase Boundary Reaction	$(1-\alpha)^n$	$1-(1-\alpha)$	S6-plane symmetry
		$2[1-(1-\alpha)^{1/2}]$	S7-cylindrical symmetry
		$3[1-(1-\alpha)^{1/3}]$	S8-spherical symmetry
Diffusion	$\frac{1}{2}\alpha^{-1}$	α^2	S9-plane symmetry
	$(-\ln(1-\alpha))^{-1}$	$(1-\alpha)\ln(1-\alpha)+\alpha$	S10-cylindrical symmetry
	$\frac{3}{2}[(1-\alpha)^{-1/3}-1]^{-1}$	$1-\frac{2}{3}\alpha-(1-\alpha)^{2/3}$	S11-spherical symmetry
	$\frac{3}{2}(1-\alpha)^{1/3}[(1-\alpha)^{-1/3}-1]^{-1}$	$[(1-\alpha)^{1/3}-1]^2$	S18-Jander's type
Potential law	$\frac{1}{n}\alpha^{1-n}$	$\alpha^n (0<n<2)$	S12 – n = 1/4
			S13 – n = 1/3
			S14 – n = 1/2
			S17 – n = 3/2
Reaction order	$\frac{1}{n}(1-\alpha)^{1-n}$	$1-(1-\alpha)^{1/2}$	S15 – n = 1/2
		$1-(1-\alpha)^{1/3}$	S16 – n = 1/3

taining the average temperature $T_{i,c}$ for the lowest 10 volume % of the sample.

Thermal Analyses

Thermogravimetric analyses were carried out using four heating rates (β_v: 4.4, 7.7, 10.4 and 12.9°C/min) under conditions previously given elsewhere [4]. The computation of kinetic data using the IKP method was reported in the Appendixes of Reference 6. (Development of the method uses theoretical considerations from References [14–16]). The computation of the probabilities of the degradation functions was carried out considering eighteen kinetic functions reported in Table 1.

RESULTS AND DISCUSSION

Oxygen Consumption Calorimetry

Heat release has long been recognized as the major fire reaction parameter because it defines fire size [17]. Illustrative measurements of rhr versus time on TGDDM/DDA and TGDDM/DDS are shown in

Figure 2. rhr curves of TGDDM/DDA vs. time.

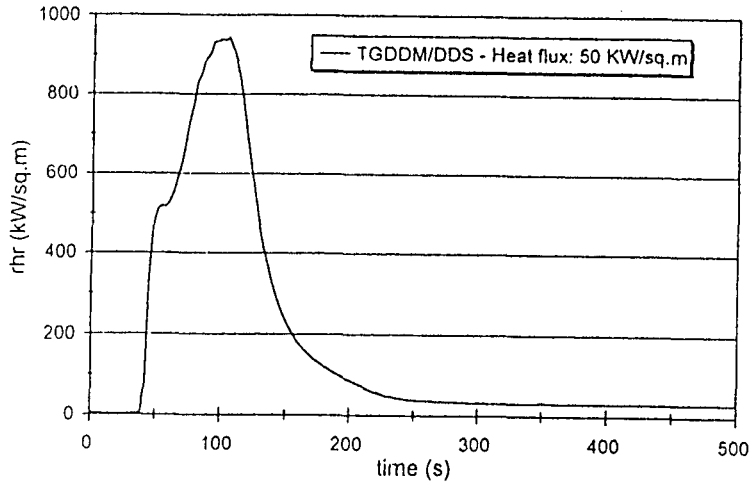

Figure 3. rhr curves of TGDDM/DDS vs. time.

Figures 2 and 3. Maxima of rhr are, respectively, about 1900 kW/m² (60-75 s) and 900 kW/m₂ (90-120 s).

Associated data for the TGDDM/DDA system are: ignition time: 24 s, time for extinction: about 120 s, soot emission from 24 to about 120 s, post-glowing of a residue whose degradation rate is low from 100 s and finally, the total heat evolved computed at 300 s is 900 kJ.

Associated data for the TGDDM/DDS system are: ignition time: 45 s, time for extinction: about 220 s, soot emission from 45 to about 200 s, post-glowing of a residue whose degradation rate is low from 100 s and finally, the total heat evolved computed at 300 s is 800 kJ. It is interesting to note that the respective values of the observed maxima of rhr and of ignition times agree well with the classification of the fire retardancy of the material deduced from the LOI values.

The rhr curves vs. times of the two resins present under our experimental conditions an intermediate plateau when their rhr increase with time. This plateau may be related to the plateau at about 45 s in the differential thermogravetry (DTG) curve of TGDDM/DDA (Figure 4) and to the decrease of the rate of weight loss of TGDDM/DDS at about 45 s (Figure 5). This phenomenon may be explained either by the formation of materials which present an intermediate thermal stability under the experimental conditions or by the formation of insulative materials "on the surface" of the materials.

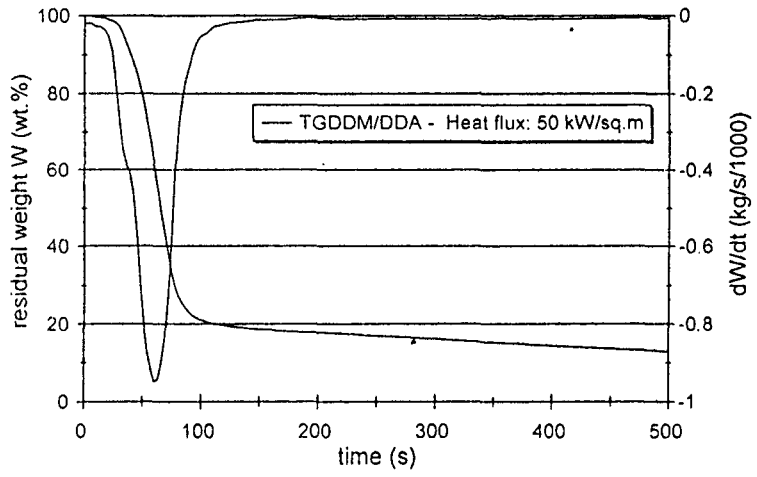

Figure 4. TG and DTG curves of TGDDM/DDA in fire conditions.

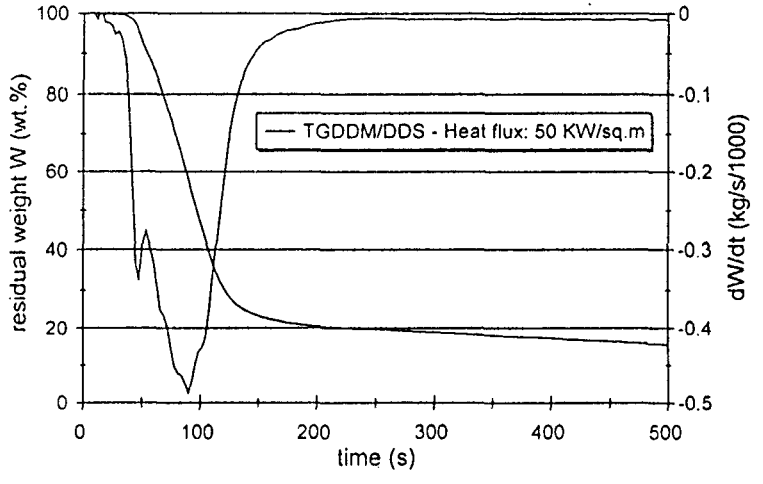

Figure 5. TG and DTG curves of TGDDM/DDS in fire conditions.

The degradation of the two resins is not complete and leads to the formation of thermally stable residues after, respectively, 100 s and about 150 s of the heat treatment of TGDDM/DDA and TGDDM/DDS. Initial mass of these residues and their rates of weight loss are nearly the same. The degradations of the residues correspond to the glowing processes, i.e., low rate oxidation of solid "carbon" into carbon oxides (mainly carbon dioxide from i.r. analysis of combustion gases using the cone calorimeter [5]) under air.

These last degradations do not lead to evolved "fuel" and, as a matter of fact, give no contribution to the flame. It may be proposed that the production of gaseous fuel occurs during conversion of the resins into the residue. So the flammabilities of the materials may be discussed, taking into account their conversion degrees (α) for residue synthesis. In this domain, the conversion occurs with formation of gaseous products (fuel or oxides (H_2O and SO_2) resulting from a pyrolysis process), of smoke and soot (polyaromatic compounds resulting from both pyrolysis and oxidative process) and eventually of oxidized products (carbon oxides, NO_x, aldehyde and ketone which result from a thermo-oxidative degradation).

The curves of the rhr values of the two resins versus α (Figures 6 and 7) and of the weight loss rates (dW/dt) versus α (Figures 8 and 9) allow the discrimination of three distinct steps:

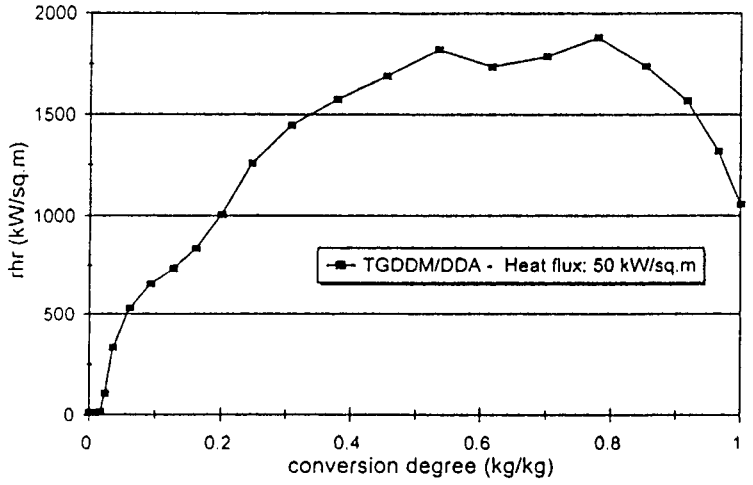

Figure 6. rhr curve of TGDDM/DDA vs. the conversion degree.

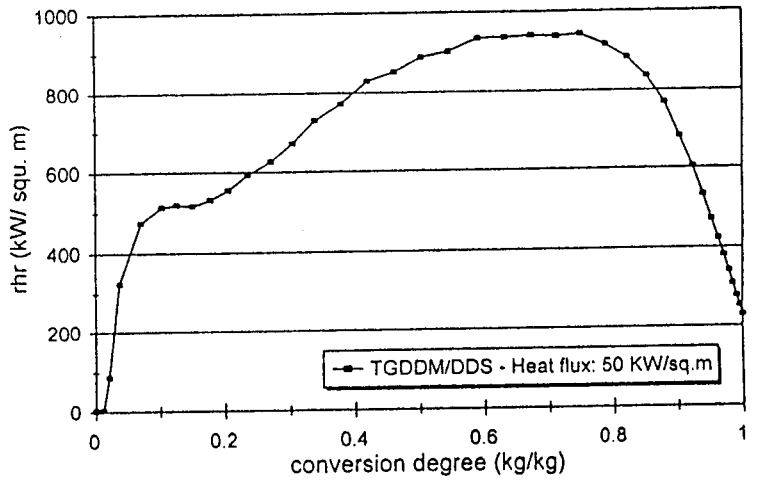

Figure 7. rhr curve of TGDDM/DDS vs. the conversion degree.

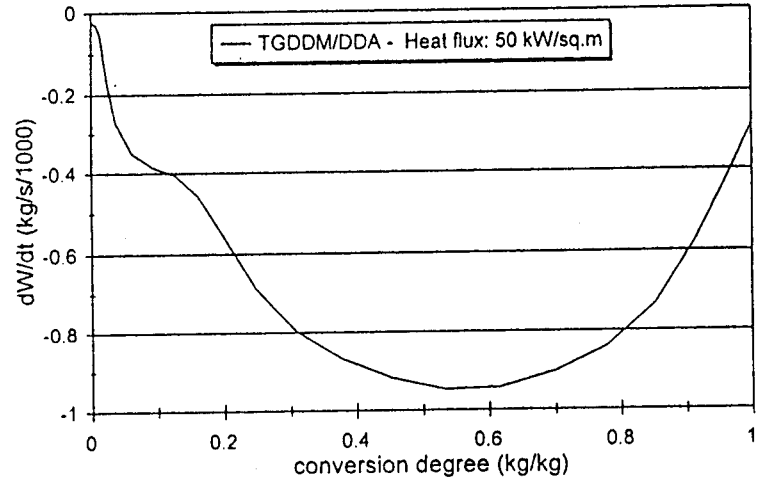

Figure 8. Rate of weight loss of TGDDM/DDA vs. the conversion degree.

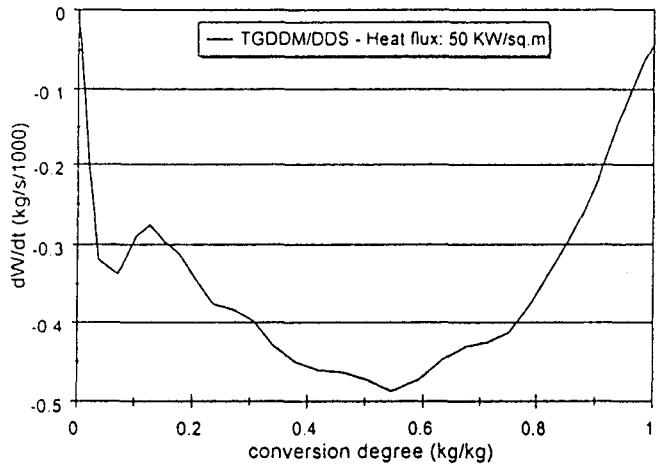

Figure 9. Rate of weight loss of TGDDM/DDS vs. the conversion degree.

- The rhr values increase ($0 < \alpha < 0.1$) to reach nearly constant values ($0.1 < \alpha < 0.18$) when the apparent degradation rates, respectively, increase and remain nearly constant (TGDDM/DDA) or decrease (TGDDM/DDS). In this zone, the rhr values are nearly the same versus α.
- Then, the rhr values increase ($0.18 < \alpha < 0.5$ with TGDDM/DDA and $0.18 < \alpha < 0.55$ with TGDDM/DDS) and lie at constant maximum values ($\alpha < 0.72$). The corresponding degradation rates increase ($\alpha < 0.55$) and then decrease slowly.
- Finally, when $\alpha < 0.75$, strong decreases of the *rhr* values and of the degradation rates are observed.

Thermogravimetry and Kinetic Study

Curves of weight losses of TGDDM/DDA and TGDDM/DDS under air and under nitrogen in Figures 10 and 11 confirm that oxygen plays a part in the formation of a carbonaceous material stable in the temperature range 300–400°C and, then, in the degradation of the material in the temperature range 400–650°C. The thermo-oxidative of TGDDM/DDA is similar to the pyrolysis process up to a 40% weight loss, whereas the thermo-oxidative degradation of TGDDM/DDS is always different.

This last result implies that the "protection" of the resin by oxygen occurs from the beginning of the degradation process.

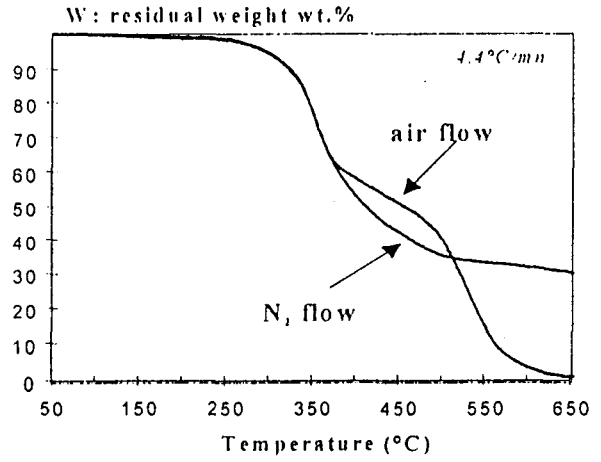

Figure 10. TG curves of TGDDM/DDA under air and nitrogen flows.

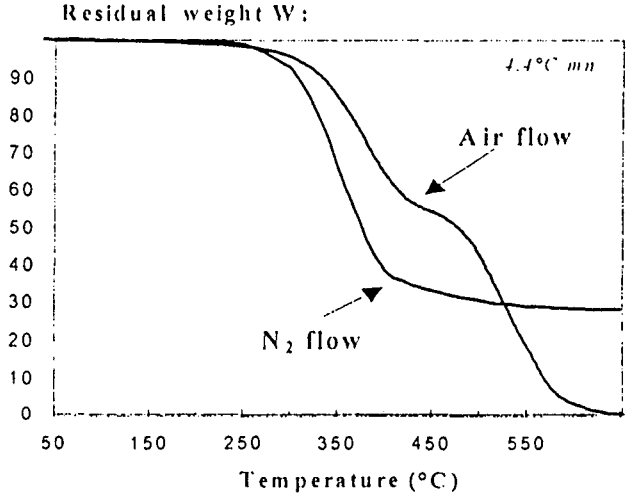

Figure 11. TG curves of TGDDM/DDS under air and nitrogen flows.

The DTG curve of TGDDM/DDA (Figure 12) shows that the formation of the carbonaceous material occurs in two successive steps in the temperature ranges 250–300°C and 300–450°C. The first step may be assigned to the formation of a new resin network via a dehydration reaction [4]. Indeed, it has been previously shown that the first step may be described using five probable kinetic functions and that its rate is lowered by a diffusion process [5].

Such a degradation does not lead to the production of a high amount of evolved fuels and, as a matter of fact, probably gives a poor contribution to the flame. In this work, we assume that the process which is rate determining for the synthesis of fuel corresponds to the second step of the degradation which leads to the formation of the stable carbonaceous material.

The thermo-oxidative degradation of this last material occurs then in two separate steps, i.e., a low rate degradation between 380 and 500°C and complete degradation in the higher temperature range.

Figure 13 shows that the thermo-oxidative degradation of TGDDM/DDS occurs in three successive steps: formation of the carbonaceous material between 300 and 425°C, low rate degradation of this material between 425 and 500°C and finally, complete degradation in the higher temperature range. In this work, we assume that the first process is rate determining for the synthesis of fuel under fire conditions.

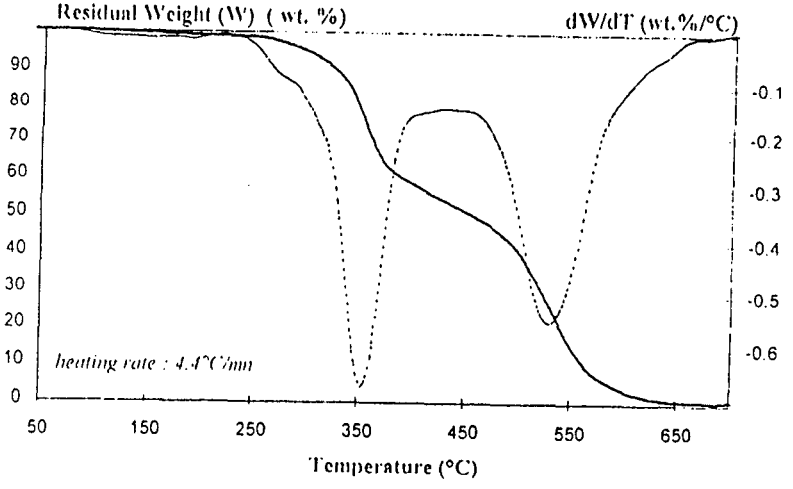

Figure 12. TG and DTG curves of TGDDM/DDA under air flow.

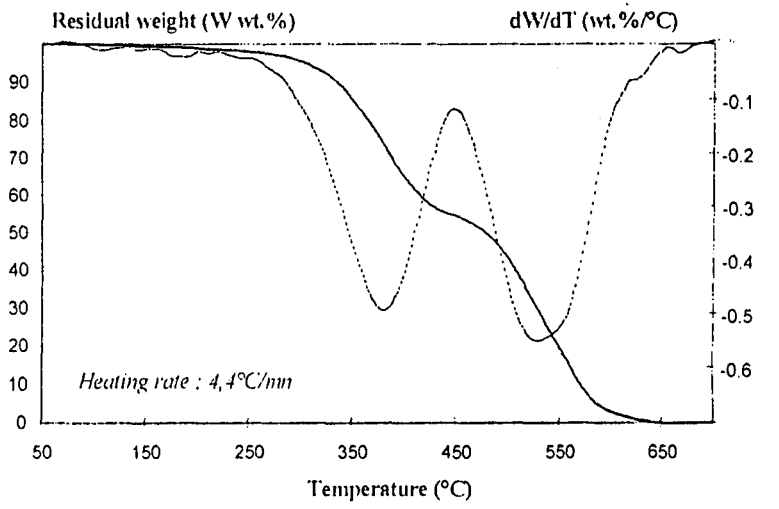

Figure 13. TG and DTG curves of TGDDM/DDS under air flow.

The IKP method allows computation of the invariant kinetic parameters with the two resins considering only residual weight values in the temperature ranges previously defined (i.e., 275–380°C and 275–425°C, with, respectively. TGDDM/DDA and TGDDM/DDS when $\beta_v = 4.4$°C/min.).

Using eighteen degradation functions, eighteen couples A_{jv} and E_{jv} (A_{jv}: apparent pre-exponential factor calculated with a function $f_j(\alpha)$ at β_v; E_{jv}: calculated apparent activation energy) per β_v are obtained.

Figures 14 and 15 show that compensation effects are observed with the two resins for each β_v. Indeed, linear relations:

$$\log A_{jv} = B_v + I_v E_{jv} = \log (k_v) + E_{jv}/2.3\ RT_v$$

with

k_v = the invariant rate constant at T_v
$B_v = \log (k_v)$
$I_v = (2.3\ RT_v)^{-1}$

are verified.

The values of B_v and I_v for the two resins are then calculated from the

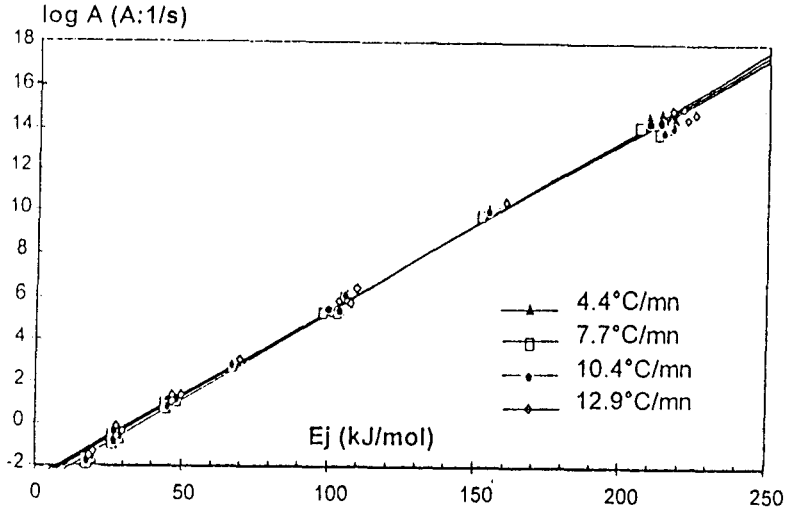

Figure 14. Compensation effect for TGDDM/DDA vs. β_v.

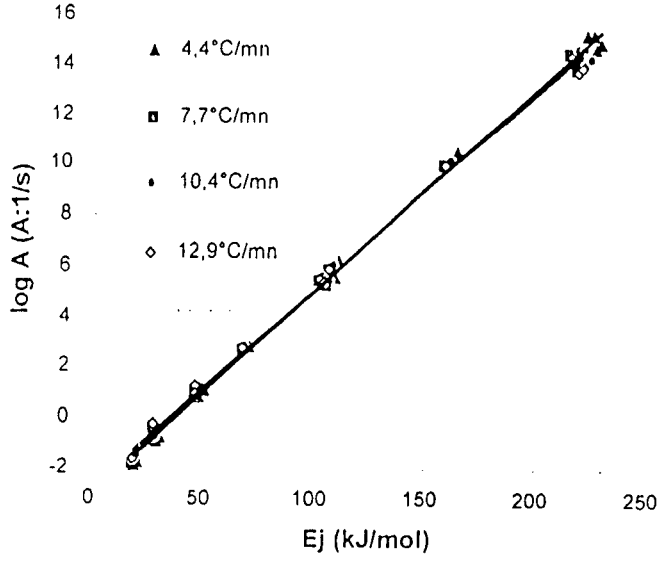

Figure 15. Compensation effect for TGDDM/DDS vs. β_v.

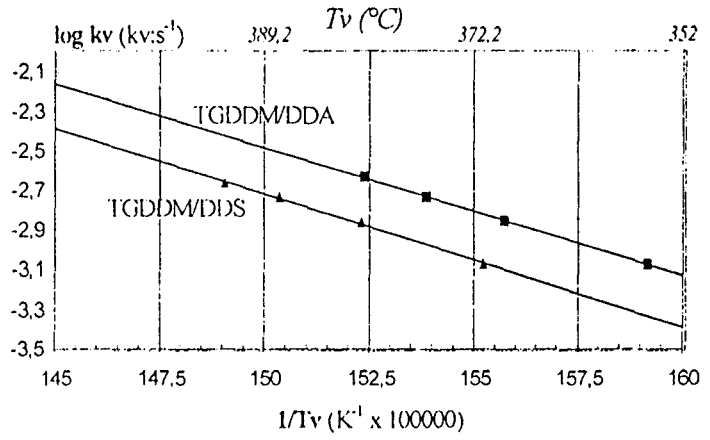

Figure 16. Compensation of the invariant rate constants of TGDDM/DDA and TGDDM/DDS vs. temperature T_v.

slopes and the intercepts of the corresponding straight lines obtained. The curves $\log k_v = f(1/T_v)$ (Figure 16) verifies that the Arrhenius law:

$$\log k_v = \log A_{inv} - E_{inv}/2.3\ RT_v$$

is followed. Consequently, the values of the invariant activation energy and of the invariant pre-exponential factors are calculated from the curves.

Table 2 shows that the invariant kinetic parameters of the two systems are quite the same and, as a matter of fact, may not be considered to explain the different fire behaviors of the systems.

The probabilities associated with each kinetic function (deduced from the experimental TG curves) are presented in Figures 17 and 18. The system TGDDM/DDA has two main probable degradation laws:

Table 2. Invariant kinetic parameters of the TGDDM/DDA and TGDDM/DDS systems.

Invariant Kinetics Parameters	TGDDM/DDA	TGDDM/DDS
$\log (A_{inv})$ (A_{inv} : s^{-1})	7.241 (±0.006)	7.298 (±0.007)
E_{inv} (kJ/mol)	123.9 (±2.4)	127.7 (±3.0)

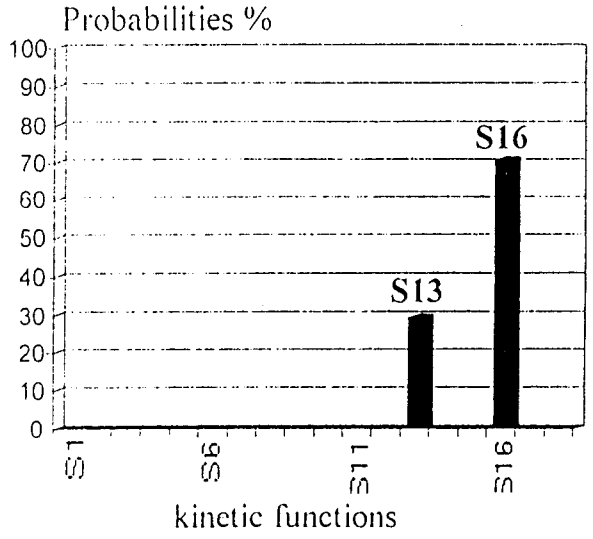

Figure 17. Distribution of the probable kinetic functions for the degradation of TGDDM/DDA.

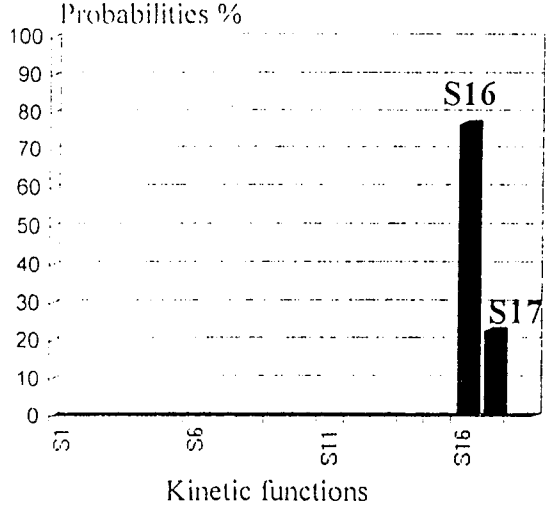

Figure 18. Distribution of the probable kinetic functions for the degradation of TGDDM/DDS.

reaction order law (*S*16): $f(\alpha) = 3(1 - \alpha)^{2/3}$

potential law (*S*13): $f(\alpha) = 3\alpha^{2/3}$

The system TGDDM/DDS may be also represented using two main probable degradation laws:

reaction order law (*S*16): $f(\alpha) = 3(1 - \alpha)^{2/3}$

potential law (*S*17): $f(\alpha) = \frac{2}{3}\alpha^{-1/2}$

The comparison of the values of the kinetic functions *S*13, *S*16 and *S*17 versus the conversion degree are given in Figure 19. An auto-protective character considering the potential laws may only be assumed with the system TGDDM/DDS.

General Discussion

Previous studies of the thermo-oxidative degradation of epoxy resins [4–5 and References therein] show that it may be represented by a three-step process: degradation of the initial network with some break-

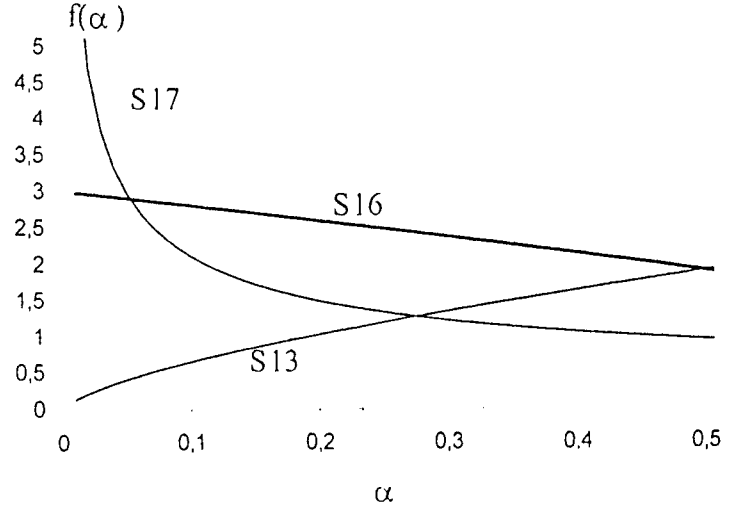

Figure 19. Degradation kinetic functions vs. α.

down reactions, formation of a polyaromatic structure corresponding to turbostratic carbon (polyaromatic species which grow by arranging in parallel layers) and finally oxidation of the carbon in the condensed phase. The three steps of the degradation of TGDDM/DDA occur successively during the TG experiments; the two first steps of the degradation of TGDDM/DDS are not separate in the TG curves.

In the condensed phase, the two first steps of the degradation correspond to both a pyrolysis (endothermic chain breakdown via a radical mechanism) and to an oxidation process (exothermal reaction consecutive to the diffusion of oxygen in the material) with formation of solid and/or gaseous oxidized products (from chemical and FTIR analyses reported in [4] and [5]). These two steps take part in the formation of the flame via the evolution of fuels, i.e., hydrocarbons as gases (alcanes, mainly methane, ethane and propane, alcynes (C_2H_2) and aromatics (benzene and toluene) (from FTIR analyses reported in [5]), liquids as droplets (tar) and solid particles (soot and/or char) (from smoke opacity measurements reported in [5]).

The combustion is generally considered a process which occurs in the gas phase. The process in the cone calorimeter can proceed, in part, as a premixed combustion–transient process nearly homogeneous throughout the entire system or in waves (deflagrations)–and in another part, as a nonpremixed combustion–process not intrinsically propagatory in which diffusion of fuels and oxidizers is essential. The initial stage of the combustion process in the cone calorimeter corresponds to inert heat conduction in the solid and in the gas phase (heat layer develops at the surface and spreads into the interior). Reaching a critical time, a reactive-diffusive zone adjacent at the surface forms. Ignition (explosion process) occurs then when the critical temperature is reached. This temperature depends on the partial pressures of the combustible gases (evolving from the reactive zone) or of the oxidizer which may be deduced from explosion pressure-temperature diagrams, and as a matter of fact, of both the pressure of inert gases and the rate of degradation of the resins.

Ignition time of TGDDM/DDA is about two times shorter than the ignition time of TGDDM/DDS. This characteristic of the resin may be directly related to the times required to observe a significant weight loss under the external heat flux (Figures 4 and 5). The thermo-oxidative degradation of the two resins begins at the same temperature i.e., 250°C (Figures 11 and 12). So, it may be assumed that an insulative material forms in the reactive-diffusive zone of the surface of TGDDM/DDS which limits the heat conduction in the solid and, as a consequence, the rate of emission of fuels.

The first step of the degradation of the two resins (destruction of the initial network with evolving of inert gases such as H_2O arising from the dehydration process) is never seen in cone calorimeter observations separate from the second stage (formation of "carbon"). It is obvious that the rate of the corresponding chemical reaction(s) depends on the temperature of the reaction zone and heat conduction in the solids and that, as a consequence, the reactions occur (in a same time) in zones of the solids lower than those where the formation of the "carbon" takes places. The observed weight losses correspond then to the evolution of gases arising from the two processes.

These two observations agree well with the degradation front model: the rate of evolution of "vapors" depends on the presence in the solid of a more or less insulative layer characterized by a temperature corresponding to the loss of its insulative character.

In a combustion process, heat is generated as a result of the chemical reaction between pyrolysing materials "vapors" and oxygen in the gas phase and pyrolysing material and oxygen in the solid phase [18]. Heat generated in chemical reactions is defined as chemical heat [19] and its rate is defined as the chemical heat release rate. Oxygen consumption calorimetry allows estimation of this chemical heat release rate. The oxygen consumption principle stipulates that, for a large number of organic solids, a quite constant net amount of heat is released per unit of oxygen consumed for complete combustion [20]. The change of oxygen concentration in combustion gases can thus be used to assess the *rhr* of a combustible.

In the energy conservation equation of a combustion process [21], three kinds of energy are seen to arise–chemical energy, thermal energy and kinetic energy. The first energy is only considered in the *rhr*. In these three terms, chemical energy (assumed special to combustion) is associated with the different binding energies of the different molecules in their ground state. It provides a chemical-kinetic contribution to the change in thermal energy, i.e., enthalpy, of the material. The other terms of the balance (diffusive and convective effects in particular, heat conduction, additional transient energy accumulation through pressure increase and radiant energy input) eventually used in a further discussion are not measured in this study.

The curves of the rhr values and of the weight losses versus time of the resins (Figures 2 to 5) show that the ratios of the maxima of the rhr to the rates' maxima of the weight losses show nearly the same value. So, they verify that the rhr values are related to the rate of conversion.

The curves of the rhr values versus the conversion degree (Figures 6 and 7) show that rhr values of the two resins are close to 0 when α is

low. The null values allow a proposal that the first step of the degradation of the resins corresponding to the formation of a carbonaceous material (dehydration [5] network breakdown and intramolecular formation of cycles [22]) and of the surface "carbon" insulative layers lead to evolution of inert gaseous products (mainly H_2O arising from the radical process of formation of the new networks and of the oxidative process leading to the formation of the polyaromatic material). More, the dilution of the evolved combustible products by the inert gases and/or the low evolution rate of the fuels gives conditions which do not correspond to explosion limits and do not allow the formation of oxidized products via a flame.

After ignition, the rhr values of the two resins increase to reach nearly constant values when α increases (an intermediate plateau is observed in the two curves) and then decrease. These variations may be related to the observed variation of the rates of weight loss.

Figure 20 compares the values of the effective heat of combustion of the two resins [ehc = rhr/(dW/dt)] versus the conversion degree. It shows that a steady state corresponding to a constant value of the ehc is observed in the conversion range $0.15 < \alpha < 0.65$ with TGDDM/DDA. Such a steady state is not observed with TGDDM/DDS with which ehc increases when $0.02 < \alpha < 0.15$, decreases when

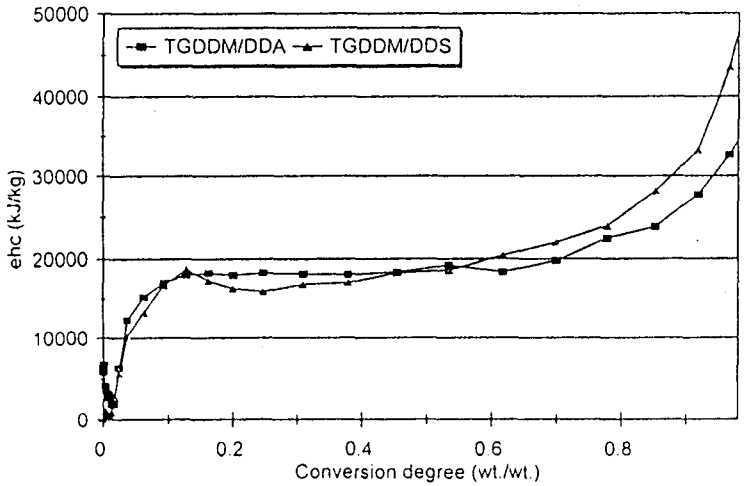

Figure 20. Effective heat of combustion of TGDDM/DDA and TGDDM/DDS vs. the conversion degree.

$0.15 < \alpha < 0.25$ and finally, increases with α. It is to be noted that the ehc of the TGDDM/DDS resin is lower than the ehc of the TGDDM/DDA resin in the conversion range $0.15 < \alpha < 0.55$ and higher when $\alpha < 0.55$.

The curve of the ehc versus the degradation degree of TGDDM/DDA confirms that the curve of rhr is directly related to the weight losses of the systems. The steady state observed in the range $0.15 < \alpha < 0.65$ may be explained by a nearly constant regime of the flame in particular, a constant chemical composition of the fuel, negligible variation of the rate of fuel synthesis and negligible variation of the temperature of the flame and of the corresponding distribution of the selectivities for oxidized products. The beginning of the steady state ($\alpha = 0.15$) corresponds to the plateau in the curves of rhr and weight losses versus the conversion degree and may be explained by the successive formation and presence of the protective material under equilibrium conditions, i.e., the rate of formation of the carbon of interest equals the rate of its degradation.

The sharp increase of the ehc of TGDDM/DDA when $\alpha < 0.80$ corresponds to the extinction of the flame and a post-glowing process. This last process leads to the synthesis of carbon oxides, mainly CO_2 (from a FTIR analysis [5]) from low rate oxidation of the residual "carbon."

The comparison of the ehc values in the two last degradation steps confirms that the consumption of oxygen occurs, at least for a part, in incomplete oxidation (less exothermic) reactions. Several reactions corresponding to incomplete oxidation processes may be considered: formation of the carbon-based char (dehydrogenation, breakdown of the polymer chains-solid fuel and cyclisation), formation of aldehydes, ketones and phenol in the condensed and/or the gaseous phases, formation of tar (growth of large molecular weight polycyclic aromatics hydrocarbons [23]), soot nucleation from tar [24] in the gaseous phase and formation of coke (residue of softening solid fuel).

These products may also be fuel components. They are also concerned in a further combustion process depending on either the presence of catalytic species in the flame or the temperature of the zones of the flame. As an example, partial oxidation of soot occurs at 380°C [25] and its combustion is complete at 765°C [26].

In the cone calorimeter apparatus, the flame admits both a pre-mixed and a diffusion regime. The trends previously observed for the formation of soot from fuel,

- in the premixed conditions: aromatics > alkanes > alkenes > alkynes [27]

- in diffusion conditions: aromatics > alkynes > alkenes > alkanes [28]

show that the presence of aromatic compounds in the "fuel" increases the tendency to form soot and, as a matter of fact, decrease the ehc.

A phenomenological relation between the presence of aromatic groups in DDS and the observed volume of smoke production (vsp) of TGDDM/DDS higher than the vsp of TGDDM/DDA may be proposed (Figure 21), which should explain the corresponding lowest ehc values.

The curve of the ehc versus the degradation degree of TGDDM/DDS shows that the curve of rhr is not directly related to the weight losses of the systems because a stationary state is never deduced from the ehc values of this resin. The formation of the carbonaceous surface material leads ($0.15 < \alpha < 0.25$) to a decrease of ehc linked to the decrease of the rhr and of the weight loss rate. The ehc then increases continuously when the conversion degree increases ($0.25 < \alpha < 0.75$) and becomes higher than the ehc of TGDDM/DDA when $\alpha > 0.05$. In this particular case, the exothermicity of the oxidative process (i.e., the selectivity for complete combustion) is a function of the conversion degree. As this stage, a corresponding chemical process may not be proposed from the results obtained from calorimetry results. When $\alpha > 0.75$, a sharp increase of the rhr of TGDDM/DDS is observed which may be, as previously, assigned to the complete oxidation of "carbon" in the condensed phase (glowing).

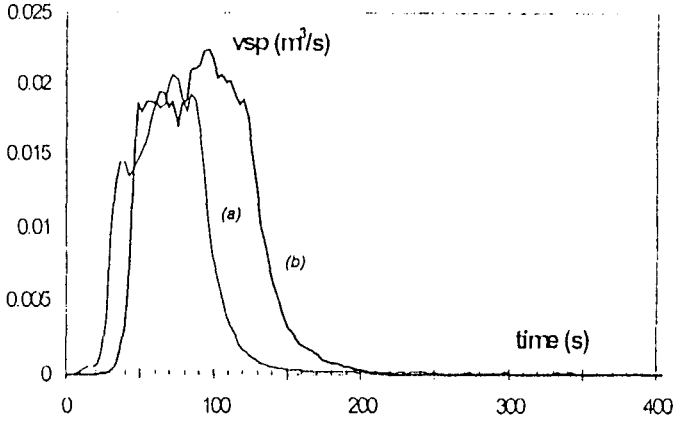

Figure 21. Volumes of smoke production of TGDDM/DDA (a) and TGDDM/DDS (b) vs. time (from N. Rose, Doctoral Dissertation [5]).

The comparison of the TG curves of TGDDM/DDA and TGDDM/DDS under air and nitrogen (Figures 11 and 12) confirms that oxygen plays a part in the formation of a carbonaceous material stable in the temperature range 320–500°C and, then, in the complete degradation of the material in the temperature range 500–650°C.

The oxidative stabilization of a carbonaceous material resulting from the thermal degradation of a resin, previously observed with intumescent thermoplastic polymer formulations [29], has to be discussed by analogy with the oxidative stabilization of pitch [30 and references therein]. Such a stabilization of "carbon" by oxygen remains an area requiring further clarification. Although a great deal of work has been done on the subject, the actual chemical processes [31] involved (changes of kinetics, oxygen functionality, "caged" aromatic radicals) are yet poorly understood.

The DTG curve of TGDDM/DDA in air shows that the formation of the carbonaceous material results from two successive steps in the temperature ranges 250–300°C and 300–450°C. The first step, which is assigned to the formation of a new resin network as previously discussed, is not observed in the DTG curve of TGDDM/DDS, which degrades to give the carbonaceous shield in an apparent single step.

The IKP method allows comparison of the kinetics of the carbonization processes of the two resins which are fuel productive processes. Compensation effects are observed. The compensation effects of this kind are classified, rather, into false or superifical effects [32] resulting from parameter distortion by an inappropriate kinetic model function [33].

The curves of Figure 16 verify that the Arrhenius law is followed. The comparison of the values of the invariant rate constant vs. the temperature may allow comparison of the thermal stabilities and, as a consequence, the fire behaviors of the resins [34]. The sequence $k_{v\ TGDDM/DDA} > k_{v\ TGDDM/DDS}$ agrees well with the sequence $LOI_{TGDDM/DDA} > LOI_{TGDDM/DDS}$ and $rhr_{TGDDM/DDA} > rhr_{TGDDM/DDS}$. So, we may propose once more that this parameter may be selected as a criterion for the classification of the fire performances of polymers.

The computed probabilities distribution of the kinetic functions are well discriminated. Then, the degradation mode

$$f(\alpha) = \sum_{j=1}^{j=16} P_j f_j(\alpha)$$

of the resins may be modelised using the conversion degree α:

$$f(\alpha)_{TGDDM/DDS} = 0{,}77\ S16 + 0{,}23\ S17$$

$$f(\alpha)_{TGDDM/DDA} = 0{,}71\ S16 + 0{,}29\ S13$$

and the thermo-oxidative degradation rates of the resins finally described by the equation:

$$d\alpha/dt_i = A_{inv_i} \exp(-E_{inv_i}/RT) \cdot f(\alpha)_i$$

where the subscript i is the resin considered. The plots of $d\alpha/d_{t_i}$ versus the conversion degree and the temperature (Figure 22) give interesting estimations of the emission of gaseous fuel resulting from the degradation of the resins. The degradation rate of TGDDM/DDA (Curve a) remains, whatever the temperature and the conversion degree, always higher than that of TGDDM/DDS (Curve b). The degradation rates of the two resins decrease with the conversion degree and, as a matter of fact, their degradation may be assumed decelerating (auto-protective) in fire. It may be noticed that identical rates for equal values of the conversion degree are observed with TGDDM/DDA in a temperature range 50–100°C lower than this of TGDDM/DDS. These observations explain the sequences: $\text{rhr}_{TGDDM/DDA} > \text{rhr}_{TGDDM/DDS}$ and $t(\text{rhr}_{TGDDM/DDA}) < t(\text{rhr}_{TGDDM/DDS})$, in which t is the time required to reach the maxima of the rhr values.

The expressions for the degradation rates:
of TGDDM/DDA

$$\frac{d\alpha}{dt} = 3A_{inv} \exp\left(\frac{-E_{inv}}{RT_d}\right)(0.71(1 - \alpha)^{2/3} + 0.29\alpha^{2/3})$$

and of TGDDM/DDS

$$\frac{d\alpha}{dt} = A_{inv} \exp\left(\frac{-E_{inv}}{RT_d}\right)[0.77(3(1 - \alpha)^{2/3}) + 0.23(2/3(\alpha^{-1/2}))]$$

are used to compute T_d (Figure 1)

The knowledge of the values of the conversion degree versus time during the degradation under the conditions of a fire allows the calculation of $d\alpha/dt$, of $f(\alpha)$ and then of the resulting temperature of degradation T_d values versus time.

Figure 23 presents the change of T_d in TGDDM/DDA versus the conversion degree: T_d increases sharply for $\alpha < 0.05$, presents a constant value ($T_d \cong 400$°C) when $0.05 < \alpha < 0.15$, then T_d increases slowly to

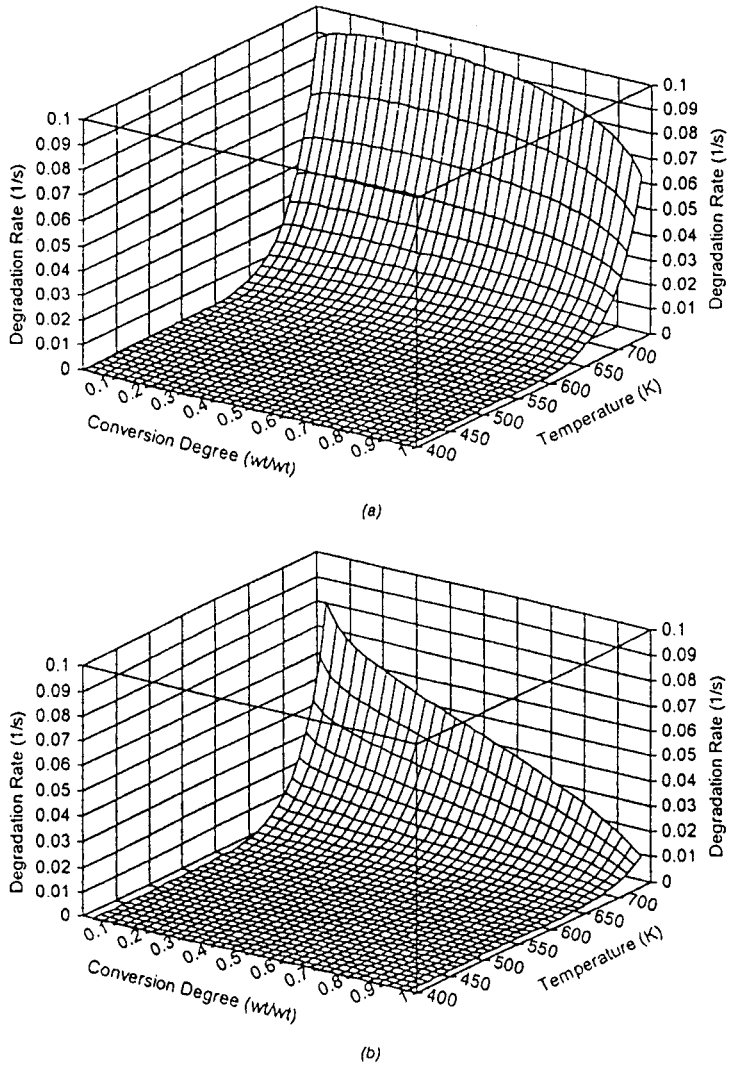

Figure 22. Degradation velocity of TGDDM/DDA (a) and TGDDM/DDS (b) versus the conversion degree α and the temperature.

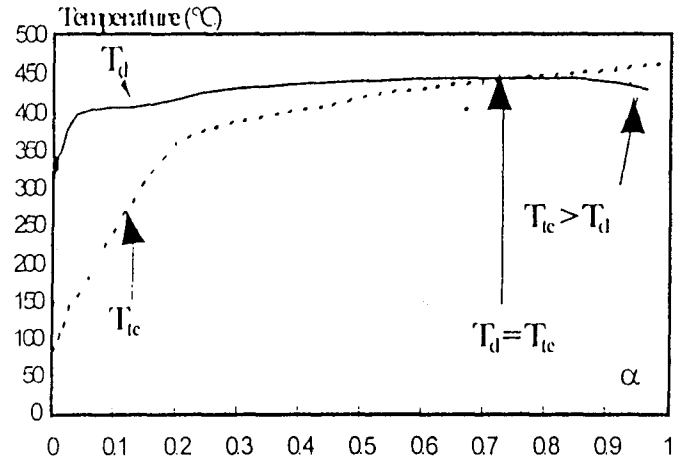

Figure 23. Comparison of the computed temperature of the degradation front T_d and the measured average temperature T_{tc} in the lower 10 volume % of the TGDDM/DDA sample versus the conversion degree.

reach 435 °C and remains close of this value ($0.15 < \alpha < 0.67$). These different ranges of T_d versus α correspond, respectively, as previously discussed, to the formation of a carbonaceous shield, the protection of the "resin" (new polymer network) by this shield, the degradation of the "resin" at a constant temperature corresponding to a balance between the heat transfer in the shield and the chemical heat consumption (pyrolysis and thermo-oxidative process in the resin and eventually in the shield).

The comparison between the computed T_d and T_{tc} shows three successive modes of degradation versus α described in a simplified diagram in Figure 24:

- $T_d > T_{tc}$ and the degradation takes place only in the upper volume of the material if $\alpha < 0.67$.
- $T_d \cong T_{tc}$ and the degradation concerns the whole of the material if $0.67 < \alpha < 0.85$.
- $T_d < T_{tc}$, the lower material is no more protected from the heat (cone and flame) flux and the degradation concerns only the carbonaceous shield (glowing) if $\alpha > 0.85$.

Figure 25 presents the change of T_d in TGDDM/DDS versus the conversion degree: T_d increases sharply for $\alpha < 0.05$ to reach 415 °C,

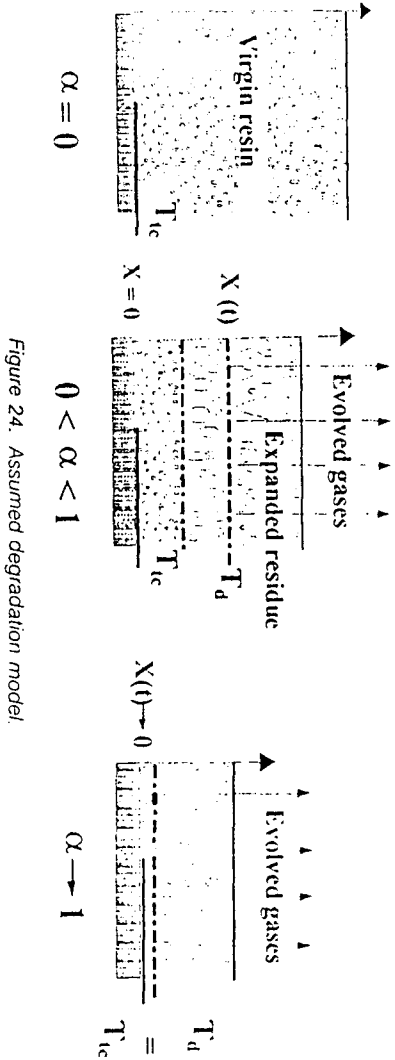

Figure 24. Assumed degradation model.

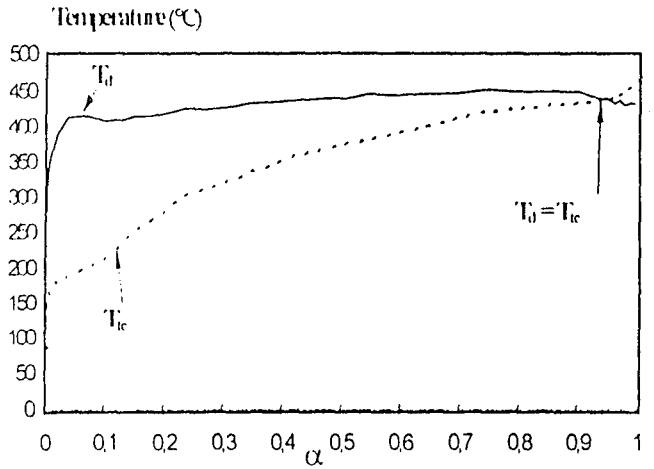

Figure 25. Comparison of the computed temperature of the degradation front and of the measured average temperature in the lower 10 volume % of the TGDDM/DDS sample versus the conversion degree.

decreases to 400°C when $0.05 < \alpha < 0.15$, then T_d increases slowly from 400 to 435°C ($0.15 < \alpha < 0.92$). Each step may be ascribed, respectively, to the formation of the carbonaceous shield and to the degradation of the "resin" corresponding to a balance between the heat transfer in the shield and the chemical heat consumption.

The comparison between the computed T_d and T_{tc} shows two degradation steps versus α:

- $T_d > T_{tc}$, and the degradation takes place only in the upper volume of the material if $\alpha < 0.95$.
- $T_d < T_{tc}$, the degradation concerns the residual "resin" and the carbonaceous shield (glowing) if $\alpha > 0.85$.

The degradation front model allows measurement of the conversion degree (0.67 and 0.92, respectively, with TGDDM/DDA and TGDDM/DDS) and as a consequence, the time for which the protective character of the upper "carbon" shield exists.

Moreover, a comparison of the differences between the values of the computed T_d and measured T_{tc} allows a classification of the protective (at least insulative) character of the carbonaceous shield [as an example: ($T_d - T_{tc}$) measured with TGDDM/DDA and TGDDM/DDS are, re-

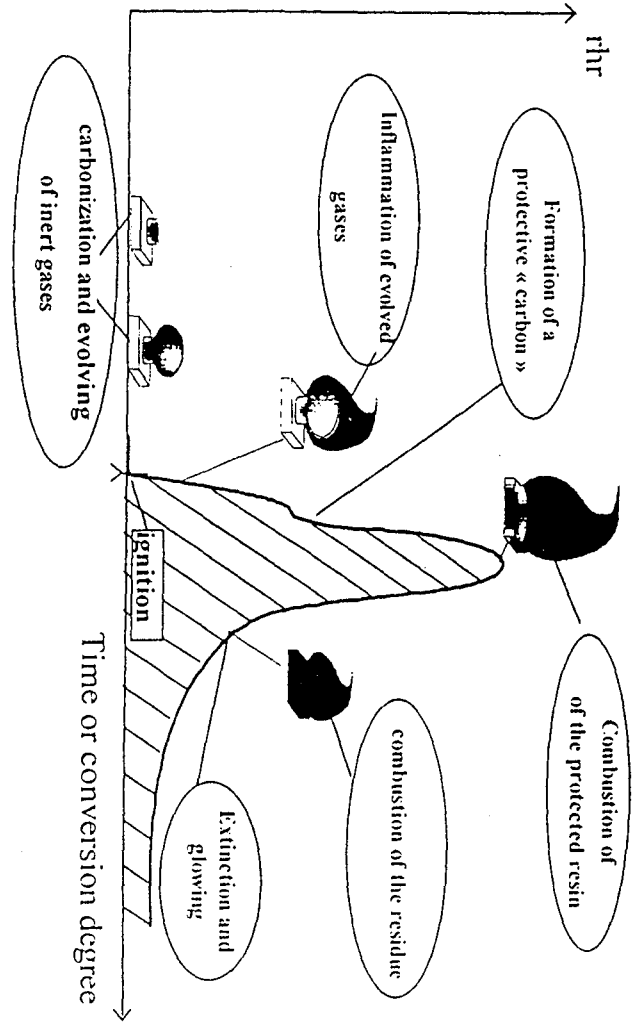

Figure 26. Thermal behavior of an epoxy resin.

spectively, about 50 and 160°C]. The corresponding classification agrees well with the measured LOI and rhr sequences.

CONCLUSION

This work studies the degradation of the model epoxy resins TGDDM/DDA and TGDDM/DDS under the conditions of a fire using the cone calorimeter. Invariant kinetic parameters computed from classical TG data in air and TG data obtained under the conditions of a fire give information on the behavior of resins in a fire. Moreover, the method allows the computation the temperature of the front of degradation for the two resins. The comparison between this temperature and temperatures measured in the material provides information on the advancement of the degradation process and then on the process of the protection of the materials. The effective heat of combustion is an additional tool to appraise the chemical process. In particular, it puts forward the existence of parallel oxidative processes and so defines the regime of the combustion.

From the results of our study, the behavior of the epoxy resins in a fire may be generalized using rhr values according to the scheme reported in Figure 26.

NOMENCLATURE

A_i, apparent pre-exponential factor claculated with 1 $f_i(\alpha)(s^{-1})$
A_{inv} invariant pre-exponential factor claculated with 18 $f_i(\alpha)(s^{-1})$
B_i and I_i parameters deduced from the linear relationship of the compensation at β_i
DDA dicyandiamine
DDS diamino 4-4′ diphenyl sulfone
dW/dt rate of weight loss (kg/s)
E_i, apparent activation energy calculated with 1 $f_i(\alpha)$(kJ/mol)
Einv invariant activation energy calculated with 18 $f_i(\alpha)$(kJ/mol)
ehc effective heat of combustion (kJ/kg)
$f_i(\alpha)$ kinetic function of the reaction
IKP invariant kinetic parameter
K_i invariant rate constant of the system at the temperature $T_i(s^{-1})$
LOI limiting oxygen index (%)
n order of the reaction

rhr rate of heat release (kW/m²)
T_d temperature of the degradation front (°C)
TGDDM *N,N,N′,N′*tetraglycidyl-*r,r′* diamino diphenyl methane
T_{in} temperature inside of the material (°C)
T_i invariant temperature deduced from the compensation effect (K)
W residual weight (wt. %)

Greek Symbols

α conversion degree (kg/kg)
β_i heating rate (°C/min)

REFERENCES

1. Dewprashad, B. and E. J. Eisenbraun. 1994. "Fundamentals of Epoxy Formulations," *J. Chem. Education,* 71(4):290.
2. FAR Part 25 Amendment 25-61, Federal Aviation Administration (1986), FAR Part 25 Amendment 25-66, Federal Aviation Administration, Atlantic City , NJ (1988) and Airbus Directives and Procedures "Fire–Smoke–Toxicity," ABD 0031 Airbus Industrie, Blagnac (1994).
3. Costes, B., Y. Henry, M. R. Buckingham, A. J. Lindsay, D. E. Stevenson, G. Muller, E. Morel, S. V. Levchick, G. Camino, M. P. Luda, L. Costa, P. L. Chambers, C. M. Chambers and A. C. Kennedy. 1995. "Development of New Materials with Improved Fire Resistance, Reduced Smoke and Toxicity (Brite-Euram Progamme 4412)," *Abstracts of Fire Retardant Polymers-5th European Conference,* Salford (September).
4. Rose, N., M. Le Bras, R. Delobel, B. Costes and Y. Henry. 1993. "Thermal Oxidative Degradation of an Epoxy Resin," *Polym. Deg. & Stab.,* 42:307.
5. Rose, N., M. Le Bras, S. Bourbigot and R. Delobel. 1994. "Thermal Oxidative Degradation of Epoxy Resins: Evaluation of their Heat Resistance using Invariant Kinetic Parameters," *Polym. Deg. & Stab.,* 45:387; Rose, N. 1995. "Etude de la Dégradation Thermique et du Comportement au Feu de Résines Epoxydes Utilisées dans l'Aéronautique," *Doctoral Dissertation,* Lille, France.
6. Bourbigot, S., M. Le Bras and R. Delobel. 1995. "Fire Degradation of an Intumescent Flame Retardant Polypropylene using Cone Calorimeter," *J. Fire Sci.,* 13(1–2):3.
7. Babraukas, V. 1984. "Development of Cone Calorimeter–A Bench Scale Heat Release Apparatus Based on Oxygen Consumption," *Fire and Materials,* 8(2):81.
8. Babraukas, V., J. R. Lawson, W. D. Walton and W. H. Twilley. 1982. "Unfoldstered Furniture Heat Release Rates Measured with a Furniture Calorimeter," NBS-IR 82-2604.
9. "Standard Test Method for Measuring the Minimum Oxygen Concentra-

tion to Support Candle-Like Combustion of Plastics (Oxygen Index)," *ASTM D2863/77,* Philadelphia: American Society for Testing Materials.

10. Bente, MP. 1993. "Réactivité à l'état fondu des systèmes époxy-cyanammide-dicyanamide-mélamine, *Doctoral Dissertation.* PAU, France.
11. Costes, B. 1989. "Etude Structurale du Réticulat tétraglycidyle Diamino-diphényle Méthane-diaminodiphényle Sulfone," *Doctoral Dissertation,* Le Mans, France.
12. Babraukas, V. 1982. "Development of Cone Calorimeter–A Bench Scale Rate of Heat Release Based on Oxygen Consumption," *NBS-1R 82-2611,* US Natl. Bur. Stand.
13. Venger, A. E., Y. E. Fraiman, and F. B. Yurevich. 1983. "Applicability of One-Stage Chemical Reaction Kinetic Equation to Describe Non-Isothermal Destruction Processes," *J. Thermal Anal.,* 27:325.
14. Lesnikovich, A. I. and S. V. Levchik. 1985. "A Method of Finding Invariant Values of Kinetic Parameters," *J. Thermal Anal.,* 30:677.
15. Bourbigot, S., M. Le Bras, R. Delobel and D. Normand. 1993. "Comparative Study of the Integral TG Methods Used in the Invariant Kinetic Parameters Method. Application to Fire Retardant Polypropylene," *J. Chim. Phys.,* 90:1909.
16. Grayson, S. J. 1992. "Heat Release in Fire," V. Babraukas and S. J. Grayson, eds., London: Elsevier Appl. Sci., 1.
17. Tewarson, A. 1994. "Flammability Parameters of Materials: Ignition, Combustion, and Fire Propagation," *J. Fire Sci.,* 12:329–356.
18. Tewarson, A. 1988. "Generation of Heat and Chemical Compounds in Fires," in P. J. DiNenno, ed *The SFPE Handbook of Fire Protection Engineering,* pp. 1–179; and Quincy, MA: National Fire Protection Association Press, pp. 1–199.
19. Hugget, C. 1980. "Estimation of the Rate of Heat Release by Means of Oxygen Consumption," *J. Fire and Flammability,* 12.
20. Linan, A. and F. A. Williams. 1993. "Fundamental Aspects of Combustion," A. Linan, ed., New York: Oxford University Press.
21. Gilbert, M. D., N. S. Schneider and W. J. McKnight. 1991. *Macromol.,* 24(2):360.
22. Howard, J. B. 1990. "Carbon Addition and Oxidation Reactions in Heterogeneous Combustion and Soot Formation," *23rd Symp. (Int.) on Combustion,* The Combustion Institute, pp. 1107–1127.
23. Glassman, I. 1990. "Soot Formation in Combustion Process," *23rd Symp. (Int.) on Combustion,* The Combustion Institute, pp. 295–311.
24. Goldenberg, E., M. Prigent and J. Caillod. 1983. "Dépollution des Gaz d'Echappement des Moteurs Diesel au Moyen de Pots Catalytiques," Revue de l'Institut Francais du Pétrole, 38(6).
25. Arques, P. 1992. "Inflammation Combustion–Pollution," Masson, ed., Paris: Collection Technologies, p. 114.
26. Calcote, H. F., D. B. Olson and D. G. Kell. *Energy and Fuels,* 2:494.
27. Schalla, R. L. and R. R. Hibbard. 1959. "Smoke and Coke Formation in Combustion of Hydrocarbon-Air Mixture," Chapter Nine in *NACA Report 1300.*

28. Delobel, R., M. Le Bras and N. Ouassou. 1990. "Fire Retardance of Polypropylene by Diammonium Pyrophosphate-Pentaerythritol: Spectroscopic Characterization of the Protective Coating," *Polym. Deg. and Stab.,* 30:41–56.
29. Drbohlav, J. and W. T. K. Stevenson. 1995. "The Oxidative Stabilization and Carbonization of a Synthetic Mesophase Pitch, Part II: The Carbonization Process," *Carbon,* 33(5):713–731.
30. Yanagida, K., T. Sasaki, K. Tate, A. Sakanishi, Y. Korai and I. Mochida. 1993. *Carbon,* 31:577.
31. Koga, N. and J. Sestak. 1991. "Further Aspects of the Kinetic Compensation Effect," *J. Thermal Anal.,* 37:1103–1108.
32. Koga, N., J. Sestak and J. Malek. 1991. "Distortion of the Arrhenius Parameters by the Inappropriate Kinetic Model Function," *Thermochimica Acta,* 188:333–336.
33. Delobel, R., S. Bourbigot, M. Le Bras, Y. Schmidt and J. M. Leroy. 1993. "Invariant Values of Kinetic Parameters–Evaluation of Fire Retardancy–*Application to the PP-APP/PER System," Makromol. Chem., Macromol. Symp.,* 74:59.

I-3-b. Complément de la discussion de l'étude TG - calorimétrie par consommation d'oxygène de la dégradation des résines

Une étude antérieure de Rose N. [59, 61] concerne l'analyse qualitative et quantitative des gaz émis avant et à l'ignition des 2 systèmes par FTIR couplée au calorimètre à cône [89, 90]. Elle montre que les produits de la dégradation thermique (SO_2, HCN et CH_4 sont les produits sondes rapportés) et de la dégradation thermo-oxydante (CO, CO_2, et l'acroléine) ne sont jamais observés avant l'ignition. La perte de masse préalable correspond donc à la modification de la structure des résines associée à la déshydratation des macromolécules. Les écarts entre les temps d'ignition impliquent donc une stabilité thermique comparativement plus élevée de la structure TGMDA/DDS initiale.

La valeur du flux calorimétrique supérieure à 1000 kW/m^2 de TGMDA/DDA montre que, malgré sa valeur du LOI (25 %), son comportement au feu est mauvais. L'utilisation de cette résine nécessite l'ajout d'adjuvants FR [91] ou la modification chimique de son monomère telle une phosphorylation [92].

Les performances de la formulation de TGMDA/DDS sont médiocres. Leur optimisation doit faire l'objet d'une étude complémentaire considérant tout particulièrement le protocole de réticulation. Une utilisation de cette résine dans l'industrie aéronautique est néanmoins improbable. En effet, la réglementation de la FAA impose comme critère de sélection la valeur maximale du flux calorimétrique 65 kW/m^2 [93], valeur qui interdit à ce jour l'utilisation de tous les matériaux composites à base de résines polyépoxydes.

Par ailleurs, le règlement FAR 25-61 [69] prend en compte la chaleur moyenne dégagée pendant les 120 premières secondes (borne maximale :7800 kJ/m^2) qui permet d'évaluer la contribution d'un matériau au processus de « flash over ». Ce critère n'exclut pas les deux résines TGMDA/DDS et TGMDA/DDA qui présentent des valeurs proches du t.h.e. à 120 s : respectivement 570 et 600 kJ.

Ces résultats sont intéressants car ils permettent de proposer une relation entre la résistance à la chaleur (rhr) et la propriété FR (LOI, temps d'ignition) alors qu'une relation entre la propriété FR et la participation du matériau à un embrasement généralisé n'existe pas.

L'ATG met en évidence une participation de l'oxygène moléculaire à la formation du matériau carboné, plus importante lors de la dégradation de TGMDA/DDS que lors de celle de TGMDA/DDA. Les spectres CP/DD-MAS RMN du ^{13}C des résidus carbonés montrent que l'oxygène est un constituant du matériau polyaromatique stable formé à 380°C avec TGMDA/DDS. Le spectre de ce dernier (Figure I-6) présente, en effet, une bande large, centrée à environ 160 ppm, caractéristique d'une liaison C - O dans une structure polyaromatique [94] toujours présente dans le résidu obtenu à 430°C (limite supérieure de la stabilité du matériau carboné). Il faut signaler qu'une comparaison des intensités relatives des signaux des différentes espèces présentes n'est pas possible dans des échantillons différents. En effet, les spectres sont accumulés en utilisant la technique de la polarisation croisée et les intensités sont en conséquence des fonctions de la concentration en protons proches voisins des C. Par contre, les spectres CP/DD-MAS RMN du ^{13}C du résidu carboné stable, issu de TGMDA/DDA à 350°C, ne présentent pas le signal des espèces oxydées qui n'est observé qu'à la température de début de la dégradation du matériau carboné (Figure I-7). La présence d'espèces oxydées dans le revêtement protecteur implique des propriétés chimiques et physiques différentes du matériau. Une relation phénoménologique entre propriété FR et présence d'espèces oxydées ne peut, bien sur, pas être proposée à partir de cette seule observation ; mais elle mérite d'être considérée lors d'études ultérieures.

L'étude cinétique de la dégradation des résines, avec discrimination des données relatives au processus de déshydratation (valeurs TG retenues dans le domaine de température correspondant aux 20°C précédant le maximum de la vitesse apparente), permet d'évaluer en terme de transfert de matière les dégradations carbonisantes des 2 résines. Elle confirme que la vitesse de dégradation de TGMDA/DDS est inférieure à celle de TGMDA/DDA dans le domaine de température considéré.

Les évolutions des vitesses avec la température et le degré de conversion sont caractéristiques d'une dégradation des deux résines qui conduit, par ablation, à une stabilité thermique accrue des deux systèmes. En effet, les vitesses diminuent en isotherme lorsque le taux de conversion en carbone augmente.

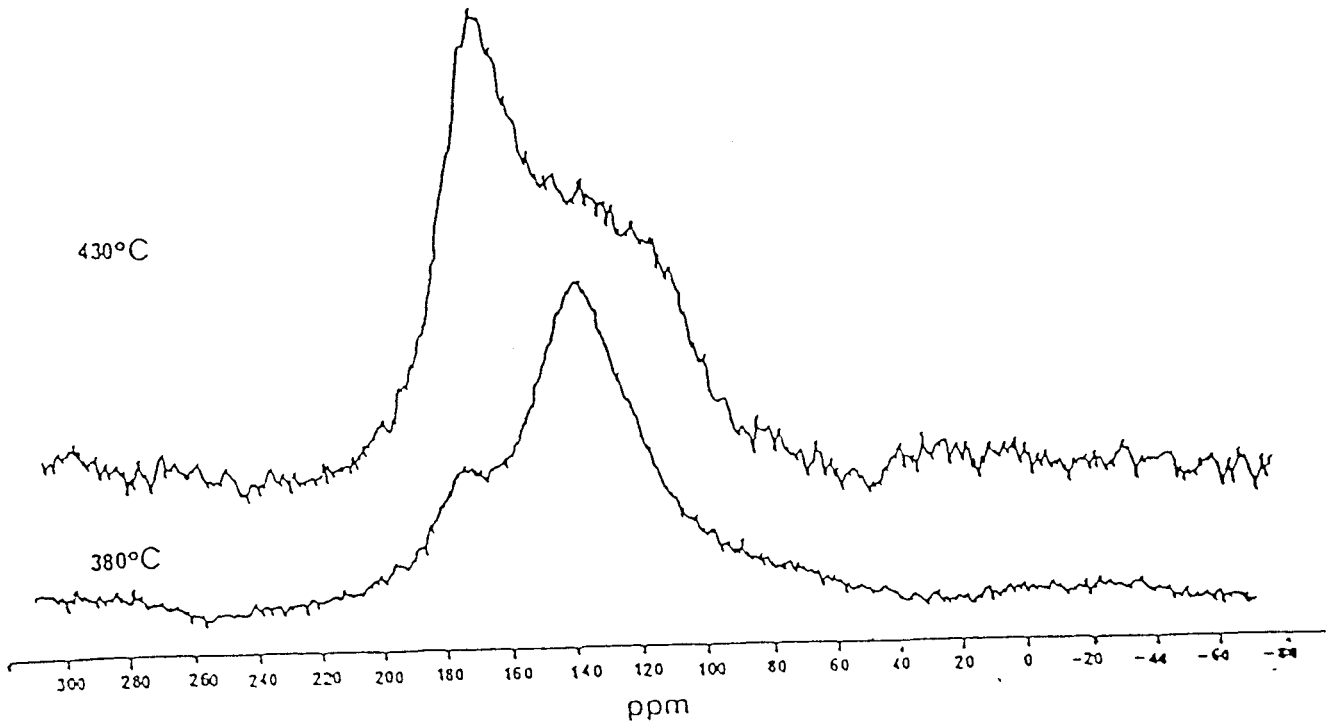

Figure I-6. Spectres CP/DD-MAS RMN du ^{13}C des résidus de TGMDA/DDS obtenus à HTT 380 et 430°C.

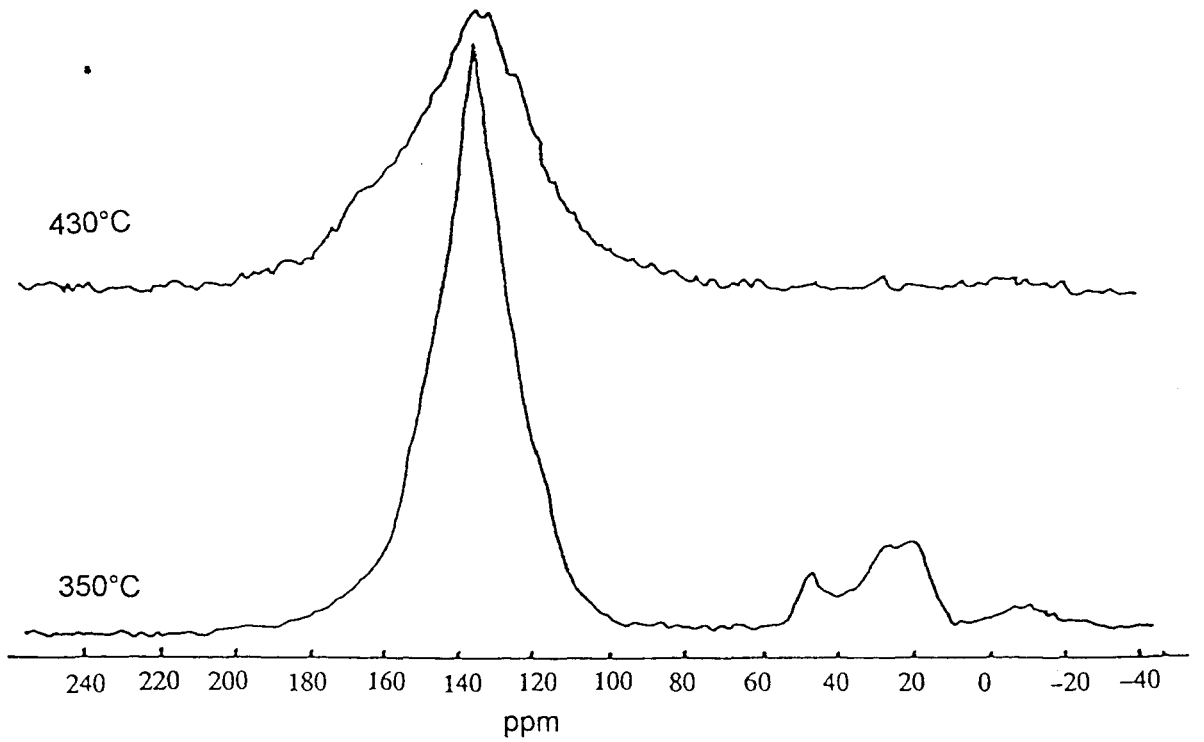

Figure I-7. Spectres CP/DD-MAS RMN du ^{13}C des résidus de TGMDA/DDA obtenus à HTT 350 et 430°C.

Le modèle du front de dégradation est validé par la comparaison des températures mesurées au sein de l'échantillon et de celles calculées en utilisant les paramètres cinétiques invariants. La convergence des deux courbes vérifie la validité des IKP et lève les soupçons sur la représentativité des résultats de l'ATG. L'application du modèle permet de préciser l'influence des comportements thermiques des résines sur leurs stabilités dans les conditions d'un feu. Le modèle montre, en particulier, que les matériaux carbonés issus de TGMDA/DDA et TGMDA/DDS sont des matériaux protecteurs pour les transferts thermiques jusqu'à des taux de conversion des résines en « carbone » de l'ordre de, respectivement, 67 et 95 % pondéral.

Finalement, l'étude propose une représentation schématique (Figure I-8) expliquant les variations du flux calorimétrique lorsqu'un matériau présentant un comportement ablatif est mis en présence d'une source de chaleur. Ce modèle permet d'expliquer les formes complexes (éventuellement plusieurs maximums observés lors de l'étude de matériaux intumescents [23, 39]) par des séquences formation - dégradation et/ou obtention - perte du caractère protecteur du revêtement.

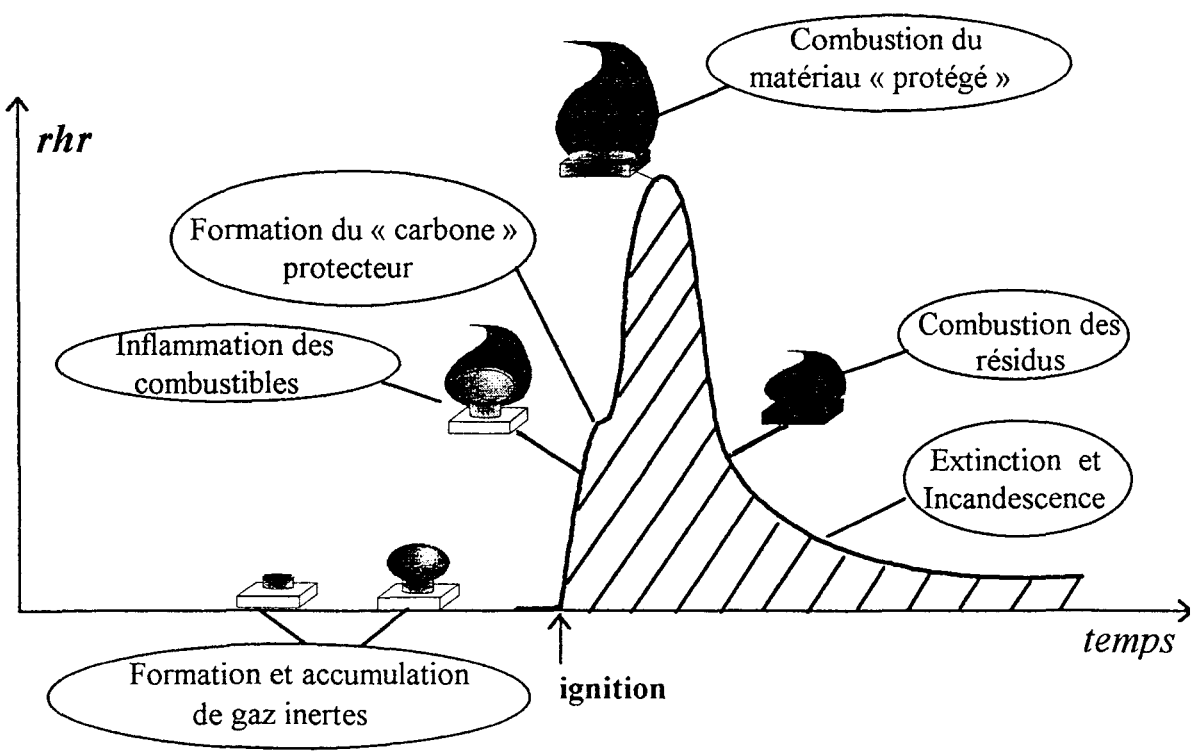

Figure I-8. Comportement thermique d'un matériau apte à la carbonisation.

En conclusion, l'étude comparative des deux résines TGMDA/DDS et TGMDA/DDA montre l'apport des techniques spectroscopiques et de la thermogravimétrie à la compréhension du comportement chimique à la chaleur et au feu de matériaux polymères autoextinguibles ou retardateurs de flamme par un processus de carbonisation.

Les spectroscopies présentées seront utilisées dans la suite de ce travail. Nous utiliserons en complément la RMN basse résolution du proton qui, outre la caractérisation des protons aromatiques, permet par mesure de la diffusion une étude de la structure des matériaux et la spectroscopie de photoélectrons (XPS) qui, outre l'évaluation des teneurs superficielles relatives aux éléments constitutifs, permet d'approcher les réactions chimiques qui se produisent dans les conditions d'un traitement thermo-oxydant ou d'un feu via la caractérisation des liaisons chimiques.

L'étude illustre l'intérêt de la mesure des paramètres cinétiques invariants en utilisant la méthode IKP pour le classement des comportements thermiques des matériaux. Dans la suite du présent rapport, nous discuterons l'existence éventuelle de relations entre ces caractéristiques des matériaux et leurs propriétés FR.

Finalement, elle vérifie la validité du modèle du front de dégradation appliqué aux matériaux aptes à carboniser. Ce modèle sera appliqué pour comprendre et/ou évaluer le mode de protection dans des matériaux intumescents.

CHAPITRE II

CONTRIBUTION A LA COMPREHENSION DU PROCESSUS D'INTUMESCENCE

ETUDE DU MELANGE MODELE (POLYPHOSPHATE D'AMMONIUM -PENTAERYTHRITOL), ADJUVANT DE FORMULATIONS INTUMESCENTES DES POLYMERES THERMOPLASTIQUES.

Le terme français « intumescence » (action par laquelle une chose s'enfle (Littré [95])) est longtemps resté une expression littéraire. A titre d'exemple, Victor Hugo définit la formation des bancs de brume sur la mer comme « l'intumescence de la mer » [96]. Le verbe « To intumesce » est utilisée par le tragédien Elisabéthain John Webster (1580-1624) avec deux significations : « grandir ou augmenter de volume avec la chaleur » ou « présenter un gonflement vers le haut en bouillonnant ». La définition de Webster permet une description tout à fait exacte des performances d'un revêtement ou d'un matériau intumescent qui, chauffés au delà d'une température critique, commencent à fondre en bouillonnant puis en gonflant. Le résultat du processus consiste en une barrière multicellulaire (alvéolaire), épaisse et ininflammable, susceptible de protéger le substrat ou le matériau résiduel de l'action de la chaleur ou de la flamme.

La combustion d'un polymère peut être modélisée classiquement (Figure II-1) en utilisant les travaux de Martel [97] et de Tkac [98].

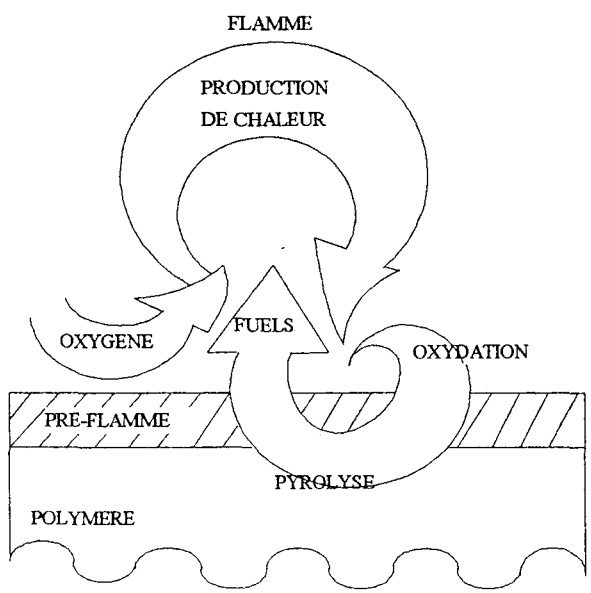

Figure II-1. Modèle de combustion d'un polymère.

La protection des polymères, par développement d'un matériau intumescent à l'interface entre les zones de pré-flamme et de pyrolyse, peut admettre trois modes :

- imperméabilité aux gaz combustibles formés par la pyrolyse du polymère, qui ne peuvent pas en conséquence contribuer au développement de la flamme. L'augmentation des pressions partielles de ces gaz, à l'interface zone de pyrolyse - intumescence, limite en outre la vitesse de la dégradation thermique du polymère,
- imperméabilité aux comburants, en particulier à l'oxygène moléculaire. La diffusion de l'oxygène ne s'effectue pas et la dégradation thermo-oxydante est impossible,
- caractère isolant qui limite le transfert de chaleur de la flamme vers le matériau résiduel. Les vitesses des dégradations thermiques et thermo-oxydantes diminuent.

L'association du CA : Pentaérythritol (PER, $C(CH_3OH)_4$) et du CP : polyphosphate d'ammonium (APP, $-(O - POONH_4 -)_{700}$) conduit à des mélanges d'adjuvants actuellement utilisés pour la formulation de peintures FR. L'utilisation et les performances FR de ces mélanges ont, par ailleurs, été testées dans les thermoplastiques et plus particulièrement dans les éthyléniques [23, 39, 99-101]. La protection est obtenue par développement d'un bouclier charbonneux expansé (Planche 1). Les travaux de notre groupe ont montré que, dans ces matériaux, le rapport pondéral APP/PER = 3/1 permet d'obtenir la propriété FR maximale avec une courbe des LOI, fonction des teneurs relatives en CA et CP, caractéristique d'un effet de synergie. Le tableau II-1 rapporte les valeurs des LOI et les classements UL-94 [102] de différentes formulations intumescentes contenant l'adjuvant à un taux de charge de 30 % pondéral. Il montre que l'adjuvant permet d'obtenir des performances intéressantes, en particulier dans des formulations du PP, du HDPE et du LRAM3.5 qui seront plus particulièrement étudiées dans la suite de ce travail.

Les raisons du manque d'intérêt industriel de ces formulations est maintenant bien connu :il résulte de leur difficulté de mise en œuvre. En effet, un mécanisme thermo-radicalaire conduit, lors de leur mise en œuvre, à une modification des propriétés du polymère initial (couleur jaune à brune [44], modification des masses

moléculaires, perte du caractère thermoplastique [103] et/ou perte des propriétés mécaniques et de l'aptitude à la mise en œuvre [42, 44]). De plus, lorsque la température de mise en œuvre est supérieure à 190°C, une migration des adjuvants ou des produits de leur réaction hors du polymère lors de la trempe ou lors du vieillissement entraîne, outre une modification de la « main » (toucher poisseux), la perte de la propriété FR [42, 45].

Tableaux I-1. Propriétés FR de formulations intumescentes obtenues par ajout du mélange adjuvant APP/PER (charge : 30% pondérale), d'après Alistiqsa et al. [104, 105], Bourbigot et al. [23, 106] et Schmidt - Le Tallec et al. [36, 39].

polymère	PP	PE	LN	FEABu5
LOI (%)	31	30	25	26
UL-94	VO	VO		
polymère	FEABu13	LYABu30	LQVA5	LQVA15
LOI (%)	27	28	29	32
UL-94				
polymère	EVA28	LRAM2,8	LRAM3,5	LYAMe30
LOI (%)	34	27	28	38
UL-94			V0	

***Glossaire** : LN : éthylène (melt index : 0,3 g/10 min), FEABu5 : éthylène (95 %) - acrylate de butyle (5%), FEABu13 : éthylène (87%) - acrylate de butyle (13), LYABu30 : éthylène (70%)- acrylate de butyle (30%), LQVA5 : éthylène (95%) - acétate de vinyle (5%), LQVA15 : éthylène (85%) - acétate de vinyle (15%), EVA28 : éthylène (72%) - acétate de vinyle (28%), LRAM2,8 : éthylène (92,2%) - acrylate de butyle (5%) - anhydride maléique (2,8%), LRAM3,5 : éthylène (91,5%) - acrylate de butyle (5%) - anhydride maléique (3,5%) et LYAMe30 : éthylène (70%) - acrylate de méthyle (30%).*

Cet adjuvant reste cependant un système de référence pour la compréhension et la modélisation de l'intumescence développée par les systèmes additifs et les formulations des thermoplastiques.

L'action du processus d'intumescence peut être illustrée par une étude préalable de la température dans le matériau polymère pendant son auto-combustion. A titre d'exemple, l'étude a été conduite sur une plaque, élaborée à partir de la formulation PP/APP/PER, dans des conditions de combustion « forcée » (après une inflammation 10 s avec un brûleur butane/O_2, l'échantillon brûle sous un

balayage (débit : 1,02 m^3/h) d'air de synthèse de teneur en O_2 : LOI + 4 % volumique). Elle montre que le matériau charbonneux superficiel se forme à 280°C et est conservé pour une température inférieure à 550°C (Figure II-2). Dans les conditions opératoires, une valeur constante de la température de surface (comprise entre 530 et 550°C) est atteinte au bout de 110 s et conservée pendant 60 s. Cette valeur constante s'interprète par l'existence d'un état stationnaire en terme de flux de chaleur provenant de la flamme, qui correspond donc à un flux de matière (gaz combustibles) sensiblement constant. Une étude du profil de la température dans le matériau montre que l'épaisseur du matériau affecté par le processus de dégradation thermique ($T > 320 \pm 10$°C) est de l'ordre de 6/1000 m.

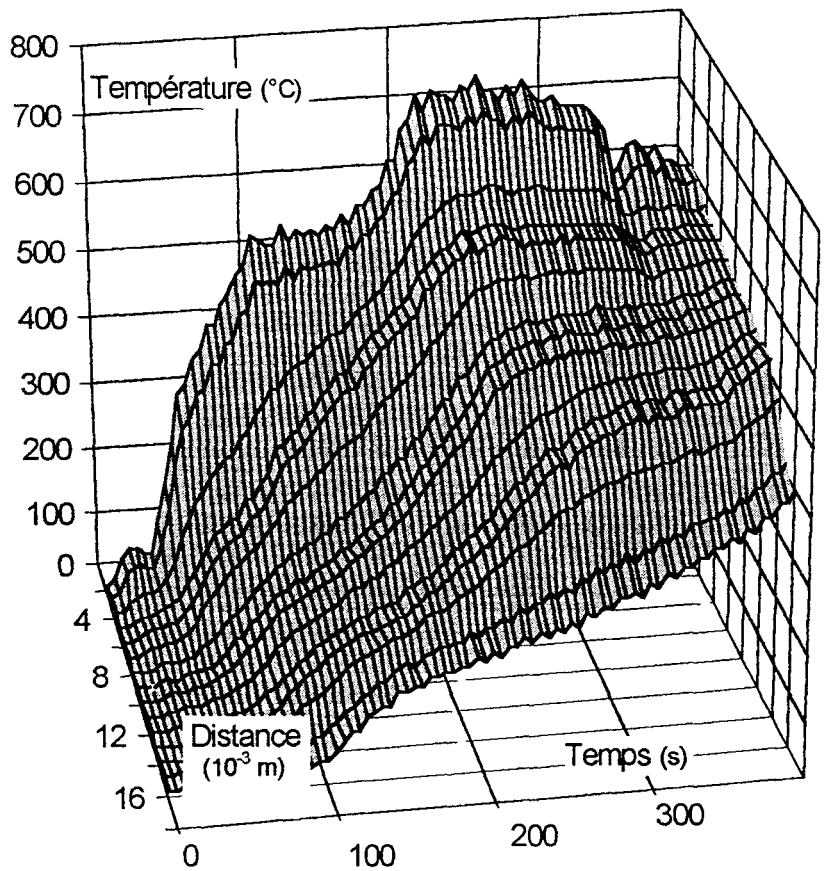

Figure II-2. Profil de la température de surface de PP/APP/PER dans les conditions du feu.

Cette étude préalable montre que le matériau superficiel utile, qui modifie le régime de la combustion de la formulation intumescente, se forme dès 280°C et se conserve aux HTT inférieures à 550°C. Dans la première partie du présent chapitre,

le comportement thermique du mélange APP/PER est considéré dans le domaine de température 280 - 550°C. Nous y portons notre attention sur les transformations des propriétés chimiques et physico-chimiques du matériau qui se développent en fonction de HTT, en considérant plus particulièrement la phase condensée.

La seconde partie du Chapitre concerne le comportement thermique, dans la même gamme de températures, des formulations polymère/APP/PER et plus particulièrement celui de la formulation LRAM3,5/APP/PER, présumé représentatif de la série des formulations étudiées. La comparaison des caractéristiques des solides, produits de la dégradation de la formulation et du mélange d'adjuvants, permet alors de discuter la participation éventuelle d'une matrice polymère à la formation du revêtement intumescent et, en conséquence, à sa protection.

La dernière étude présentée concerne le mécanisme protecteur mis en jeu dans la formulation PP/APP/PER. Une relation entre la propriété FR et les paramètres cinétiques de la dégradation thermo-oxydante est recherchée. Par ailleurs, le modèle du front de dégradation y est utilisé pour expliquer la faible valeur du flux calorifique résultant de la combustion des matériaux intumescents. Le mécanisme ablatif de la protection de tels matériaux est finalement discuté.

II-1. ***Etude de la dégradation thermo-oxydante du mélange des adjuvants,***

Les comportements thermiques du système d'adjuvants et des formulations polymères/APP/PER sont maintenant bien connus sous inerte [107, 108] et dans l'air [36, 39, 104, 109]. Les résultats de l'analyse thermogravimétrique de APP/PER doivent être rappelés. La figure II-2 compare la courbe TG expérimentale de APP/PER ($W_{APP/PERexp}$) avec la courbe TG calculée par combinaison linéaire des courbes TG des adjuvants isolés ($W_{APP/PERcalc}$)

$$(W_{APP/PERcalc} = ¼(3W_{APP} + W_{PER})$$

Elle montre que le de PER ne se sublime pas et qu'une réaction entre les adjuvants et/ou la dégradation des produits de cette réaction conduit à la formation d'un matériau comparativement stable entre 280 et 700°C.

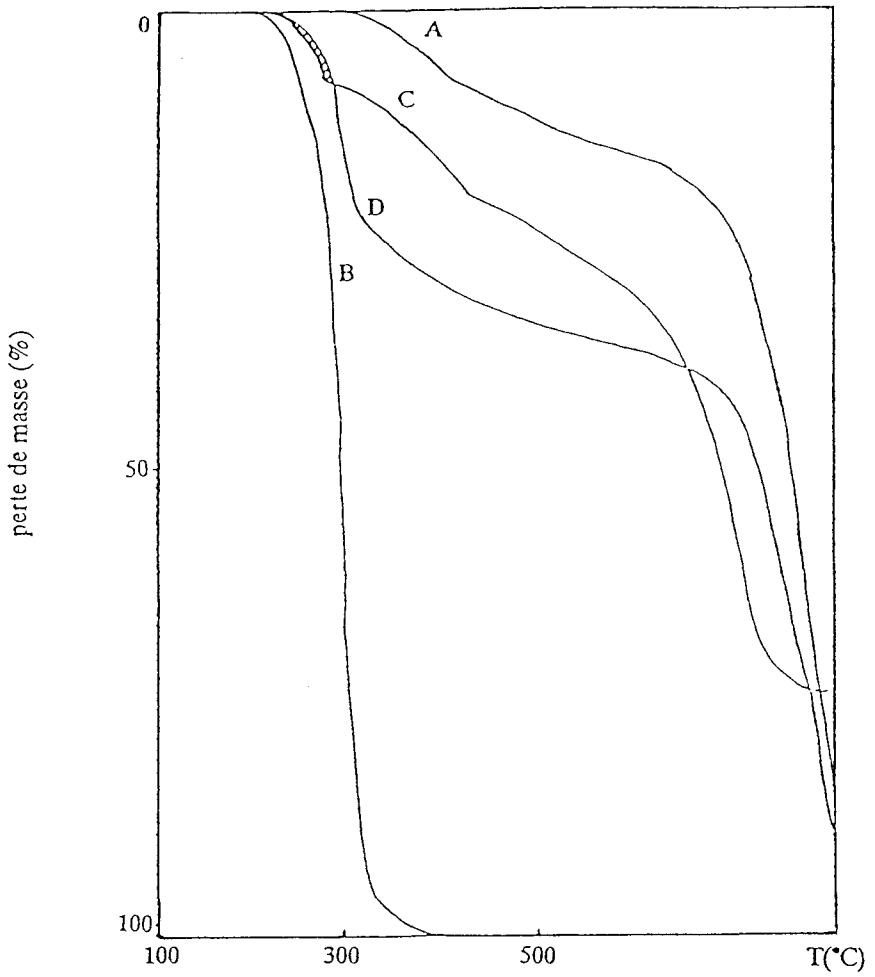

Figure II-3. Courbes thermogravimétriques sous air (β_v = 300°C/h) de APP (A), PER (B), APP/PER (C : $W_{APP/PERexp}$) et courbe calculée de APP/PER (D : $W_{APP/PERcalc}$).

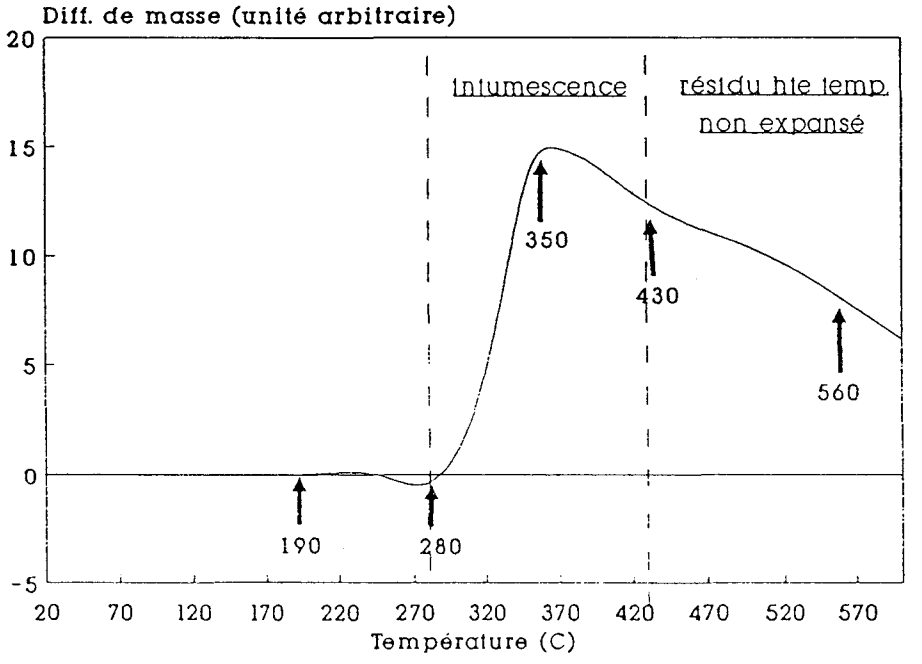

Figure II-4. Représentation schématique de la différence $\Delta W = W_{APP/PERexp} - W_{APP/PERcalc}$ calculée en fonction de la température.

La courbe de la différence ΔW

$$\Delta W = W_{APP/PERexp} - W_{APP/PERcalc}$$

en fonction de la température (Figure II-3) met en évidence trois domaines de température :

- entre 190 et 280°C : la réaction entre les adjuvants se produit avec hydrolyse de la chaîne de APP et formation d'esters des acides orthophosphorique, pyrophosphorique et polyphosphorique. La composition chimique et la structure de ces esters ont été caractérisées par notre Groupe [23, 100, 101, 104] et par Camino et al. [110, 111]. Les résultats de ces études ne seront donc pas discutés dans ce mémoire,
- entre 280 et 350°C, la décomposition du mélange des esters conduit à la formation d'un matériau charbonneux expansé, le matériau intumescent,
- au delà de 350°C, le matériau intumescent se dégrade. Cette dégradation produit un résidu charbonneux non-expansé qui se dégrade lentement via l'oxydation du « carbone » par l'oxygène de l'air et la sublimation de l'oxyde de phosphore (point d'inflexion à environ 560°C).

Les processus chimiques, qui entrent en œuvre lors du traitement thermique du système, peuvent être précisés par l'étude des matériaux solides charbonneux (« char ») ou des mélanges liquide - solide pâteux, obtenus lors d'un traitement isotherme sous balayage d'air aux HTT caractéristiques : 280, 350, 430 et 560°C.

Les données structurales de ces matériaux sont obtenues par la spectroscopie de diffusion Raman qui définit le stade de la « pré-graphitisation » du matériau carboné, la XRD qui précise la taille des domaines ordonnés et la DSC qui, par mesure des températures de transition vitreuse (T_g), peut mettre en évidence des phases de différentes structures.

L'analyse chimique permet ensuite de connaître la composition globale des échantillons. Une étude XPS y caractérise les différences entre les teneurs globales et les teneurs de « surface » des matériaux et les environnements chimiques des éléments dans le matériau, en portant une attention toute particulière à ceux de l'azote. La RMN des solides (CP/DD-MAS RMN du ^{13}C, MAS RMN du ^{1}H et DD-MAS RMN du ^{31}P) complète la caractérisation chimique. L'ensemble de l'étude doit

permettre une description de l'arrangement des structures phospho-carbonées qui composent les matériaux. La comparaison des matériaux permettra finalement de proposer des relations composition - propriétés dynamiques des matériaux.

II-1-a. Résultats et discussions

Savjetovanje POLIMERNI MATERIJALI SMANJENE GORIVOSTI
Conference Flame Retardancy of Polymeric Materials
Opatija, 18. i 19. listopad/October 1990.

AMONIJ POLIFOSFAT-PENTAERITRITOL KAO DODATAK ZA SMANJENJE GORENJA: STRUKTURNA SVOJSTVA "UGLJIKA" U NABUBRENIM SLOJEVIMA
Ammonium Polyphosphate-Pentaerythritol Fire Retardant Additive: Structural Characterization of "Carbon" in the Intumescent Coating

René DELOBEL
Serge BOURBIGOT
Michel Le BRAS
Jean-Marie LEROY

LABORATOIRE DE PHYSICO-CHIMIE DES SOLIDES
Villeneuve d'Ascq Cedex,
Francuska

Prijevod: Branimir KANOVNIK, ELKA, Zagreb

Izlaganje na znanstvenom skupu

SAŽETAK

Studija se bavi odredivanjem svojstava nabubrenih materijala na osnovu ugljika koji nastaju pouglji-vanjem amonij polifosfata - pentaeritritola. prikazuje se nastajanje i rast kuglica medufaze koje dovode do stanja predugljenjivanjem, a time i porasta anizotropije materijala kada temperatu-ra toplinske obrade poraste. Dan je odnos izmedu zaštitnog karaktera sloja ugljika i anizotropije njegove strukture.

SUMMARY

The study deals with characterization of the intu-mescent carbon-based material arising from ammonium polyphosphate - pentaerythritol additives via a carbonization process. It shows the formation and the growth of mesophase spherules leading to a pregraphitization state and, therefore, the increase of the anisotropism of the resulting material when the temperature of the thermal treatment increases. A relation between the protective character of the carbon - based shield and the anisotropy of its car bonaceous structure is proposed.

Traduction anglaise de "Savjetovanje POLIMERNI MATERIJALI SMANJENE GORIVOSTI
Conference Flame Retardancy og Polymeric Materials
Opatija, 18. i 19. listopad/October 1990

INTRODUCTION

Polyphosphates-polyols mixtures are used as fire retardant additives in polyethylene-based formulations because, contrary to the commercial antimony oxide-halogenated hydrocarbon mixtures, they do not release any toxic or corrosive agent in the conditions of fire. Previously it has been proposed that the protection of materials containing these additives is provided by carbon-based shields which result from an intumescent phenomenon [1][2].

In a previous paper [3], it has been shown that, in the particular case of polypropylene(PP)-based formulations, the protection of the polymeric matrices may be provided by two different carbon-based coatings on the undecomposed bulks. These two coatings result respectively from the intumescence process arising from the phosphate-polyol mixtures and from the reaction of oxidized products of the thermo-oxidative degradation of the polymer with the additives and (or) their degradation products.

The present paper deals with the additive mixture: ammonium polyphosphate (PPA)-pentaerythritol (PER) (PPA/PER = 3 (wt/wt)) which presents the highest synergy effect on the fire retardant performances of (PP-PPA-PER) formulations. With these formulations, it has been shown that the protective coating consists only in the carbonaceous structure resulting from a reaction between the additives. Moreover, the protective character is only observed at temperatures lower than 430°C.

The loss of the protective character of the coating may be related either to the disappearing of the acidic phosphate species, catalysts for the formation of a carbon-based shield [4], or to structural changes of this carbonaceous material.

This paper studies the structures of the carbon-based material which forms from (PPA-PER). It includes D.S.C., Raman spectroscopy and X.R.D. results. The aim of this study consists in establishing a relationship between structural changes of the material and the loss of the protective character of the shield.

EXPERIMENTAL

The commercial sample of PP (powder) was supplied by Atochem and the PER was Prolabo grade. The procedures for the characterization of the raw materials and the preparation of the initial mixtures have been described previously [3].

The D.S.C. measurements were obtained by using a NETZSCH 444 unit. Samples (15 mg in a sealed aluminium pan) were heated in flowing air at a rate of 7.5 °C x mn^{-1}. An empty aluminium pan was used as a reference. To determine the glass transition temperature (T_g), samples were first heated at respectively 190, 280, 350 and 430°C and then cooled at room temperature. After this treatment the samples were heated at 430°C (heating rate: 7.5°C x mn^{-1}).

The Raman study was performed using a Raman microspectrometer with spectrographic dispersion and multichannel detection (XY-DILOR). An optical beam produced by a continuous wave argon laser ($\lambda = 5.145 \times 10^{-7}$ m) enters in a microscope and is focused on the sample surface (power at the level of the sample = 4mW). Under these conditions, it is then possible to examine sample area as small as 10^{-12} m^2 and, therefore, to obtain informations on the local

arrangement of the sample [5].

The X-ray diffraction spectra were recorded using a Philips spectrometer (scan rate: $1° \times mn^{-1}$, $K_{\alpha Cu}$ ($\lambda = 1.540598 \times 10^{-10}$ m)). The average particle diameter d of the crystalline carbonaceous species was measured by the line-broadening of the conventional 002 peak in carbon and graphite material [ ] using the simplified Scherrer formula [6]:

$$d = Gt = Gk\lambda \, (\beta_{1/2} \, Cos \, \theta)^{-1}$$

with t: the thickness of the crystallites,

λ: the incident X-ray wavelength,

$\beta_{1/2}$: the full breadth at half maximum (in 2θ radians)

k = 0.89 (Scherrer constant in the hypothesis of a gaussian shape of the diffraction ray),

G = 4/3 (geometric factor corresponding to the hypothesis of a spheric geometry of the crystallites).).

A value of interlayer spacing of carbon lower than 0,344 nm implies the existence of a graphitization process. The graphitization level may be obtained according to Mazza et al [7] using the relation :

$$g = \frac{3{,}44 - d_{002}}{3{,}44 - 3{,}354}$$

RESULTS AND DISCUSSION

The TG analysis of (PPA-PER) under air (Fig.1) characterizes 4 domains previously discussed [3]:

- in the temperature range : $190 < T < 280°C$, a reaction between the additives occurs and the presence of trapped free radicals [1] proves the beginning of a carbonization process,
- in the temperature range : $280 < T < 350°C$, the intumescence process takes place,
- in the temperature range : $350 < T < 430°C$, the degradation of the intumescent coating can be observed,
- at higher temperatures, the formed carbonaceous residue remains stable up to 600°C.

The D.S.C. curve (Fig. 2) shows a sharp endothermic peak at 200°C which may be ascribed to an esterification process leading mainly to the "spiro" structure [8] [9]. The next endothermic phenomenon between 270 and 300°C may be ascribed to the

degradation of the esters leading to the formation of polyaromatic structures [10]. The last exothermic phenomenon observed at 350°C may then be ascribed to the degradation of the intumescent structure.

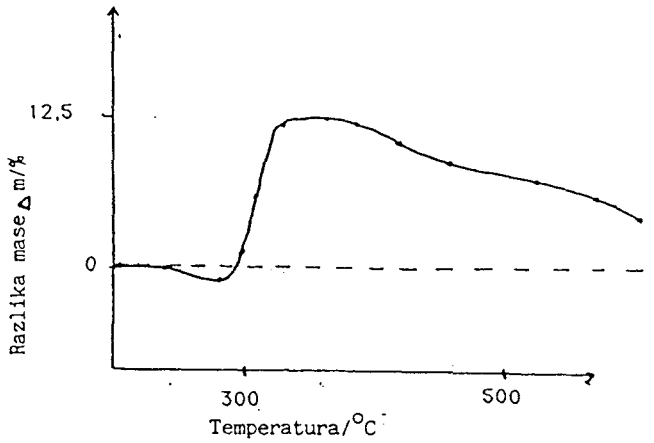

Figure 1. Differences between the experimental TG curves of (PPA-PER) and the curves calculated in the hypothesis that the thermal decompositions of PPA and PER are independent.

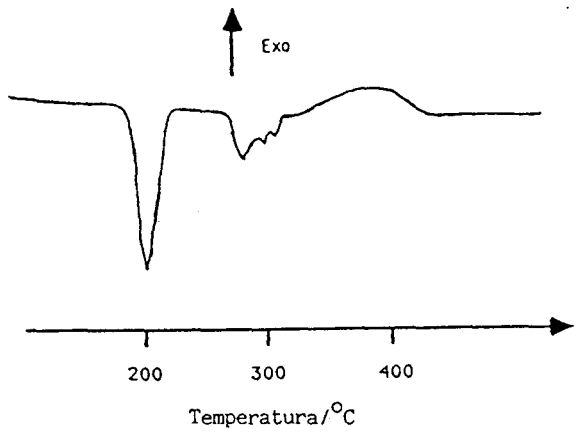

Figure 2. D.S.C. curve of (PPA-PER) in air.

Figure 3 presents the D.S.C. curves of the carbonaceous materials obtained at each characteristic temperature and Table 1 summarizes the observed T_g values..A glass transition temperature shows the frontier between the glassy and the softening states. The results show then the vitrous character of the coatings obtained when T > 280°C. Three different Tg are observed with every sample. It may be proposed that the coatings are mixtures of at least three polymers. This hypothesis has been previously confirmed by a ^{13}C CP/MAS solid state N.M.R. study which shows a broad line between 120-130 ppm corresponding to polyaromatic species [10].

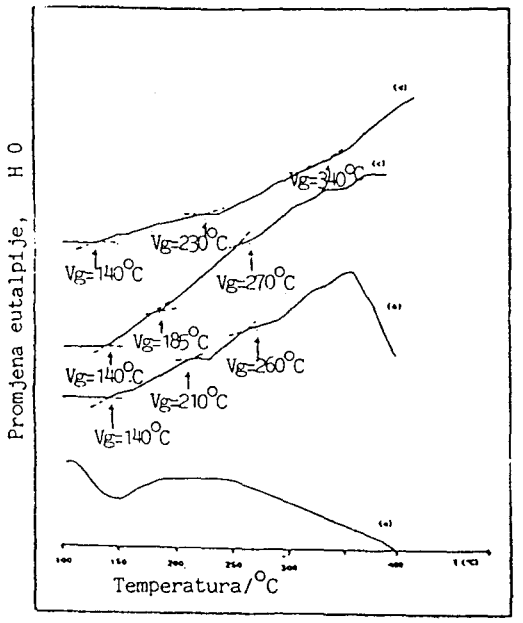

Figure 3: D.S.C. curves of the carbon-based materials obtained by a thermal treatment of (PPA-PER) in air at respectively 190°C (a), 280°C (b), 350°C (c) and 430°C (d).

Moreover, the Raman spectra of the samples obtained at temperatures higher than 190°C exhibit two broad bands around 1580 cm^{-1} and 1350 cm^{-1}, whereas a continuous background is observed for the sample heat-treated at 190°C (figure 4).

The diffusion band observed at 1580 cm^{-1} corresponds to the E_{2g} vibrational mode (C-C vibration in an aromatic layer) and the band at 1350 cm^{-1} is usually the so-called "defect band". These two broad bands are characteristic of a pregraphitic structure involving the presence of mesophase [5] [11] which allows to explain how isotropic pitches transform to anisotropic carbons [11] [12]. Generally, when carbon-based materials are heat-treated in the range: 300°-500°C, mesophase precipitates from the isotropic phase in the form of anisotropic spherules [13]. The anisotropic spherules which form during the initial stages of mesophase consist of stacks of molecules (polyaromatic species according to the previous ^{13}C N.M.R. study) which are arranged in parallel layers within the sphere [14].

The Raman microspectroscopy study confirms (at least at 280°C) the carbonization process of the esters resulting from the reaction between the two additives and reveals furthermore the presence of an anisotropic phase in the resulting materials.

Table 1. Glass transition temperatures of the carbon-based materials obtained by the thermal treatment of (PPA-PER).

treatment temperatures (°C)	Tg (°C)
190	/
280	140 210 260
350	140 185 270
430	140 230 340

The X.R.D. spectra of the samples heat-treated at 280°C and 350°C show only a broad band which is characteristic of the isotropic phase (figure 5). With samples heat-treated at 430°C and 560°C, the spectra exibit diffraction peaks at θ = 12.25° and 13.25° which correspond respectively to the d_{002} values: 0.367 and 0.337 nm.

From these results, it may be concluded that, after the treatment at 560°C, the sample is already in a pregraphitization state. The g value (0,78) allows to propose a probability of $P = g^2 = 60\%$ for the distance between two polyaromatic layers of d_{002} =0.337 nm [7].

The mesophase in the samples treated at 280°C and 350°C is not observed by X.R.D.. This result implies that their crystallite sizes are lower than 5 nm. When treated at 430°C and 560°C, the samples show $\beta_{1/2}$ values of the d_{002} ray (respectively 0.2 and 0.15°) which correspond to average spherule diameters respectively of 55 and 75 nm.

These results show therefore that the spherule size increases sharply when the temperature.of the treatment of (PPA-PER) increases. As previously proposed by

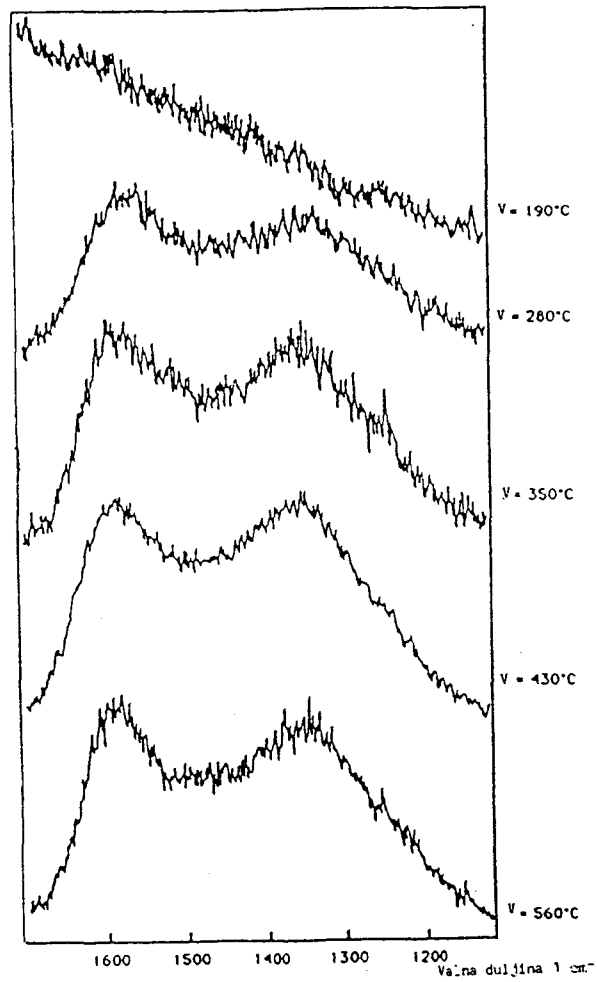

Figure 4. Raman spectra of the carbon-based materials obtained by thermal treatments of (PPA-PER) in air.

Singer and Lewis [15], this phenomenon may be explained by a coalescence process of the spherules as shown in the figure 6.

As a conclusion, the present study shows unambiguously the formation and the growth of mesophase spherules leading to a pregraphitization state and, therefore, the increase of the anisotropism of the resulting material when the temperature of the thermal treatment of (PPA-PER) increases (graphitization about 78 % at 560°C).

The loss of the protective character of the carbon-based shields resulting of (PPA-PER) at 430°C has been previously reported. From the present study, a relation between its protective character and the anisotropy of its carbon structure may be proposed. The loss of the protective character may then be explained by a change of the mechanical properties of the shield which results from the structural change and may lead to the existence of cracks in the material. In that last case, these cracks allow the existence of a polymeric matrix-air interface and then the development of the thermo-oxidative degradation of the polymeric material.

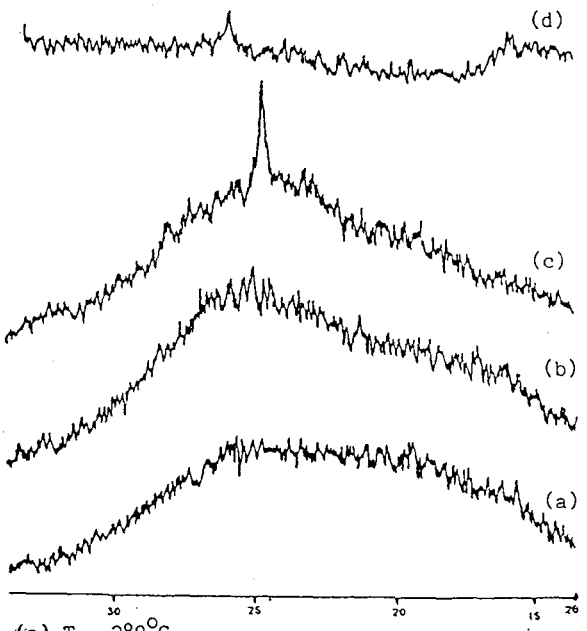

Figure 5. X.R.D. spectra of the carbon-based material resulting of (PPA-PER).

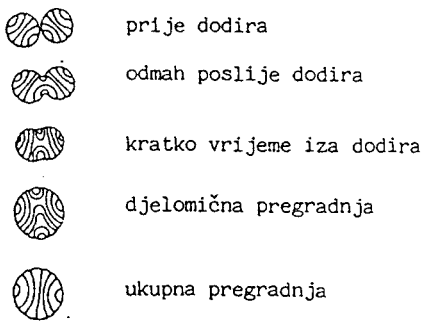

Figure 6. Schematic diagram of the collision and coalescence of mesophase spheres.

1. H.L. VANDERSLL, J. Fire and Flamm. (1971. 2,97
2. R. DELOBEL, et al: Polym Deg & Stab., 23,349 (1990)
3. R. DELOBEL et al: J.Fire Sci (u tisku)
4. R. DELOBEL et al: Polym, Deg & Stab (u tisku)
5. P. LESPADE et al: Caron 22 (1984) (4-5), 375
6. J. L. LEMAITRE, et al: "Heterogeneous Catalysts" Volume 15 F. DELANNAY ed., M.DEKKER, New-York (1984) 299.
7. M. MAZZA, et al: J. Chim. Phys (1964) 729
8. V.PAROPRSTY et al: Mag.Reson in Chem 23(1),122 (1985)
9. R.DELOBEL et al: "Proceed, of the 3rd Meeting on Fire Retardant Polymers", G.CAMINO et al.ed.,A.I.M. pub., Turin, 1989, 28
10. M.LE BRAS et al: Bull.Soc.Chim.Belges, 98(9-10) 349 (1989)
11. J.D.BROOKS and G.H.TAYLOR: Carbon 3,185 (1965)
12. L.S.SINGER, Farad.Discuss: Chem.Soc. 79,265 (1985)
13. R.A.GREINKE and L.S. SINGER: Carbon 5, 665 (1988)
14. I.C. LEWIS: J.Chim Phys. 81 (11-12) 751 (1984)
15. I.C. LEWIS and L.S.SINGER: Appl.Spectr. 36 1 52 (1982)

Carbon, Vol. 31, No. 8, pp. 1219–1230, 1993
Printed in Great Britain.

0008-6223/93 $6.00 + .00

CARBONIZATION MECHANISMS RESULTING FROM INTUMESCENCE ASSOCIATION WITH THE AMMONIUM POLYPHOSPHATE-PENTAERYTHRITOL FIRE RETARDANT SYSTEM

SERGE BOURBIGOT, MICHEL LE BRAS and RENÉ DELOBEL
Laboratoire de Physicochimie des Solides, E.N.S.C.L., Université des Sciences et Technologies de Lille, BP 108, F-59652 Villeneuve d'Ascq Cedex, France

(*Received* 4 *March* 1993; *accepted in revised form* 10 *May* 1993)

Abstract—In this work we study the thermal behavior of an ammonium polyphosphate-pentaerythritol mixture, fire-retardant additive for polyolefins, and most particularly the carbonization process resulting from an intumescent phenomenon. The study has been carried out using Micro-Raman and ^{13}C, ^{1}H, ^{31}P NMR of the solid state spectroscopies. It is shown that the structure consists in phoscarbonaceous and polyaromatic species. These latter form an anisotropic structure above 280°C. This structure grows when the temperature increases. Finally, a reactional scheme of the carbonization of the intumescent system is proposed.

Key Words—Intumescence, ammonium polyphosphate/pentaerythritol, Raman microspectroscopy, MAS NMR ^{13}C, ^{1}H, and ^{31}P.

1. INTRODUCTION

The easy combustion of synthetic materials and thermoplastics in particular has led to the development of fire-retardant (FR) systems. One new direction of research is to develop systems leading to the formation of an intumescent shield (expanded carbon-based structure[1] that limits the heat transfer from the flame to the material. A theoretical model of heat transfer proposed by Anderson *et al.*[2] leads us to conclude that the low thermal conductivity of intumescent char results from the insulating abilities of pockets of trapped gas within a porous char material. Trapping of the gases resulting from the thermal degradation of FR formulations needs a char with particular dynamic properties (viscous "solid" material).

The study of the carbonization mechanisms leading to intumescent phenomena appears essential in order to formulate new FR thermoplastics-based systems[3,4]. The first step of such a study is the chemical characterization of the "solid" char. This work has been realized on the ammonium polyphosphate (APP)-pentaerythritol (PER) intumescent system. These additives are widely used in paints and polyurethane foams[5], and may be used in thermoplastics such as PP [2–6] or PE[4–7]. A previous paper proposed that the carbonization process of the system occurred via several steps[8]. From 190°C, there is reaction between the additives, leading to a phosphate ester. Between 280°C and 350°C, development of intumescence occurs, and between 350°C and 430°C, there is degradation of this intumescent coating. At higher temperatures, there are structural changes leading to the formation of a new carbonaceous species (established in the temperature range $430°C < T < 450°C$).

It has been previously shown that the protective property of the charring material is no longer observed above 430°C[9,10]. The aim of this study is to characterize the carbonaceous structure of the precursor of the intumescent char, and to explain the chemical change of the carbon-based materials, which leads finally to loss of the protective character. This characterization was carried out using Micro-Raman spectroscopy and NMR of the solid state.

2. EXPERIMENTAL

2.1 *Material*

Raw materials were PER (Aldrich R.P. grade) and APP ($(NH_4PO_3)_n$, $n = 700$, Hoechst Exolit 422, soluble fraction in H_2O: < 1 wt%). The study has been carried out using the APP/PER mixture for the ratio APP/PER = 3 (wt/wt). In the case of the polyethylenic materials, the fire-retardant properties are maximum for this ratio[2,6]. Initial mixtures were first prepared by ballmilling after mechanical grinding and sifting (200×10^{-6} m) of the raw materials. They are then treated at five different temperatures (190, 280, 350, 430, and 560°C) during 12 hours under air flow (flow rate = 6 cm^3/s). This delay was chosen because it had been shown in a previous work[11] that the weight loss of the sample became equal to zero between 10 and 12 hours.

2.2 *Chemical analysis*

Table 1 presents the chemical composition of the samples heat treated at 280, 350, 430, and 560°C.

Table 1. Chemical analysis of the APP/PER samples heat treated at 280, 350, 430, and 560°C

Temperature (°C)	C (at.kg^{-1})	H (at.kg^{-1})	N (at.kg^{-1})	O[a] (at.kg^{-1})	P (at.kg^{-1})
280	12	39	6	30	8
350	21	35	5	26	7
430	19	30	4	27	8
560	31	25	4	22	6

[a]Obtained by difference.

2.3 *Micro Raman spectroscopy*

Raman microprobe examination was performed with a Raman microspectrometer having spectrographic dispersion and multichannel detection (Microdil 28—Dilor). An optical beam produced by a continuous-wave argon laser enters a microscope and is directed onto an objective that focuses it to a one-micrometer spot on the sample surface. To avoid sample heating, the power was kept below 4 mW. Subsequent visual examination of the surface was made systematically in order to check that no alteration had occurred around the focal point. In a typical experiment, the experimental conditions are a laser beam wavelength of 514.5 nm and a spectral slit width of 9 cm^{-1}.

2.4 *NMR measurements*

^{13}C NMR measurements were performed on a Brucker CXP100 weak field spectrometer at 25.2 MHz (2.35 T) with magic-angle spinning (MAS), high-power ^{1}H decoupling, and ^{1}H–^{13}C cross polarisation (CP). The Hartmann-Hahn matching condition was obtained by adjusting the power on ^{1}H channel for a maximum ^{13}C FID signal of adamantane. All spectra were acquired with a single contact time of 5 ms, because it has been shown that the intensities of the bands of the samples heat-treated at 280 and 350°C were near to their maxima, and those of the samples heat-treated at 430 and 560°C were at maximum[12]. A repetition time of 10 sec was used for all samples, because the spin-lattice relaxation time (T_1) always stayed below 2 sec at all temperatures (the repetition time is chosen to be five times T_1)[12]. Typically 10000 scans were necessary to obtain spectra with a good signal/noise ratio, and the reference used was the tetramethylsilane (TMS).

^{1}H NMR measurements were obtained at 100.1 MHz on the same spectrometer with MAS and a repetition time of 2 sec (T_1 always below 300 ms)[12]. All spectra were acquired with 20 scans, and the reference used was the TMS. The deconvolution of the spectra has been carried out using the software Peakfit (Jandel Scientific), assuming either Gaussian or Lorentzian bands.

^{31}P NMR measurements were performed at 40.5 MHz on the same spectrometer with MAS, with high-power decoupling protons and a repetition time of 2 sec (T_1 always below 300 ms)[12]. All spectra were acquired with 500 scans. The reference used was 85% H_3PO_4 in aqueous solution.

All spectra of the solids were obtained at the spinning speed of 3 kHz.

3. RESULTS AND DISCUSSION

3.1 *Micro Raman spectroscopy*

Raman microspectroscopy has been used to characterize carbonaceous species. Figure 1 shows the diffusion spectra of the samples treated, respectively, at 190, 280, 350, 430, and 560°C.

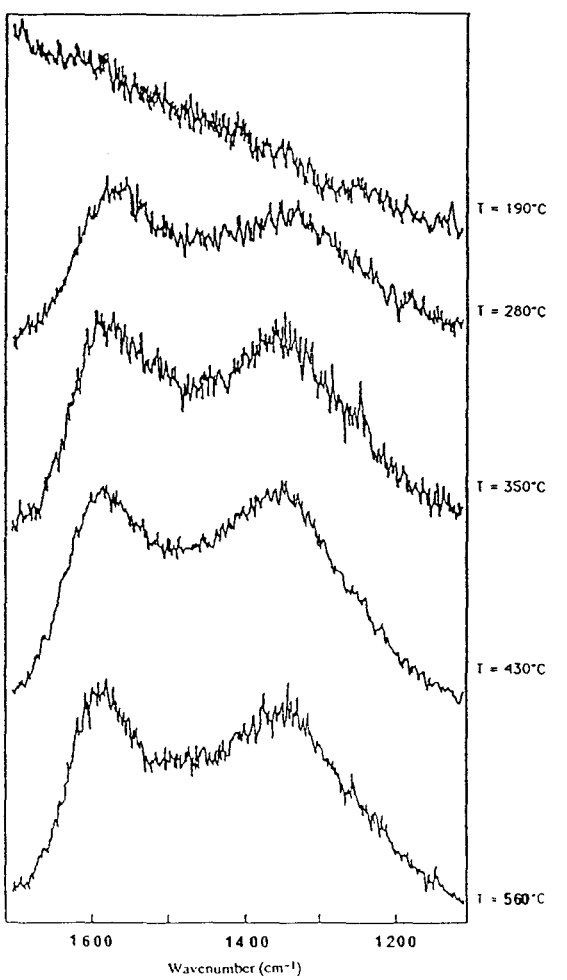

Fig. 1. Raman spectra of the APP/PER samples heat-treated at 190, 280, 350, 430, and 560°C.

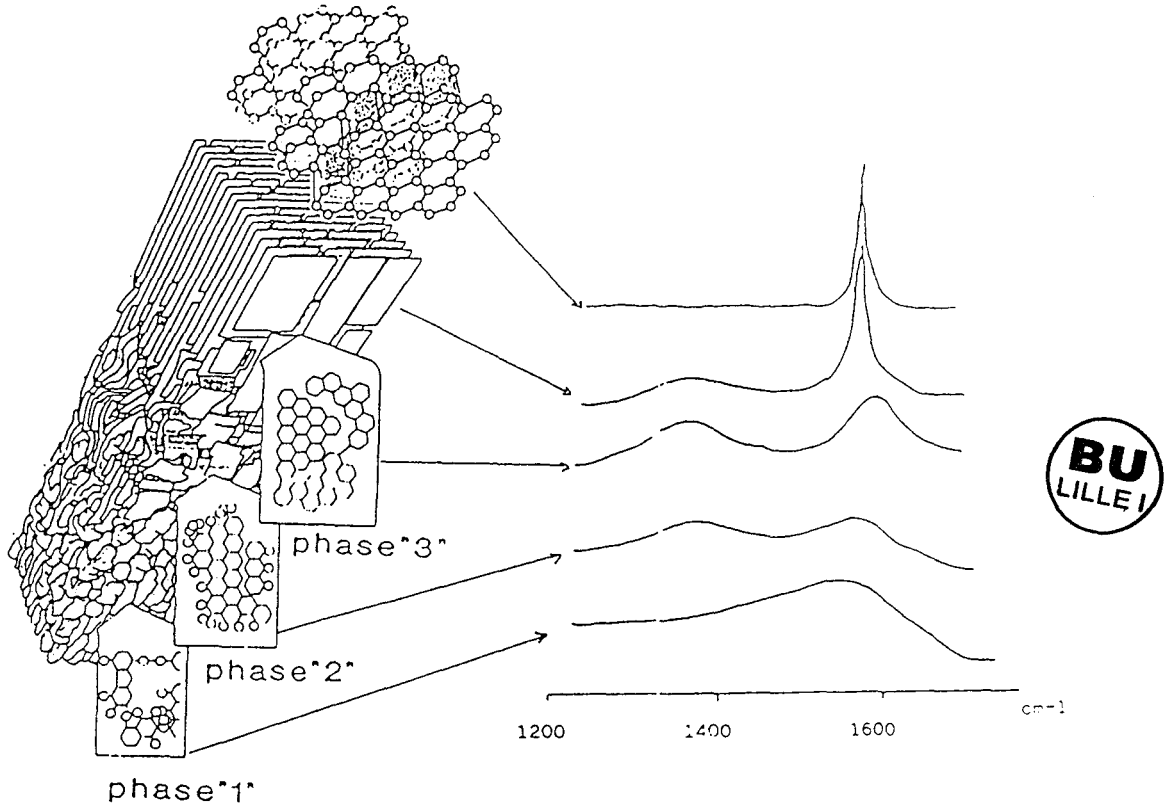

Fig. 2. Raman spectra of "carbon" related to the carbonization scheme (from refs. [17] and [18]).

A continuous background is only observed for the sample heat-treated at 190°C, whereas at 280°C, the spectra always exhibit two broad bands around 1580 cm^{-1} and 1350 cm^{-1}. The diffusion band observed at 1580 cm^{-1} corresponds to the E_{2g} vibrational mode (C-C vibrations in the aromatic layers). The band at 1350 cm^{-1} is usually the so-called *defect band*[13], is assigned to A_{1g} vibrational mode, and may be related to the structural organization of the carbonaceous matter (in particular shape and size)[14]. So, the process of carbonization begins to develop in the temperature range 190–280°C. It is interesting to note that the band around 1350 cm^{-1} becomes better defined when the temperature increases. This change is a characteristic of the formation of carbonaceous matter[15], and it may be proposed that the appearance of the A_{1g} vibrational mode above 280°C is due to the formation of a turbostratic carbon, which grows by arranging itself in parallel polyaromatic layers when the temperature increases.

In a previous study, we showed that the reaction between APP and PER formed phosphate esters with a spiro structure above 190°C[16]. Therefore, the Raman spectroscopy study allows us to propose that a carbonization process develops from these esters to form anisotropic carbonaceous species. To explain this structure, we can take the scheme of Griffiths *et al.*[17] and Cottinet *et al.*[18] (Fig. 2), which shows that the spectra obtained correspond to steps 2 and/or 3. This result allows us to propose that the structures of our carbonaceous species may consist of polyaromatic species bridged by alkyl groups (e.g., methylene).

3.2 *CP/DD-MAS NMR ^{13}C*

CP/DD-MAS ^{13}C spectroscopy is a powerful tool to characterize carbonaceous materials and so, to explain the hypothesis deduced from the Raman spectroscopy study.

CP/DD-MAS ^{13}C NMR spectra are presented in Fig. 3. The attributions of the absorption bands are presented in Table 2.

A band is only observed between 10 and 30 ppm at 280°C, which may be assigned to aliphatic carbons. The spectra show a broad band between 100 and 160 ppm, which implies the presence of several non-magnetically equivalent carbons[19]. We observe, therefore, that aromatic species appear from 280°C, and that aliphatic carbons are no longer characterized for $T > 280$°C. This behaviour may be explained by the development of reactions of cyclisation and by a condensation process to form aromatic species. Nevertheless, the absence of aliphatic carbons in the spectra does not mean that these species have completely disappeared. Indeed, both Suwelack[23] *and* Oliver[24] have observed that for a given pitch the intensity of aliphatic carbon bands obtained in the conditions of rotation at magic angle decreased very strongly and sometimes disap-

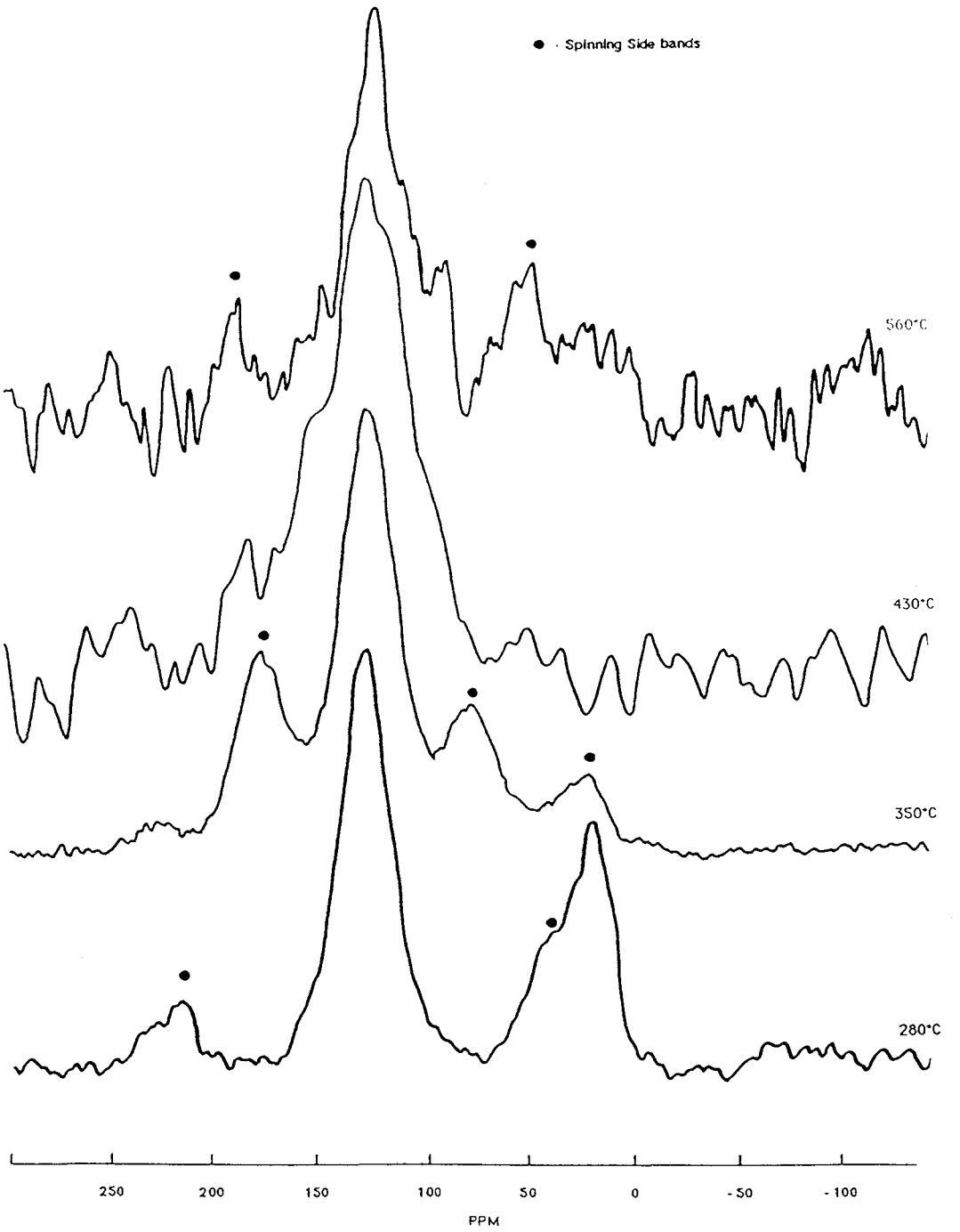

Fig. 3. CP/DD-MAS NMR ^{13}C spectra of the heat-treated APP/PER samples.

peared. They considered that motion of sufficiently low frequency coupled with MAS results in complete decoupling of the proton-carbon dipolar interaction, and the CP process may be effectively blocked. So we may only conclude that there is a reduction of the number in aliphatic carbons in the materials above 350°C.

The hypothesis of aromatic species with nitrogen in the cycle may be suggested, first, because the ^{13}C NMR does not allow us to distinguish between aromatic heterocycles and aromatic cycles, and second, because the presence of nitrogen has been shown by chemical analysis. Moreover, the ammonium species of the APP may evolve ammonia or react to create amines, amides, or nitrogenated aromatic heterocycles when the temperature increases. The amine and amide groups are not observed, but may exist in low content.

The presence of C_{ar-O} may be explained by the formation of phenolic species, and/or a phosphocarbonaceous structure, and/or C_{ar-O-C}. Nevertheless, the maintenance of phenolic species at high temper-

Table 2. Chemical shifts and attributions of the CP/DD-MAS ^{13}C NMR spectra

Temperature (°C)	Chemical shift (ppm)	Attribution	Ref.
280	20 (10–30)	branched aliphatic carbons	[19,20]
	129 (bd : 110–160)	C_{ar-H}, C_{ar-C}, C_{ar-N}, C_{ar-O}	[19,21,22]
350	129 (bd : 100–160)	C_{ar-H}, C_{ar-C}, C_{ar-N}, C_{ar-O}	[19,21,22]
430	124 (bd : 80–180)	C_{ar-H}, C_{ar-C}, C_{ar-N}, C_{ar-O}	[19,21,22]
560	119 (bd : 90–170)	C_{ar-H}, C_{ar-C}, C_{ar-N}, C_{ar-O}	[19,21,22]

C_{ar-H}: protonated aromatic carbons. C_{ar-C}: not protonated aromatic carbons. C_{ar-O}: oxygenated aromatic carbons. C_{ar-N}: nitrogenated aromatic carbons and/or nitrogenated carbons with conjugated bondings in heterocycles. bd: broad band.

atures is doubtful, because these species would have reacted with acidic phosphate species to form a phosphocarbonaceous structure and/or with carboxilic groups created in the material. So we propose that C_{ar-O} is due principally to the presence of C_{ar-O-P} and C_{ar-O-C}.

To explain the carbonaceous structure observed, we have used a high field spectrometer (B = 7 T). The spectrum obtained for the sample heat-treated at 560°C is presented in Fig. 4. It has been recorded without CP, and we note the presence of four based bands centered at 25, 70, 125, and 180 ppm, which may be attributed, respectively, to branched aliphatic carbons, oxygenated aliphatic carbons as $R_1R_2R_3$–C–O–R_4 ($R_1R_2R_3$ = aliphatic groups or protons and R_4 = aliphatic groups, protons, or phosphorus), aromatic carbons (C_{ar-H}, C_{ar-C}, C_{ar-N}, and C_{ar-O}), and carboxylic carbons[19,21,22]. The band of aliphatic carbons is observed and the hypothesis of Suwelack[23] and Oliver[24] is confirmed. The presence of C—O bondings may be explained by a phosphonaceous structure (C—O—P) and/or etheroxide species (C—O—C), not by the presence of alcohol groups, because these latter may react with acidic species formed in the material. Moreover, the spectrum permits the maintenance of carboxylated species at high temperatures. It can be noted that the C=O groups were not observed on the weak field spectrometer, perhaps due to the large anisotropy of the chemical shift tensor of C=O[21] and insufficient resolution of the spectrometer.

3.3 *MAS-NMR ^1H*

MAS-NMR ^1H study completes the analytical results obtained by CP/DD-MAS NMR ^{13}C. The spectra are presented in Fig. 5 with the deconvolution of their bands, assuming either Lorenztian or Gaussian curves. It is interesting to note that the spectra are relatively well defined, and that CRAMPS technology is not absolutely necessary to increase the resolution of the bands[25]. The attributions are given in Table 3.

These results show the formation of aromatic species from 280°C that confirms the attributions

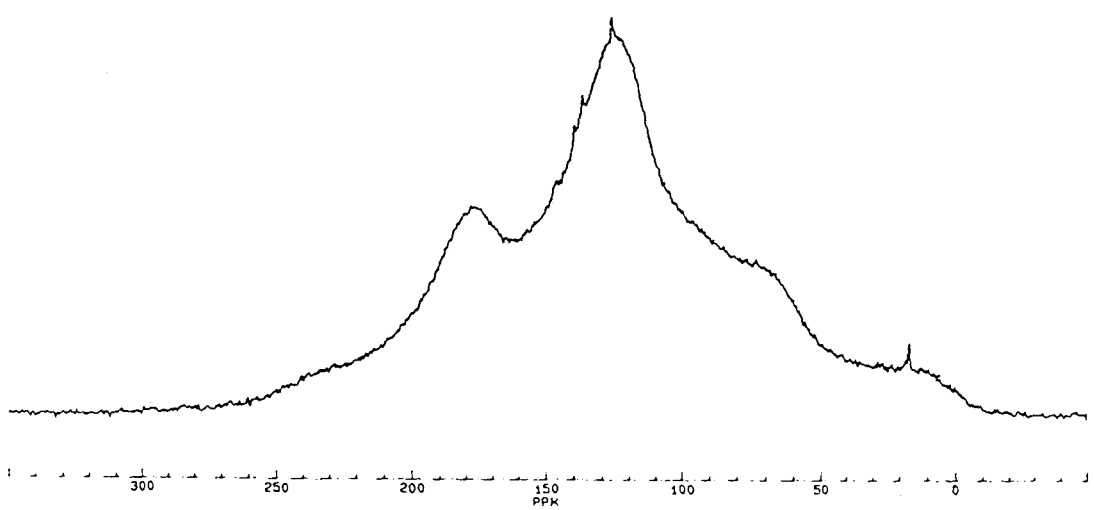

Fig. 4. DD-MAS NMR ^{13}C spectrum of the APP/PER sample heat-treated at 560°C (high field spectrometry).

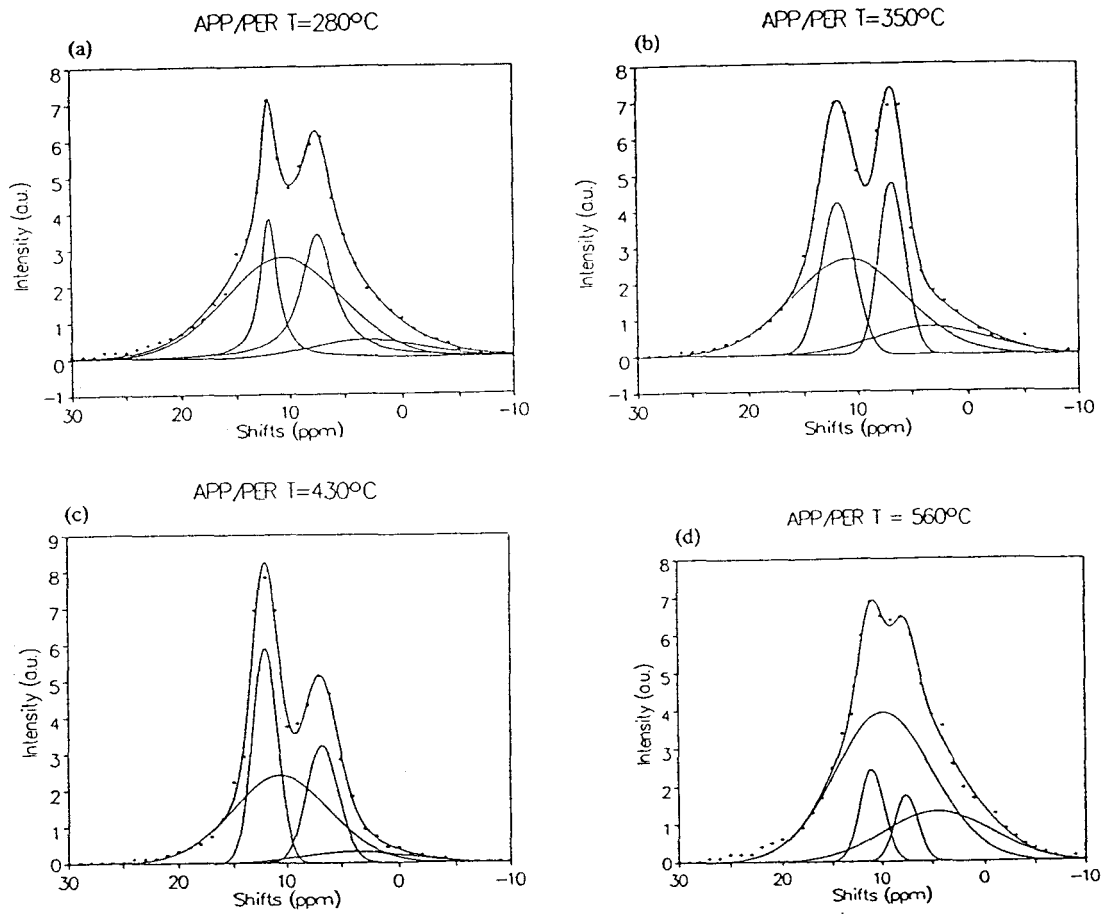

Fig. 5. Deconvolution of the MAS NMR ^{1}H spectra of the heat-treated APP/PER samples.

obtained by Raman microspectroscopy and CP/DD-MAS NMR ^{13}C. The attribution of the chemical shifts between 9 and 10.5 ppm may appear doubtful, because it is generally admitted that the shifts of aromatic protons are situated in the range 6 to 9 ppm[26–27]. But in a recent work, Rosenberger *et al.*[28] have shown that with a weak field spectrometer and in the particular case of coals, the shifts may be more important (up to 13 ppm). The bands observed between 11 and 12 ppm are characteristic of protons in a carboxilic group. We confirm, therefore, the presence of carboxylic groups at all temperatures, as has been proposed previously.

The bands around 7 ppm may be assigned to H_{POH}, H_{ar-OH}[26], and/or to H_{ar}[26]. But as has been explained above, the contribution of H_{OH} is very weak. The hypothesis of an attribution only to aromatic species cannot be considered. Indeed, the IR study characterizes the presence of phosphate species at every temperature and, in particular, shows the presence of P—OH groups[29]. Moreover, the CP/DD-MAS ^{13}C NMR has shown aromatic carbons linked to protons. As the band around 11 ppm has already been assigned to aromatic protons, it may be concluded that the band around 7 ppm is principally the contribution of H_{POH}.

The bands observed around 3 and 4.5 ppm may be assigned to $—CH_3$, to $—CH_2—$ linked to aromatic species[26,27], and also to $—OCH_3$ linked to phosphate and/or to end oxo species. It is interesting to note that the increase of the chemical shift at 560°C may be explained by an increase of $—CH_2—$ bridging groups. Moreover, it is noted that the number of $—CH_3$ protons decreases strongly at 560°C; it may be proposed that in an oxidative atmosphere the reaction that transforms the $—CH_3$ groups into —COOH group may occur. Aliphatic protons are observed at all temperatures. This result confirms, therefore, the previously proposed hypothesis that in CP/DD-MAS-NMR ^{13}C, there is an intensity loss of the band corresponding to aliphatic carbons.

Now it is interesting to discuss the four signals' forms of the spectra obtained with our deconvolution hypothesis (Fig. 5). It can be noted that the bands are narrow (for spectra obtained without homonuclear decoupling), and therefore, that the line-broadening effects of homonuclear $^{1}H—^{1}H$ dipolar interactions and chemical shift anisotropy have been in part removed by magic-angle spinning. Indeed, the static spectra show one single relatively narrow band with a width at half maximum between 2500–3000 Hz[12]. It means that the $^{1}H—^{1}H$ interac-

Table 3. Chemical shifts' attributions of the MAS–NMR ^1H spectra

Temperature (°C)	Chemical shift (ppm)	Attribution	Fit results			Ref.
			Curve type	r^2	F statistic	
280	3.1	H_{CH_3}, H_{CH_2}, H_{OR}	Gaussian	0.997	1065	[26,27]
	7.4	H_{POH}	Lorentzian			[a]
	10.5	H_{ar}	Gaussian			[26,27]
	12.0	H_{COOH}	Lorentzian			[26,27]
350	3.3	H_{CH_3}, H_{CH_2}, H_{OR}	Gaussian	0.995	560	[26,27]
	6.8	H_{POH}	Gaussian			[a]
	10.2	H_{ar}	Gaussian			[26,27]
	11.8	H_{COOH}	Gaussian			[26,27]
430	3.3	H_{CH_3}, H_{CH_2}, H_{OR}	Gaussian	0.993	400	[26,27]
	6.7	H_{POH}	Gaussian			[a]
	10.3	H_{ar}	Gaussian			[26,27]
	12.0	H_{COOH}	Gaussian			[26,27]
560	4.5	$H_{CH_{2b}}$, H_{OR}	Gaussian	0.996	700	[26,27]
	7.6	H_{POH}	Gaussian			[a]
	9.9	H_{ar}	Gaussian			[26,27]
	11.1	H_{COOH}	Gaussian			[26,27]

H_{CH_3}: $-CH_3$ protons linked to aromatic species. H_{CH_2}: $-CH_2-$ protons linked to an aromatic species. $H_{CH_{2b}}$: $-CH_2-$ bridging groups between aromatic species. H_{POH}: protons linked to a —P—OH phosphate group. H_{ar}: protons linked to aromatic carbons. H_{COOH}: protons linked to a carboxylic group. H_{OR}: protons linked to aliphatic or aromatic group. [a]This study: attributions from comparisons with the spectra of several acidic phosphate species.

tions in the sample are weak because of low ^1H concentration and/or partial averaging of dipolar interactions by molecular motions.

These remarks explain our hypothesis of deconvolution. Indeed, the line width attributed to the aromatic groups (peaks at 10 ppm) tends to be larger than the other groups. One possible explanation is the large anisotropy in bulk magnetic susceptibility characteristic of aromatic compounds, and the fact that, with powdered samples, MAS does not completely average this kind of effect to yield sharp lines[30]. Moreover another phenomenon may be superimposed to yield broad lines. Aromatic protons may be in different ranges of conformation, which may give a superposition of peaks, leading to a broad band. The band corresponding to the aliphatic group (peak at 3–4 ppm) is relatively broad and weak. It may be proposed that the aliphatic protons are coupled because of a rigid conformation (e.g., —CH_2— bridges between aromatic groups). The other bands (carboxilic protons (peak at 12 ppm) and phosphate protons (peak at 7 ppm)) are relatively well resolved. The dipolar interactions are weak and so removed by MAS, and it may be proposed that the structure of the material allows relative mobility of these protons.

3.4 *DD-MAS NMR ^{31}P*

Spectroscopic studies, IR in particular, on APP/PER systems have previously shown that the intumescent coating was partially composed of phosphocarbonaceous structures[29]. To explain these phosphocarbonaceous structures a DD-MAS NMR ^{31}P study has been made. The spectra are presented in Fig. 6. The attributions of the different bands are presented in Table 4.

At 280°C, APP reacted with PER and degraded to form ortho- and pyrophosphate species. The band around −11 ppm may be attributed to orthophosphate groups linked to aromatic rings and/or to polyphosphate end groups belonging mainly to pyrophosphate species[3,31,32]. Taking account of the previous IR study and the CP/DD-MAS ^{13}C and MAS ^1H results, these attributions are justified.

At 350°C, a decrease of the intensity of the band at around −11 ppm is observed. It may be explained by a degradation of the pyrophosphate species to form orthophosphate groups. Moreover, it is observed that the polyphosphate chains present at 280°C are degraded at this temperature.

At 430°C, an additional band appears around −7 ppm, which may be assigned to pyrophosphate groups[31,32]. To explain the differences of shift between two pyrophosphate groups, it is interesting to recall some results. There are three major influences of the molecular structures on the chemical shifts of phosphates[33]: (a) the charge and radius of the next neighbour ions[34], (b) the P—O—X bond angle[35], and (c) the bond strength[36]. Nevertheless, it has been demonstrated by Un *et al.*[37] that these three factors depend on each other, and that the chemical shift interactions in ^{31}P NMR of the solid state are dominated by d_P—p_O π bonding effects. So it may be proposed that the differences of the chemical shifts between the two pyrophosphate groups are due to different units R (R=H or alkyl groups) in P—O—P—OR species, which lead to different P—OR bond length, and thus to a variation in the P—O—P bond angle and, finally, to a change of the π-bond order of the concomittant P—O bond.

At 560°C, an increase of the species defined by the band at −11 ppm compared with the band of

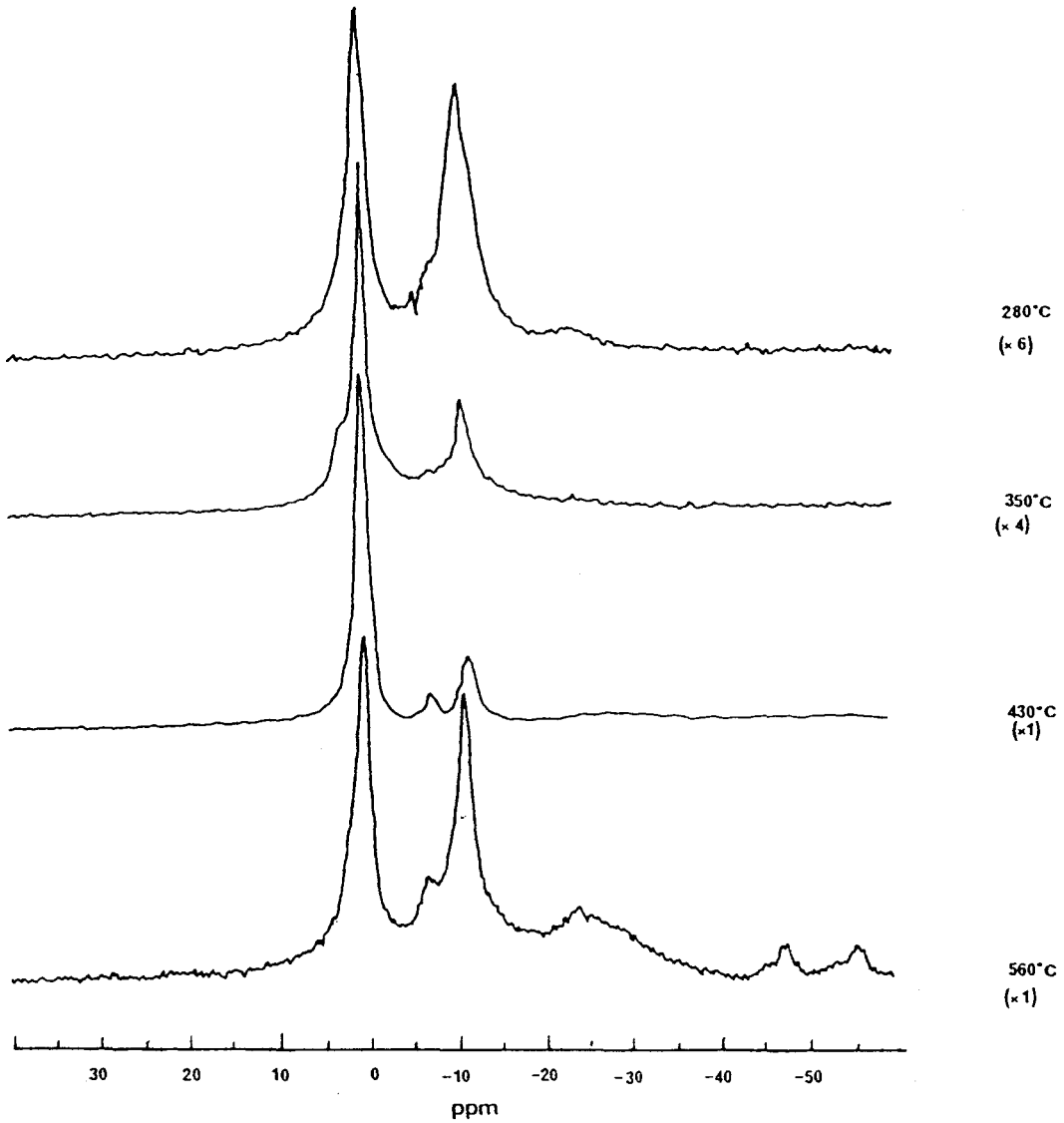

Fig. 6. DD-MAS NMR ^{31}P spectra of the heat-treated APP/PER samples.

the orthophosphate species and the presence of polyphosphate chains are observed. Two additional bands appear at −48 and −56 ppm, which may be assigned to a cage structure of P_4O_{10} type with different P—O—P bond angles[33]. These observations suggest that between 430°C and 560°C phosphate species (mainly orthophosphates) recondense to form pyrophosphate and polyphosphate groups.

4. CONCLUSION

To conclude this work, we propose a reaction scheme for the carbonization process from 280°C up to 560°C:

- at 280°C, formation of small aromatic molecules with alkyl groups branched, which may be bridged by phosphate species (Fig. 7);
- from 350°C to 430°C, condensation of the aromatic molecules which begin to arrange in parallel layers (Fig. 8); the anisotropy in the material increases (Fig. 9);
- up to 560°C, formation of large polyaromatic molecules with an increase of the anisotropy and the appearance of P_4O_{10} crystals (Fig. 10).

When the temperature increases, the intumescent structure develops. It is formed by polyaromatic stacks linked mainly with ortho- and pyrophosphate bridges. At 280°C, it may be proposed that the structure is formed principally by aromatic or aliphatic molecules bridged by phosphate species. These bridges imply good dynamical properties of the structure by allowing to this latter, the accomodation of the stresses. At higher temperatures, there is a condensation of the aromatic molecules and, concurrently, there is a decrease of phosphocarbonaceous species (scission of the P—O—C linkages by heating). Consequently, the increase of the polyaromatic edifice size may lead to a drastic

Table 4. Chemical shifts attributions of the DD-MAS NMR ^{31}P spectra

Temperature (°C)	Chemical shift (ppm)	Attribution	Ref.
280	−0.5	$-PO_4$ units in R_2HPO_4, RH_2PO_4 and/or H_3PO_4.	
	−11.1	$-PO_4$ units in Φ_2RPO_4 and/or Φ_2HPO_4 and/or pyrophosphate group and/or polyphosphate chain (end group).	[3,31,32]
	−24	Polyphosphate chain (central group).	
350	−0.3	$-PO_4$ units in R_2HPO_4, RH_2PO_4, and/or H_3PO_4.	
	−11.4	$-PO_4$ units in Φ_2RPO_4 and/or Φ_2HPO_4, and/or pyrophosphate group.	[3,31,32]
430	−0.13	$-PO_4$ units in R_2HPO_4, RH_2PO_4, and/or H_3PO_4.	
	−7.6	Pyrophosphate.	[3,31,32]
	−11.7	$-PO_4$ units in Φ_2RPO_4, and/or Φ_2HPO_4, and/or pyrophosphate group.	
560	0.3	$-PO_4$ units in R_2HPO_4, RH_2PO_4, and/or H_3PO_4.	
	−7.1	Pyrophosphate.	[3,31,32]
	−10.9	$-PO_4$ units in Φ_2RPO_4, and/or Φ_2HPO_4, and/or pyrophosphate group, and/or polyphosphate chain (end group).	
	−24.2	Polyphosphate chain (central group).	
	−48.3 and −55.7	Phosphoric oxydes (type P_4O_{10} cage structure).	[33]

R = alkyl groups and Φ = aromatic or polyaromatic groups.

increase of the apparent viscosity of the material and, as a matter of fact, to the loss of the interesting properties of the char. At 560°C, the condensation process of the polyaromatic molecules develops. The presence of methylene groups bridging aromatic molecules may be noted. These groups are predominant among the aliphatic groups. The structure is, therefore, more rigid and the stress accommodation becomes difficult. Moreover, it is revealed that there is condensation of phosphate species and formation of P_4O_{10} crystals. It may be proposed that the P_4O_{10} crystals create a stress concentration around them,

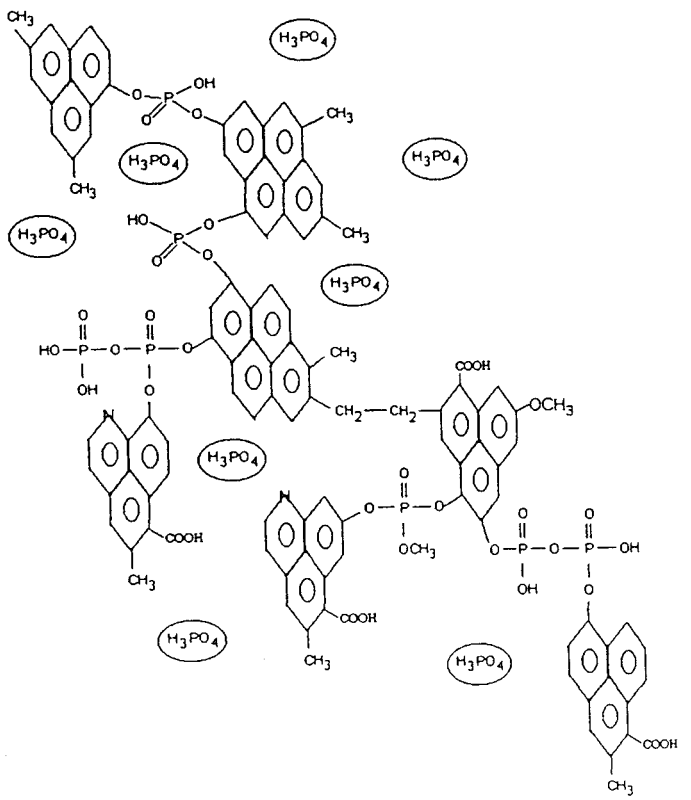

Fig. 7. Phosphocarbonaceous structure of the APP/PER sample heat-treated at 280°C.

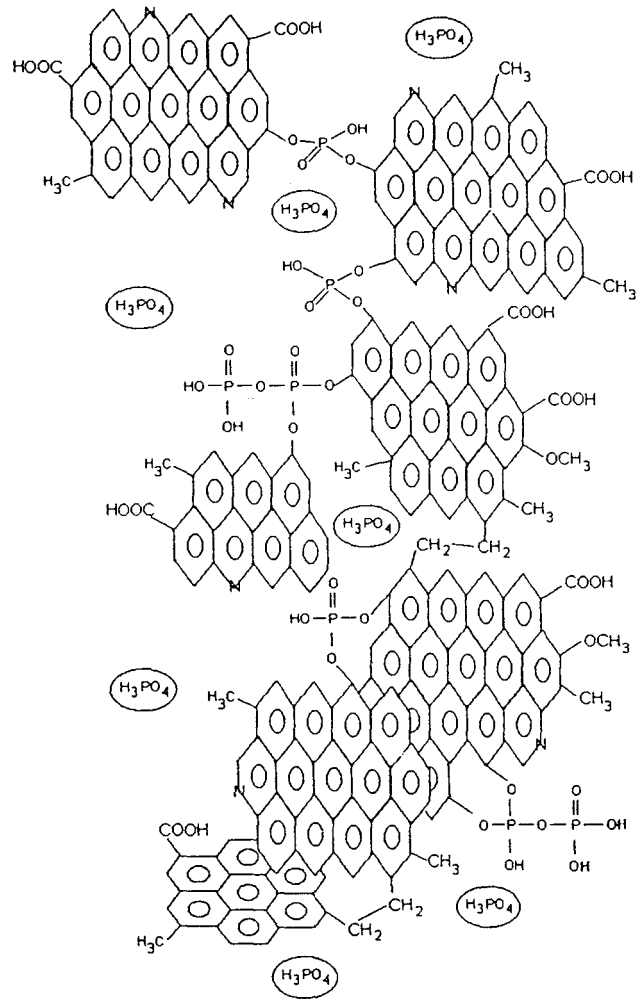

Fig. 8. Phosphocarbonaceous structure of the APP/PER sample heat-treated at 350°C.

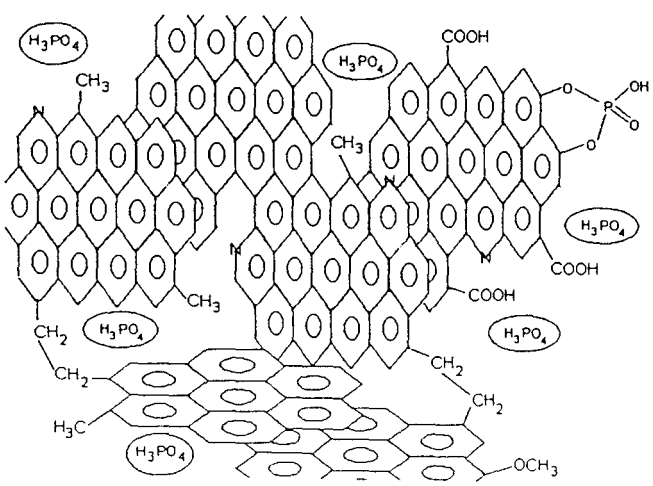

Fig. 9. Phosphocarbonaceous structure of the APP/PER sample heat-treated at 430°C.

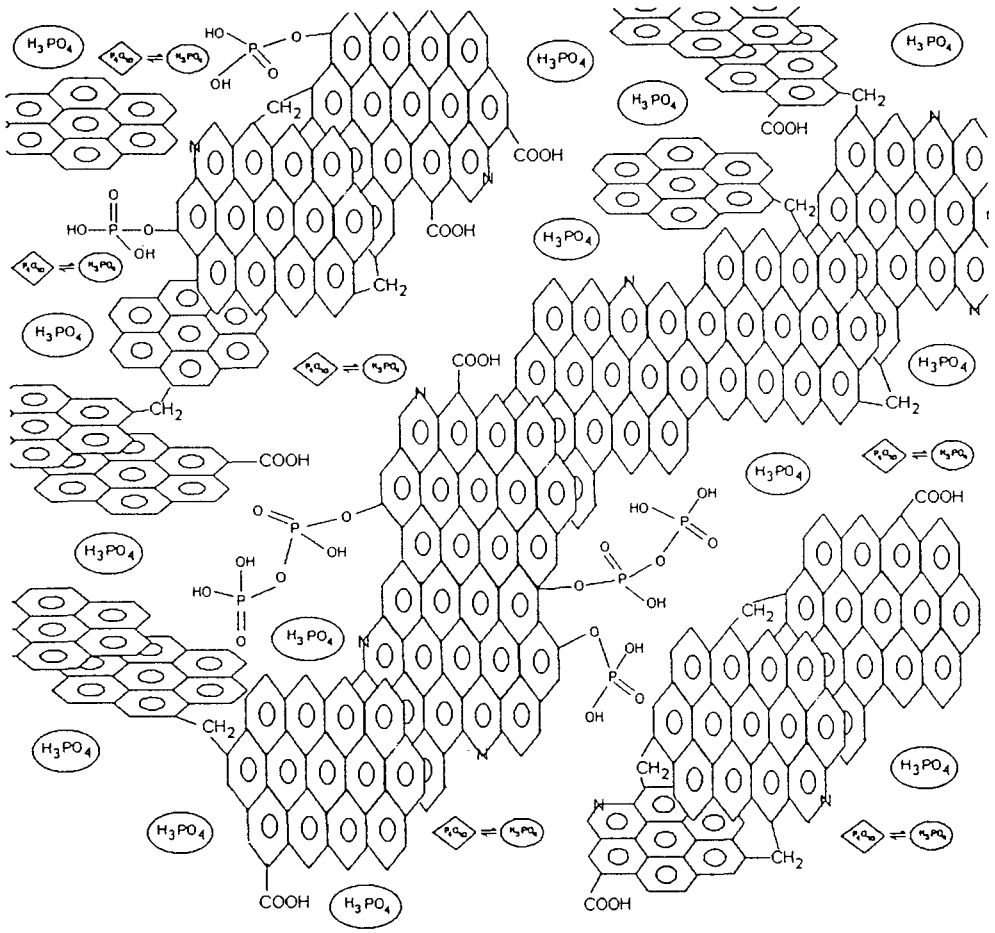

Fig. 10. Phosphocarbonaceous structure of the APP/PER sample heat-treated at 560°C.

allowing easier crack creation and propagation (Fig. 10).

This work demonstrates that the dynamic properties of the char may be explained by the chemistry of the system (aromaticity, thermal polymerisation of aromatic molecules, etc.). So, to formulate a new fire-retardant intumescent system, the carbonization mechanism must be adjusted to obtain the dynamic properties of interest.

REFERENCES

1. R. Delobel, S. Bourbigot, M. Le Bras, and J. M. Leroy, In *Flame Retardancy of Polymeric Materials* (Edited by V. Z. Janovic), pp. 8/1–8/4. Society of Plastic and Rubber Eng., Zagreb (1990).
2. R. Delobel, M. Le Bras, N. Ouassou, and F. Alistiqsa, *J. Fire Sci.* **8**, 85 (1991).
3. N. Ouassou, doctoral dissertation, University of Lille (1991).
4. Y. Schmidt-Le Tallec, doctoral dissertation, University of Lille (1992).
5. In *Handbook of Flame Retardant Chemicals and Fire Testing Services* (Edited by Technomic Publishing Company) Lancaster, PA (1988).
6. G. Camino, L. Costa, and L. Trossarelli, *Polym. Deg. & Stab.* **12**, 213 (1985).
7. Y. Schmidt, S. Bourbigot, A. Marchal, M. Le Bras, and R. Delobel, In *Actes du 4e congrès de la société française de Chimie* (Edited by Université Louis Pasteur), pp 108. Sociéte Française de Chimie (SFC), Strasbourg (1991).
8. R. Delobel, N. Ouassou, M. Le Bras, and J. M. Leroy, *Polym. Deg. & Stab.* **30**, 41 (1990).
9. C. E. Anderson, S. Dziur, W. A. Mallow, and J. Buckmaster, *J. Fire Sci.* **3**, 161 (1985).
10. C. E. Anderson, D. E. Ketchum, and W. P. Mountain, *J. Fire Sci*, **6**, 390 (1988).
11. R. Delobel, N. Ouassou, M. Le Bras, and J. M. Leroy, *Polym. Deg. & Stab.* **23**, 349 (1989).
12. S. Bourbigot, doctoral dissertation, University of Lille (1993).
13. M. Nakamizo, R. Kammereck, and P. L. Walker, Jr., *Carbon* **12**, 259 (1974).
14. F. Tuinsta and J. L. Koenig, *J. Chem. Phys.* **53**, 1128 (1970).
15. M. Nakamizo, *Carbon* **29**, 757 (1991).
16. F. Alistiqsa, doctoral dissertation, University of Lille, (1993).
17. J. A. Griffiths and H. Marsh, *Carbon '80*, Baden Baden (1980), p. 17.
18. D. Cottinet, P. Couderc, J. L. Saint Romain, and P. Dhamelincourt, *Carbon* **26**, 339 (1988).
19. A. Grint, G. P. Proud, I. J. F. Poplett, K. D. Bartle, S. Wallace, and R. S. Matthews, *Fuel* **68**, 1490 (1989).
20. G. E. Maciel, V. J. Bartuska, and F. P. Miknis, *Fuel* **58**, 391 (1979).
21. W. L. Earl and D. L. Vanderhart, *J. Magn. Res.* **48**, 35 (1982).
22. S. Supaluknari, I. Burgar, and F. P. Larkins, *Org. Geochim.* **15**, 509 (1990).

23. D. Suwelack, W. P. Rothewell, and J. S. Waugh, *J. Chem. Phys.* **73**, 2559 (1980).
24. P. Ollivier and B. C. Gerstein, *Carbon* **22**, 409 (1984).
25. S. F. Dec, C. E. Bronnimann, R. A. Wind, and G. E. Maciel, *J. Magn. Res.* **82**, 454 (1989).
26. C. E. Bronnimann, B. L. Hawkins, M. Zhang, and G. E. Maciel, *Anal. Chem.* **60**, 1743 (1988).
27. L. M. Ryan, R. E. Taylor, A. J. Paff, and B. C. Gerstein, *J. Phys. Chem.* **72**, 508 (1980).
28. H. Rosenberger and G. Sheler, *Z. Chem.* **23**, 34 (1983).
29. R. Delobel, M. Le Bras, Y. Schmidt, and S. Bourbigot, In *Actes du MOFFIS 91* (Edited by GFP), pp. 79–85. GFP, Le Mans (1991).
30. D. L. VanderHart, W. L. Earl, A. N. Garroway, *J. Magn. Res.* **44**, 361 (1981).
31. J. R. Van Wazer, C. F. Callis, J. N. Shoolery, and R. C. Jones, *J. Am. Chem. Soc.* **78**, 5715 (1956).
32. T. M. Duncan and D. C. Douglass, *J. Chem. Phys.* **87**, 339 (1984).
33. U. Sternberg, F. Pietrowski, and W. Priess, *Z. Phys. Chem.* **168**, 115 (1990).
34. U. Haubenreißer, doctoral dissertation, University of Jena (1984).
35. D. Müller, E. Jahn, and G. Ladwig, *Chem. Phys. Lett.* **109**, 332 (1984).
36. A. K. Cheetham, H. J. Clayden, C. M. Dobson, and R. J. B. Jakeman, *J. Chem. Soc. Chem. Commun.*, 195 (1986).
37. S. Un and M. P. Klein, *J. Am. Chem. Soc.* **111**, 5119 (1989).

Applied Surface Science 81 (1994) 299–307

XPS study of an intumescent coating Application to the ammonium polyphosphate/pentaerythritol fire-retardant system

Serge Bourbigot [a,*], Michel Le Bras [a], Léon Gengembre [b], René Delobel [a]

[a] *Laboratoire de Chimie Analytique et Physicochimie des Solides, ENSCL, Université des Sciences et Technologies de Lille, BP 108, F-59652 Villeneuve d'Ascq Cedex, France*

[b] *Laboratoire de Catalyse Hétérogène et Homogène, URA-CNRS D04020, USTL, F-59650 Villeneuve d'Ascq, France*

Received 10 May 1994; accepted for publication 15 July 1994

Abstract

Fire retardancy of polymers may be due to the formation of a protective surface coating, i.e. a swollen charred layer (intumescence). An intumescent coating resulting from thermal treatments of the association of ammonium polyphosphate (APP) and pentaerythritol (PER) is studied by X-ray photoelectron spectroscopy. The O 1s, P 2p, C 1s and N 1s spectra are discussed. In the formation of the intumescent material the presence is shown of nitrogen in pyrrole and pyridine type structures of aromatic phosphate esters. A degradation mechanism is suggested which involves a reaction with O_2 via the formation of carbonyl and carboxylic groups.

1. Introduction

The large diffusion of synthetic polymeric materials which occurred in the last few decades, has increased fire risks as well as fire hazards. The easy combustion of organic polymers has led to the development of fire-retardant (FR) systems. The most effective FR systems are halogen-based materials. Nevertheless, these systems are known to be a source of corrosive, obscuring and toxic smoke when the materials burn. The general tendency is to limit the use of halogen-based FR systems and to turn research and development towards halogen-free FR systems. One of the most attractive solutions is the use of intumescent insulative materials [1]. They form on heating a foamed cellular charred layer on their surface which protects the underlying material from the action of the flames. The proposed action mechanism is based on the charred layer acting in the condensed phase as a physical barrier which slows down heat and mass transfer [2,3].

The study of the formation mechanisms of the resulting surface charred layer appears essential to formulate new FR systems [4]. This work has been carried out on the ammonium polyphosphate (APP) – pentaerythritol (PER) intumescent system. These additives are widely used in paints and polyurethane foams [5] and may be used in thermoplastics such as PP [2,6] and PE [4,7]. In the case of polyethylenic materials, the fire-retardant properties are maximum for the ratio APP/PER = 3 (wt/wt) [2,6]. A previ-

applied surface science

ous paper suggested that the carbonization process of the system occurs via several steps [8]. From 190°C the additives react and form phosphate esters. Between 280 and 350°C intumescence develops and between 350 and 430°C, the intumescent coating degrades. At higher temperatures, there are structural changes leading to the formation of a new carbonaceous species (established in the temperature range $430 < T < 560$°C).

The mixture of APP/PER develops an intumescent structure when it is heat-treated. This structure is formed by stacks of polyaromatic species linked mainly by phosphate compounds [9]. The atoms present in the material are carbon, oxygen, phosphorus and probably nitrogen. Indeed, the reaction between APP and PER, when the temperature increases, evolves ammonia. This latter may react to form amine, amide and/or nitrogenated aromatic species.

Low-power spectroscopies apart from XPS allow easy observation of the nitrogen surroundings. The ^{15}N NMR of the solid state cannot be used because of the low isotopic abundance of ^{15}N (0.4%) which would require a very high scan number to obtain only a very weak signal. The other spectroscopies such as infra-red, ^{13}C and ^{1}H NMR, do not directly characterize nitrogen and in our case the presence of nitrogen compounds forming the intumescent structure was only a probable hypothesis [9]. The aim of this study is to characterize the intumescent coating by X-ray photoelectron spectroscopy (XPS). This work complements a previous paper [9] and should enable us to specify the intumescent structure. Indeed, XPS is a powerful tool to characterize the carbonaceous matter and in particular, the nitrogen compounds.

2. Experimental details

2.1. Material

Raw materials were PER (Aldrich R.P. grade) and APP ($(NH_4PO_3)_n$, $n = 700$, Hoechst Exolit 422, soluble fraction in H_2O: < 1 wt%). The study has been carried out using the APP/PER mixture for the ratio APP/PER = 3 (wt/wt). Initial mixtures were first prepared by ballmilling after mechanical grinding and sifting (200 μm) of the raw materials. They were then treated at five different temperatures (190, 280, 350, 430 and 560°C) during 12 h under flowing air (flow rate = 6 cm^3/s). An intumescent coating was obtained at temperatures higher than 190°C and then analyzed after recooling. The analyses are carried out after grinding in such a way as to obtain representative data of the material.

Table 1
Chemical analysis of the APP/PER samples heat-treated at 280, 350, 430 and 560°C

Temperature (°C)	C (at/kg)	H (at/kg)	N (at/kg)	O [a] (at/kg)	P (at/kg)
280	12	39	6	30	8
350	21	35	5	26	7
430	19	30	4	27	8
560	31	25	4	22	6

[a] Obtained by difference.

2.2. Chemical analysis

Table 1 presents the chemical composition of the samples heat-treated at 280, 350, 430 and 560°C.

2.3. XPS

The samples were examined by XPS on a AEI ES 200B spectrometer using Al Kα radiation ($h\nu$ = 1486.6 eV). The spectrometer was run in fixed analyser transmission mode at a pass energy of 65 eV with an X-ray power source of 250 W. Under these conditions the full-width at half-maximum (FWHM) of the Au 4f peak is 1.4 eV. Samples were mounted by pressing into the indium holder and introduced in a prechamber to obtain a pressure of 10^{-5} Torr. In the main analyzer chamber, the pressure was between 10^{-7} and 10^{-8} Torr. Finally it was necessary to cool the samples to around -70°C to avoid any degradation of the material.

Data acquisition was controlled by a AEI DS 200B data system connected to a computer. In order to obtain N 1s spectra of sufficient quality to permit resolution of different nitrogen components, several hours of data accumulation were required. X-ray-induced sample degradation was not observed versus time. To compensate for sample charging all binding energies were referenced to C 1s at 285 eV.

The peaks were resolved using peak analysis software (Peakfit of Jandel Scientific) assuming a Lorentzian/Gaussian line shape [10]. Initial assumptions on the possible species were derived from the results of previous studies [2,4,9].

3. Results and discussion

The XPS wide-scan spectra of the heat-treated APP/PER system show at each temperature very intense O 1s and C 1s peaks and P 2p and N 1s readily distinguishable peaks. The XPS analysis ("surface" analysis) results are resumed in Table 2 and are compared to the "bulk" analysis (Fig. 1). The P/C and O/C ratios are quite similar up to 430°C and become very different between 430 and 560°C, whereas the N/C ratios are the same between 350 and 560°C.

The decrease of the P/C and O/C ratios from 280 up to 430°C may be assigned to the degradation of the phosphorus compounds formed by reaction between APP and PER [2] which releases free radicals like $PO^{\cdot}$ or $PO_2^{\cdot}$ not trapped in the intumescent shield. Between 430 and 560°C, the decrease of the ratios in the case of the "bulk" analysis may be due to the volatilization of the phosphorus oxides formed [9]. There is migration of the phosphorus species at the surface (P/C increases in the case of the "surface" analysis) and there is a strong oxidation at the surface of the coating (O/C increases).

Both the N/C curves show at 280°C that the nitrogenated compounds are principally in the bulk. When the temperature increases, they migrate to the surface (between 280 and 350°C) and may evolve in the form of ammonia or NO_x species.

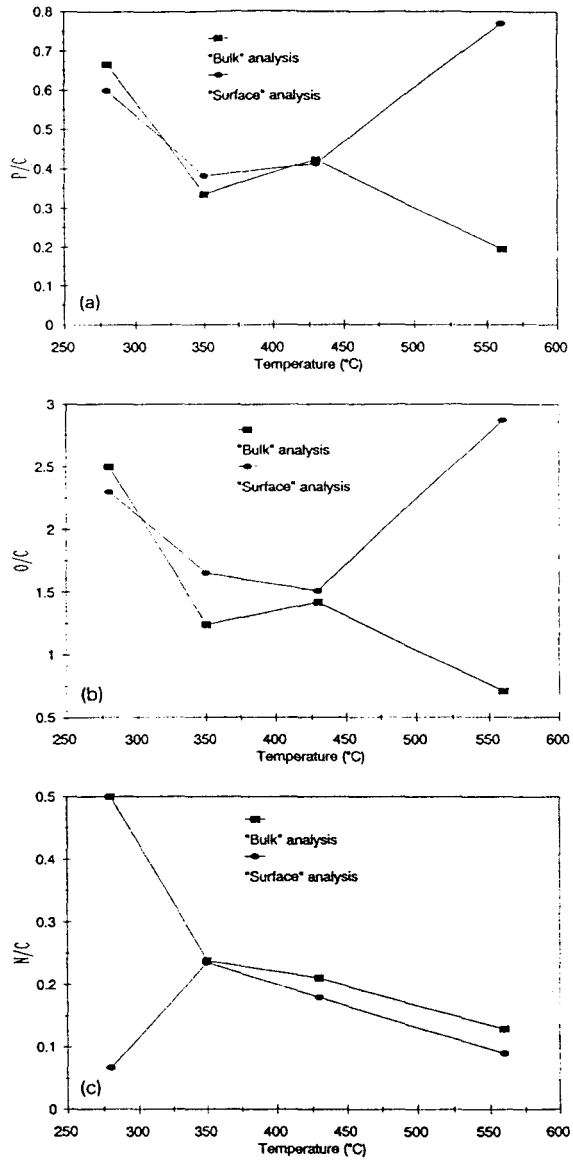

Fig. 1. Comparison of P/C (a), O/C (b) and N/C (c) ratios measured from chemical and XPS analyses.

Table 2
XPS analysis of the APP/PER samples heat-treated at 280, 350, 430 and 560°C

Temperature (°C)	P/C	O/C	N/C
280	0.6	2.3	0.067
350	0.38	1.65	0.235
430	0.41	1.51	0.18
560	0.77	2.87	0.09

3.1. O 1s spectra

The XPS spectra of the heat-treated APP/PER systems are shown in Fig. 2. The results of our fit assumptions are summarized in Table 3.

At each temperature two bands are observed with binding energies (E) at around 532 and 533.5 eV. Since the O 1s band is structureless, it is impossible

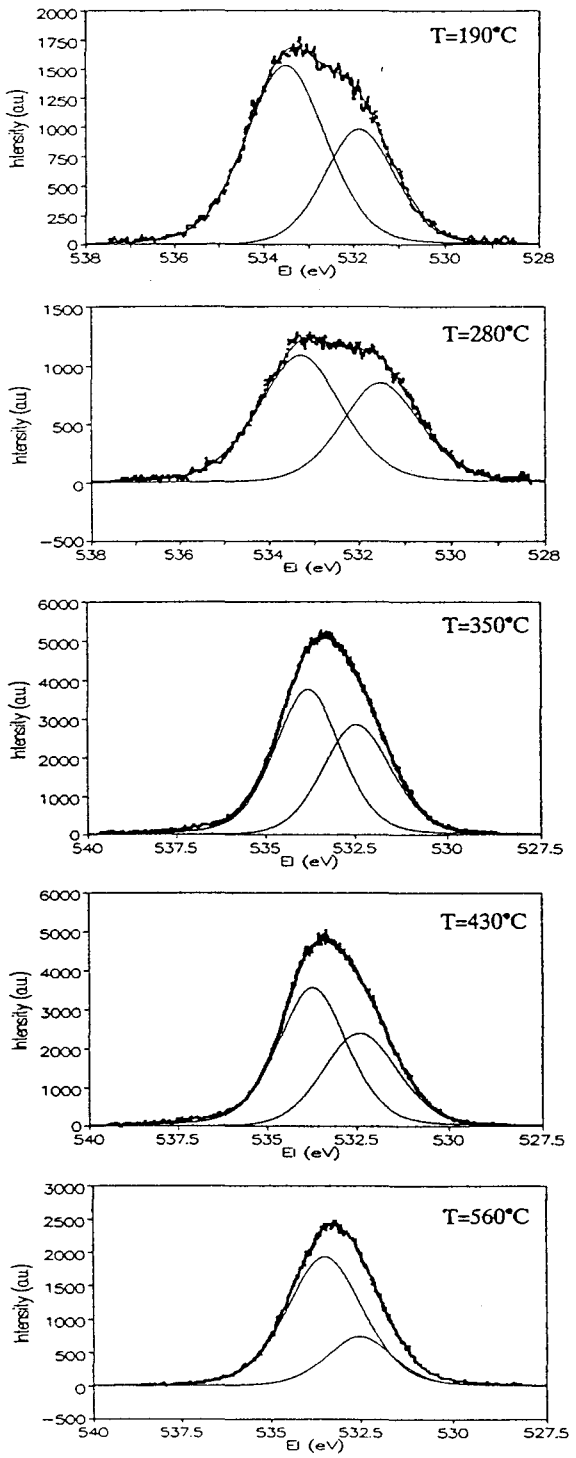

Fig. 2. O 1s spectra of the heat-treated APP/PER system.

Table 3
Fit results of the O1s spectra of the heat-treated APP/PER system

Temperature (°C)	Binding energy (eV)	Fit statistics	
		r^2	F
190	531.9	0.996	31685
	533.5		
280	531.5	0.996	40648
	533.3		
350	532.5	0.998	348821
	533.8		
430	532.4	0.998	198026
	533.7		
560	532.5	0.999	216402
	533.5		

to monitor the separate contributions of inorganic (e.g. O in phosphate) and organic oxygen (e.g. O in carboxyl, alcoolxyl or ether groups) [11]. The bands centred around 532 eV can be assigned to double binding =O in phosphate or carbonyl groups [10–12] as assumed in a previous work [9]. The presence of an amidic function may be suggested but should be verified by the C1s and N1s spectra. The bands centred around 533.5 eV can be assigned to –O– in C–O–C, C–O–P and/or C–OH groups. Moreover, the value of 533.5 eV suggests that –O– is bound to aromatic species as it has been proposed in a previous NMR study [4,9].

Fig. 3 presents the –O–/=O ratio versus temperature. The ratio decreases between 190 and 350°C and then increases at higher temperatures. It suggests that O_2 reacts with the aliphatic chains to form hydroperoxides which are not stable and give cetonic groups and that part of the phosphorus compounds may have been evolved (degradation of the phosphate esters) via radical reactions creating $PO^{\cdot}$ and $PO_2^{\cdot}$ ($190 < T < 350$°C). At temperatures higher than 350°C, the carbonyl and carboxylic groups may evolve into CO and CO_2 and at 560°C, principally stable phosphate esters remain in the material (the ratio near three confirms this hypothesis).

3.2. P 2p spectra

Fig. 4 shows the P 2p spectra obtained and Table 4 summarizes the results of the fit hypothesis. It is to note that the bands are always wide (FWHM ≥ 2.3

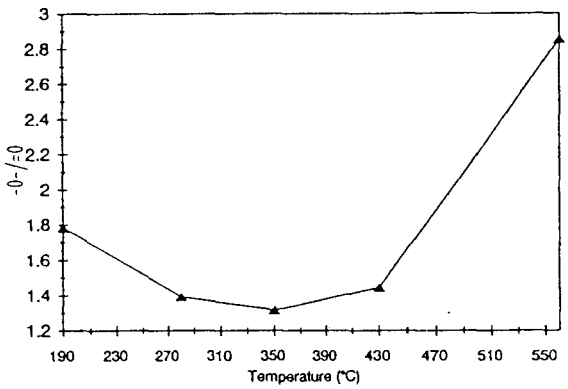

Fig. 3. -O-/=O ratio versus temperature.

eV) for a fit hypothesis of one single peak but it is known, in the case of P 2p that the resulting line observed is core-line doublets corresponding to $P\,2p_{1/2}$ and $P\,2p_{3/2}$ [10]. The binding energies measured between 134 and 135 eV can be assigned to P–O–C and/or PO_3^- groups in phosphate species and/or P_2O_5 [10] according to a previous ^{31}P NMR study [4,9]. The increase of the binding energies values may be explained by the formation of P_2O_5 when the temperature increases. Indeed, from 430°C the presence of P_2O_5 has been observed in the intumescent structure [4,9].

3.3. C 1s spectra

The C 1s spectra are shown in Fig. 5 and Table 5 summarizes the results of the most probable fit hypothesis. At 190°C three bands are observed at 284.7, 286.4 and 288.9 eV which can be assigned to C–H and C–C (aliphatic and aromatic species), C–O (ether and/or hydroxyl groups) and/or C–O–P (in hydrocarbonated phosphate), O=C–O (ester and/or carboxylic groups) bonds [10–11,13].

It is to note that the number of oxidized carbon atoms (58%) is high with respect to that at the other temperatures. It can be explained by the reaction between APP and PER which forms ester phosphates [2,8] (spiro-like structure) and low aromatic species.

Between 280 and 430°C, our fit hypotheses imply four bands instead of three previously. The band at 284.7 eV is the contribution of C–H and C–C in aliphatic and aromatic species in the material. The bands between 285.7 and 286.1 eV may be assigned

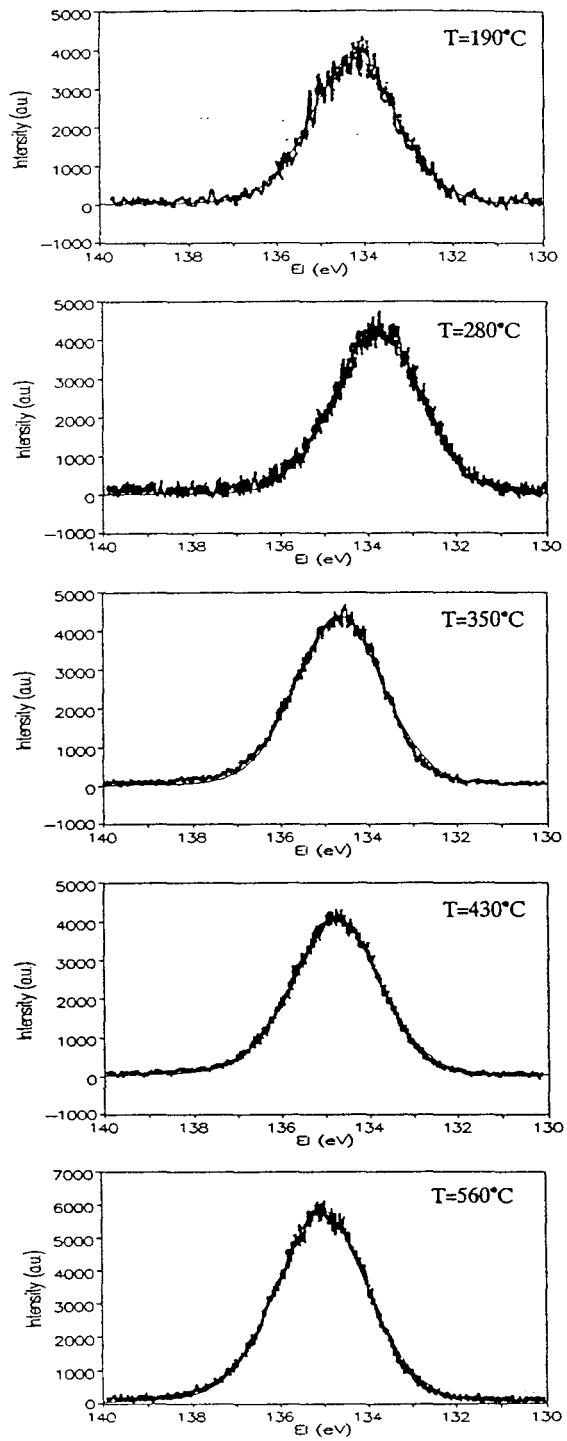

Fig. 4. P 2p spectra of the heat-treated APP/PER system.

Table 4
Fit results of the P2p spectra of the heat-treated APP/PER system

Temperature (°C)	Binding energy (eV)	Fit statistics	
		r^2	F
190	134.3	0.981	49899
280	134.1	0.988	115098
350	134.7	0.993	151952
430	134.7	0.996	262285
560	135.0	0.995	272853

to C–O (as previously) and/or C–N in cyclized compounds [10,14,15]. The other peaks are characteristic of carbonyl (around 287.5 eV) and carboxyl (around 289.5 eV) groups.

At 560°C we can observe another band at around 291.4 eV which may be assigned to a shake-up peak [14,16]. It corresponds to π to π^* type transitions in aromatic species. The other bands can be attributed as in the preceding cases.

It can be noted that the amidic group is not observed as previously suggested. Oxidized species are present at every temperature and it is interesting to plot C_{ox}/C_a (C_{ox}: oxidized carbons and C_a: aliphatic and aromatic carbons) versus the temperature (Fig. 6).

Between 190 and 280°C C_{ox}/C_a decreases, the ester phosphates observed at 190°C degrade to form olefinic bonds and, finally, via Diels–Alder type reactions aromatic species [17]. Therefore, C_a increases and C_{ox}/C_a decreases. Between 280 and 430°C, C_{ox}/C_a increases when the temperature increases, the aromatic species condenses and oxidizes to form phenolic and/or carboxilic species (the area increase of the peak at 289.5 eV confirms this hypothesis) [4,9]. At higher temperatures, the decrease of C_{ox}/C_a can be explained by the transformation of carboxylic groups into CO_2 (between 430 and 560°C, the peak area of the band at 289.5 eV decreases).

It is now interesting to compare the three ratios C_{C-O}/C_a, $C_{C=O}/C_a$ and $C_{O=C-O}/C_a$ (C_{C-O}: ether or nitrogenated carbons; $C_{C=O}$: carbonyl carbons; $C_{O=C-O}$: carboxylic carbons) versus temperature (Fig. 7). The C_{C-O}/C_a ratio presents the same behavior as the C_{ox}/C_a ratio. Between 190 and 280°C, phosphate esters degrade (breaking of the P–O–C bonds) and the cyclized nitrogenated species begin to form. Up to 430°C, the increase of the ratio may be

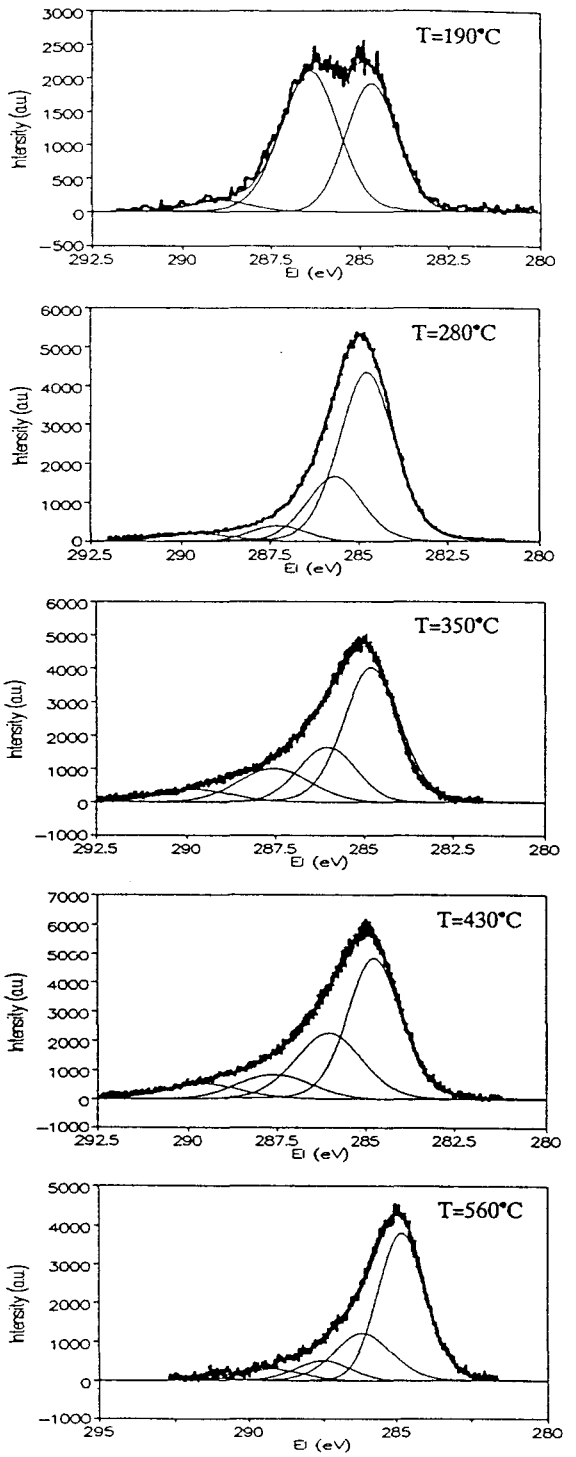

Fig. 5. C 1s spectra of the heat-treated APP/PER system.

Table 5
Fit results of the C1s spectra of the heat-treated APP/PER system

Temperature (°C)	Binding system (eV)	Fit statistics	
		r^2	F
190	284.7	0.990	29275
	286.4		
	288.9		
280	284.7	0.997	55451
	285.7		
	287.3		
	289.5		
350	284.8	0.992	28957
	286.1		
	287.5		
	289.7		
430	284.8	0.996	53000
	286.1		
	287.6		
	289.5		
560	284.8	0.993	20758
	286.2		
	287.5		
	289.2		
	291.4		

explained by the presence of stable phosphate esters and the creation of nitrogenated heterocycles. Then the ratio decreases because of the volatilization of the P_2O_5 formed.

The $C_{C=O}/C_a$ ratio increases up to 350°C, the material oxidizes by reacting with O_2 via the formation of hydroperoxides creating carbonyl groups. At higher temperatures, it decreases due, according to the $-O-/=O$ ratio versus temperature curve, to the transformation of C=O into CO and CO_2.

The $C_{O=C-O}/C_a$ ratio decreases between 190 and

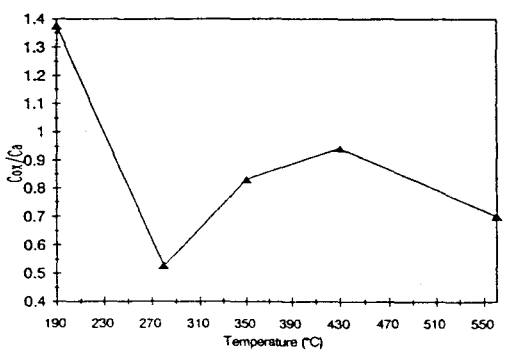

Fig. 6. C_{ox}/C_a versus temperature.

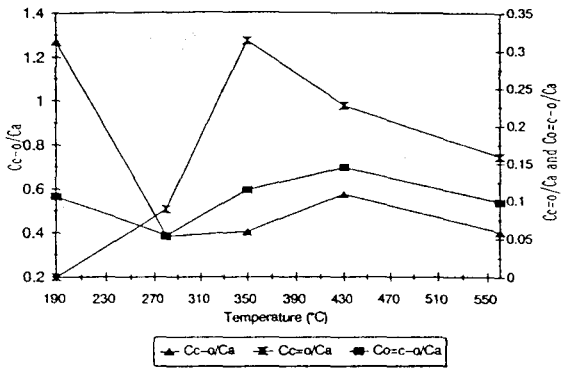

Fig. 7. C_{C-O}/C_a, $C_{C=O}/C_a$ and $C_{O=C-O}/C_a$ ratios versus temperature.

280°C due to the formation of aromatic species. The increase of this ratio between 280 and 430°C may be explained by the oxidation of the intumescent coating. Between 430 and 560°C, the carboxylic groups transform into CO and CO_2.

3.4. N1s spectra

Each material gives rise to a single broad N1s peak. The core-level binding energy of the nitrogen atom depends on the oxidation state and the environment of the atom. The binding energy is, however, largely independent of the bulk of the molecule, although conjugation effects give rise to a chemical shift dispersion and a consequent peak broadening. Since different functional group types exhibit a particular chemical shift, it is possible to resolve a single broad peak by reference to a range of suitable model compounds [19]. The N1s spectra could be resolved into two major components (Fig. 8 and Table 6) except for the spectrum of the heat-treated system at 190°C.

At 190°C one single band is observed centred at 401.7 eV which can be assigned to NH_4^+ groups in phosphate species [10]. Indeed, at this temperature APP reacts with PER without (or little) release of ammonia. At higher temperatures, ammonia is evolved and may react to form nitrogenated aromatic species. This hypothesis is confirmed by the chemical shift measured in the XPS spectra. Two bands at around 401.2 and 399.6 eV are observed corresponding to NH_4^+ groups and nitrogen in pyrrole- and/or pyridine-type structures, respectively [10,18–20].

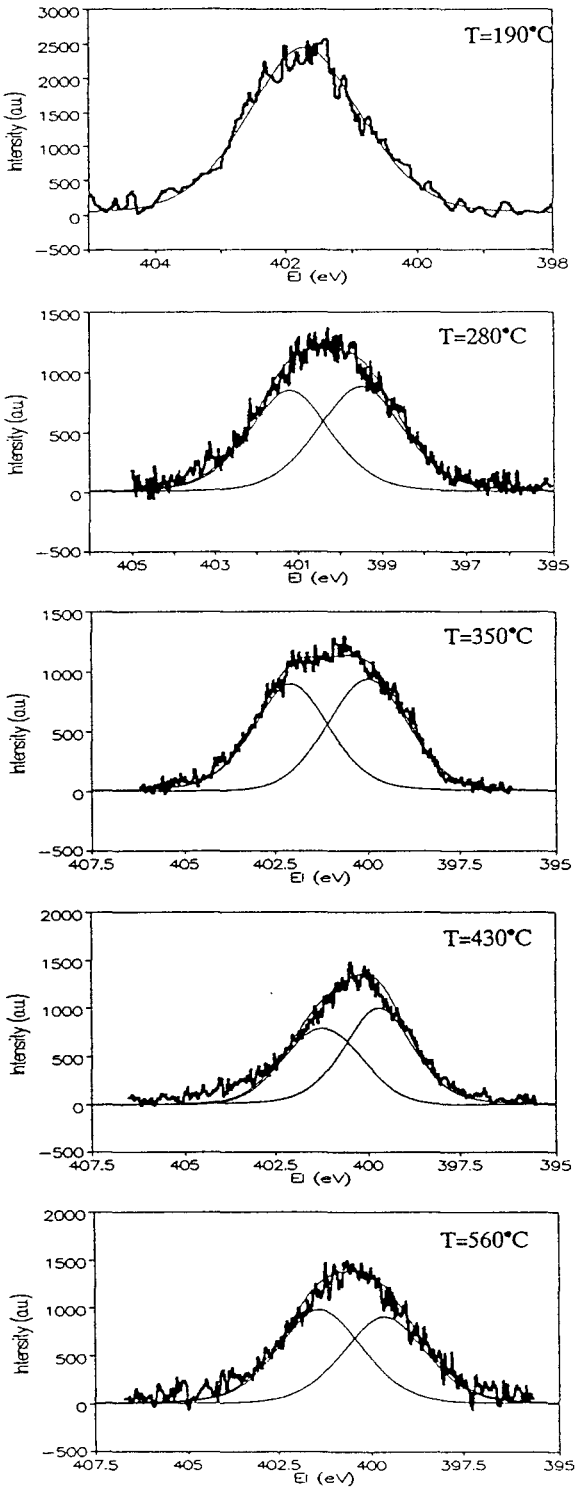

Fig. 8. N 1s spectra of the heat-treated APP/PER system.

Table 6
Fit results of the N1s spectra of the heat-treated APP/PER system

Temperature (°C)	Binding energy (eV)	Fit statistics	
		r^2	F
190	401.8	0.974	30903
280	399.5	0.970	21291
	401.2		
350	400.0	0.983	25880
	402.1		
430	399.7	0.964	11568
	401.2		
560	399.6	0.954	15128
	401.4		

It is to note that NO_x species may form because of our experimental conditions (the samples are heat-treated in the air). A previous IR study has not shown NO_x species trapped in the intumescent shield [4]. So, the presence of these species may not be assumed.

The hypothesis of ammonium salts may be surprising at these temperatures because of the low stability of ammonium phosphates at high temperatures. Nevertheless, the intumescent material can trap ammonia in its structure [21] and, during recooling, NH_3 can react with acidic phosphates and/or carboxylic groups to form ammonium salts.

The analysis does not suggest the presence of any amine or amide groups. This may be explained by the reactivity of these functional groups which may be reaction intermediates to form nitrogenated heterocycles. Indeed, evolved ammonia can react with ketones to form amides which can give amines by the Hoffman degradation and/or nitriles by heating. Nitriles can then react with alcohols in acid medium to form iminoether which can condensate with amines to form heterocycles. These cycles may also be formed by reaction of ammonia or amines with furanes or 1,4-diketones.

To resume, the fire-retardant system APP/PER develops an intumescent coating from 280 up to 560°C but it has been shown that this is very efficient at 350°C [2]. At this temperature, we have observed that the number of oxidized species (carbonyl and carboxylic groups) is maximum. It may be assumed that these reactive species play a part in the protective property of the material.

The FR properties of an intumescent shield have been previously connected to particular dynamic properties of the material [9,22]. The presence of N-containing organic species may not explain the properties of interest because samples treated at 430°C (protective material) and at 560°C (no protection) have the same N content.

4. Conclusion

This study allows us to specify the intumescent structure developed from the thermal treatment of the APP/PER system. It confirms the presence of P–O–C bonds belonging to stable phosphate esters and the decomposition of the material by reaction with O_2 via carbonyl and carboxylic species. Moreover, it shows first, that there are nitrogenated compounds in the intumescent coating and second, that the ammonia evolved reacts to form nitrogenated aromatic species in pyrrole- and pyridine type structures but there are no amine and amide in the intumescent shield.

References

[1] H.L. Vandersall, J. Fire Flammability 2 (1971) 97.
[2] R. Delobel, M. Le Bras, N. Ouassou and F. Alistiqsa, J. Fire Sci. 8 (2) (1990) 85.
[3] G. Camino, L. Costa and M.P.L. di Cortemiglia, Polym. Deg. Stab. 33 (1991) 131.
[4] S. Bourbigot, doctoral dissertation, University of Lille (1993).
[5] Handbook of Flame Retardant Chemicals and Fire Testing Services (Technomic, Lancaster, 1988).
[6] G. Camino, L. Costa and L. Trossarelli, Polym. Deg. Stab. 12 (1985) 213.
[7] Y. Schmidt-Le Tallec, doctoral dissertation, University of Lille (1992).
[8] R. Delobel, N. Ouassou, M. Le Bras and J.M. Leroy, Polym. Deg. Stab. 30 (1990) 41.
[9] S. Bourbigot, M. Le Bras and R. Delobel, Carbon 8 (1993) 1219.
[10] G. Beamson and D. Briggs, in: High Resolution XPS of Organic Polymers (Wiley, Chichester, 1992).
[11] A.R. Gonzalez-Elipe, A. Martinez-Alonso and J.M.D. Tascon, Surf. Interf. Anal. 12 (1988) 565.
[12] G. Marletta, C. Oliveri, G. Feria and S. Pignatoro, Surf. Interf. Anal. 12 (1988) 447.
[13] Y. Nakayama, F. Soeda and A. Ishitani, Carbon 28 (1990) 21.
[14] D.L. Perry and A. Grint, Fuel 62 (1983) 1024.
[15] D.T. Clark and R. Wilson, Fuel 62 (1983) 1034.
[16] S.R. Kelemen, K.D. Rose and P.J. Kwiatek, Appl. Surf. Sci. 64 (1993) 167.
[17] G. Camino, G. Martinasso, L. Costa and R. Gobetto, Polym. Deg. Stab. 28 (1990) 17.
[18] K.D. Bartle, D.L. Perry and S. Wallace, Fuel Proc. Technol. 15 (1987) 351.
[19] S. Wallace, K.D. Bartle and D.L. Perry, Fuel 68 (1989) 1450.
[20] P. Burchill and L.S. Welch, Fuel 68 (1989) 100.
[21] C.E. Anderson, S. Dziur, W.A. Mallow and J. Buckmaster, J. Fire Sci. 3 (1985) 161.
[22] R. Delobel, M. Le Bras, Y. Schmidt and S. Bourbigot, in: Actes Int. Symp. on Mineral and Organic Functional Fillers in Polymers (GFEAP, Le Mans, 1991).

ELSEVIER

0169-4332/94/$07.00
SSDI 0169-4332(94)00185-5

II-1-b. Discussion synthétique

L'étude structurale des matériaux montre l'existence de plusieurs phases quelque soit la température du traitement. Il est proposé que ces matériaux sont donc des mélange de plusieurs composés de type polymère polyaromatique. Les deux bandes du spectre de diffusion Raman, identiques à celles des spectres des produits de la carbonisation de TDMGA/DDS, impliquent une structure carbonée

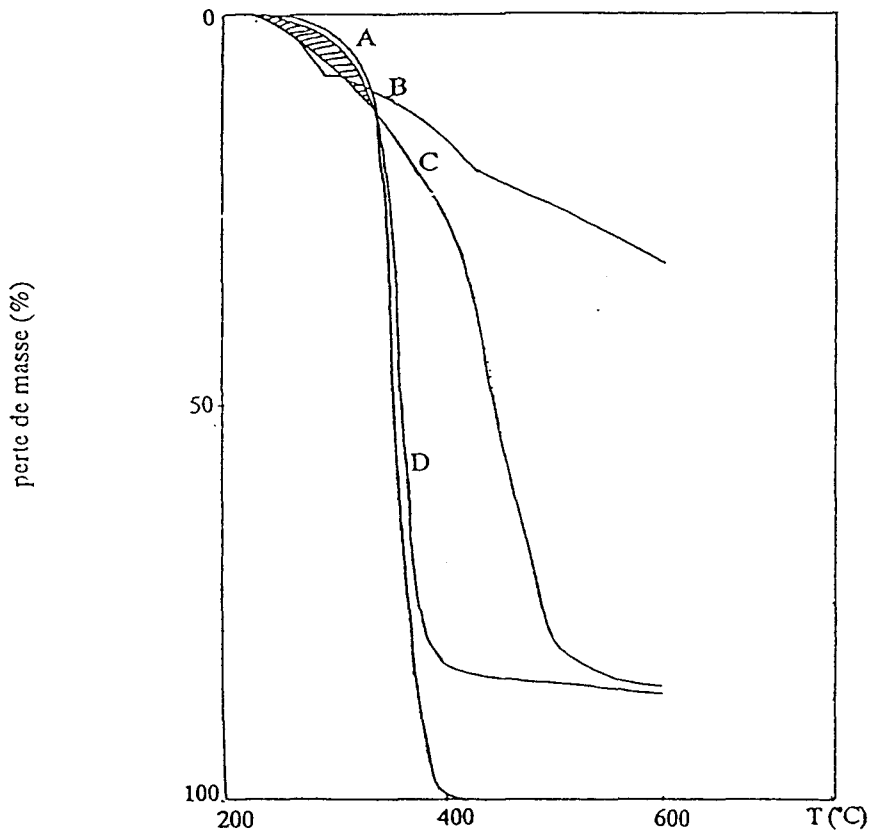

Figure II-5. Courbes thermogravimétriques sous air (β_v = 300°C/h) de PP (A), APP/PER (B), PP/APP/PER (C : $W_{PP/APP/PER exp}$) et courbe calculée de PP/APP/PER (D : $W_{PP/APP/PER calc}$).

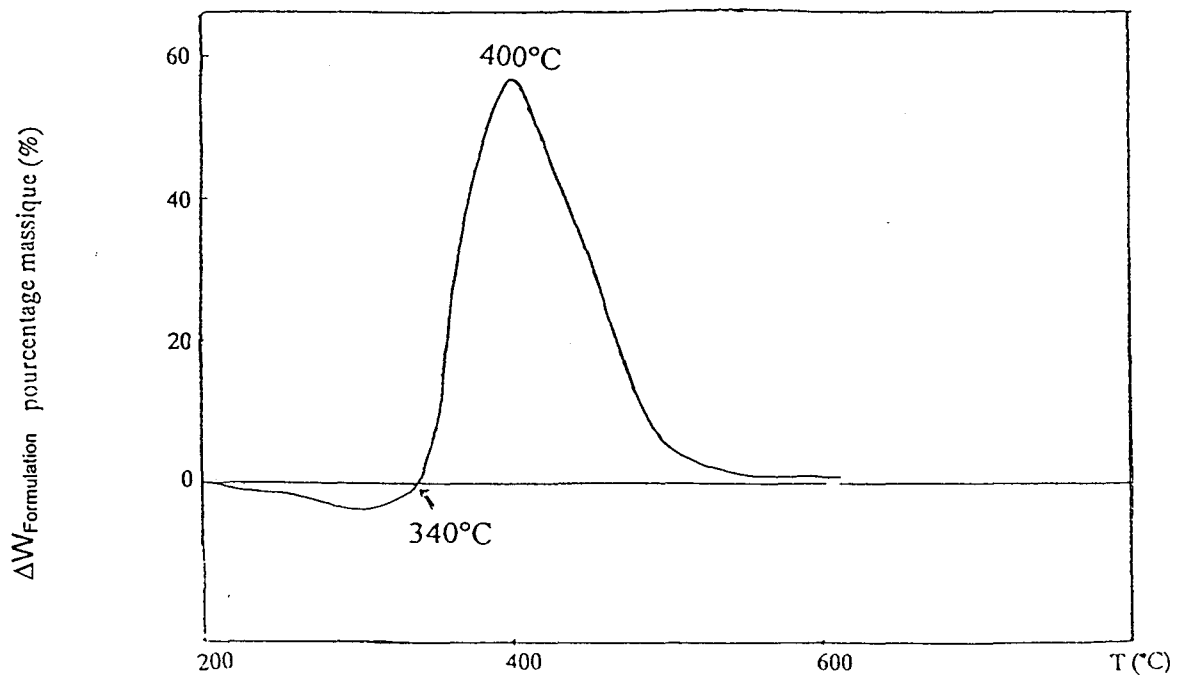

Figure II-6. .Différence $\Delta W_{Formulation}$ calculée en fonction de la température avec PP/APP/PER sous air.

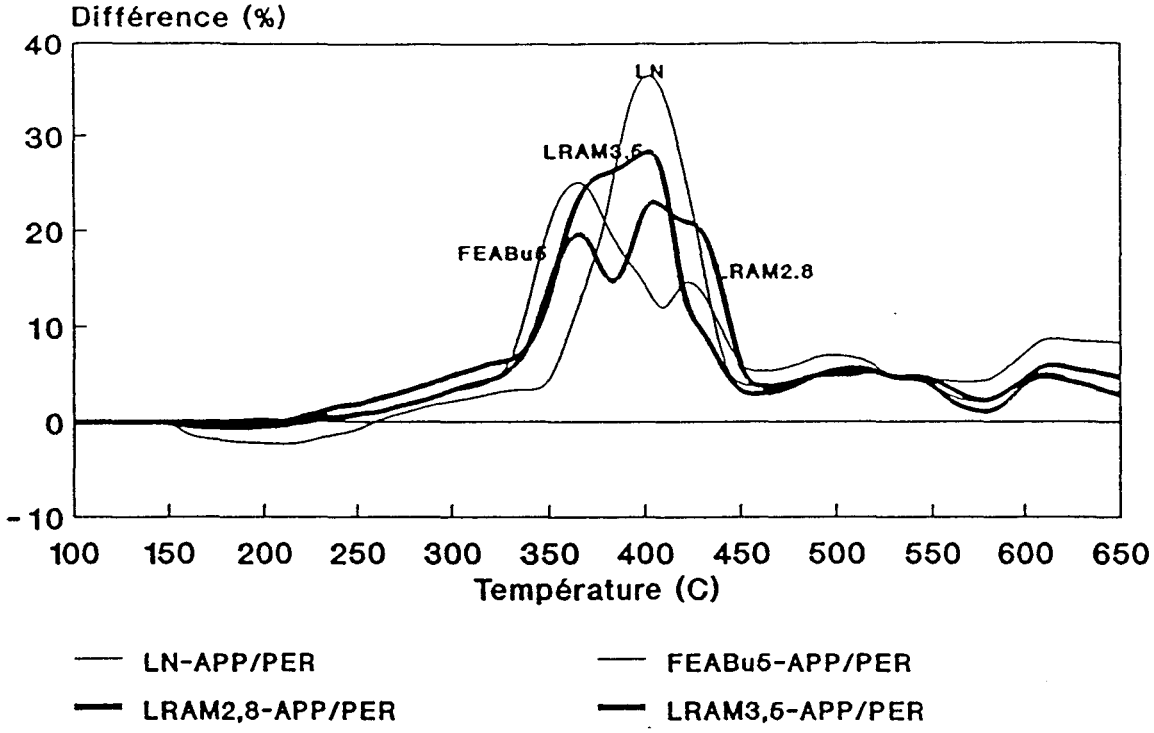

Figure II-7. Différences $\Delta W_{Formulation}$ calculées en fonction de la température de systèmes polymère/APP/PER sous air.

Le rôle joué par l'oxygène dans la dégradation de PP/APP/PER est mis en évidence par la comparaison entre les courbes des ATG conduites respectivement sous air (Figures II-5 et II-6) et sous inerte (Figures II-8 et II-9).

La stabilité sous inerte est comparativement élevée entre 200 et 350°C. Il est connu que l'oxygène participe dans le domaine des « basses températures » à la dégradation du PP lors de la séquence : diffusion (absorption) de l'oxygène, formation d'un « macroradical », conversion de ce radical en radical peroxy et formation d'un hydroperoxyde [1201]. L'auto-oxydation du polymère s'effectue ensuite par un processus radicalaire en chaînes branchées initié par la décomposition des hydroperoxydes. Les produits de cette dégradation ont été préalablement rapportés [109]. La présence de l'adjuvant dans le PP diminue la stabilité dans cette zone (surface hachurée de la figure II-8). Un processus mécano-chimique lors de la mise en forme explique cette différence.

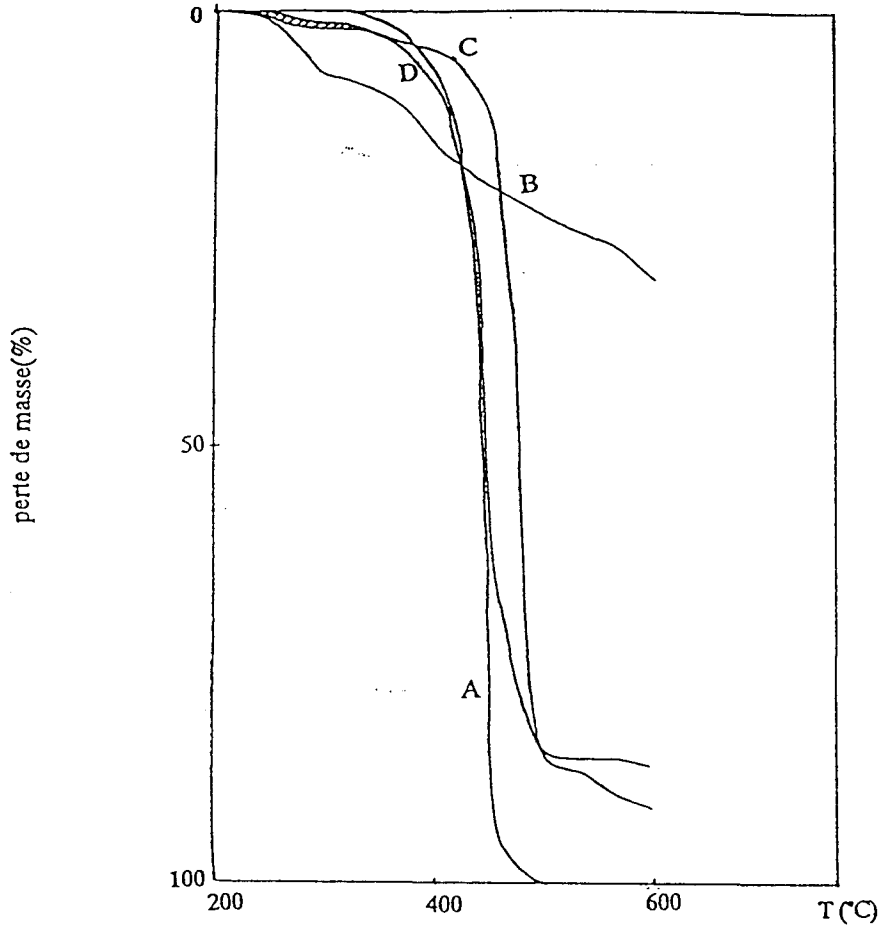

Figure II-8. Courbes thermogravimétriques sous azote (β_v = 300°C/h) de PP (A), APP/PER (B), PP/APP/PER (C : $W_{PP/APP/PERexp}$) et courbe calculée de PP/APP/PER (D : $W_{PP/APP/PERcalc}$).

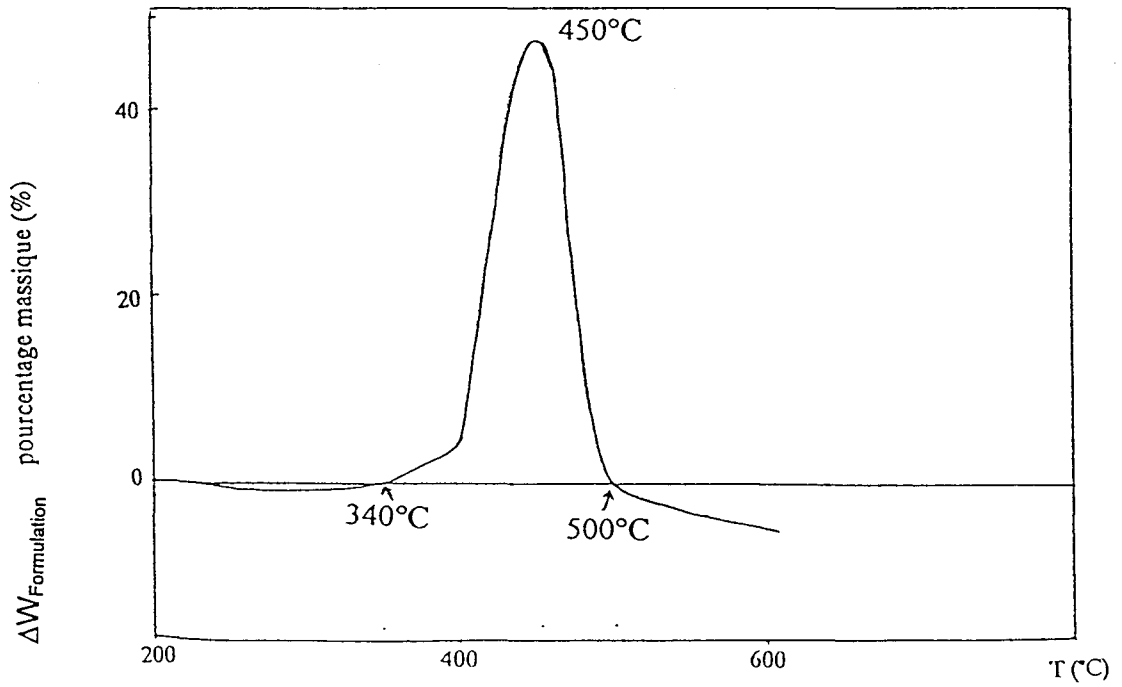

Figure II-9. Différence $\Delta W_{Formulation}$ calculée en fonction de la température avec PP/APP/PER sous azote.

La dégradation rapide et complète du PP, observée sous air à environ 350°C, se produit entre 400 et 480°C sous inerte. Elle prend place entre 430 et 510°C dans PP/APP/PER.

Les courbes de différence de masse montrent que, dans cette étape, une protection de la matrice polymère existe entre 340 et 500°C sous air et sous inerte. A ces températures, la dégradation (pyrolyse) se produit par scission des chaînes avec formation de chaînes plus courtes éventuellement volatiles ou par dépolymérisation (dégrafage) avec formation du monomère [121-124]. Ces réactions sont des réactions radicalaires. Les réactions avec les produits de la dégradation de APP/PER limitent donc le développement du processus de pyrolyse. La protection lors d'une dégradation thermique sera discutée au Chapitre III par un mécanisme de terminaison des chaînes réactionnelles via une réaction avec le produit de la dégradation de APP/PER.

L'étude des résines polyépoxydes a montré que l'oxygène moléculaire réagit lors de la dégradation pour former des produits constituants du matériau protecteur. La présence de ces produits dans les matériaux intumescents doit, dans un premier temps, d'être vérifiée lors de la dégradation thermo-oxydante. Le présent paragraphe présente l'analyse quantitative et la caractérisation des espèces chimiques des matériaux carbonés formés lors de la dégradation thermo-oxydante de la formulation LRAM3,5/APP/PER. L'étude utilise les spectroscopies RMN et IR qui permettent de caractériser les groupements chimiques présents dans le matériau protecteur.

Le polymère est choisi pour mettre en évidence l'influence éventuelle des chaînes des co-monomères acrylate de butyle et anhydride maléique sur la composition du matériau protecteur. Les résultats seront discutés par référence à une étude similaire du système PP/APP/PER [104, 105].

II-2-a. Résultats

Pergamon

Carbon, Vol. 33, No. 3, pp. 283–294, 1995

0008-6223/95 $9.50 + .00

0008-6223(94)00131-6

CARBONIZATION MECHANISMS RESULTING FROM INTUMESCENCE—PART II. ASSOCIATION WITH AN ETHYLENE TERPOLYMER AND THE AMMONIUM POLYPHOSPHATE-PENTAERYTHRITOL FIRE RETARDANT SYSTEM

SERGE BOURBIGOT, MICHEL LE BRAS, and RENÉ DELOBEL
Laboratoire de Physicochimie des Solides, E.N.S.C.L.,
Université des Sciences et Technologies de Lille, BP 108,
F-59652 Villeneuve d'Ascq Cedex, France

PATRICE BRÉANT
Cerdato (Elf-Atochem), F-27470 Serquigny, France

and

JEAN-MICHEL TRÉMILLON
GRL (Elf-Atochem), BP 34, F-64170 Lacq, France

(*Received* 4 *February* 1994; *accepted in revised form* 7 *October* 1994)

Abstract—In this work we study the carbonization resulting from an intumescence phenomenon of the fire-retardant formulation: ethylene terpolymer-ammonium polyphosphate/pentaerythritol. Characterisation of the intumescent coating is carried out using infrared spectroscopy and MAS-NMR of the solid state. The study shows the formation of organic phosphocarbonaceous esters, which limits depolymerisation or the evolution of gaseous hydrocarbons. These esters prevent the development of condensed polyaromatic structures. These latter are bridged by the polyethylenic links, which provide the mechanical properties of interest in the protective shield.

Key Words—Intumescence, ethylene terpolymer/ammonium polyphosphate/pentaerythritol, infrared spectroscopy, MAS NMR ^{13}C, ^{1}H, and ^{31}P.

1. INTRODUCTION

In a previous paper, we studied the carbonization mechanisms resulting from an intumescence phenomenon between the ammonium polyphosphate (APP) and the pentaerythritol[1]. Between 280°C and 350°C development of intumescence (the protective cellular carbon-based coating) occurs, and between 350°C and 430°C degradation of this intumescent coating takes place. At higher temperatures, structural changes lead to the formation of a new carbonaceous species (established in the temperature range 430°C < T < 560°C). We demonstrated that the dynamic properties of the char could be explained by the chemistry of the system (aromaticity, thermal polymerisation of aromatic molecules, etc.).

The APP/PER fire-retardant (FR) system is very efficient in polyolefin-based formulations[2–3] and, in particular, in the ethylene-butyl acrylate-Maleic anhydride (LRAM3.5)[4]. For example, the formulation has a Limiting Oxygen Index (LOI)[5] equal to 30%, and admits the classification V-O of the UL-94 test[6] for an additives level of 30%. A previous study in this laboratory[7] showed that olefinic species take part in this protective process. A chemical process explaining this role has to be determined.

The aim of this study is to characterize the intumescent char resulting from the formulation LRAM3.5-APP/PER (Fig. 1) and to understand the protection mechanisms of the formulation. This characterization is carried out using infrared spectroscopy and NMR of the solid state.

2. EXPERIMENTAL

2.1 *Material*

Raw materials were LRAM3.5 (Lotader P3200 supplied by Elf-Atochem, ethylene terpolymer: ethylene (91.5%)-butyl acrylate (5%)-Maleic anhydride (3.5%)), PER (Aldrich R.P. grade), and APP ($(NH_4PO_3)_n$, $n = 700$, Hoechst Exolit 422, soluble fraction in H_2O: <1 wt%). The study was carried out using the APP/PER mixture for the ratio APP/PER = 3 (wt/wt). In the case of the polyethylenic materials, the fire-retardant properties are maximum for a ratio[2–4]. The additives are incorporated at 30% (wt/wt) in the polymer. Initial mixtures were first prepared by ball-milling after mechanical grinding and sifting (200×10^{-6} m) of the raw materials. They were then treated at four different temperatures (280, 350, 430, 560°C) during 12 hours under air flow (flow rate = 6 cm^3/s). An intumescent coating was obtained at every temperature and then analysed.

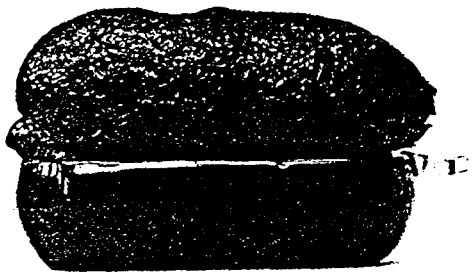

Fig. 1. Intumescence coating resulting from the carbonization of the LRAM3.5-APP/PER formulation.

2.2 *Infra-red spectroscopy*

Samples were ground and mixed with KBr to make pellets. Spectra were recorded using a Perkin-Elmer 683 instrument connected with a PE3600 data station.

2.3 *NMR measurements*

^{13}C NMR measurements were performed on a Brucker CXP100 weak field spectrometer at 25.2 MHz (2.35 T) with magic-angle spinning (MAS), with high-power ^{1}H decoupling and ^{1}H-^{13}C cross polarisation (CP). The Hartmann-Hahn matching condition was obtained by adjusting the power on ^{1}H channel for a maximum ^{13}C FID signal of adamantane. All spectra were acquired with contact times of 1 ms (samples heat-treated at 280 and 350°C) or 1.5 ms (samples heat-treated at 430 and 560°C). It was shown that the intensities of the bands of the samples were maximized[4]. A repetition time of 10 sec was used for all samples because the spin-lattice relaxation time (T_1) stayed below 2 sec at all temperatures (the repetition time was chosen to be five times T_1)[4]. Typically, 10,000 scans were necessary to obtain spectra with a good signal/noise ratio, and the reference used was tetramethylsilane (TMS).

^{1}H NMR measurements were obtained at 100.1 MHz on the same spectrometer with MAS and a repetition time of 2 sec (T_1 always below 300 ms)[4]. All spectra were acquired with 20 scans, and the reference used was the TMS. The deconvolution of the spectra was carried out using Peakfit software (Jandel Scientific), assuming either Gaussian or Lorentzian bands.

^{31}P NMR measurements were performed at 40.5 MHz on the same spectrometer with MAS, with high power decoupling protons and a repetition time of 2 sec (T_1 always below 300 ms)[4]. All spectra were acquired with 500 scans. The reference used was 85% H_3PO_4 in aqueous solution.

All spectra of the solids were obtained at a spinning speed of 3 kHz.

3. RESULTS AND DISCUSSION

3.1 *Chemical analysis*

Table 1 presents the chemical composition of the samples heat treated at 280, 350, 430, and 560°C.

Figure 2 shows the ratio P/C of the formulation LRAM3.5-APP/PER plotted against temperature in comparison with the ratio of the APP/PER system. The curve of the formulation increases up to 430°C, and then remains constant, which means that in the "high-temperature" range, stabilisation of phosphorus species is favored compared to carbonaceous species, contrary to what is observed with the APP/PER system. This suggests that the presence of the polymer stabilizes the phosphorus species in the protective shield. Moreover, the relatively low P/C values observed at 280 and 350°C may be explained by the higher carbon content of the intumescent material.

Figure 3 shows the ratio N/C of the formulation LRAM3.5-APP/PER plotted against temperature in comparison with the ratio of the APP/PER system. The curves have two different evolutions. In the case of the additives, the carbonaceous species are stabilized compared to phosphorus compounds when the ratio N/C remains constant in the case of polymer additives. This suggests that the polymer orients the reactions to form stable nitrogenated compounds. Indeed, the reaction between APP and PER evolves ammonia, which may react, for example, on the maleic anhydride functions of the polymer.

This study shows, therefore, that an interaction between the polymeric matrix and the additives takes place, and that the intumescent coating develops not only from these latter to protect the material.

3.2 *Infra-red spectroscopy*

The spectra of the formulation are presented (Fig. 4) in the wavelength ranges between 850 and 1350 cm^{-1} and between 2500 and 3700 cm^{-1}. The first spectral region corresponds to the absorption range of the P—O bonds and allows us to characterize, on one hand, the phosphate species and, on the other hand, to prove the formation of a phosphocarbonaceous structure (Table 2). The second spectral region is an absorption range of aliphatic groups, which allows us to show the stability of the polymeric matrix in the intumescent coating (Table 2).

At every temperature, the spectra present broad bands between 1150 and 1300 cm^{-1} assigned according to McKee *et al.*[10], to P—O—C bonds in "phosphate-carbon" complexes, and broad bands about 1000 cm^{-1} assigned to modes of symmetric vibrations of PO_2 and PO_3, characteristic of phosphocarbonaceous complexes[8-11]. These results show, therefore, the formation of phosphocarbonaceous structure from 280°C, which is kept up to 560°C.

It is interesting to note that two bands are observed at about 950 cm^{-1} and 1090 cm^{-1}, assigned, respectively, to the modes of asymmetric and symmetric vibrations of a P—O bond in a chain P—O—P. The

Table 1. Chemical composition of the heat-treated LRAM3.5-APP/PER formulation

	Temperature (°C)			
Elements	280	350	430	560
C (% mol)	4.7	3	1	1
H (% mol)	10.6	5.1	4.3	1.9
N (% mol)	0.1	0.1	0.02	0.05
O (% mol)	1.4	2.5	3.8	3.9
P (% mol)	0.2	0.4	0.6	0.7

band about 1090 cm^{-1} disappears above 350°C, which implies an increase in asymmetry of the P—O—P bonds. Moreover, these condensed phosphate species are observed at every temperature.

In comparison with the APP/PER system[12–13], the spectra exhibit two additional absorptions at 2920 and 2850 cm^{-1}, which characterize aliphatic groups [14]. The intensity of these bands decreases when the temperature decreases, and they are no longer observed at 560°C. The spectra of APP/PER vs the temperature showed only aliphatic groups up to 225°C, which are formed by reaction between the additives. It may be proposed that the aliphatic groups observed are assigned to $-(-CH_2-)_n-$ and that therefore the FR APP/PER system inhibits the degradation of the polymer by blocking polyethylenic links in the intumescent coating.

3.3 *CP/DD-MAS NMR ^{13}C*

The CP/DD-MAS ^{13}C spectroscopy is a powerful tool to characterize the carbonaceous materials and, thus, to confirm the hypothesis deduced from the infrared spectroscopy.

CP/DD-MAS ^{13}C NMR spectra are presented in Fig. 5. The attributions of the absorption bands are presented in Table 3.

At every temperature, an intense band is observed about 33 ppm assigned to $-CH_2-$ groups in polyethylenic chains[15–16] belonging probably to fragments of nondegraded polymer. This hypothesis may appear surprising, because it is well known that the polyethylenic chains are degraded at temperatures lower than 200°C. Nevertheless, this result has already been observed by several authors[17–20]. Moreover, it is confirmed, on the one hand, by the infrared study and, on the other hand, by the spectrum of the sole polymer (Fig. 6).

A band of low intensity is observed at about 14 ppm at 280°C and 350°C. It may be assigned to $-CH_3$ groups belonging to the chain-end of the polymer[15–16]. Nevertheless, to observe these end-groups $-CH_3$, the ratio number of $-CH_3$ groups to $-CH_2-$ groups

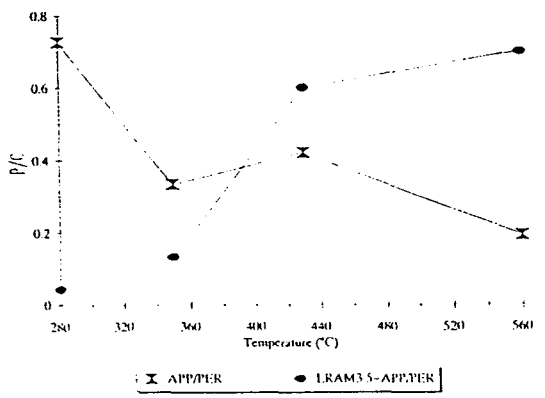

Fig. 2. P/C ratio vs temperature.

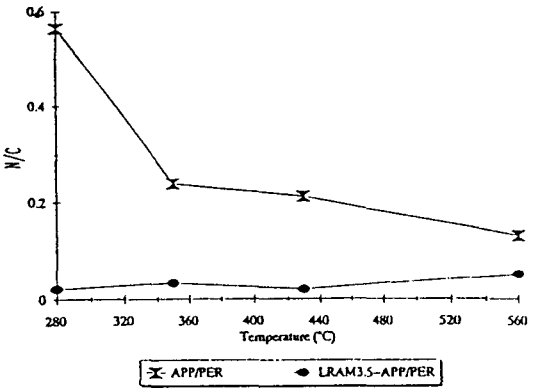

Fig. 3. N/C ratio vs temperature.

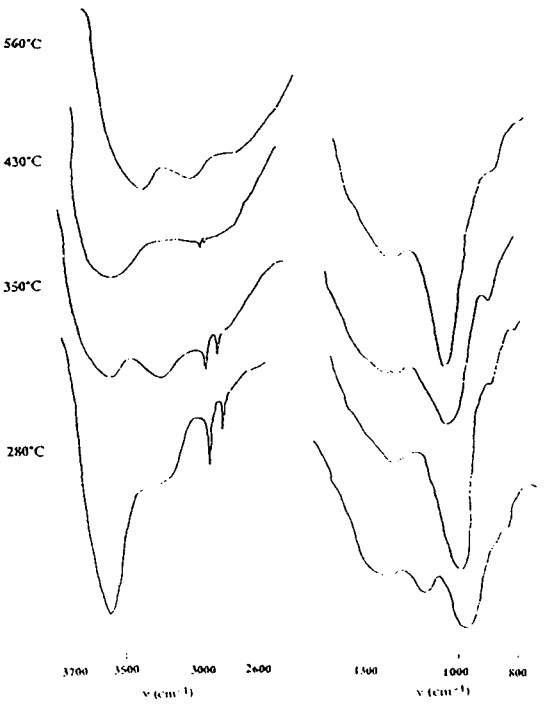

Fig. 4. Infrared spectra of the LRAM3.5-APP/PER formulation.

Table 2. Absorptions' attributions of the heat-treated LRAM3.5-APP/PER formulation

Absorption bands (cm^{-1})	Attributions	Ref.
910-940	ν_{as} of P—O in P—O—P	[8,9]
980-1020	ν_{sym} of PO_2 and PO_3 in complexes Phosphate—Carbon	[9-11]
1080-1100 (in overlap and up to 350°C)	ν_{sym} of P—O in P—O—P	[8,9]
1150-1300	Stretching mode of P—O—C in comlexes Phosphate—Carbon	[9-11]
1250-1260 (in overlap)	Stretching mode in P=O	[8,9]
2850	ν_{sym} of C—H in $-(-CH_2-)_n-$	[12]
2920	ν_{as} of C—H in $-(-CH_2-)_n-$	
3200-3600	Valence vibration of O—H in P—OH and H_2O	[9-12]

Table 3. Chemical shifts' attributions of the CP/DD-MAS ^{13}C NMR spectra

Temperature (°C)	Chemical shift (ppm)	Attribution	Ref.
280	14.5	C_{CH_3}	[15,16]
	33	C_{CH_2}	[15,16]
	111	C_{ar-H}	[15,17,18]
350	14.5	C_{CH_3}	[15,16]
	33	C_{CH_2}	[15,16]
	128 (bd: 115-160)	C_{ar-H}, C_{ar-C}, C_{ar-N}, C_{ar-O}	[15,17,18]
430	32	C_{CH_2}	[15,16]
	140 (bd: 115-160)	C_{ar-H}, C_{ar-C}, C_{ar-N}, C_{ar-O}	[15,17,18]
560	32.6	C_{CH_2}	[15,16]
	123 (bd: 100-160)	C_{ar-H}, C_{ar-C}, C_{ar-N}, C_{ar-O}	[15,17,18]

C_{CH_3}: alkyle carbon $-CH_3$ type; C_{CH_2}: alkyle carbon type $-CH_2-$; C_{ar-H}: protonated aromatic carbons; C_{ar-C}: not protonated aromatic carbons; C_{ar-O}: oxygenated aromatic carbons; C_{ar-N}: nitrogenated aromatic carbons and/or nitrogenated carbons with conjugated bondings in heterocycles; bd: broad band.

have to be high enough. Therefore, a scission of the polyethylenic chains leading to the formation of shorter chains, which are in the intumescent coating or involved in its formation, must be assumed. The disappearance of the band at 430°C and 560°C implies oxidation of these end-group $-CH_3$. This oxidation leads, via a radical mechanism, to oxidized groups (cetonic groups, hydroperoxydes etc.), which react with phosphate acidic species[3] to form phosphocarbonaceous structures and/or aromatic species bridged by polyethylenic chains.

Table 3 shows, as in the case of the APP/PER system[1], that the carbonization process is characterized by the appearance of aromatic species (bands about 111 ppm) observed from 280°C. These bands about 111 ppm may be assigned, according to Hasan *et al.*[21], to aromatic or polyaromatic species of small size (benzene, naphthalene, anthracene, etc.). From 350°C, a broad band between 110 and 150 ppm is observed, which implies the presence of several non-magnetically equivalent carbons[15]. As discussed before in the case of the APP/PER system[1], this band may be due to several types of aromatic and polyaromatic species[15, 22,23].

In comparison with the APP/PER system, the NMR ^{13}C study has shown that the presence of the polymer in the formulation LRAM3.5-APP/PER puts off the carbonization of the system. The polymer par-

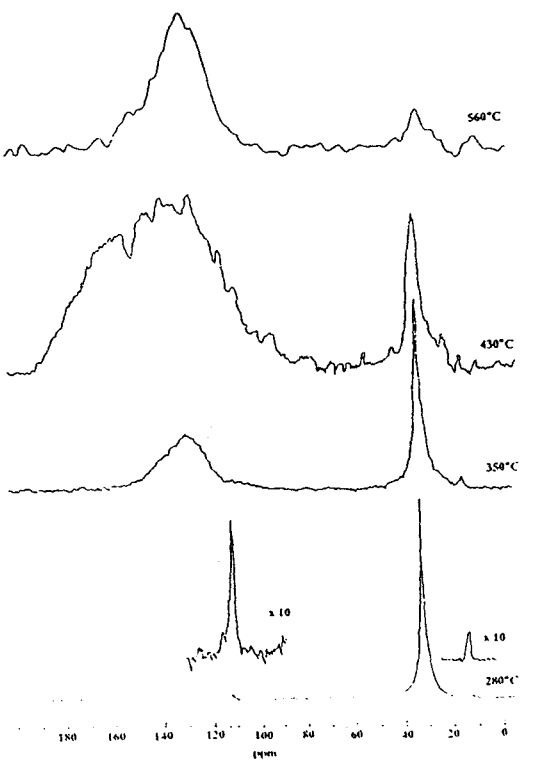

Fig. 5. CD/DD-MAS NMR ^{13}C spectra of the LRAM3.5-APP/PER formulation

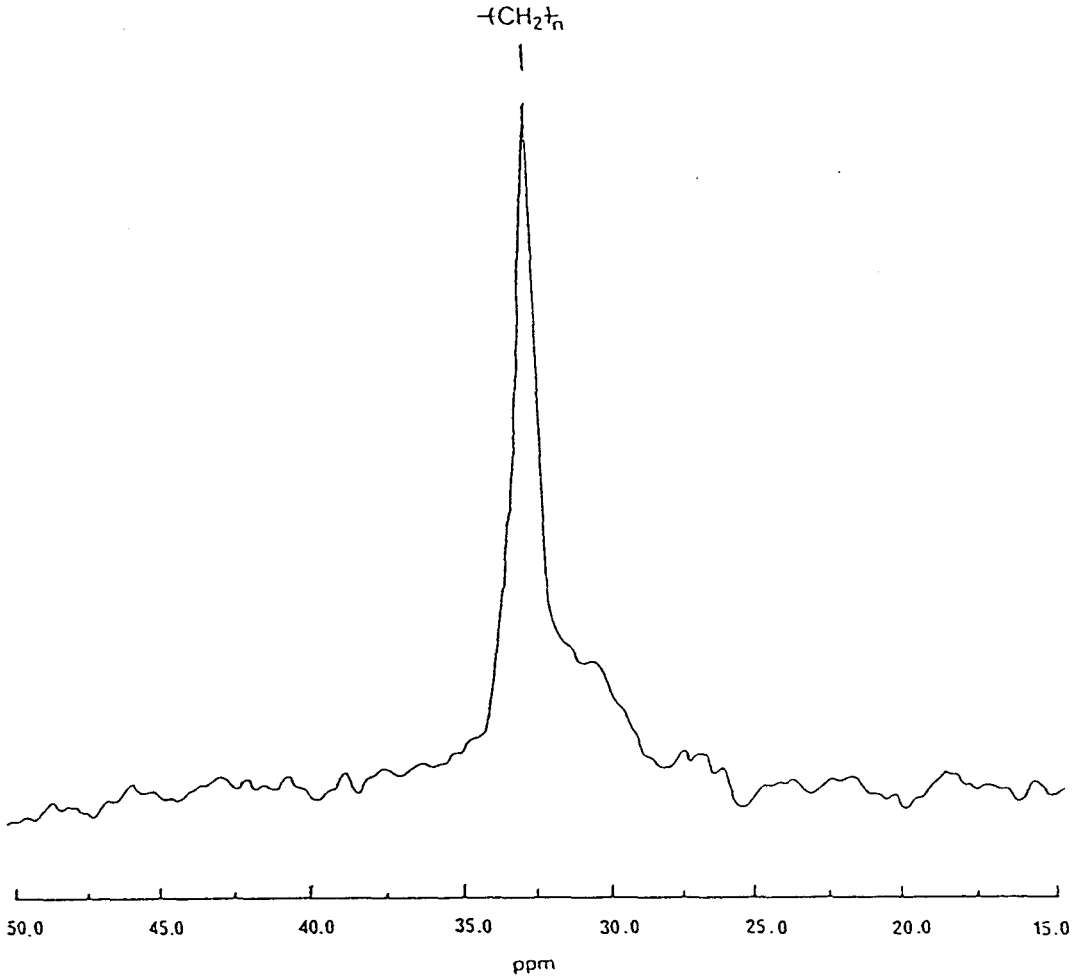

Fig. 6. CD/DD-MAS NMR ^{13}C of the polymer LRAM3.5.

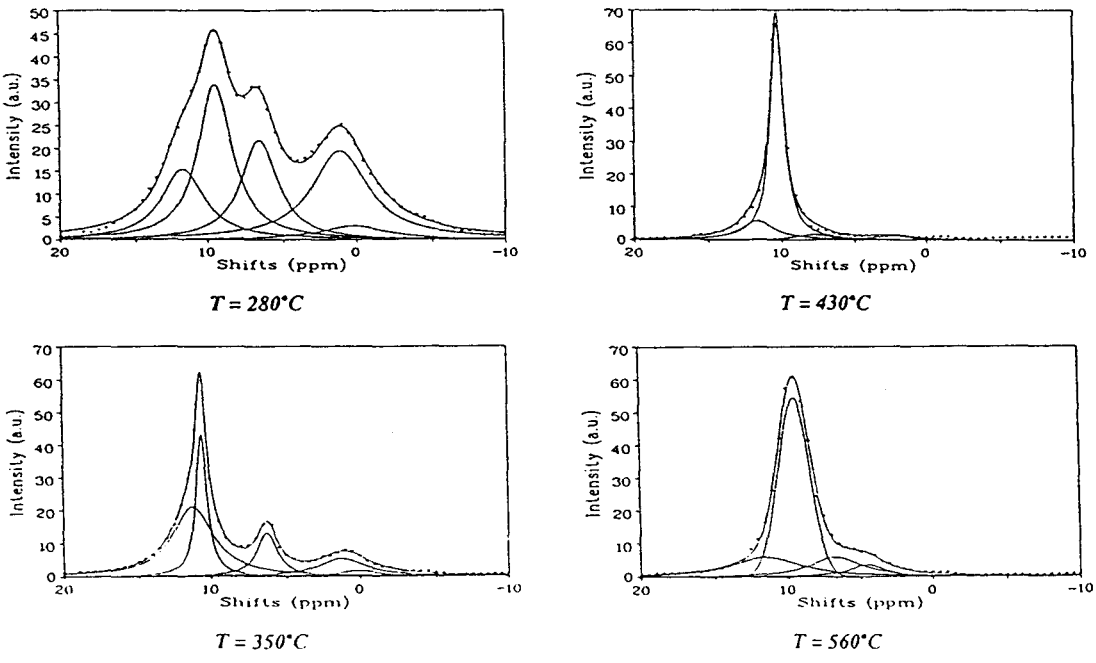

Fig. 7. MAS RMN ^{1}H spectra of the LRAM3.5-APP/PER formulation (. = experimental points).

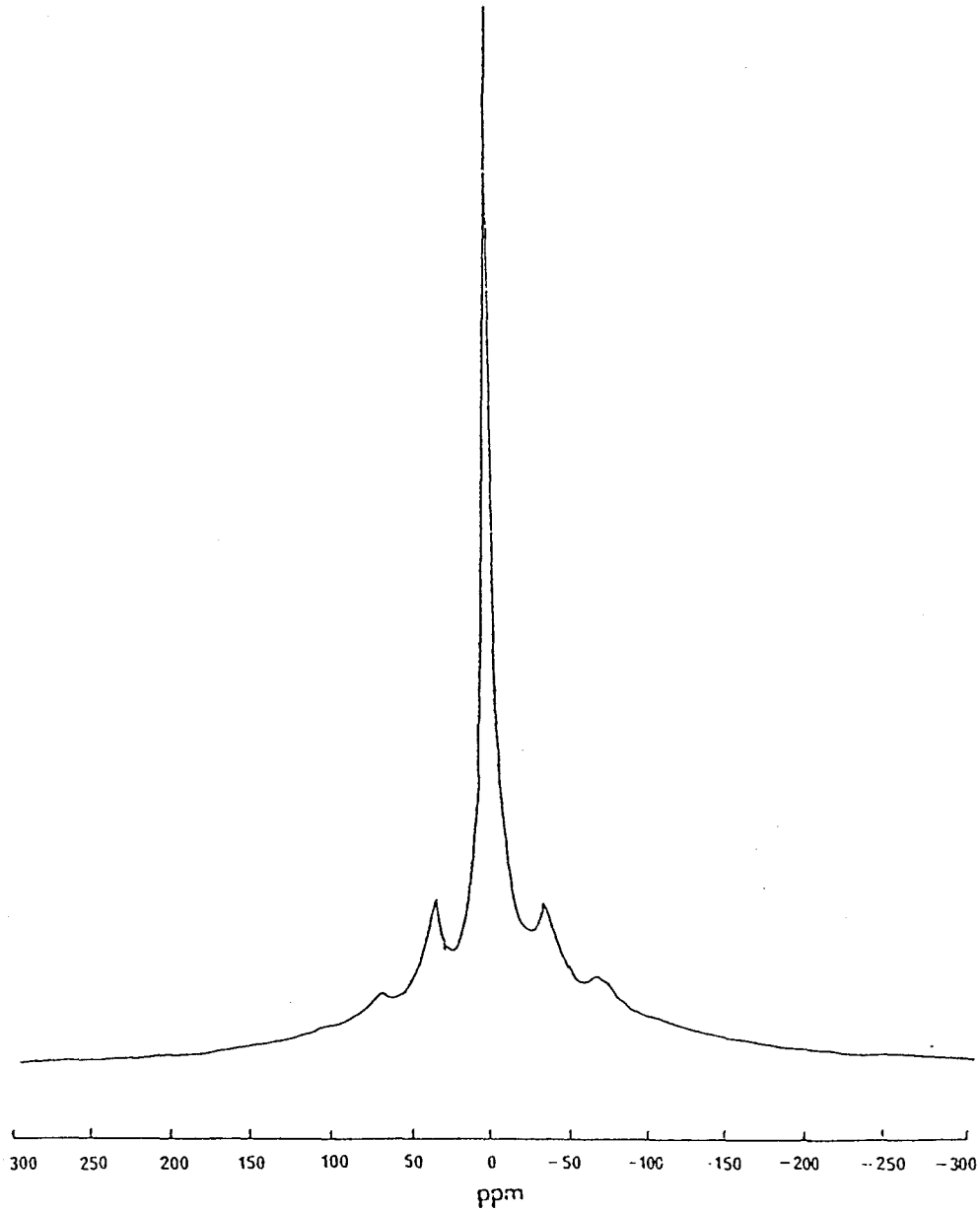

Fig. 8. MAS RMN ^{1}H spectra of the polymer LRAM3.5.

ticipates in the formation of the intumescent shield, and may hinder aromatization.

3.4 *MAS-NMR ^{1}H*

The MAS-NMR ^{1}H study completes the analytical results obtained by CP/DD-MAS NMR ^{13}C. The spectra are presented (Fig. 7) with the deconvolution of their bands assuming either Lorenztian or Gaussian curves. As in the case of APP/PER system[1], the spectra are relatively well defined, and CRAMPS technology is not absolutely necessary to assign the bands [24]. The attributions are given in Table 4.

Table 4 puts forward the formation of aromatic species from 280°C, which confirms the hypothesis deduced from CP/DD-MAS NMR ^{13}C. The bands around 12, 9, and 7 ppm have already been observed and discussed in the case of the APP/PER system[1]. In the presence of the polymer in the carbonization process, additional bands appear. These bands around 1 ppm may be assigned, according to the NMR ^{13}C study, to undegraded chains' fragments $-(-CH_2-)_n-$ of the polymer. Moreover, the spectra of the sole polymer confirms this hypothesis (Fig. 8).

The bands at 0.2 and 0.6 ppm observed, respectively, at 280 and 350°C may be assigned, according to NMR ^{13}C study, to $-CH_3$ end-groups belonging to $-(-CH_2-)_n-$ chains. The band around 2.5 ppm corresponds to aliphatic protons in $-CH_3$ groups

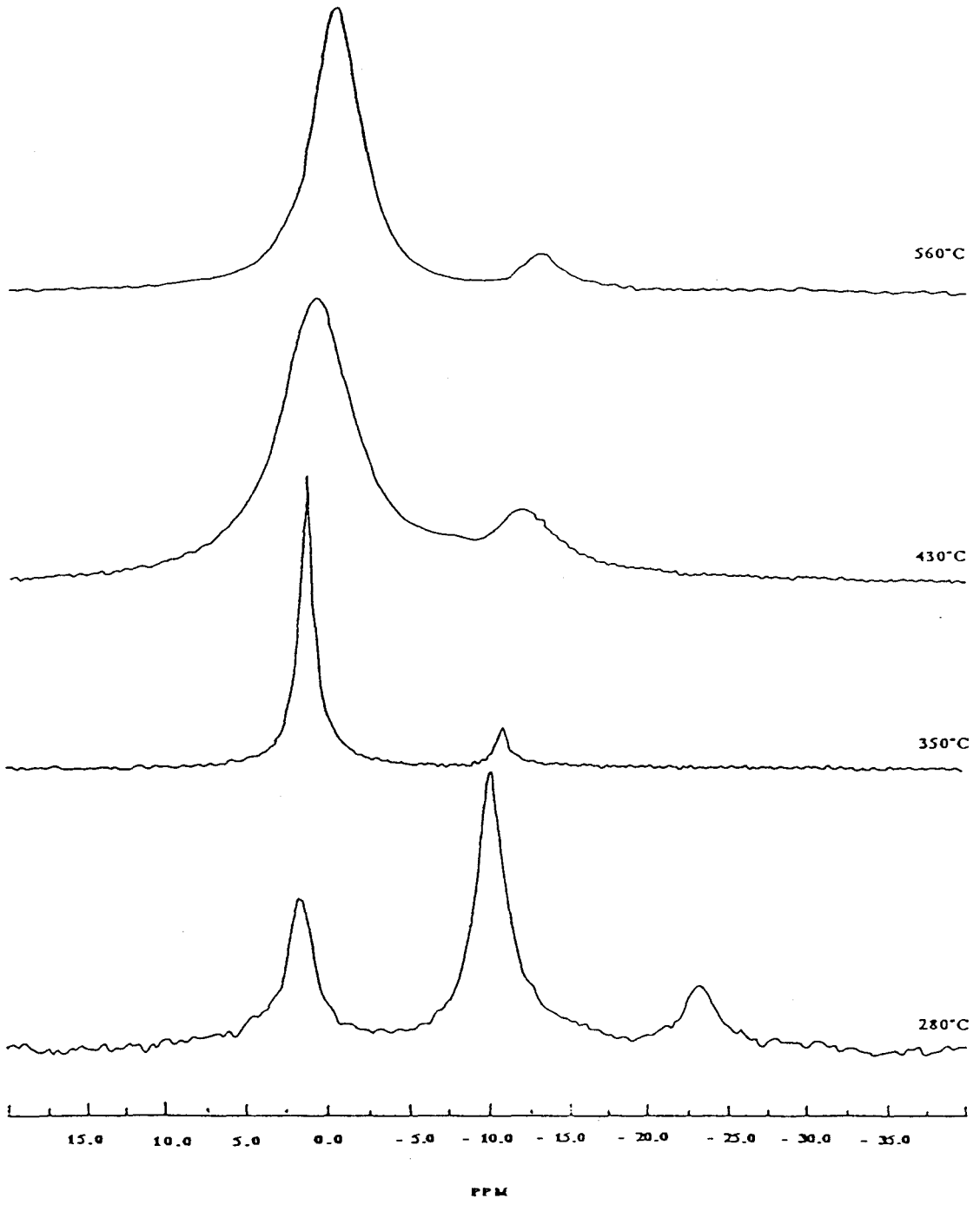

Fig. 9. DD-MAS NMR ^{31}P spectra of the LRAM3.5-APP/PER formulation.

linked to aromatic species and/or to $=CH-$ groups [25–26]. These latter would stem from the first degradation and fragmentation of the polyethylenic chains, then recombination of these with other chains and/or with the additives. The band around 4.5 ppm may be assigned to aliphatic protons belonging to methylene groups bridging polyaromatic species[24–26].

The width of the bands associated to aliphatic groups are larger than those of other groups. This suggests that these protons have significant homonuclear ^1H-^1H interactions because of proton-proton couplings in the $-(-CH_2-)_n-$ chains or rigid conformation. The other bands assigned to phosphate, carboxylic, and aromatic protons are well resolved. The dipolar interactions are therefore weak, and so removed by MAS. Thus, the material structure allows relative mobility of these protons and/or low couplings between these protons. It is noteworthy that in

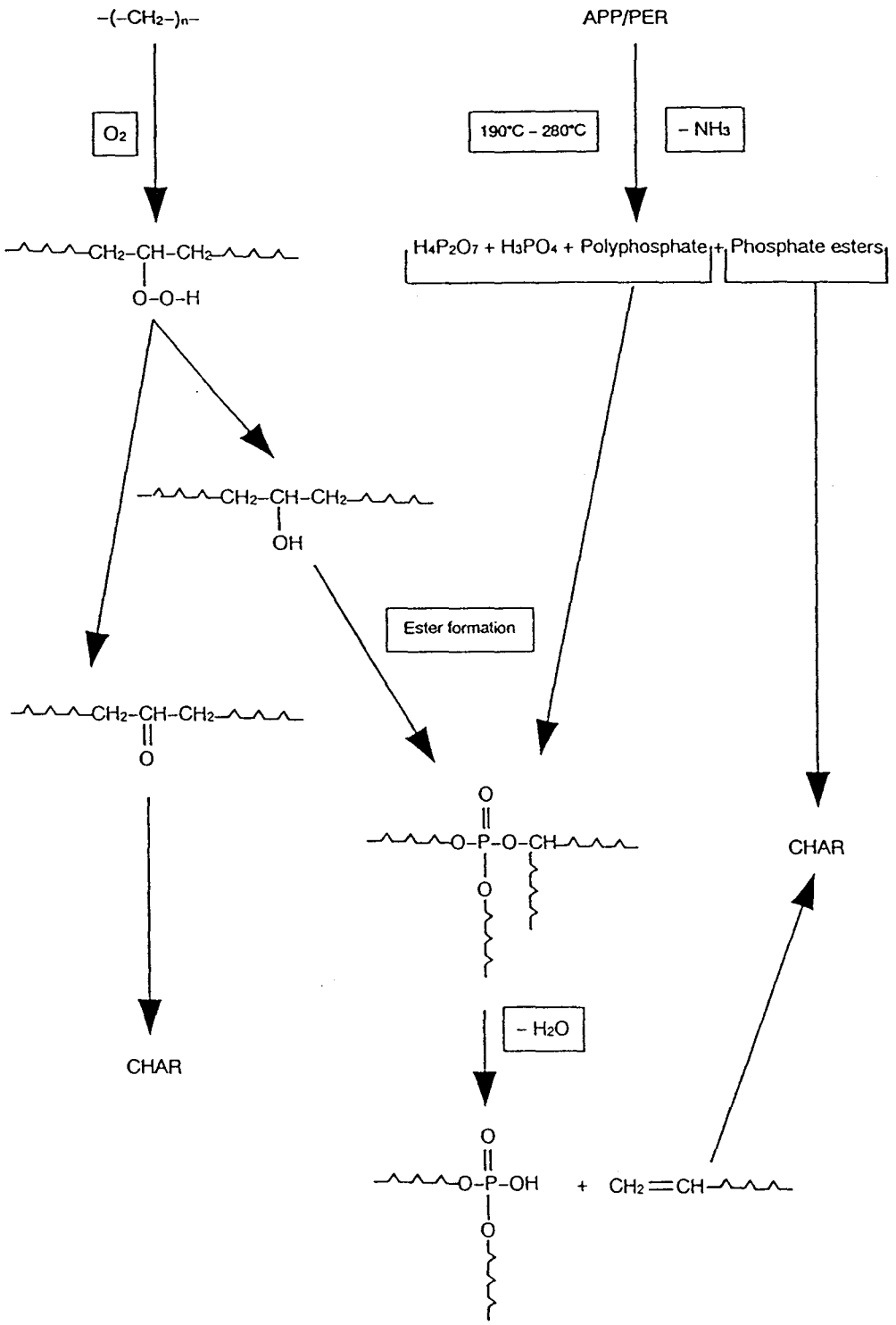

Fig. 10. Reactional scheme showing the formation of phosphocarbonaceous esters.

the case of the APP/PER system[1], the bands assigned to aromatic protons were large. This suggests a polymer-additive interaction, which leads to the formation of a structure allowing relative mobility of protons.

3.5 *DD-MAS NMR ^{31}P*

The infrared study has shown that the intumescent shield was partially composed of phosphocarbonaceous structures. To characterise this structure, a DD-MAS NMR ^{31}P study has been made. The spectra are

Table 4. Chemical shifts' attributions of the MAS-NMR ^1H spectra

Temperature (°C)	Chemical shift (ppm)	Attribution	Fit results			Ref.
			Curve type	r^2	F statistic	
280	0.2	H_{CH_3}	Lorentzian	0.998	1800	[25,26]
	1.1	H_{CH_2}	Lorentzian			[25,26]
	6.7	H_{POH}	Lorentzian			*
	9.5	H_{ar}	Lorentzian			[24,26]
	11.5	H_{COOH}	Lorentzian			[24,26]
350	0.6	H_{CH_3}	Lorentzian	0.999	2920	[25,26]
	1.2	H_{CH_2}	Lorentzian			[25,26]
	6.3	H_{POH}	Lorentzian			*
	10.5	H_{ar}	Lorentzian			[24-26]
	11.7	H_{COOH}	Lorentzian			[24-26]
430	2.5	H_{ar-CH_3} and/or H_{CH}	Gaussian	0.993	750	[25,26]
	7.7	H_{POH}	Lorentzian			*
	10.3	H_{ar}	Lorentzian			[24-26]
	11.6	H_{COOH}	Lorentzian			[24-26]
560	4.5	$H_{CH_{2b}}$, H_{OR}	Lorentzian	0.998	2630	[25,26]
	6.7	H_{POH}	Lorentzian			*
	9.6	H_{ar}	Gaussian			[24-26]
	11.5	H_{COOH}	Lorentzian			[24-26]

H_{CH_3}: $-CH_3$ protons; H_{ar-CH_3}: $-CH_3$ protons linked to aromatic species; H_{CH}: $=CH-$ protons; H_{CH_2}: $-CH_2-$ protons; $H_{CH_{2b}}$: $-CH_2-$ bridging groups between aromatic species; H_{POH}: protons linked to a $-P-OH$ phosphate group; H_{ar}: protons linked to aromatic carbons; H_{COOH}: protons linked to a carboxylic group; H_{OR}: protons linked to aliphatic or aromatic group.

*This study: assignments from comparisons with the spectra of seveal acidic phosphate species.

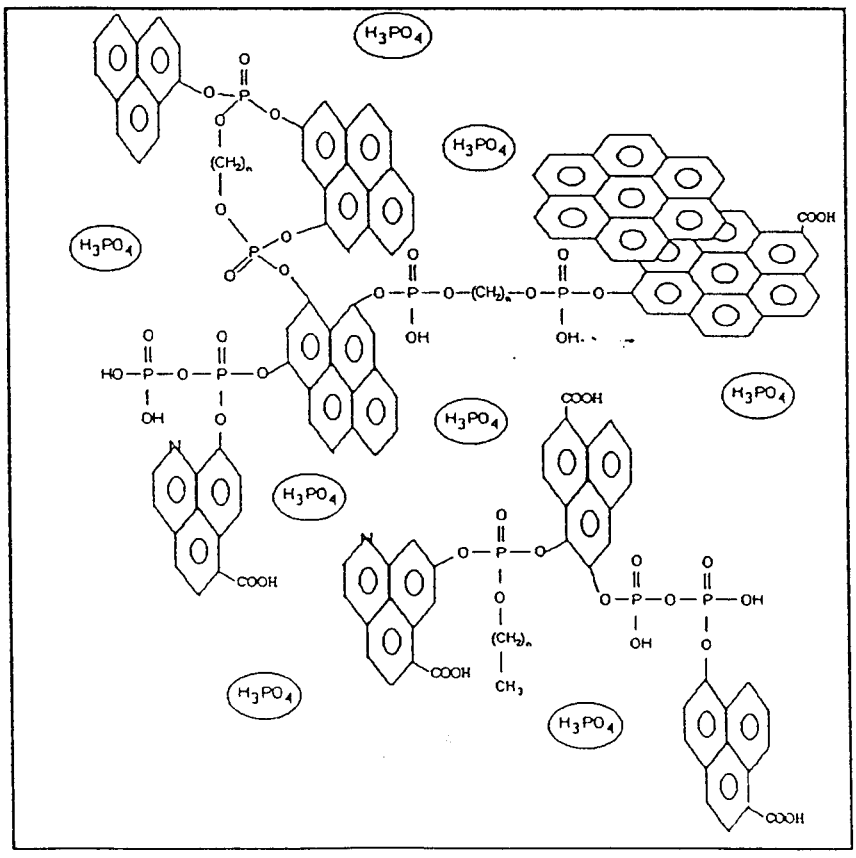

Fig. 11. The intumescent coating resulting from the LRAM3.5-APP/PER formulation heat-treated at 280°C.

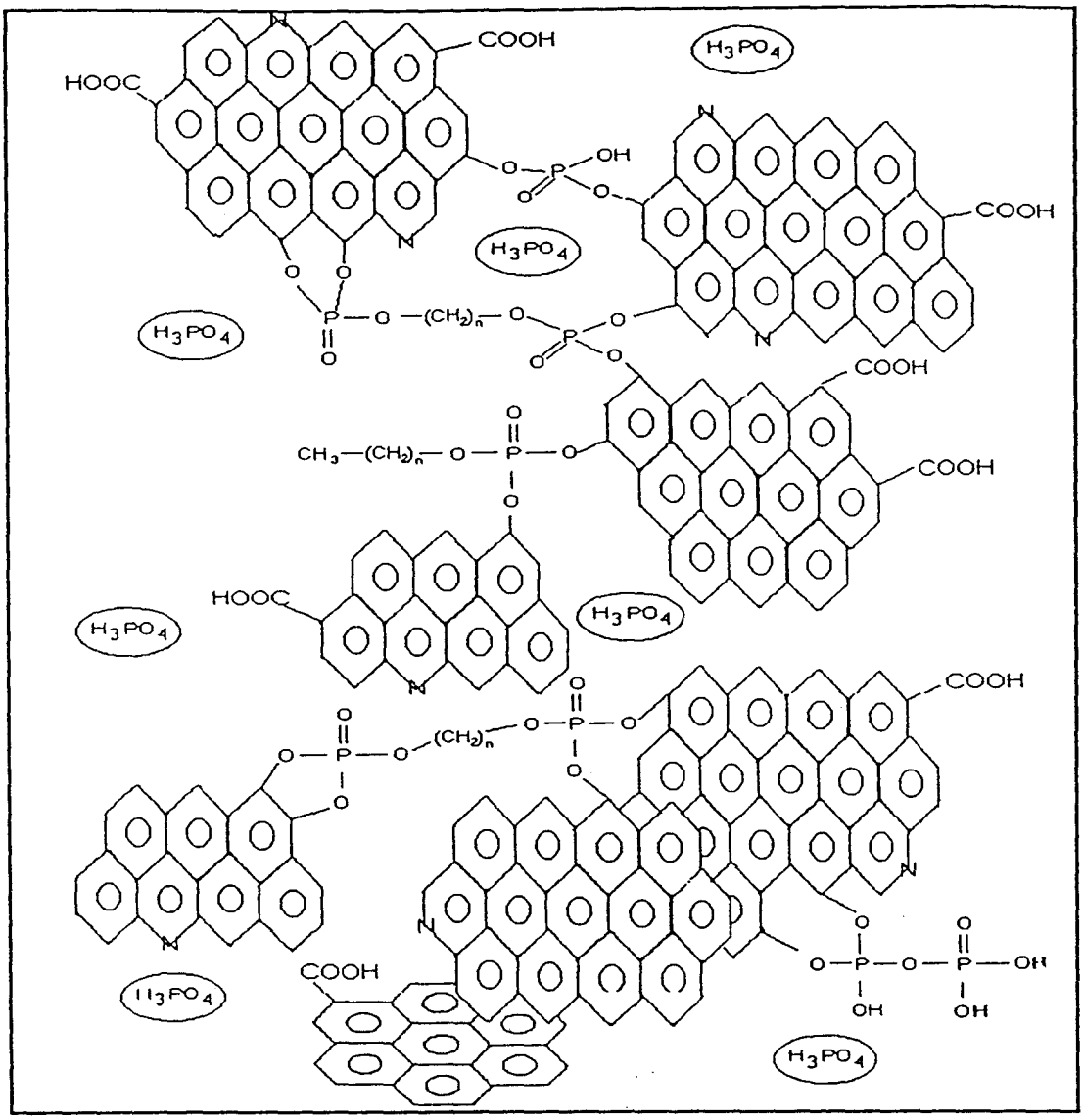

Fig. 12. The intumescent coating resulting from the LRAM3.5-APP/PER formulation heat-treated at 350°C.

Table 5. Chemical shifts' attributions of the DD-MAS NMR ^{31}P spectra

Temperature (°C)	Chemical shift (ppm)	Attribution	Ref.
280	1.5	—PO_4 units in R_2HPO_4, RH_2PO_4, and/or H_3PO_4	[8,27,28]
	−10.2	—PO_4 units in Φ_2RPO_4, and/or Φ_2HPO_4, and/or pyrophosphate group, and/or polyphosphate chain (end group)	
	−22.9	—Polyphosphate chain (central group)	
350	1	—PO_4 units in R_2HPO_4, RH_2PO_4, and/or H_3PO_4	[8,27,28]
	−10.9	—PO_4 units in Φ_2RPO_4, and/or Φ_2HPO_4, and/or pyrophosphate group	
430	0.8	—PO_4 units in R_2HPO_4, RH_2PO_4, and/or H_3PO_4	[8,27,28]
	−12	—PO_4 units in Φ_2RPO_4, and/or Φ_2HPO_4, and/or pyrophosphate group	
560	−0.4	—PO_4 units in R_2HPO_4, RH_2PO_4, and/or H_3PO_4	[8,27,28]
	−12.6	—PO_4 units in Φ_2RPO_4, and/or Φ_2HPO_4, and/or pyrophosphate group, and/or polyphosphate chain (end group)	

R = alkyl groups and Φ = aromatic or polyaromatic groups.

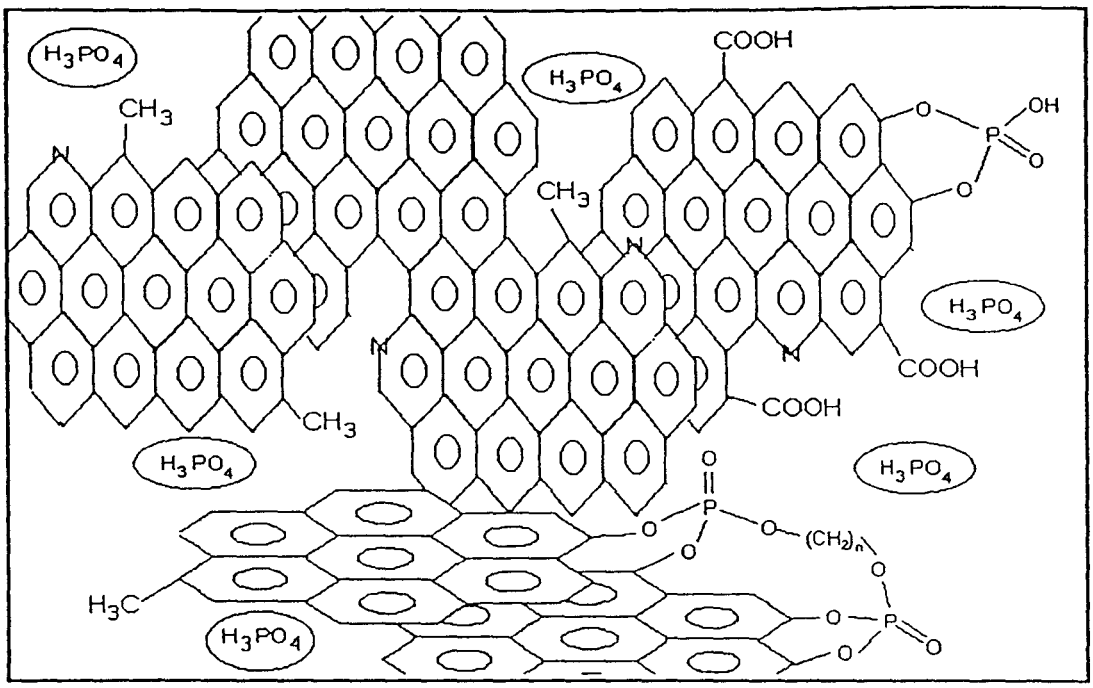

Fig. 13. The intumescent coating resulting from the LRAM3.5-APP/PER formulation heat-treated at 430°C.

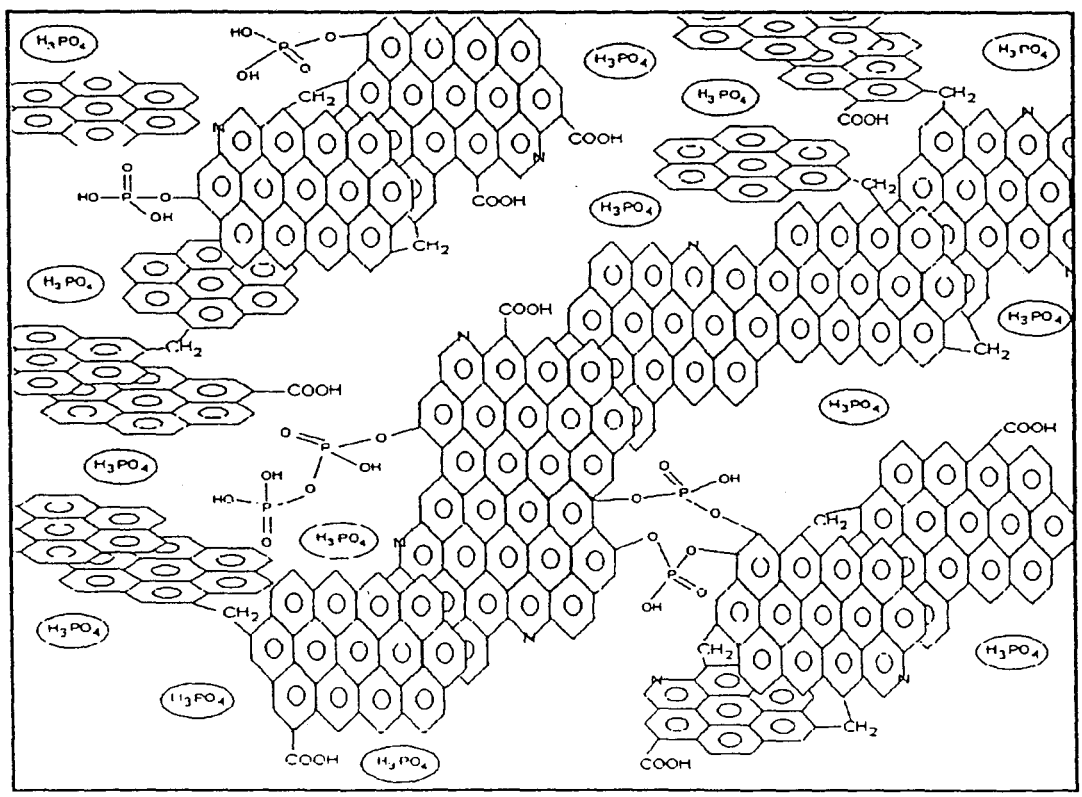

Fig. 14. The intumescent coating resulting from the LRAM3.5-APP/PER formulation heat-treated at 560°C.

presented in Fig. 9. The attributions of the different bands were already justified in our previous work[1], and are given in Table 5.

The ortho- and pyrophosphate groups are observed at every temperature. At 280°C, APP reacts with PER to form ortho- and pyrophosphate species, probably via a hydrolysis reaction. The bands around −10 ppm correspond to orthophosphate groups linked to aromatic cycles and/or to pyrophosphate species[27–28]. Infrared, NMR ^{13}C, and ^{1}H studies justify these attributions. At the other temperatures, the intensity of the bands around −11 ppm decreases very significantly. The polyphosphate chains observed at 280°C are degraded at higher temperatures. This evolution corresponds to a hydrolysis phenomenon, which is amplified for the polymer in comparison with the sole additives system[1].

In comparison with the APP/PER system, the formation of P_4O_{10} is not observed. Indeed, the degradation of the polymer evolves water, and the chemical equilibrium between H_3PO_4 and P_4O_{10} is strongly moved to the formation of the acid.

4. CONCLUSION

In this work, we have shown that the incorporation of the FR APP/PER system in the polymer stabilizes polyethylenic links; consequently, the depolymerization is limited to the formation of small flammable molecules. These links make bridges between polyaromatic species, which provide the mechanical properties of interest of the intumescent coating. They give the flexibility to the carbonaceous shield which, in the conditions of a fire, allow it a retarded creation and propagation of cracks in which the air can diffuse to the polymeric matrix.

To explain the presence of fragments of polyethylenic chains in the material, we may propose according to Kishore *et al.*[29] the scheme of Fig. 10. This scheme shows the formation of phosphocarbonaceous esters that are thermally stable, and therefore may keep polyethylenic links in the coating.

The results of the spectroscopic studies allow us to propose a reaction scheme for the carbonization process from 280°C up to 560°C. When the temperature increases, the intumescent structure develops. At 280°C (Fig. 11), it is formed by stacks of polyaromatic species linked principally by phosphohydrocarbonaceous bridges.

The condensation of aromatic species and concurrently the decrease of phosphocarbonaceous species by scission of P—O—C bonds appear when the temperature increases (Fig. 12–14). Consequently, a key to the intumescence is, on the one hand, to reduce the scission of P—O—C bonds and, therefore, the increase of the size of the aromatic structure, and, on the other hand, to keep polyethylenic links at high temperature.

REFERENCES

1. S. Bourbigot, M. Le Bras, and R. Delobel, *Carbon* **31**, 1219 (1993).
2. G. Camino, L. Costa, and L. Trossarelli, *Polym. Deg. & Stab.* **12**, 213 (1985).
3. R. Delobel, M. Le Bras, N. Ouassou, and F. Alistiqsa, *J. Fire Sci.* **8**, 85 (1991).
4. S. Bourbigot, Doctoral dissertation, Lille (1993).
5. ASTM D-2863-77.
6. ANSI/ASTM D-635-77.
7. R. Delobel, N. Ouassou, M. Le Bras, and J. M. Leroy, *Polym. Deg. & Stab.* **23**, 349 (1989).
8. N. Ouassou, Doctoral dissertation, Lille (1991).
9. R.S. Brown, R. Anderson, and L.J. Shannon, *Adv. Chem. Eng.* **7**, 68 (1968).
10. D.W. McKee, C.L. Spiro, and E.J. Lamby, *Carbon* **22**, 285 (1984).
11. R.A. Nyquist, *Appl. Spectrosc.* **11**, 161 (1957).
12. F. Alistiqsa, Doctoral dissertation, Lille (1993).
13. R. Delobel, M. Le Bras, Y. Schmidt, and S. Bourbigot, In *Actes du MOFFIS 91* (Edited by GFP), pp. 79–85. GFP, Le Mans (1991).
14. *The Coblenz Society Desk Book of Infrared Spectra* (Edited by C.D. Craver), Kirwood (1980).
15. G.E. Maciel, V.J. Bartuska, and F.P. Miknis, *Fuel* **58**, 391 (1979).
16. G.E. Maciel, M.J. Sullivan, L. Petrakis, and D.W. Grandy, *Fuel* **61**, 411 (1982).
17. G. Camino, L. Costa, G. Clouet, A. Chiotis, J. Brossas, M. Bert, and A. Guyot, *Polym. Deg. & Stab.* **6**, 105 (1984).
18. Y. Schmidt-Le Tallec, Doctoral dissertation, Lille (1992).
19. S.K. Brauman, *J. Fire Ret. Chem.* **8**, 8 (1981).
20. G. Montaudo, E. Scamporino, and D. Vitalini, *J. Polym. Sci.* **21**, 3361 (1983).
21. M.U. Hasan, M.F. Ali, and A. Bukhari, *Fuel* **62**, 518 (1983).
22. W.L. Earl and D.L. Vanderhart, *J. Magn. Res.* **48**, 35 (1982).
23. S. Supaluknari, I. Burgar, and F.P. Larkins, *Org. Geochim.* **15**, 509 (1990).
24. S.F. Dec, C.E. Bronnimann, R.A. Wind, and G.E. Maciel, *J. Magn. Res.* **82**, 454 (1989).
25. C.E. Bronnimann, B.L. Hawkins, M. Zhang, and G.E. Maciel, *Anal. Chem.* **60**, 1743 (1988).
26. L.M. Ryan, R.E. Taylor, A.J. Paff, and B.C. Gerstein, *J. Phys. Chem.* **72**, 508 (1980).
27. J.R. Van Wazer, C.F. Callis, J.N. Shoolery, and R.C. Jones, *J. Am. Chem. Soc.* **78**, 5715 (1956).
28. T.M. Duncan and D.C. Douglass, *J. Chem. Phys.* **87**, 339 (1984).
29. K. Kishore and K. Mohandas, *Combustion & Flame* **43**, 145 (1981).

II-2-b. Discussion synthétique

Le LRAM3,5 présente trois dégradations successives (les ATG sous air du LRAM3,5 et de LRAM3,5/APP/PER sont présentées dans ce mémoire dans le paragraphe III-2-a). La première (200 < T < 280°C) peut être expliquée par la dégradation thermo-oxydante à « basse température » du terpolymère, associée à la décomposition des maillons anhydride maléique de la chaîne polymère. La seconde (350 < T < 370°C) et la troisième (380 < T < 430°C) peuvent être expliquées par le dégrafage successif des maillons éthylène et acrylate de butyle. La destruction du matériau est complète à 515°C.

Ces trois étapes ne sont pas observées lors de la dégradation thermo-oxydante de LRAM3,5/APP/PER, comparativement peu rapide entre 200 et 380°C, qui présente une étape rapide entre 390 et 440°C qui conduit à la formation d'un résidu (30 % pondéral). La dégradation de ce résidu rapide entre 530 et 580°C laisse un nouveau résidu qui se dégrade lentement aux températures supérieures (5 % pondéral à 650°C). Les quantités de ces résidus sont identiques à celles obtenues lors de la dégradation de LN/APP/PER dans des conditions opératoires similaires. La présence des maillons oxydés dans le polymère n'implique apparemment pas une stabilité supérieure du revêtement intumescent.

La complexité de la courbe de $\Delta W_{Formulation}$ s'explique par le maintien des maillons anhydride maléique puis par la « protection » globale du matériau qui interdit les deux dégradations rapides de LRAM3,5. Il faut signaler que le matériau résiduel charbonneux conserve un caractère expansé à 560°C.

Le rapport O/P dans le matériau intumescent, toujours proche de 6 at./at., semble indépendant de HTT (il est toujours proche de 4 dans les produits carbonés ex-APP/PER). Il implique le maintien des espèces anhydride carboxylique et acrylate dans le matériau.

Le rapport O/C augmente de 0.3 à 3.8 at./at. entre 280 et 430°C puis reste sensiblement constant aux températures supérieures. Cette évolution est liée à l'augmentation de la teneur relative en espèces phosphates du matériau dont la concentration à 560°C, d'un ordre de magnitude plus importante que celle de APP/PER (0,07 at.%), implique une relative stabilité de ces espèces dans le

matériau. Cette stabilité est confirmée par une disparition des espèces phosphates de la phase condensée (de l'ordre de 45 at.% entre 430 et 560°C) inférieure à la dégradation du matériau (supérieure à 80 % pondéral entre 430 et 560°C). Finalement, l'augmentation de la teneur en azote entre 430 et 560°C s'explique par une stabilité supérieure des espèces carbonées contenant cet hétéroélément.

L'étude spectroscopique montre que les matériaux intumescents issus de LRAM3,5/APP/PER sont constitués d'édifices polyaromatiques pontés par des espèces orthophosphates et pyrophosphates. Ces édifices sont, comme ceux des matériaux ex-APP/PER, des supports des espèces acides carboxyliques et phosphate acides [125]. L'oxyde de phosphore n'est pas formé quelle que soit HTT. La dégradation thermo-oxydante du polymère et de chaînes méthylènes libère H_2O qui hydrolyse les espèces phosphates et interdit, de ce fait, leur condensation et la formation de l'oxyde. La relative stabilité des espèces phosphates entre 430 et 560°C peut s'expliquer par une compétition entre l'hydrolyse et la sublimation de P_4O_{10}.

En accord avec le modèle de Kishore, le polymère participe à la formation du matériau protecteur par formation de chaînes polyéthylènes constituants des ponts inter-polyaromatiques. Cette participation est observée jusque au moins 430°C. La perte du caractère protecteur du matériau à environ 550°C peut être phénoménologiquement reliée à la disparition de ces chaînes polyéthyléniques.

Une étude parallèle de PP/APP/PER confirme la participation de chaînes du PP au matériau intumescent. En effet, le spectre CP/DD-MAS RMN du ^{13}C du matériau intumescent obtenu à 280°C (Figure II-10) montre la présence des 3 types de C de PP (glissements chimiques δ : 20, 24,6 et 42 ppm). La stabilité thermique des chaînes ex-PP dans le matériau est comparativement faible puisque ces signaux ne sont plus observés après le traitement à 360°C. Le spectre RMN présente alors uniquement le signal large (δ maximum 125 ppm) caractéristique des C aromatiques.

Une analyse IR (Figure II-11) complète ces résultats. Les spectres de PP/APP/PER à 360 et 400°C présentent des absorptions dans le domaine spectral 2800-3000 cm^{-1} et une absorption entre 1450 et 1460 cm^{-1} caractéristiques des groupements aliphatiques du polymère. La disparition du dernier signal lorsque PP/APP/PER est traité à 500°C permet de proposer une dégradation thermique des

chaînes polymères du matériau carboné à cette température, avec formation de produits gazeux et/ou de structures condensées éthyléniques ou aromatiques. La perte du caractère expansé du système PP/APP/PER à 430°C peut ainsi résulter de la disparition complète des chaînes linéaires du polymère qui pontent les édifices aromatiques

Le spectre IR de PP/APP/PER à 500°C ne présente plus le signal large (entre 2500 et 3600 cm^{-1}) attribué traditionnellement aux groupements OH des acides phosphoriques. Ce résultat implique une diminution sévère de la teneur en espèces phosphates acides et la formation des espèces polyphosphates ou oxydes susceptibles de sublimer.

La comparaison des comportements thermiques permet donc de présumer un « effet » de la matrice polymère qui sera étudié au Chapitre III.

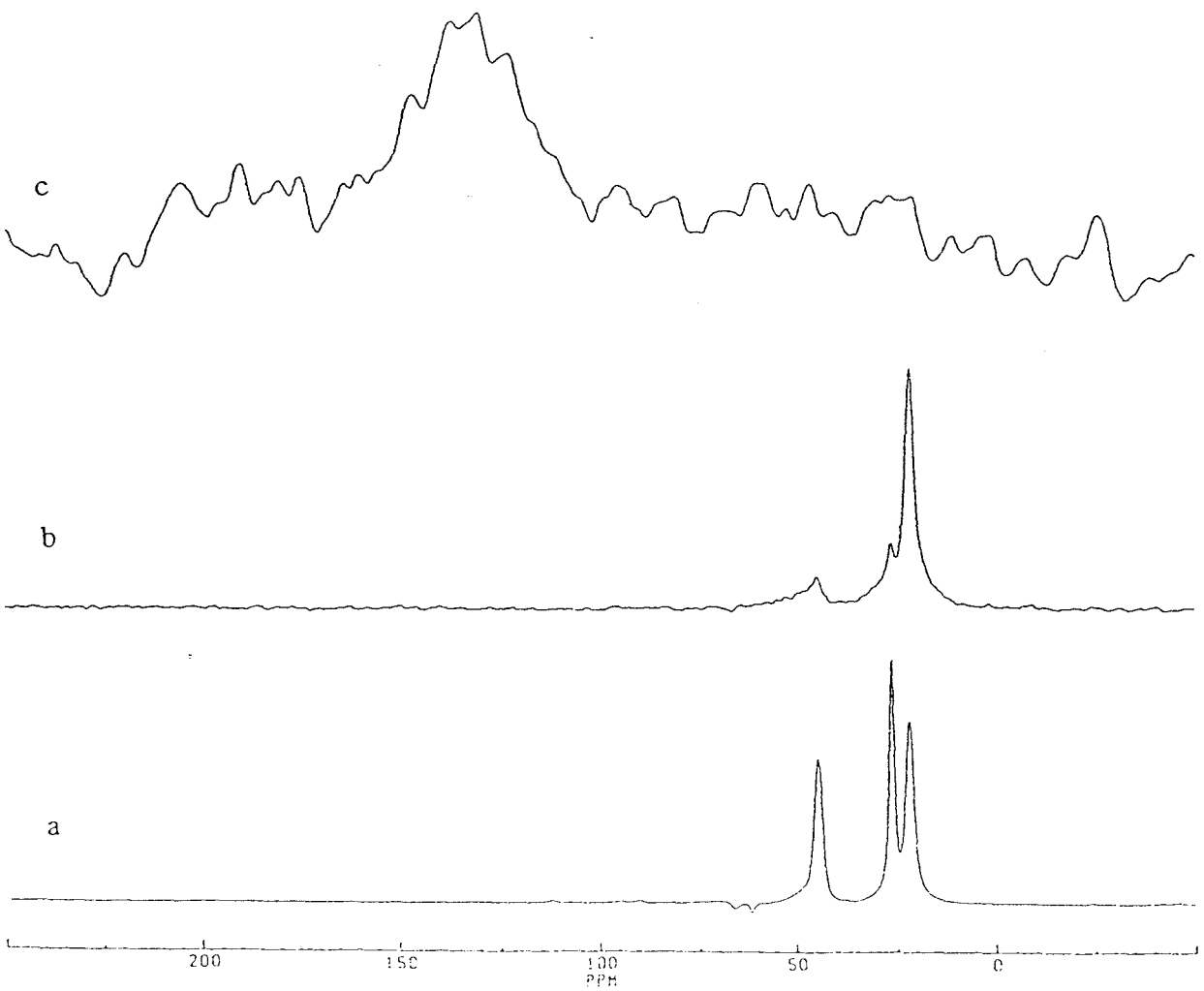

Figure II-10. Spectres CP/DD-MAS du 13C de PP (a) et de PP/APP/PER dégradé sous air à 280°C (b) et 360°C (c).

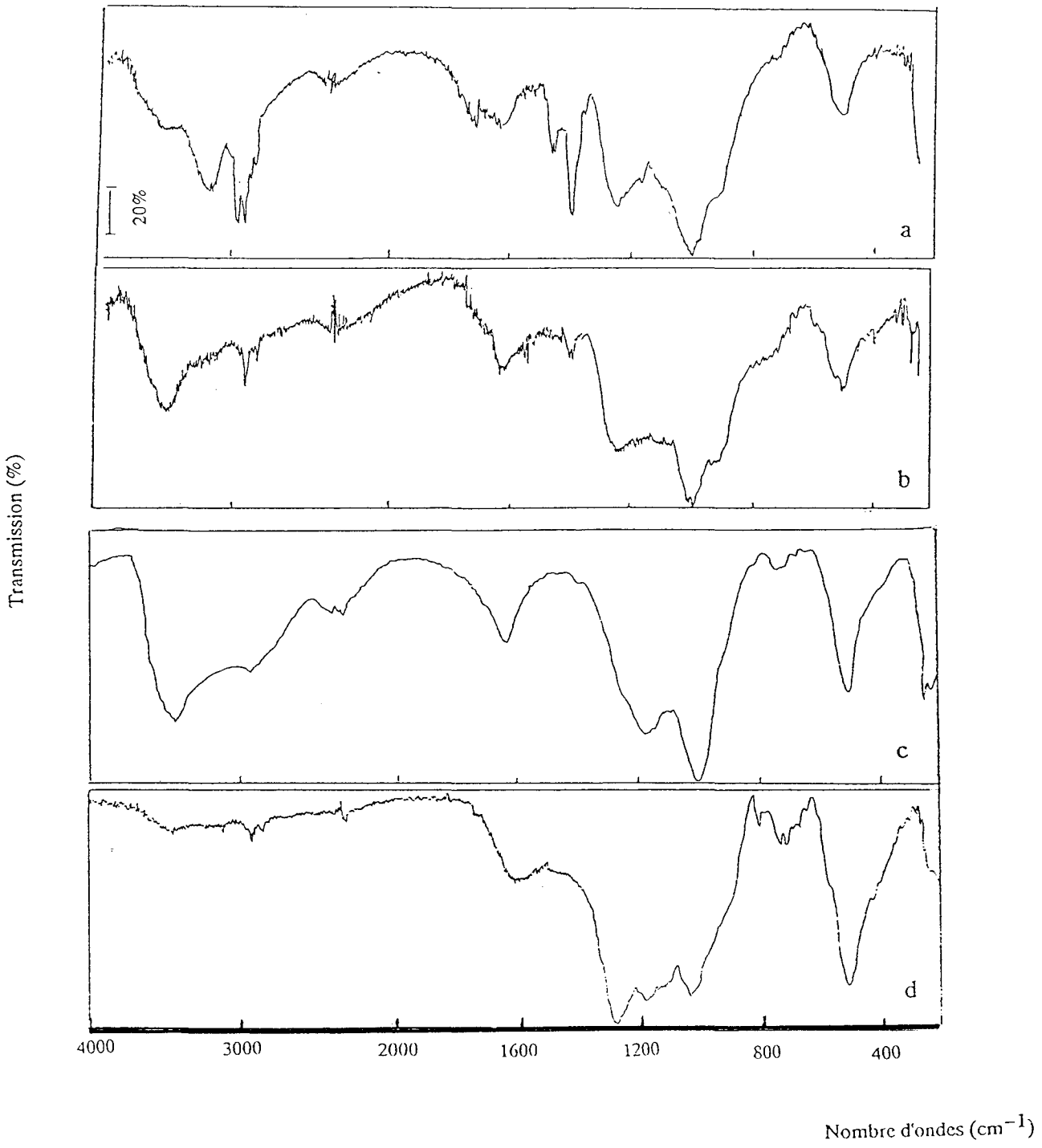

Figure II-11. Spectres IR de PP/APP/PER dégradé sous air à 250°C (a), 360°C (b), 400°C (c) et 500°C (d).

II-3. ***- Contribution à l'étude du mécanisme de protection au feu par un matériau intumescent***

Depuis le « First International Fire Prevention Congress » en 1903 [126], le débit calorimétrique (rhr) produit par un matériau lors d'un incendie est reconnu comme le paramètre majeur pour l'évaluation quantitative des comportements au feu du matériau. Les évaluations antérieures à 1980 faisaient appel aux analyses thermogravimétriques associées aux bilans thermiques. Ces techniques permettent d'approcher la mesure du rhr avec une erreur liée à la mesure des températures et au caractère non adiabatique des systèmes [127].

Comme l'illustre l'étude des résines polyépoxydes, rapportée dans le chapitre I du mémoire, le calorimètre à cône permet la mesure du rhr « en temps réel ». Les courbes obtenues sont des fonctions de l'apport de chaleur externe [128] et l'étude des t.h.e. montre qu'un même matériau est, selon l'irradiance, un « retardant de flamme » (t.h.e. égal à celui du polymère vierge) ou un « limiteur de flamme » (le t.h.e. du matériau est inférieur à celui du polymère en fin de combustion)

Nous présentons, dans ce paragraphe, une compilation des modifications chimiques et thermiques de différentes formulations intumescentes originales EVA/APP/polyol, où les deux types de comportements des matériaux intumescents FR (illustrés par l'étude du système EVA/APP/PER) sont discutés.

La Chimie des systèmes intumescents est ensuite considérée en utilisant les données gravimétriques obtenues au calorimètre à cône dans les conditions d'un feu. Cette étude nécessite le calcul préalable des paramètres cinétiques invariants de la dégradation de ces systèmes. Nous rapportons dans ce paragraphe trois travaux complémentaires qui permettent l'étude.

Le premier donne une représentation de la stabilité thermique d'un matériau intumescent et présente une relation entre les valeurs des énergies d'activation invariantes et le classement feu (les valeurs des LOI). Il permet de comprendre, en terme de stabilité thermique, les modifications de la propriété FR en fonction des teneurs en adjuvant FR [79].

Le second travail discute la validité des calculs des paramètres invariants et rapporte, ensuite, une méthode pour le calcul de la répartition la plus probable des fonctions de dégradation.

Le dernier utilise finalement le modèle du front de dégradation pour calculer la température de la zone où se produit la perte de masse. Cette température calculée permet de définir les étapes de la dégradation d'un matériau intumescent dans les conditions d'un feu et de la formation des gaz combustibles.

La formulation intumescente PP/APP/PER, qui présente une valeur du LOI :32±1 % volumique et un classement UL-94 : V0, fait l'objet de l'étude. Elle a été choisie car elle présente, parmi les formulations intumescentes développées au Laboratoire aux performances FR similaires, la chimie la plus complexe. En effet, elle permet, outre l'étude de la dégradation du polymère et de sa contribution au matériau protecteur, celle des modifications du matériau protecteur qui se produisent à des températures basses [129].

L'ATG permettra de comparer les dégradations de PP et de la formulation intumescente. En particulier, la « stabilité » de PP/APP/PER sera considérée en fonction de la conversion des chaînes du polymère.

L'étude au calorimètre à cône est conduite dans les conditions où le flux de chaleur externe ne permet pas à la formulation EVA/APP/PER de présenter le caractère « limiteur de flamme ». Le comportement différent de PP/APP/PER permettra de discuter un éventuel effet de la matrice.

Le profil de la température du front de dégradation sera finalement comparé à celui mesuré dans le matériau lors l'auto-combustion du matériau dans un mélange gazeux riche en oxygène. Cette comparaison fournit des informations sur l'action du bouclier thermique en fonction du degré de conversion du matériau.

II-3-a Résultats et discussion

Polymer Degradation and Stability 44 (1994) 263–272

ELSEVIER

Effect of intumescence on polymer degradation

Arnaud Marchal,* Rene Delobel, Michel Le Bras, Jean-Marie Leroy

Ecole Nationale Supérieure de Chimie de Lille, BP 108, 59652 Villeneuve d'Ascq Cedex, France

&

Denis Price

Department of Chemistry and Applied Chemistry, University of Salford, Salford UK, M5 4WT

(Received 5 January 1994; accepted 17 January 1994)

In the area of polymer flame retardancy, intumescent formulations offer an attractive alternative to mineral and halogenated components. Polymer protection by formation of an intumescent layer during a conflagration is a complex phenomenon involving both chemical and physical processes. This paper reports a comparative study of a number of intumescent systems for commercial ethylene–vinyl acetate polymers and based on ammonium polyphosphate and polyol. It is shown that intumescent shield formation involves the presence of a stable phosphocarbonaceous structure. The efficiency of such protection has been assessed. Temperature profiles have been studied during the combustion of these materials in the LOI apparatus. The temperature–time profiles obtained show a plateau region indicating heat transfer limitation within the intumescent coating. Moreover, cone calorimeter studies show that the maximum rate of heat release from these intumescent coatings is four times less than that for the virgin polymer samples. Several models have been set up and used to analyse the heat transfer phenomena observed during the degradation of the various polymer systems under fire conditions.

INTRODUCTION

'We are not far from believing that fire is definitely the first object, the first phenomenon to give human spirit food for thought'.[1] This long reflection has lead to the description of classical fire as a vicious circle, or more precisely, a vicious triangle (Fig. 1). At the three apices of this figure, heat, fuel and oxygen will be found, and the centre is the location of the flame. Indeed, when a material, particularly a polymer, is heated, it will produce fuel. When fuel and oxygen are correctly mixed, they will turn into a flame. Flame will produce heat, the heat fuel, fuel and oxygen a flame, and so on. The role of fire prevention is to break this triangle. In order to achieve this, three main kinds of additives are nowadays used.

First of all, halogenated compounds are widely used as flame retardants (FRS). They act as a gas phase inhibitor, interfering with the highly reactive $H^{\cdot}$ and $OH^{\cdot}$ free radicals and thus with propagation reactions. In spite of their great efficiency, different international regulations tend to limit the use of such products on account of their toxic or corrosive combustion effluents.[2]

The inorganic hydroxide compounds represent the second main type of FR. Their endothermic dehydration at high temperature reduces the heat flux towards the polymer. They are considered as

* To whom correspondence should be addressed.

This paper was presented at the 18th Annual Meeting of the UK Polymer Degradation Discussion Group held at the Bolton Institute on 15–17 September 1993.

Polymer Degradation and Stability 0141-3910/94/$07.00

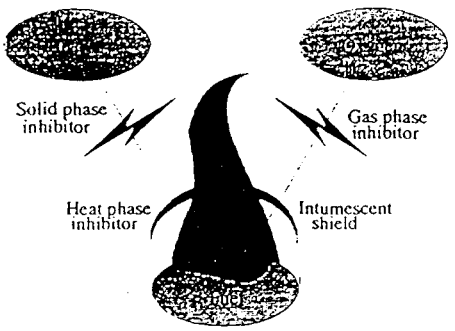

Fig. 1. The 'vicious' triangle of fire.

solid phase FRS. The water released during this reaction can act as a blanket, keeping fuel and oxygen apart, or at least diluting the mixture. Unfortunately, a large amount of such components is needed to obtain a good fire behaviour, which is predudicial to the mechanical properties of samples.[3,4]

The last type of FR is the subject of this study. The intumescent additives can be considered as 'heat phase FRS'. The role of these FRS is to produce a thermal shield, able to protect the bulk material from an external heat flux and to inhibit the escape of volatile fuels and oxygen diffusion (Fig. 2). Usually, this protection is assumed by the creation of an expanded carbonaceous structure on the flame front.[5,6] Thus, a dual approach is needed to understand both the chemical and physical (thermal) phenomena involved and thus to suggest ways to improve intumescent protection of polymer systems.

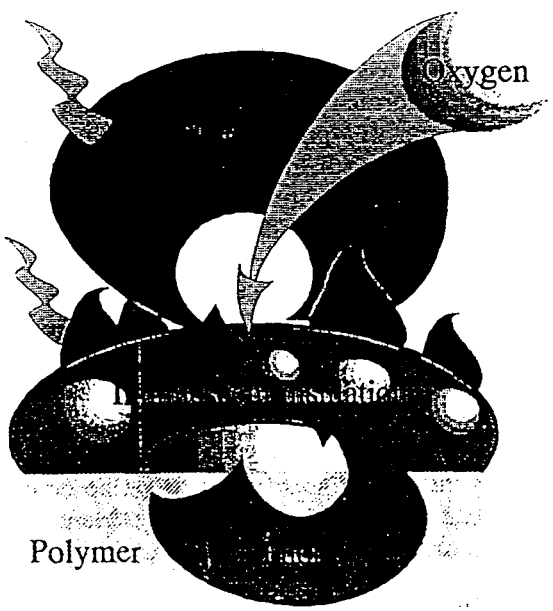

Fig. 2. Intumescence presumed behaviour.

EXPERIMENTAL

Materials

The polymer used in this study was a commercial ethylene–vinylacetate (EVA) (ELVAX 260) with a melt index of 7 g/10 mn. The intumescent formulations were composed of PER (pentaerythritol, Prolabo RP grade), βcD (β-cyclodextrin, Prolabo RP grade), PPA (ammonium polyphosphate, Hoescht, Exolit 422), PY (diammonium pyrophosphate, synthesised in the laboratory, using the previously published procedure proposed by Swanson *et al.*[7]), and Bzn (borax, zinc borate 2335). The present work was restricted to four series of formulations with an EVA/additives ratio of 70/30 (w/w) (Table 1). Samples were mixed at 180°C for 10 min, using a Brabender mixer measuring head.

Tests

The tests used to assess fire properties of materials were the LOI (ASTM D2863/77) and the UL 94 (ASTM D635/77).

Analytical

Thermogravimetric analyses were carried out under air, using a Setaram MTB 10-8 load cell in the range 20–600°C. Raman microspectroscopy was performed using a Microdil 28-Dilor multichannel detector with a 514·5 nm laser beam wavelength. IR spectra were recorded on a Perkin–Elmer 683 instrument, using a PE 3600 data station. X-ray experiments were performed on a Siemens D500 diffractometer. Electron paramagnetic resonance (EPR) spectra were recorded at 25°C on a Varian 'E line'

Table 1. Formulations summary

Samples	PY (%)	PPA (%)	PER (%)	βcD	Bzn (phr
A	20	—	10	—	—
B	—	20	—	10	—
C	—	20	10	—	—
D	—	20	10	—	2

spectrophotometer. Solid ^{13}C-NMR measurements were performed on a Brucker CXP 100 weak field spectrometer at 25·2 MHz (2·35T) with magic-angle spinning (MAS); high power ^{1}H decoupling and ^{1}H–^{13}C cross-polarization.

Thermal

Temperature profiles were obtained with a modified LOI apparatus (see Fig. 9(a)). Samples of 100 mm^3 × 100 mm^3 × 3 mm^3 were exposed to different heat fluxes in a cone calorimeter (PL Thermal Science) according to ASTM 1356-90. Data were processed with software developed at the laboratory.

RESULTS AND DISCUSSION

Chemical aspect

The results presented in this paper are restricted to the (EVA/A) and (EVA/B) systems, since the chemical behaviour of (EVA/C) and (EVA/D) are quite similar to that of the (EVA/A) formulation.

Fire retarding performance

Variations of the LOI values versus the PY and the PPA contents (Fig. 3) show the existence of a synergistic phenomenon with the (EVA/PY/PER) system (EVA/A) at a PY/PER weight ratio of 3/1. As the (EVA/PPA/BcD) system (EVA/B) keeps roughly a constant value of oxygen index, further studies were performed with this ratio for each system.

The aim of these chemical studies is to compare these two quite similar (polyphosphate/polyol) formulations, which have very different fire properties. Emphasis will be laid on correlation between fire behaviour and carbonaceous coating structure produced by these samples, in order to know how to bring about an intumescence phenomenon.

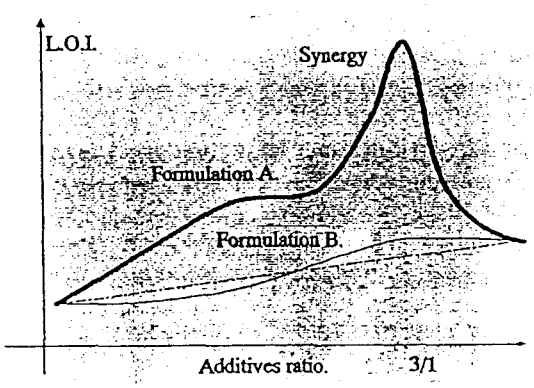

Fig. 3. LOI versus weight additives ratio.

Thermogravimetric analysis

Although it is obvious that reactions during a TGA experiment and reactions under real fire conditions may be, in all probability, quite different, TGA is one of the simplest techniques with which to study the thermal behaviour of materials. The experimental TG curve of the mixture of additives was compared to the respective TG 'theoretical' curve calculated as a linear combination of the TG curves for the single additives (in respect of their weight ratio) (Fig. 4). These 'theoretical' curves represent the degradation of the mixture when no interaction between additives occurs. In the temperature range of the study, some temperature domains can be discussed for each mixture, as indicated in Table 2. To follow the evolution process of each sample, some characteristic temperatures, corresponding to the different steps indicated by Fig. 3, were chosen. Samples were submitted to an isothermal treatment at each of these selected characteristic temperatures (CT) under air during 6 h.

Spectroscopic analysis: carbonisation

The intumescence phenomenon is induced by the expansion of a carbonaceous coating. Figure 5 presents the solid state ^{13}C-NMR (CP/MAS) spectra of the samples produced at the various characteristic temperatures. The study confirms that the reaction between additives for the A system, at 190°C, leads to the formation of three types of phosphoric acid ester previously proposed by Delobel *et al.*,[8] while the B system curve, at this same temperature is the spectrum from βcD. The difference in behaviour of the two formulations does not stop here. Degradation of the ester developed by the A system, for $245 < CT < 350$°C, gives hydrocarbonaceous products with delocalised ethylenic bonds ($135 < \delta < 150$ ppm), aromatic structures ($100 < \delta < 120$ ppm) and alkyl groups probably linked to aromatics ($\delta \approx 20$ ppm). The changes then observed in the spectra with the increase of

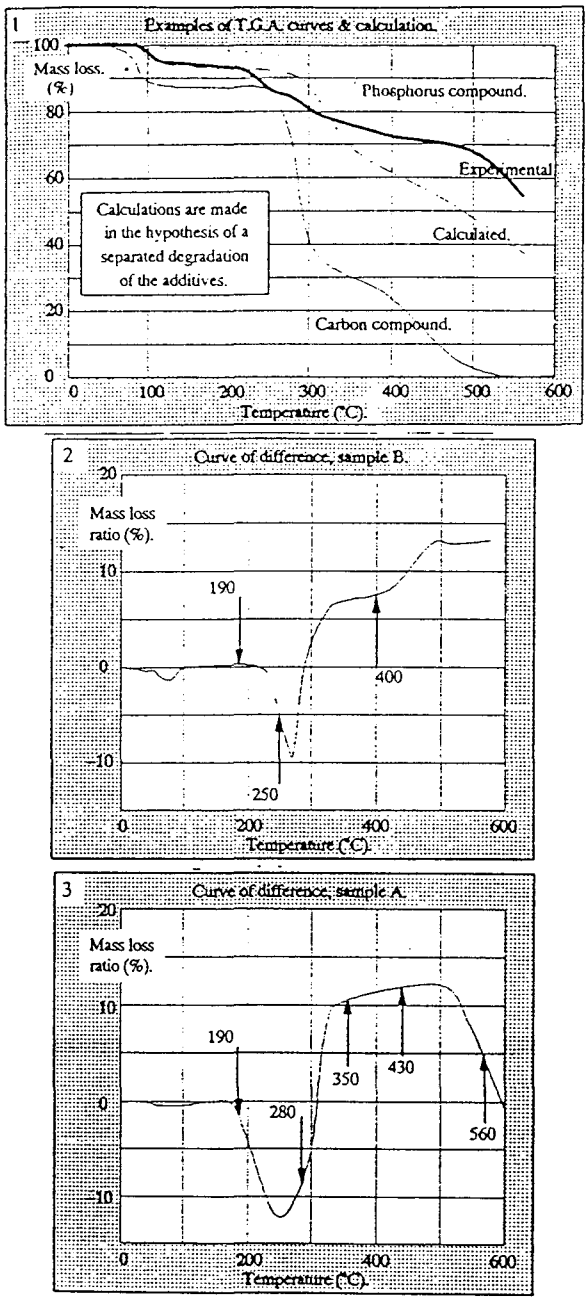

Fig. 4. Thermogravimetric analysis, under air, 180°C/h.

temperature show an aromatic structures development by dealkylation (signals fading near 20 ppm) and by ethylenic condensation. The B system spectra change differently. Indeed, thermal treatments of PPA/βcD lead to a very complex carbonaceous material, including aromatic species and alkyl groups (Table 3).

An EPR spectroscopic study has also been carried out in order to obtain more information

Table 2. TGA temperature domains

Formulations	Temp. Range (°C)	Remarks	Refs
A	150–245	Reaction between additives with ammonia and water loss	
	245–350	Carbonaceous intumescent material development	
	350–550	Intumescent material 'stability'	6, 8
	>550	Coating degradation	
B	50–90	Dehydration	
	220–270	Reaction between additives	
	>270	Nonexpansed carbonaceous material formation	

about the formation of these carbonaceous structures. Only the concentration of paramagnetic species (N_{sp}) will be discussed here. The results (Fig. 6) show that, for the A system, a radical process takes place up to 280°C. The decrease of the signal could then be explained by a competition between a bond breaking process (dealkylation, dehydrogenation) and a condensation phenomenon (recombination of radical species). The B system curve points to a carbonisation process that is incomplete ($\log N_{sp} < 10^{-19}$). There is no specific temperature or temperature range where a carbonisation process occured.[9]

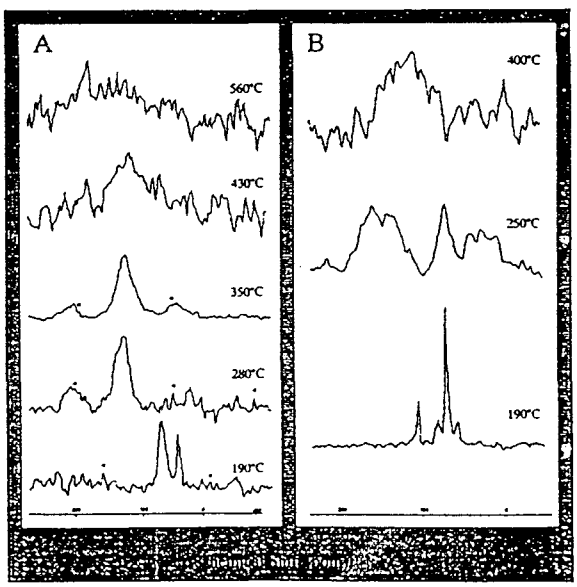

Fig. 5. ^{13}C NMR spectra versus CT. (Asterisk: spinning bands.)

Table 3. ^{13}C assignment summary

Formulations	Temperature (°C)	Chemical shift, δ (ppm)	Assignments	Refs
A	20	48. 1[1]	CH20H CH20H C[1]	26
		68. 8[2]	C[2]H20H CH20H	27
		40. 1	Quaternary C	
	190	60. 2	Methylene[a]	26
		68. 3	Methylene[b]	27
		77. 1	Methylene[c]	28
		20	Aliphatics	26
	280	120	Aromatic species	27
		135	Delocalised ethylenics	
	350	123	Condensed species	26
	430	118	Polyaromatics	26, 27
	560	120	Polyaromatics	26, 27
B	20–190	60, 8[6] 72[2,3,5] 81, 4[4] 102, 3[1]	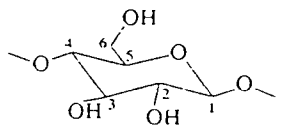	29
		20–30	Aliphatics	26
	250	72	Carbon of βcD	27
		130	Condensed species	
	400	2	Alkyls	26
		110	Polyaromatics	27

[a–c] Methylene groups bound to phosphate species.[3]

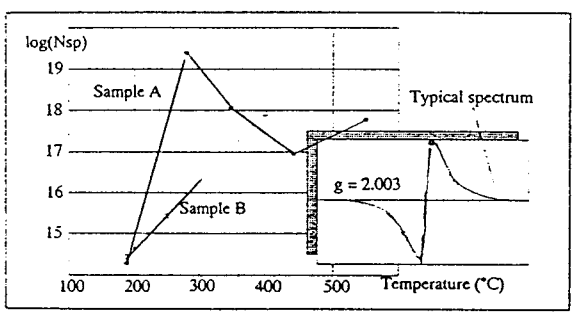

Fig. 6. EPR, spin concentration versus CT.

Raman microspectroscopy has been used to investigate the nature of the polyaromatic species (Fig. 7). The two broad bands observed for the A sample after 190°C (1580 and 1350 cm^{-1}, respectively, assigned to E2g and A1g vibration modes) confirm that a structured carbonaceous material is beginning to develop.[10] X-ray diffraction allows assessment of the nature and size of the structural state of this material.[11] For the A sample, treated above 280°C, a broad band appears at around 12°, this indicates the formation of small domains of turbostratic carbon.[12] None of these features were obtained for the B system.

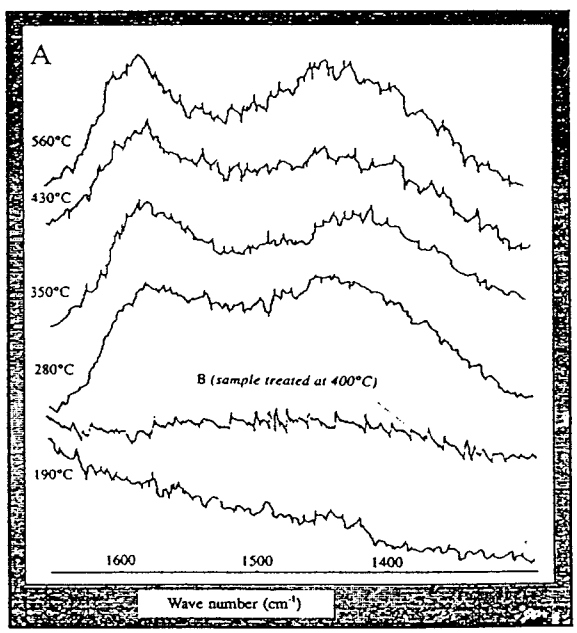

Fig. 7. Raman spectra.

The IR study of both these materials confirms these results (Fig. 8). Indeed, the three characteristic bands of the deformation mode of aromatic CH bonds in polyaromatic structures (700–800 cm^{-1}) have been found for sample A,

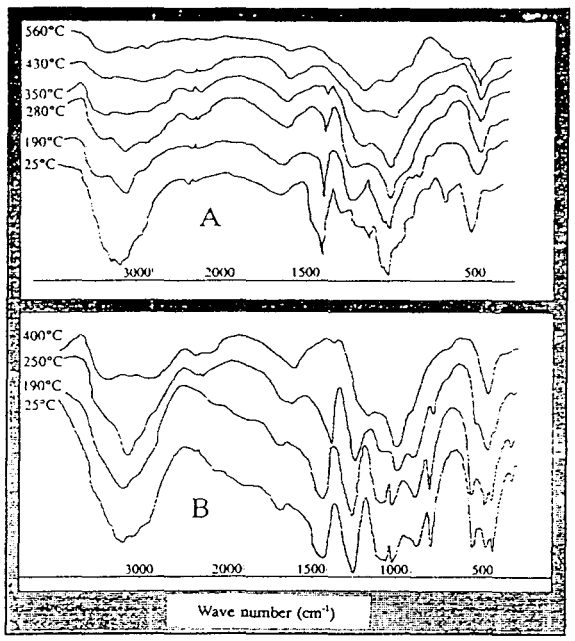

Fig. 8. IR absorption.

none for system B. Moreover, with increasing temperature, the A sample spectra show a progressive fading of the symmetric vibration mode absorptions due to PO_2 and PO_3 to give an intense band centred on 1000 cm^{-1}, characteristic of PO bonds in phosphocarbonaceous complexes.[13] Their existence is confirmed up to 430°C by a large band (1100–1300 cm^{-1}) assigned to POC chains in these complexes (overlapping with phosphoryl groups at 1210 cm^{-1}).[14] At a higher temperature, some characteristic bands assigned to phosphoric oxide are shown, which indicate the beginning of degradation of these species. IR spectra of sample B just show an increasing intensity of absorption bands with temperature, probably due to the hydrolysis and the decomposition of PPA.

Chemical conclusion

These chemical studies show that, for PY/PER system (A), the degradation of phosphoric acid esters (created between 190–280°C) leads to the formation of a carbonaceous material containing polyaromatic structures. Moreover, solubility experiments combined with IR studies show the existence of phosphocarbonaceous species, stable between 280 and 430°C and hardly soluble. The thermal treatment of PPA/βcD system (B) induces the formation of a very complex carbonaceous material with acid and aromatic species. This carbonisation process is not complete at 400°C. No phosphocarbonaceous structure is observed.

The spectroscopic analysis of these formations reveals the main factors leading to creation, formation, and development of an intumescent coating. Nevertheless, it is not easy to link these features directly to the main part that the intumescent barrier is given to play, it is to say, the thermal shield.

Physical aspect

Temperature profiles

In order to study the thermal behaviour of an intumescence shield, temperature profiles have been measured during the sustained combustion of samples in the LOI equipment as shown in Fig. 9(a). Figure 9(b) presents the profile obtained for a typical intumescent formulation (EVA/C) at an oxygen index of LOI + 1, chosen in order to get a sustained combustion process.

The first thermocouple (X1) underwent

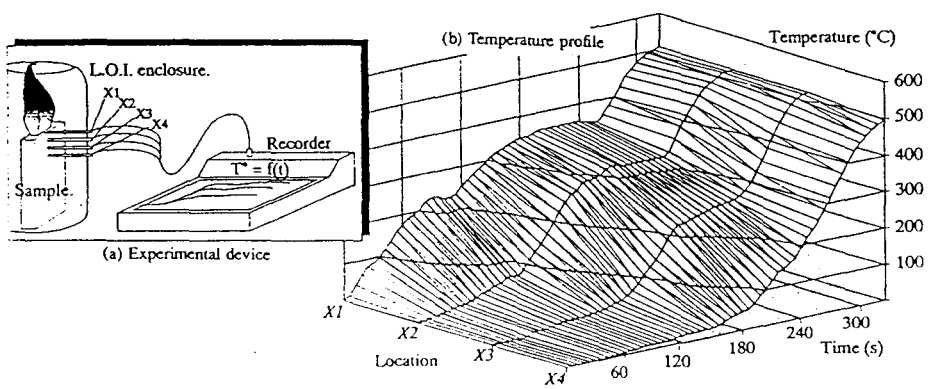

Fig. 9. Temperature profiles: (a) experimental device and (b) example for an intumescent formulation.

temperature increase up to 200°C within the 2 m, without any significant heating of the bulk material. Then, the occurrence of a temperature plateau between 180 and 240 s proves the efficiency of the thermal protection brought about by the formation of the intumescent coating. In fact, the sample, still exposed to the flame, shows isothermal behaviour near the surface and follows only a very progressive increase of temperature in its bulk. This protection ends at around 300 s, as is shown by the abrupt temperature increase of the four thermocouples. As the material collapses after this time, the temperatures after 300 s are irrelevant. The 'thermal insulation' property disappears when the temperature gradient inside the material becomes nil.

This kind of experiment is quite delicate to set up. Various factors such as 'shrinkage' or 'flaming drop release' can lead to a wrong evaluation of the temperature profiles. Nevertheless, if none of these perturbations occurs, good reproducibility is observed.

Rate of heat release profiles

Heat release has long been recognised as the major reaction to fire parameter because it defines fire size.[15] Relevant rate of heat release measurement has become accessible only since the advent of the cone calorimeter. Developed by the NIST in the 1980s, this apparatus allows a new qualification and quantification of phenomena relevant to fire development.[16] This test, using quasi-real conditions, avoids many of the errors inherent in regular calorimetry methods, because it is based on the oxygen consumption principle. This principle stipulates that, for a large number of organic solids, a quite constant net amount of heat is released per unit of oxygen consumed (by weight) for complete combustion, with an average value of 13·1 kJ/kg of $O_2 \pm 5\%$. The change of oxygen concentration in combustion gases can thus be used to assess the heat release rate (r.h.r.) of a combustible.[17]

Virgin polymer and intumescent formulations were tested in a cone calorimeter under different heat fluxes, according to ASTM 1354-90. Under 50 kW/m^2 (Fig. 10), the presence of intumescent additives noticeably decreases the maximum value of the heat release rate of the polymer (ratio 1/4). This constitutes additional evidence that such a protection is efficient. Unexpectedly, the addition of intumescent FR decreases the

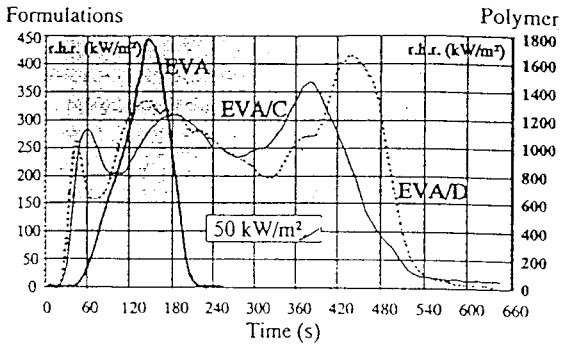

Fig. 10. Rates of heat release of EVA and EVA/FR systems.

ignition time, which seems specific to the intumescence shield formation behaviour. The general shape of EVA/FR formulations r.h.r. curves is also very characteristic. Although interpreting this kind of curve is not easy, some assumptions can be made. The first peak, and especially the slope of the first peak, can be assigned to the abrupt inflammation of the material. This phenomenon is explained by a very rapid flame propagation on the surface of the sample, due to gas accumulation before ignition. After a transitory phase, a second 'band', the broadest one, is certainly due to the protection assumed by the intumescent coating (hypothesis supported by the effective heat of combustion curves study).[18] Subsequent destruction of this structure must be the cause of the last peak with its residual r.h.r.

Thermal modelling

All the data warrant further investigation, and especially with regard to the heat transfer mode during the existence of an intumescent coating. First of all, the evolution of the temperature gradient presented in Fig. 9(b) leads naturally to the construction of a heat balance model. No equations will be presented here, but they are fully developed in many engineering books.[19] In order to deal with this heat balance in a simple way, different assumptions have been made. To a first approximation, only conduction heat transfer is considered and the sample is studied as a one-dimensional system. From these basic assumptions, equations can be solved according to different heat transfer mode hypotheses. Figure 11 presents the variation of one of the parameters (P/λ) as predicted by the model. This value is the ratio between the volumic calorific power (P) of the sample (different from

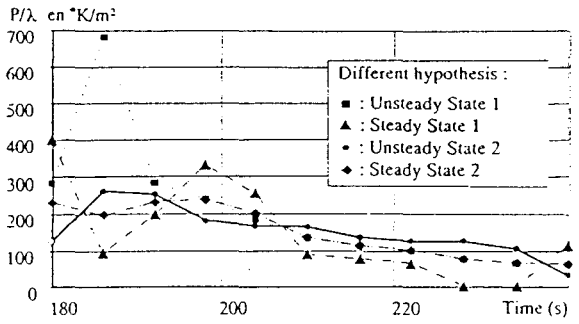

Fig. 11. Evolution of the P/λ parameter.

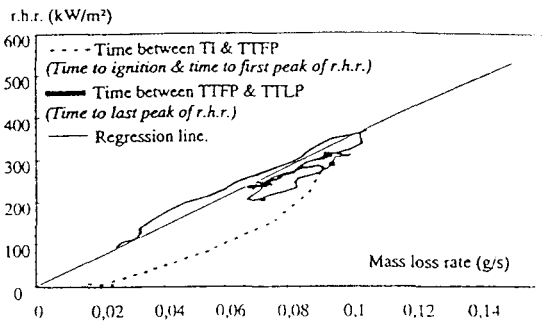

Fig. 12. Result of the 'bilayer' model.

combustion enthalpy) and its thermal conductivity (λ). The good reproducibility of this parameter whichever heat transfer mode hypothesis is used, indicates that, between 180 and 240 s, heat transfer must be in a steady state mode. Other parameters, especially the thermal diffusibility coefficient, have been considered, but they show absurd values. This is due to mathematical instability during the Laplacian discretisation (Cranck–Nicholson condition unrespected).[20] Nevertheless, modifications of the procedure could solve this problem.

The steady state mode of heat transfer during the existence of an intumescence shield has been confirmed by the results of the 'bilayer' model. Numerous models divide the material submitted to a fire into two layers: a reaction area and a transfer area. This approach has been applied to wood (charring area/uncharred area),[21] to polymers in the first step of degradation (melt area/solid area)[22] and also to intumescent formulation (expanded coating/polymer). The 'bilayer' model has been adapted to the cone calorimeter application. The mass loss of the sample is considered to be located at the interface of the two layers, with only a negligible role for the degradation products in the reaction area. It is obviously very difficult to link such assumptions with the real phenomenon. Nevertheless, a very simple relationship between heat rate and derivative mass loss can be tested with our sample. The regression line presented in Fig. 12 shows a good correlation (Fisher coefficient > 600) with the experimental curve between the time to first r.h.r. peak and time to last r.h.r. peak. This implies that the heat transfer mode during this time range is in a steady state. Such results were not found for the virgin polymer, thus this heat transfer mode appears to be 'characteristic' of the thermal shield brought about by intumescence formation.

Thermal conclusions and perspectives

The thermal aspect of FR studies, especially in thermoplastic polymers, has often been disregarded. This is not the case for building products applications,[23] moreover, a large number of concepts used in this field are valid for our studies. For example, a thermal model for wood ignition has been applied to our samples. This model allows definition of the critical heat flux in ignition and an apparent thermal inertia of the material (Fig. 13). The plots obtained show good linearity and give credence to the analogy between wood and intumescent polymer thermal studies.

The cone calorimeter is a powerful tool for formulation studies. The exploitation of the total heat evolved (t.h.e.) curves (≈integrated r.h.r. curves) gives some very interesting results. Figure 14 shows the effect of external heat flux on the difference between the t.h.e. curve of an

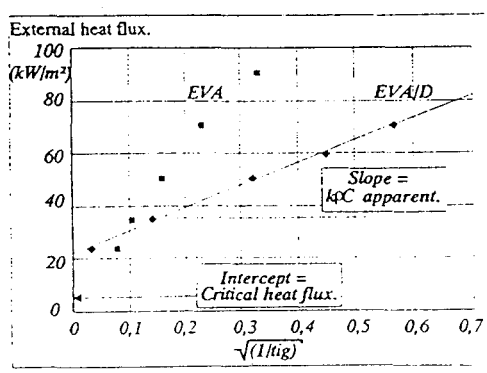

Fig. 13. Thermal wood ignition model applied to intumescent formulations studies.

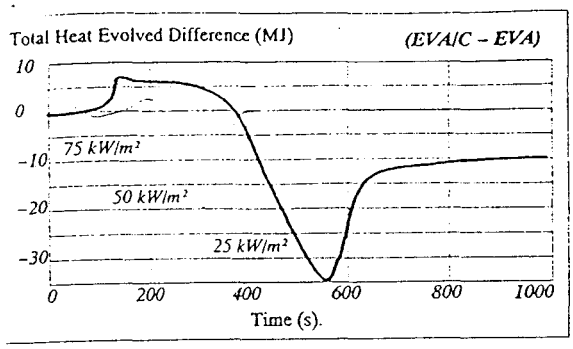

Fig. 14. Influence of external heat flux on total heat evolved difference (EVA – EVA/FR).

EVA/FR formulation and the t.h.e. curve of the virgin polymer. This diagram indicates two different behaviours of FR. The 75 and 100 kW/m^2 curves show that, after an energy difference decrease, the plot returns to the zero difference baseline. The total heat developed by the EVA/FR sample is the same as that for the polymer. The additives formulation is considered as a *fire retardant* system, insofar as the return to the zero baseline is retarded. At 25 kW/m^2, the EVA/FR formulation shows a decrease in the total heat developed, so it can be considered as a *fire restrictant*. This work shows the fundamental importance of the choice of the external heat flux in FR studies, and even in standardisation.

GENERAL CONCLUSION

'If you are wrong with the exhibition of Fire Nature, your mistake will spread in all fields of Physics (. . .).'[25] The very complex nature of fire development, especially when the intumescence phenomenon is induced, remains difficult to study. This work shows that a dual approach, both chemical and physical, is needed. These two complementary aspects have to be linked in order to develop a global view of intumescent shield efficiency. In particular, more coherence between spectroscopic analysis and physical behaviour in fire should be sought. Thermogravimetric analysis, temperature profiling to obtain profiles such as those in Fig. 9(b), and FTIR combined with cone calorimeter experiments, are some techniques which should create a consistent bridge between these two aspects.

Another possibility is to consider the intumescent samples as chemical reactors, these kinds of materials representing a good example of a heat and chemical exchanger. Some analogy with chemical engineering calculations could lead to a more general comprehensive study of the effect of intumescence insulation on polymer degradation.

ACKNOWLEDGEMENTS

The authors wish to thank Alcatel-Alsthom-Recherche, and especially Mme Prigent, for the technical and financial support.

REFERENCES

1. Bachelard, G., *La Phychanalyse du Feu.*, trans., (ed.) Gallimard, Paris, 1949, p. 93.
2. Piechota, *J. Cellular Plastics* (1965) 186.
3. Brossas, J., *2ième Colloque Sur L'Ignifugation des Polymères*, ed. L. Delfosse, USTLFA, Lille, 1987.
4. Camino, G., *et al.*, *Fire Safety Res*, **2** (1980) 257.
5. Delobel, R., Le Bras, M. & Ouassou, N., *Polym. Deg. & Stab.*, 30(1) (1990) 41.
6. Delobel, R., *et al.*, *J. Fire Sci.*, **8**(2) (1990) 85.
7. Swanson, C. & McCollough, F., *Inorg. Synth.*, 7 (1963) 65.
8. Delobel, R., Le Bras, M., Ouasssou, N. & Descressain, R., *Polym. Deg. & Stab.* **28**(2) (1989) 67.
9. Alger, R. S., *Electron Paramagnetic Resonance: Techniques and Applications*, ed., R. S. Alger, Wiley Interscience, New York, 1974, p. 146.
10. Cottinet, P., Couderc, P., Romain, J. L. & Dhamelincourt, P., *Carbon*, **26**(3) (1988) 339.
11. Morterra, L., Louv, M. J. D. & Severdia, A. G., *Carbon*, **22**(1) (1984) 5–12.
12. Rose, N., *et al.*, *Polym. Deg. & Stab.*, **42** (1993) 307–16.
13. Schmidt-Letallec, Y., Thèse de doctorate, Lille, 1992.
14. Ouassou, N., Thèse de doctorat. Lille, 1991.
15. Grayson, S. J., *Heat Release in Fire*, eds, V. Babrauskas & S. J. Grayson, Elsevier, London, 1992, Chapt. 1.
16. Babrauskas, V., Development of Cone Calorimeter—a bench scale rate of heat release based on oxygen consumption, *NBS-IR 82-2611, U.S. Natl. Bur. Stand.*, 1982.
17. Huggett, C., *J. Fire & Flammability*, **12** (1980).
18. Marchal, A., *Polymères & Civilisation*, ed., M. Grenier-Loustalot, Groupement francais des polymères, Pau, 1993.
19. Krieth, F., *Transmission de la Chaleur et Thermodynamique*, ed., F. Kreith, Masson et Cie, Paris, France, 1967.
20. Crank, J. & Nicholson, P., *Proc. Camb. Phil. Soc.*, **43** (1947) 50–67.
21. Mikkola, E., Charring of wood. Internal report 689, VTT, Espoo, 1990.
22. Baillat, C., Vantelon, J. P., Most, J. M. & Joulain, A., *J. Chim. Phys.*, **11–12**(75) (1978) 1051–9.
23. Karlsson, B., Report TVBB-1099, Lund University, Sweden, 1992.
24. Janssens, M., Fire Safetv Science. *Proceedings of the Third International Symposium*, Hemisphere Publishing, New York, 1991, pp. 167–76.
25. Boerhaave, *Eléments de Chimie*, trans., vol. 2, Leide, 1752, p. 144.
26. Ducan, P. M., *J. Phys. Chem., Ref. Data*, **16**(1) (1987) 125.
27. Paroprsty, V., Malik, L. & Golsar, I., *Magn. Reson. Chem.*, 23(1) (1985) 122.
28. Halpern, Y., Mott, D. M. & Niswander, R. H. *Eng. Chem., Prod. Res. Dev.*, (23) (1984) 233.
29. Grint, A., Proud, G. P., Poplett, I. J. F., Bartle, K. Wallace, S. & Mattews, R. S., *Fuel* **68** (1989) 1490.

J Chim Phys (1992) 89, 1835-1852

Relation between limiting oxygen index and invariant activation energy. Application to the polypropylene - ammonium polyphosphate - pentaerythritol system

S Bourbigot*, R Delobel, M Le Bras, Y Schmidt

Laboratoire de Physicochimie des Solides, ENSCL, Université des Sciences et Techniques de Lille Frandres-Artois, BP 108, 59652 Villeneuve d'Ascq Cedex, France

(Received 18 November 1991; accepted 1st June 1992)

RESUME

Une méthode permettant l'évaluation des propriétés "retard au feu" est présentée dans le cas d'une formulation intumescente agissant par un mécanisme en phase condensée. La méthode consiste en la détermination de paramètres physicochimiques invariants calculés à partir de l'analyse thermogravimétrique, c'est-à-dire l'énergie d'activation et le facteur d'Arrhénius invariants. Dans le cas du polypropylène "retard au feu", une corrélation entre la valeur donnée par un test d'évaluation (LOI, norme ASTM D2863/77) et l'énergie d'activation invariante est proposée.

ABSTRACT

A method allowing the evaluation of fire retardancy properties is presented in the case of an intumescent formulation. In that case, the protection is obtained via a condensed mechanism. The method consists in the determination of invariant physicochemical parameters deduced from TG analysis : invariant activation energy and invariant preexponential factor. In the case of fire retardant polypropylene based formulation, there is a correlation between the value given by an evaluation test, i.e. the LOI (ASTM D 2863/77) and the invariant activation energy.

INTRODUCTION

The easy combustion of synthetical materials and thermoplastics in particular, has led to the developpment of fire-retardant systems. These

additives are incorporated at the time of the moulding of the material at varying additive levels and thus allow a "fire-retardant" action or an uninflammability of the material.

Up to now the most widely used flame-retardant systems by industry contain halogenated compounds which evolve toxic and corrosive agents. In our Laboratory, new flame-retardant systems which do not contain halogens are studied and developped. The protection of these systems is provided by a shield (formation of foamed layer of char *(1)*) which arises from an intumescence phenomenon *(2-3)*.

The evaluation of "fire-retardant" performances still remains empirical (vertical flame test (UL-94), epiradiator test, glow wire resistance, ...), only the Limiting Oxygen Index (LOI) method allows a quantitative comparison of these performances for different materials. JHA et al tried to establish a correlation between the LOI and the apparent activation energy calculated from the TG analyses, on polypropylene-halogenated additives systems but did not obtain conclusive results *(4)*.

The aim of our study is to correlate the LOI values of our intumescent formulations, with the values of invariant kinetic parameters obtained by thermogravimetric analysis. The method of determining invariant kinetic parameters has been developped by Lesnikovich et al *(5)*. In recent studies, these autors demonstrated, for the flame-retardant polyethylene terephtalate, that the invariant activation energy could be used to characterize the thermal oxidative degradation of material during the combustion *(6)*. More recently, Vyazovkin et al used the same method to study the influence of a flame-retardant additive on the polypropylene pyrolysis by measuring invariant kinetic parameters *(7)*.

The study has been realized for the intumescent flame-retardant formulation polypropylene (PP)- ammonium polyphosphate (APP)-pentaerythritol (PER) with different additive levels. This study is restricted to one additives mixture (APP/PER = 3(wt/wt)) which correspond to the higher synergistic effect *(8)*.

EXPERIMENTAL

Materials :

Raw materials were PP (powder supplied by Atochem), PER (Prolabo R.P. grade), APP ($(NH_4PO_3)_n$, n=700, Hoechst Exolit 422, soluble fraction in H_2O: < 1 wt %)

Initial mixtures were first prepared after a mechanical grinding and a sifting (200.10^{-6} m) of the raw materials. Sheets were then obtained using a Darragon press at T = 190°C with a pressure of 3 MPa.

Limiting Oxygen Index Test :

Limiting oxygen index was measured using a Stanton Redcroft instrument on sheets ($(6.5x10^{-3})x(6.5x10^{-2})x0.2$ m^3) according to the standard "oxygen index" test (ASTM D2863/77).

This test provides a comparative numerical value for research and quality control.It is based on the determination of the limiting percentage of oxygen in a gas mixture which will just sustain the candle like burning of a sample. The main drawback of the test is it is not directly relevant to the natural fire situation.

Thermogravimetric analysis :

Thermogravimetric analysis were carried out at heating rates of 255°C/h, 420°C/h, 670°C/h, 1070°C/h and 1230°C/h in a flowing air (Air Liquid grade) atmosphere (flow rate = $5x10^{-7}$ Nm^3/s) using a Setaram MTB 10^{-8} thermobalance. In each case, samples were $20x10^{-6}$ kg and were positioned in open vitrous silica pans. The precision on the temperatures measurements is +/- 1.5°C in the range 20°C-650°C.

Remark: The errors have been estimated by working in the conditions of the thermal analysis (described above) with a thermocouple inside the pan with and without the sample. For each heating rate, the difference between the temperature of the measure thermocouple and the temperature of the lecture thermocouple was (in the domain of the application of the method (200-400°C)) ΔT_{moy}=1.25°C with a standard deviation of 1°C.

Computation:

The computation has been carried out with a software made in our Laboratory using the spreadsheet Quattro Pro 4.

RESULTS AND DISCUSSION

1 - Evaluation of "fire retardant" performances :

The incorporation of the additives in polypropylene allows a significant improvement of "fire-retardant" performances of the polymer.

The LOI values for different additive levels are shown in **TABLE 1**.

TABLE 1:
LOI values vs. the additive levels

APP/PER (%)	LOI (%)
0	18(+/-0.5)
5	19(+/-0.5)
10	20,5(+/-0.5)
15	22(+/-0.5)
20	25(+/-1)
25	29(+/-1)
30	32(+/-1)
35	34(+/-1)
40	42(+/-1)
45	45(+/-1)
50	50(+/-1)

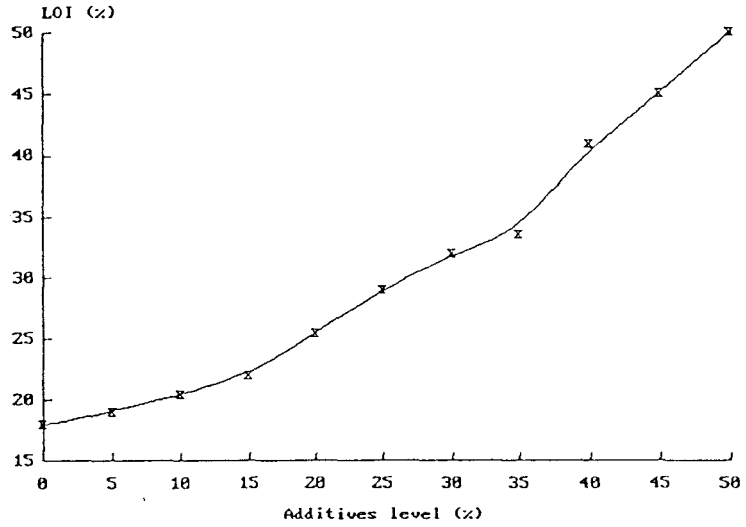

Figure 1 : Evolution of the LOI vs. additive levels

Figure 1 which describes the LOI evolution with the additive level, caracterises three zones :

- up to an additive level of 15 %, the curve slope remains weak and the LOI values increase weakly,
- from 15 % to 35 %, the improvement of performances becomes important to reach a LOI value of 33,5 %,
- from 35 % to 50 %, the LOI values increase strongly and a LOI of 50 % is reached for a loading of 50 %.

It is interesting to note that there is no "saturation" phenomenon when the additive level is increased. Indeed the LOI values continue to increase with the loading, in an opposite with the results obtained by JHA et al in the case of halogenated additives *(4)*.

2 - Invariant kinetic parameters of the PP-APP/PER system :

The thermogravimetric analysis methods are often used to study the kinetic of polymer degradation. In this part, we present a determination method of invariant kinetic parameters for the PP-APP/PER system.

The advantages of this method are first, not to put forward the hypothesis on the form of the kinetic degradation function and secondly, to be independent of the experimental conditions (in particular the heating

rate). Therefore the values obtained are no longer apparent, but real characteristics of the system.

2 - 1 - Presentation of the method :

The thermal decomposition of solids is a complex process which may be described by the following reaction :

$$A_{(s)} \longrightarrow B_{(s)} + C_{(g)}$$

This process takes place in several stages, e.g. : the chemical act of breaking of bonds ; destruction of initial crystal lattice ; formation of the crystal lattice of the solid product B (consisting of the formation of crystallization centers and the growth of these centers); adsorption-desorption of the gaseous product C ; diffusion of C ; heat transfer.

Taking into account the complexity of the process, there is little chance to find a general equation able to describe the kinetics of all thermal decomposition reactions, mainly for cases where the kinetics change during the process*(9)*. Many attempts have been made to obtain kinetic equations and from these latter, different mathematical treatments have been developped to obtain kinetic parameters*(10-12)*.

In this method, we do not use just one kinetic law but several functions presenting the advantage not to put forward hypothesis on the degradation type. We only assume that the rate expression $d\alpha/dt$, where α is the degree of conversion, can be defined by the equation (like in isothermal conditions) :

$$\frac{d\alpha}{dt} = k\, f(\alpha) \qquad (1)$$

where $f(\alpha)$ is a certain function of α and k can be considered to be the rate constant.

When thermal oxidative degradation takes place under the conditions of thermogravimetric analysis, k cannot remain constant and depends upon temperature. The validity of the Arrhenius equation can be presumed for this dependance :

$$k = A \exp\left(-\frac{E}{RT}\right) \qquad (2)$$

where A and E are respectively the preexponentiel factor and the activation energy.

In the case of a linear heating rate $\beta = \frac{dT}{dt}$, the combination of the above two equations gives the following relationship :

$$\frac{d\alpha}{f(\alpha)} = \frac{A}{\beta} \exp\left(-\frac{E}{RT}\right) dT \qquad (3)$$

The integration of the equation (3) by Ozawa's method*(13)* using Doyle's approximation*(14)* leads to the relationship :

$$\log [F(\alpha)] = \log\left(\frac{AE}{\beta R}\right) - 2{,}315 - 0{,}457 \frac{E}{RT} \qquad (4)$$

The apparent activation energy E can therefore be obtained from a plot of log $[F(\alpha)]$ against 1/T for a fixed heating rate and a chosen degradation function since the slope of such a line is given by - 0,457 E/R. In addition, the value of log A can be found from the intercept on the log $[F(\alpha)]$ axis.

In this study we use sixteen functions $f(\alpha)$ given in the litterature*(16)* (described in **TABLE 2**) and called $fj(\alpha)$ $(1 < j < 16)$ which are associated to a preexponential factor Aj and apparent activation energy Ej. Indeed, the thermal decomposition of a solid, accompanied by release of a gazeous product being a heterogenous process, is usually caracterized by several mechanisms (nucleation, one two or three-dimensioned diffusion) and consequently by another form of the function $f(\alpha)$*(16)*. Thus it is very useful in this case not to put forward the hypothesis of function $f(\alpha)$ rather than another one.

The application of the method is based on the study of the compensation effect*(17-18)*. Indeed, Ozawa's method applied to several functions $fj(\alpha)$ implies significant changes of activation energies and preexponential factors. For each function $fj(\alpha)$, log (Aj) versus Ej is plotted (Aj and Ej being obtained using equation *(4)*) and if a compensation effect is observed, a linear relation defined by the following equation:

$$\log A_j = B_V + l_V E_j \qquad (5)$$

is obtained for a given heating rate β_v ($1 < v < n$; with n the number of used heating rates).

TABLE 2 - Simple kinetic models *(16)*

	Kinetic model	$f_j(\alpha)$	$F_j(\alpha)$	
1.	Nucleation and nucleus growing, KOLMOGOROV, EROFEEV, KAZEEV, AVRAMI and MAMPEL (KEKAM)	$\frac{1}{n}(1-\alpha)(-\mathrm{Ln}(1-\alpha))^{1-n}$	1. $(-\mathrm{Ln}(1-\alpha))^n$	1.1. n = 1/4 1.2. n = 1/3 1.3. n = 1/2 1.4. n = 2/3 1.5. n = 1
2.	Phase boundary reaction	$(1-\alpha)^{1-(1/Fp)}$	2.2 $1-(1-\alpha)$ 2.2 $1-(1-\alpha)^{1/2}$ 2.3 $1-(1-\alpha)^{1/3}$	plane symmetry cylindrical symmetry spherical symmetry
3.	Diffusion	3.1 α^{-1} 3.2 $(-\mathrm{Ln}(1-\alpha))^{-1}$ 3.3 $((1-\alpha)^{1/3}-1)^{-1}$	3.1 α^2 3.2 $(1-\alpha)\,\mathrm{Ln}(1-\alpha)+\alpha$ 3.3 $3/2(1-.2/3\,\alpha-(1-\alpha))^{2/3}$	plane symmetry cylindrical symmetry sperical symmetry
4.	Potential law	$\frac{1}{n}\alpha^{1-n}$	4. α^n $(0 < n < 2)$	4.1 n = 1/4 4.2 n = 1/3 4.3 n = 1/2
5.	Reaction order	$\frac{1}{n}(1-\alpha)^{1-n}$	5.1. $1-(1-\alpha)^2$ 5.2. $1-(1-\alpha)^3$	order 2 order 3

The signification of B_V and l_V has been discussed elsewhere*(19)* and it has been demonstrated that :

$$B_V = \log (\hat{k}_V)$$

$$l_V = \frac{1}{2.3\, R\hat{T}_V}$$

Where the sign ^ denotes an invariant parameter and k_V represents the invariant rate constant of the system at the temperature T_V, these two parameters being caracteristics of the experimental conditions.

The essence of the method is to obtain a pencil of lines by varying the experimental conditions and to find the coordinates of its centre, i.e., A et E. The coordinates are in an ellipsoidal domain that may be defined with a straight line*(20)*.

$$B_V = \log \hat{A} - \hat{E}\, l_V.$$

To resume, for n heating rates, n pairs of values (B_V, l_V) are obtained and by plotting $B_V = f(l_V)$ the compensation effect implies the linear relation $B_V = \log \hat{A} - \hat{E} l_V$ with a slope equal to $-\hat{E}$ and an intercept equal to $\log \hat{A}$, and thus the values of invariant activation energy and invariant preexponential factor of the system.

2 - 2 - Application of the method to the thermal oxidative degradation of PP-APP/PER :

The study has been carried out using the sixteen above presented functions $f_j(\alpha)$ and five heating rates. The different thermograms are shown in the **figure 2**. The primary derivatives of the TG curves show two significant changes in the slopes which may be attributed to two successive stages of the decomposition of the system. The method is applied to the temperature range (depending on the heating rate) which correspond to the first stage, i.e. the thermal oxidative decomposition of the polymer*(8)*.

It is shown by plotting $\log A_j = f(E_j)$ that the compensation effect is observed for each heating rate (**figure 3**); indeed the relation *(5)* is always verified.

The values of $\hat{T}_V$ and $\hat{k}_V$ are then calculated from the slopes and intercepts of these above straight lines. The obtained datas are presented in TABLE 3.

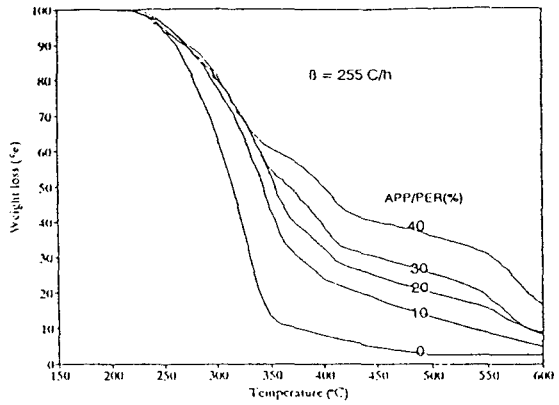

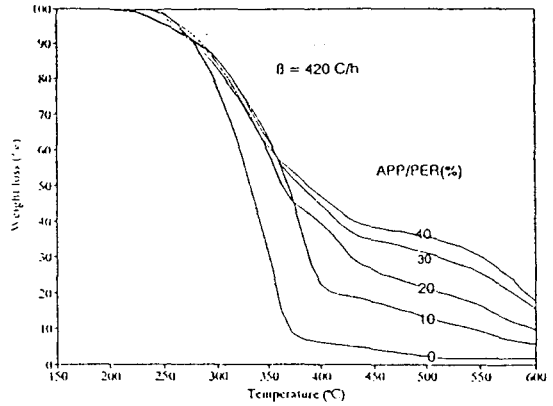

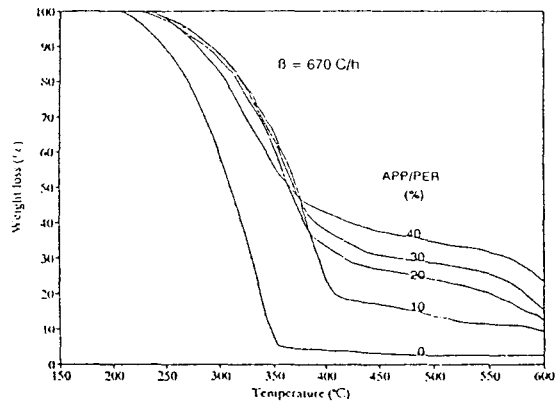

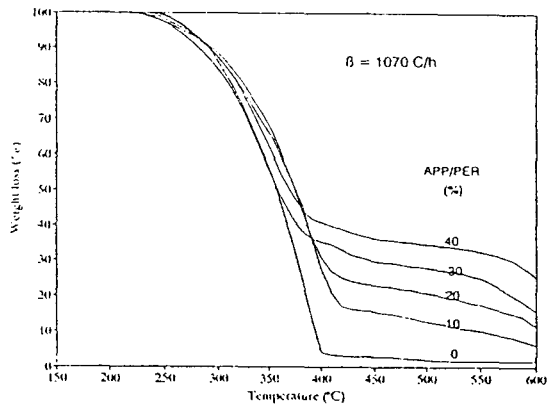

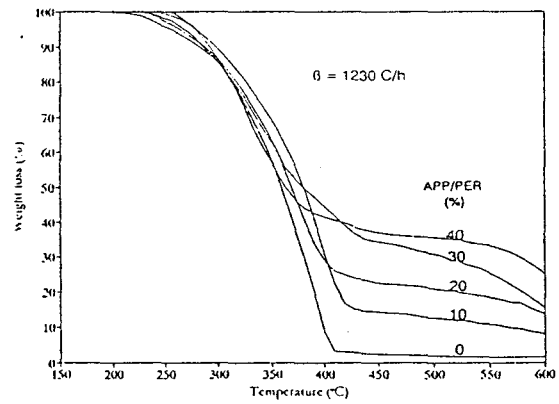

Figure 2: Thermogravimetric analysis curves of the PP-APP/PER systems for each heating rate.

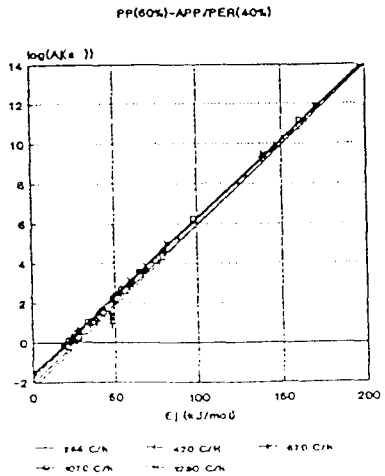

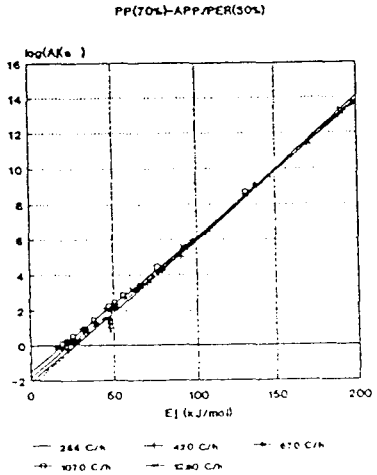

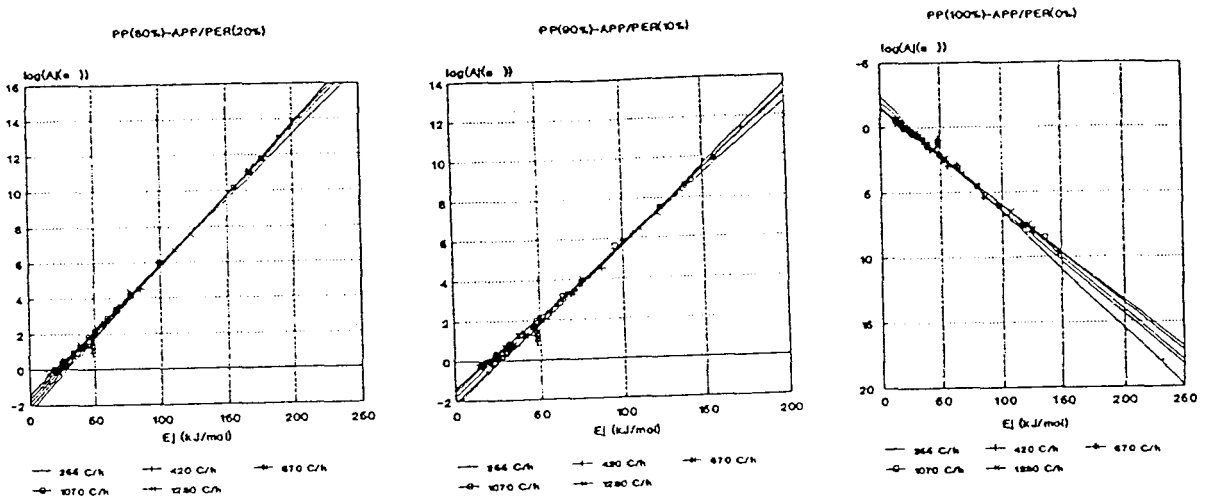

Figure 3 : Compensation effect log A_j vs. E_j

TABLE 3

T_v and k_v values computed for each heating rate and additives level

APP/PER (%)	β_v (K/h)	B_v-log($\hat{k}_v$) (k_v : s^{-1})	I_v (x10^5) (mol/J)	T_v (°C)
0	255	- 2.28(+/-0.28)	8.42(+/-0.21)	348(+/-8)
	420	- 2.07(+/-0.26)	8.14(+/-0.17)	369(+/-8)
	670	- 1.67(+/-0.30)	7.98(+/-0.23)	382(+/-11)
	1020	- 1.5(+/-0.21)	7.46(+/-0.15)	428(+/-9)
	1230	- 1.38(+/-0.21)	7.27(+/-0.17)	446(+/-10)
10	255	- 2.23(+/-0.22)	7.92(+/-0.15)	387(+/-7)
	420	- 2.07(+/-0.20)	7.69(+/-0.10)	407(+/-5)
	670	- 1.77(+/-0.20)	7.47(+/-0.12)	427(+/-7)
	1020	- 1.51(+/-0.20)	7.31(+/-0.13)	442(+/-8)
	1230	- 1.39(+/-0.18)	7.06(+/-0.14)	468(+/-9)
20	255	- 2.34(+/-0.24)	8.08(+/-0.11)	374(+/-5)
	420	- 2.09(+/-0.22)	7.91(+/-0.11)	388(+/-5)
	670	- 1.84(+/-0.21)	7.77(+/-0.12)	400(+/-6)
	1020	- 1.6(+/-0.19)	7.56(+/-0.11)	419(+/-6)
	1230	- 1.38(+/-0.20)	7.27(+/-0.16)	446(+/-10)
30	255	- 2.34(+/-0.26)	8.23(+/-0.12)	362(+/-5)
	420	- 2.09(+/-0.23)	7.95(+/-0.11)	385(+/-5)
	670	- 1.82(+/-0.22)	7.8(+/-0.13)	397(+/-7)
	1020	- 1.49(+/-0.24)	7.63(+/-0.17)	412(+/-9)
	1230	- 1.48(+/-0.21)	7.56(+/-0.14)	419(+/-8)
40	255	- 2.19(+/-0.27)	8.04(+/-0.18)	377(+/-8)
	420	- 1.99(+/-0.26)	7.98(+/-0.18)	382(+/-8)
	670	- 1.75(+/-0.26)	7.91(+/-0.17)	388(+/-8)
	1020	- 1.63(+/-0.23)	7.89(+/-0.13)	390(+/-6)
	1230	- 1.48(+/-0.24)	7.77(+/-0.16)	400(+/-8)

These calculated values allow to plot the curves log $\hat{k}_V = f(1/\hat{T}_V)$ (**figure 4**). The plotted curves in figure 4 are straight lines so, the Arrhenius law is followed.

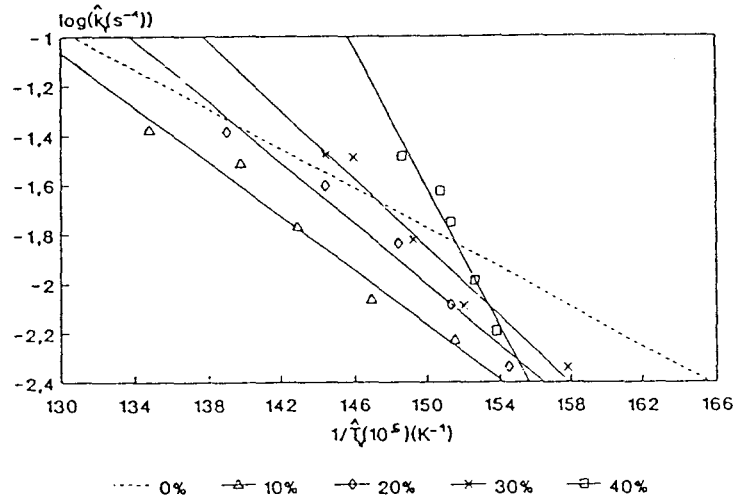

Figure 4 : log $\hat{k}_V$ vs. $f(1/\hat{T}_V)$

The regression coefficients can be computed from the plot of the straight lines in **figure 4**, and thus, the values of the invariant activation energy and the invariant preexponential factor can be obtained (**TABLE 4**).

TABLE 4:
$\hat{E}$ and log $\hat{A}$ values computed from the slopes and intercepts of the straight lines presented in figure 4.

APP/PER (%)	$\hat{E}$ (kJ/mol)	log$\hat{A}$ ($A:s^{-1}$)	r
0	77(+/-15)	4,24(+/-0.14)	0,95
10	105(+/-10)	6,13(+/-0.07)	0,98
20	118(+/-11)	7,27(+/-0.07)	0,98
30	136(+/-14)	8,86(+/-0.07)	0,98
40	269(+/-36)	19,51+/-0.07)	0,98

The value of E = 77 kJ/mol found in the case of the sole polymer is in accordance with the work of Vyazovkin et al*(7)*.

To verify the invariance of the calculated parameters, the experiences have been completed with a lower heating rate (144 K/h) for the system

with an additive level of 30%. The results obtained (**TABLE 5**) show that the values of the activation energies remain in the error range and so, the method gives results which are independant from the experimental conditions.

TABLE 5:

Invariant activation energies of the system for an additives level of 30% and for different ranges of heating rate.

β ($K \times mn^{-1}$)	E ($kJ \times mole^{-1}$)	r
2,4 - 4,25 - 7 - 11,2 - 17	146 ± 13	0,98
4,25 - 7 - 11,2 - 17 - 20,5	136 ± 14	0,98
2,4 - 4,25 - 7 - 11,2 - 17 - 20,5	142 ± 12	0,98

3 - Discussion :

Figure 4 is particularly interesting. Indeed, it is observed that the decomposition rate of the system becomes superior to the one of the sole polymer when the temperatures decrease and the additives level, therefore the fire-retardant performances, increases. This suggests that an early decomposition of the system is necessary to increase the performances. This proposal is apparently paradoxal. However in the particular case, where the protection is insured by a coating resulting from a condensed phase mechanism, the latter forms when the polymeric matrix decomposes. Therefore it may be proposed that there is a relation between the rate of developpment of the protective coating and the rate of the matrix decomposition.

In order to establish a correlation between the evolution of the LOI values and the invariant energy activation of the systems, the LOI and $\hat{E}$ curves are plotted versus the additives level. **Figure 5** shows that the "fire-retardant" performance of the system increases when the invariant activation energy increases.

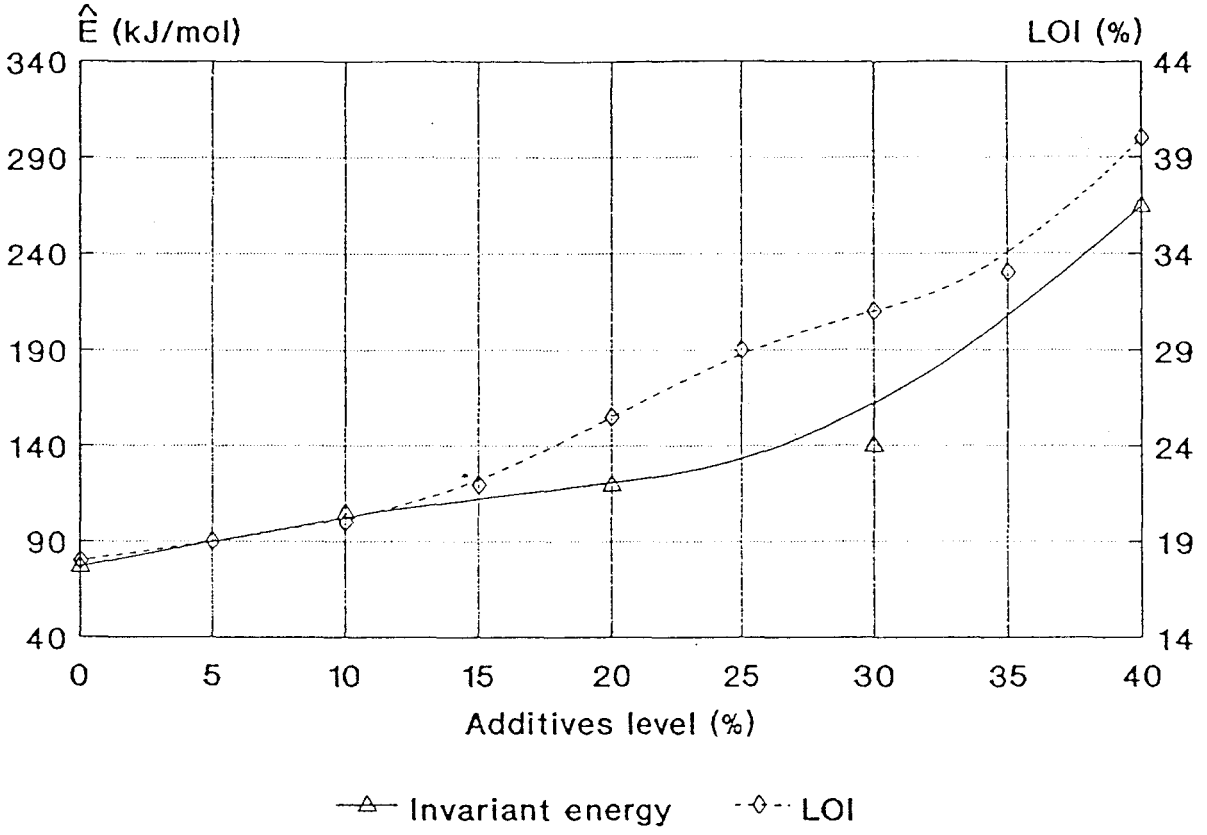

Figure 5 : LOI and E vs. additives level

Such a relation has not been previously put forward by the computation of apparent activation energy of systems containing fire-retardant additives , in the hypothesis of the degradation function $f(\alpha) = 1-\alpha$ (indeed, it is admitted that the function $f(\alpha) = 1-\alpha$ is a good approximation for the representation of the degradation of a polymer).

The curves presented in the **figure 6** show that, whatever the heating rates are, there is no correlation between the apparent activation energies of the systems and the LOI values. Thus it has been demonstrated that the invariant kinetic parameters characterize the thermal oxidative degradation of the systems PP-APP/PER in the conditions of a fire.

The curve which presents LOI against invariant activation energy (**figure 7**), shows that a linear relation ($r = 0,94$ and $0.01<\alpha<0.1$; with α: the risk of the null hypothesis) between these two parameters may be proposed.

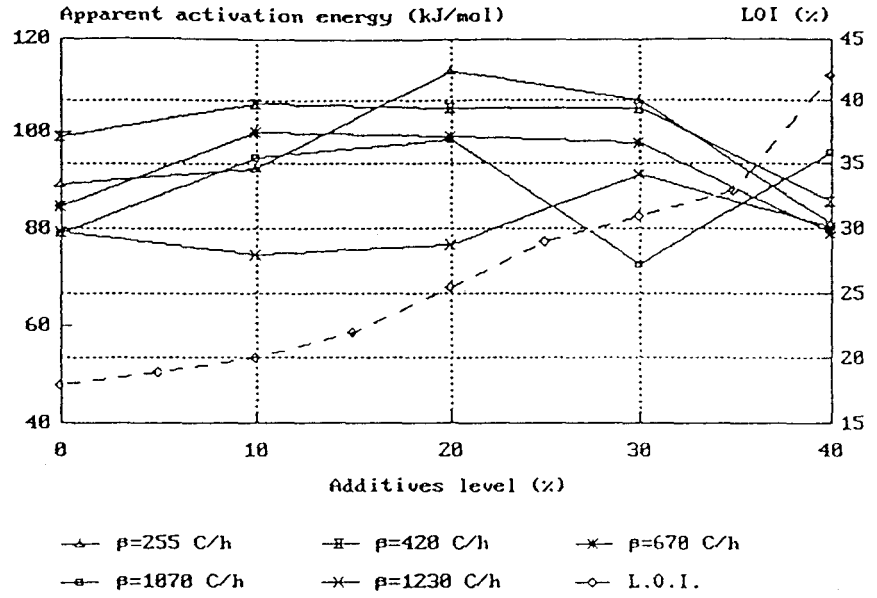

Figure 6 : LOI and apparent activation energies vs. additives level.

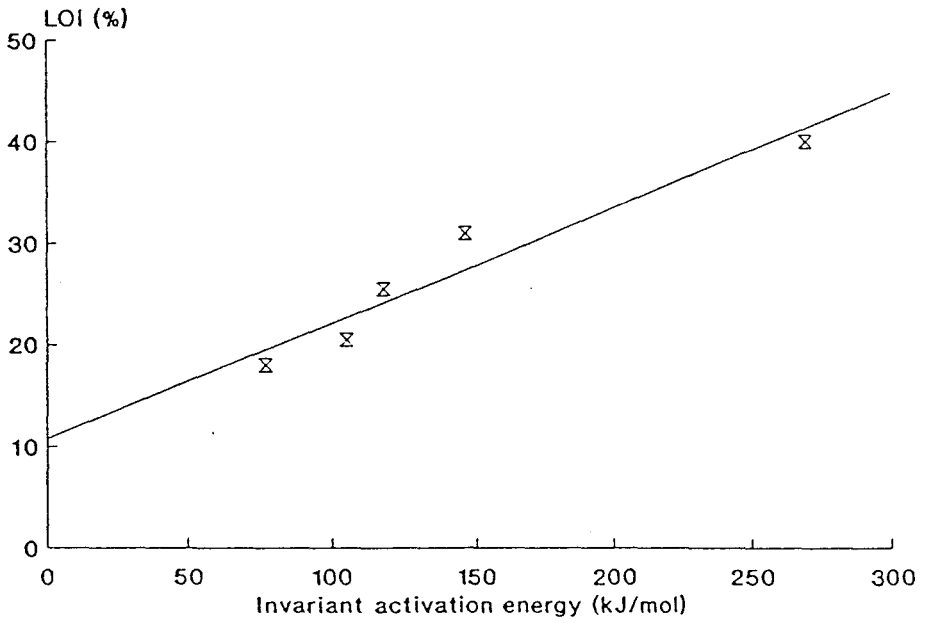

Figure 7 : LOI vs. invariant activation energy.

CONCLUSION

To conclude, this work has shown that, in the case of fire-retardant polypropylene based formulation, there is a correlation between the value given by an evaluation test, i.e.the LOI and a physicochemical characteristic of the system, i.e. the invariant activation energy.

Finally, we propose that Lesnikovich's method may be used to obtain comparative numerical values from TG data. These values allow a classification of fire-retardant formulations.

REFERENCES

1 - **R. DELOBEL, S. BOURBIGOT, M. LE BRAS, J. M. LEROY.** - "Flame Retardancy of Polymeric Materials", V. Z. JANOVIC ed., Society of Plastics and Rubber Engineers, Zagreb, 1990, 08/1.

2 - **H. L. VANDERSALL.** - J. Fire Flammability, 1971, **2**, 97.

3 - **R. DELOBEL, N. OUASSOU, M. LE BRAS, J. M. LEROY.** - Polym. Deg. & Stab., 1989, **23**, 349.

4 - **N. K. JHA, P. BAJAJ, A. C. MISRA, P. L. MAURIA.** - J. Appl. Polym. Sci., 1986, **32**, 4393.

5 - **A. I. LESNIKOVICH, S. V. LEVCHIK.** - J. Thermal Anal., 1985, **30**, 677.

6 - **A. I. LESNIKOVICH, S. V. LEVCHIK, G. F. LEVCHIK.** - J. Appl. Polym. Sci., 1986, **31**, 1943.

7 - **S. V. VYAZOVKIN, V .V. BOGDANOVA, I. A. KLIMVTSOVA, A. I. LESNIKOVITCH.** - J. Appl. Polym. Sci., 1991, **42**, 2095.

8 - **R. DELOBEL, M. LE BRAS, N. OUASSOU, F. ALISTIQSA.** - J. Fire Sci., 1990, **8**(2), 85.

9 - **J. Z. SAKO.** - J. of Phys. Chem., 1968, **72**(7), 2406.

10 - **H. TANAKA, S. OHSIMA, S. ICHIBA, H. NEGITA.** - Thermochim. Acta, 1981, **48**, 137.

11 - **C. SANTIAGO GONZALES DE GARIBAY, A. IRABIEN GULIAS, A. R. ARNAIZ LAZARO.** - Thermochim. Acta, 1984, **75**, 1.

12 - **A. ROMERO SALVADOR, E. GARCIA CALVO, A. IRABIEN GULIAS.** - Thermochim. Acta, 1984, 73, 101.

13 - **T. OSAWA.** - Bull. Soc. of Japan, 1965, **38**(11), 1881.

14 - **C. D. DOYLE.** - J. of App. Polymer Science, 1961, **5**(15), 285.

15 - **A. IRABIEN GULIAS, C. SANTIAGO GONZALES DE GARIBAY, A. R. ARNAIZ LAZARO.** - J. of Therm. Anal., 1984, **29**, 1131.

16 - A. E. VENGER, Yu. E. FRAIMAN, F. B. YUREVICH. - J. of Therm. Anal., 1983, 27, 325.

17 - A. V. NIKOALEV, V.A. LOGVINENKO, V. M. GORBARCHEV. - J. of Therm. Anal., 1974, 6, 473.

18 - J. M. CRIADO et M. GONZALES. - Thermochim. Acta., 1981, 46, 201.

19 - A. I. LESNIKOVICH, S. V. LEVCHIK, V. G. GUSLEV. - Thermochim. Acta, 1984, 77, 357.

20 - A. I. LESNIKOVICH, S. V. LEVCHIK. - J. of Therm. Anal., 1983, 27, 89.

J Chim Phys (1993) 90, 1909-1928

Comparative study of the integral TG-methods used in the invariant kinetic parameter method. Application to the fire-retardant polypropylene

S Bourbigot[1]*, R Delobel[1], M Le Bras[1], D Normand[2]

[1] *Laboratoire de physicochimie des solides, ENSCL, Université des sciences et technologies de Lille, BP 108, F59652 Villeneuve d'Ascq Cedex;* [2] *Laboratoire d'application de physicochimie, Netzsch Frères SARL, 32-34 av des Chardons, BP 101, F77341 Pontault-Combault Cedex, France*

(Received 5 November 1992; accepted 23 April 1993)

Résumé : le calcul de paramètres cinétiques invariants : énergie d'activation et facteur préexponentiel, à partir d'analyses thermogravimétriques est conduit selon trois méthodes intégrales. Il permet de tester la probabilité de différentes fonctions de dégradation. Dans le cas d'une formulation intumescente du polypropylène, dix-huit fonctions de dégradation sont comparées. Il est montré que la formation du matériau intumescent ne peut être décrite par un seul mode de dégradation. Il est proposé que la matrice polymère interagisse avec les additifs pour former un nouveau matériau protecteur.

Abstract : the computation of invariant kinetic parameters : activation energy and preexponential factor, from thermogravimetric analyses is carried out using three integral methods. It allows to test the probability of different kinetic functions. In the case of an intumescent polypropylene based formulation, eighteen degradation functions are compared. It is shown that the formation of the intumescent material cannot be described by one single mode of degradation. It is proposed that the interaction polymer matrix - additives creates a new material presenting fire-retardancy properties.

INTRODUCTION :

The determination of kinetic parameters from data of non isothermal experiments is one of the most difficult kinetic problem. The diversity of the calculation methods does not allow to give preference to any one of them. Nevertheless, the different methods of calculation of the kinetic parameters may lead to different results.

Recently, a method has been developed by Lesnikovich et al. to compute invariant kinetic parameters [1–4]. These latters are independent of the experimental conditions and they are computed without making a hypothesis on the form of the kinetic degradation function. So, the values obtained are no longer apparent but real characteristics of the system studied.

In previous papers [5–6], we have used the invariant kinetic parameter (IKP) method to correlate the fire–proofing properties of intumescent formulations in polypropylene [7] with the invariant activation energy of these systems. The present work is complementary of these studies and deals with a comparative study of integral methods communently applied in thermogravimetry which may be used in the IKP method. These integral methods allow the computation of apparent kinetic parameters for all degradation functions used and so, the compensation effect [8–9] may be studied from the values obtained. The methods used in this work are the Ozawa method [10], the Ozawa method corrected by the Flynn algorithm [11] and the Coats & Redfern method [12]. For each method, the results obtained are compared and discussed, then the kinetic functions are discriminated and their probabilities are calculated. They are computed with the three precedently methods for each degradation function and by using the Fisher distribution. It is expected to obtain a characterisation of the degradation process of the material.

The comparative study is applied to the intumescent fire–retardant system : Ammonium Polyphosphate (APP) – Pentaerythritol (PER) in Polypropylene (PP). The microthermogravimetric analysis allows to study the reaction area which leads to the formation of the intumescent protective coating. It is then expected that the form of kinetic functions will allow the discussion of the degradation mode of the material and so, will provide further information about the thermal process leading to the formation of the protective shield.

THEORY :

The invariant kinetic parameter method :

In this method, several kinetic laws (18 functions $f_j(\alpha)$) indexed in **table 1** [2,8]) and different heating rates β_v are used.

We only assume that the rate expression $d\alpha/dt$, where α is the degree of conversion can be defined (like in isothermal condition) by the equation *(1)* :

$$d\alpha/dt = k\, f(\alpha) \qquad (1)$$

and that the rate constant k follows the Arrhenius law *(2)* :

$$k = A \exp(-E/RT) \qquad (2).$$

Kinetic models	$f_j(\alpha)$	$g_j(\alpha)$	
Nucleation and nucleus growing	$\frac{1}{n}(1-\alpha)(-\ln(1-\alpha))^{1-n}$	$(-\ln(1-\alpha))^n$	S1– n = 1/4 S2– n = 1/3 S3– n = 1/2 S4– n = 2/3 S5– n = 1
Phase boundary reaction	$(1-\alpha)^n$	$1-(1-\alpha)$ $1-(1-\alpha)^{1/2}$ $1-(1-\alpha)^{1/3}$	S6– plane symmetry S7– cylindrical symmetry S8– spherical symmetry
Diffusion	α^{-1} $(-\ln(1-\alpha))^{-1}$ $((1-\alpha)^{1/3}-1)^{-1}$	α^2 $(1-\alpha)\ln(1-\alpha)+\alpha$ $3/2(1-2/3\,\alpha-(1-\alpha))^{2/3}$	S9– plane symmetry S10– cylindrical symmetry S11– spherical symmetry
Potential law	$\frac{1}{n}\alpha^{1-n}$	$\alpha^n\ (0<n<2)$	S12– n = 1/4 S13– n = 1/3 S14– n = 1/2 S17– n = 2/3 S18– n = 3/4
Reaction order	$\frac{1}{n}(1-\alpha)^{1-n}$	$1-(1-\alpha)^2$ $1-(1-\alpha)^3$	S15– order 2 S16– order 3

Table 1 : kinetic models used.

The apparent activation energies (E_{jv}) and preexponential factors (A_{jv}) are determined :

–*Firstly*, by the Ozawa method [10] using the relationship *(3)* for the i–th experimental point :

$$\log(g_j(\alpha_{iv})) = \log\left(\frac{A_{jv}E_{jv}}{\beta_v R}\right) - 2.315 - 0.457\frac{E_{jv}}{RT_{iv}} \qquad (3)$$

with $20 \le \frac{E_{jv}}{RT_{iv}} \le 60$ and $g_j(\alpha) = \int_0^{\alpha} \frac{d\alpha}{f_j(\alpha)}$

The apparent activation energy E_{jv} can therefore be obtained from a plot of $\log[g_j(\alpha_{iv})]$ against $1/T_{iv}$ for a fixed heating rate and a chosen degradation function since the slope of such a line is given by $-0.457(E_{jv}/R)$. In addition, the value of $\log A_{jv}$ can be found from the intercept on the $\log[g_j(\alpha)]$ axis.

–*Secondly*, these apparent kinetic parameters have been calculated once more using the Flynn algorithm [11]. This algorithm is an iterative method which allows the correction of the errors of the approximation of Doyle [13] used in *(3)* and so, in a first approximation to break away from the limit of E/RT values.

–*Thirdly*, the eighteen apparent kinetic parameters are computed by the Coats & Redfern method [12] using the relationship *(4)* :

$$\log\left(\frac{g_j(\alpha_{iv})}{T_{iv}^2}\right) = \log\left(\frac{A_{jv}R}{\beta_v E_{jv}}\right) - \frac{E_{jv}}{2.3RT_{iv}} \qquad (4)$$

with $g_j(\alpha) = \int_0^{\alpha} \frac{d\alpha}{f_j(\alpha)}$

By plotting $\log\left(\frac{g_j(\alpha_{iv})}{T_{iv}^2}\right)$ versus $1/T_{iv}$, the apparent activation energy E_{jv} and the apparent preexponential factor A_{jv} may be obtained.

The application of the IKP method is based on the study of the compensation effect (CE) [8–9]. For each function $f_i(\alpha)$, $\log A_i$ versus E_i is plotted and if a compensation effect is observed, a linear relation defined by the following equation : $\log A_{jv} = B_v + l_v E_{jv}$ is obtained for each heating rate β_V [3]. The significance of B_v and l_v has been discussed by Lesnikovich et al. [3] and it has been demonstrated that *(5)* :

$$\begin{cases} B_v = \log(k_v) \\ l_v = \dfrac{1}{2.3RT_v} \end{cases} \qquad (5)$$

where k_v is the invariant rate constant of the system at the temperature T_v, these two parameters being characteristics of the experimental conditions.

The essence of the method is to obtain a pencil of lines by varying the experimental conditions and to find the coordinates of its centre, i.e. E_{inv} et A_{inv} (invariant activation energy and preexponential factor). The coordinates are in an ellipsoidal domain that may be defined by a straight line [2] :

$$B_v = \log A_{inv} - E_{inv}\, l_v \qquad (6).$$

Probabilities of the kinetic degradation functions :

The kinetic functions $f_j(\alpha)$ may then be discriminated using the $\log A_{inv}$ and E_{inv} values obtained. Having n of the i–th of the experimental values of $\left(\frac{d\alpha}{dT}\right)_{iv}$, the residual sum of squares for each $f_j(\alpha)$ and

for each heating rate β_v may be computed *(7)* :

$$(n-1)S_{jv}^2 = \sum_{i=1}^{i=n}\left|(\frac{d\alpha}{dT})_{iv} - \frac{A_{inv}}{\beta_v}\exp(\frac{E_{inv}}{RT_{iv}})f_j(\alpha_{iv})\right|^2 \qquad (7)$$

The most probable function is then chosen by the average minimum value of $\bar{S}_j$ defined by the relationship *(8)* :

$$\bar{S}_j = \frac{1}{p}\sum_{v=1}^{v=p} S_{jv} \qquad (8)$$

with p the number of heating rates used.

The probability associated with each $f_j(\alpha)$ can be calculated by defining the ratio *(9)*

$$F_j = \frac{\bar{S}_j^{-2}}{S_{min}^{-2}} \qquad (9)$$

where $\bar{S}_j^{-2} = \frac{1}{p}\sum_{v=1}^{v=p} S_{jv}^{-2}$ and S_{min}^{-2} is the average minimum of residual dispersion.

This ratio obeys to the F–distribution *(10)* :

$$q(F_j) = \frac{\Gamma(\nu)}{\Gamma^2(\frac{\nu}{2})} \times \frac{F_j^{\frac{\nu}{2}-1}}{(1+F_j)^{\nu}} \qquad (10)$$

where ν is the number of degrees of freedom equal for every dispersions and Γ is the Gamma function [15]. It is interesting to note that the average of the residual dispersion and not simply the residual dispersion has been chosen to define the ratio F_j because the average $\bar{S}_j^{-2}$ is a good non–bias estimator of all S_{jv}^2 and it gives a better statistic representation of the process.

The probabilities of the j–th function are computed on the assumption that the experimental data with L kinetic functions are described by a complete and independent events' systems *(11)* :

$$\sum_{j=1}^{j=L} P_j = 1 \qquad (11)$$

Therefore we obtain *(12)* :

$$P_j = \frac{Z_j}{\sum_{j=1}^{j=L} Z_j} \qquad (12)$$

with $Z_j = 1 - \frac{\Gamma(\nu)}{\Gamma^2(\frac{\nu}{2})} \int_0^{F_j} x^{\frac{\nu}{2}-1}(1+x)^{-\nu} dx.$

EXPERIMENTAL :

Materials :

Raw materials were PP (powder supplied by ATOCHEM), PER (PROLABO R.P. grade), APP ($(NH_4PO_3)_n$, n=700, Hoechst Exolit 422, soluble fraction in H_2O : < 1 wt%).
Initial mixtures PP–APP/PER were first prepared after a mechanical grinding and a sifting (200.10^{-6} m) of the raw materials. The composition of the mixture (PP/APP/PER : 70/22.5/7.5 ponderal ratio) corresponds to the highest fire–retardant performances of this PP–based system [7].

Thermogravimetric analysis :

Thermogravimetric analysis were carried out at heating rates of 3, 5, 7, 10 K/min under synthetic air (Air Liquid grade) (flow rate = $5x10^{-7}$ Nm^3/s) using a NETZSCH STA 409 thermobalance. In each case, samples were 20 mg and were positioned in open Pt/Ir crucibles. The thermocouple is in the heart of the sample and the precision on the temperature measurements is ± 0.25 K in the range 323 K–1023 K. The corrections of the Archimede strength are systematically carried out by substraction of the curve of the system obtained in blank tests.

Computation :

The computation of the kinetic parameters values and of the probabilities of the degradation function has been carried out with a software developed by the Laboratory using the spreadsheet Quattro Pro 4 (Borland).

RESULTS AND DISCUSSION :

The different thermograms are shown in **figure 1**. The method is applied to the temperature range (determinated with the first derivative curve) which corresponds to the thermal oxidative decomposition

of the material ($0.1 < \alpha < 0.45$). In this range of temperature, it has been previously shown that the intumescent phenomenon occurs and that the resulting material is stable [7].

From these TG curves, we obtain 18 couples (A_{jv}, E_{jv}) per heating rates β_v depending of the kinetic functions $f_j(\alpha)$ used in the computation. The parameters are only apparent values of the degradation process. They are presented **table 2**.

Heating rates β_v (K/min)	Kinetic functions	Coats & Redfern		Ozawa		Ozawa with the Flynn algoritm	
		$\log(A_{jv})$ ($A : s^{-1}$)	E_{jv} (kJ/mol)	$\log(A_{jv})$ ($A : s^{-1}$)	E_{jv} (kJ/mol)	$\log(A_{jv})$ ($A : s^{-1}$)	E_{jv} (kJ/mol)
3	S1	-2.92	11.12	-0.7	19.9	-0.53	13.43
	S2	-2.16	18.1	-0.27	26.53	-0.14	19.5
	S3	-0.8	32.04	0.66	39.8	0.74	33.28
	S4	0.46	45.99	1.64	53.07	1.69	47.11
	S5	2.89	73.88	3.68	79.6	3.71	74.38
	S6	2.14	66.47	3.02	72.56	3.05	67.29
	S7	-1.2	28.34	0.35	36.28	0.44	29.41
	S8	-2.45	15.63	-0.47	24.19	-0.33	17.78
	S9	8.42	142.74	8.67	145.12	8.68	143.14
	S10	8.58	147.48	8.8	149.63	8.81	147.88
	S11	1.16	50.65	0.6	48.18	0.66	42.1
	S12	-3.18	9.27	-0.84	18.14	-0.6	10.58
	S13	-2.45	15.63	-0.47	24.19	-0.33	17.78
	S14	-1.2	28.34	0.35	36.28	0.44	29.41
	S15	2.72	66.08	2.72	66.08	2.76	60.14
	S16	2.34	60.15	2.34	60.15	2.39	54.12
	S17	-0.05	41.05	1.22	48.37	1.27	42.26
	S18	0.51	47.41	1.66	54.42	1.71	48.31
5	S1	-2.88	9.83	-0.57	18.91	-0.4	12.76
	S2	-2.14	16.46	-0.17	25.21	-0.04	18.53
	S3	-0.85	29.71	0.69	37.82	0.78	30.65
	S4	0.35	42.96	1.6	50.43	1.66	44.05
	S5	2.63	69.46	3.5	75.64	3.53	70.14
	S6	1.73	60.45	2.71	67.06	2.75	61.04
	S7	-1.34	25.2	0.32	33.53	0.43	26.09
	S8	-2.51	13.45	-0.4	22.35	-0.23	15.08
	S9	7.45	130.93	7.8	134.12	7.81	131.37
	S10	7.7	136.65	8.01	139.56	8.02	137.04
	S11	1.16	50.65	0.82	48.18	0.89	41.27
	S12	-3.21	7.58	-0.72	16.77	-0.49	9.78
	S13	-2.51	13.45	-0.4	22.35	-0.23	15.08
	S14	-1.34	25.2	0.32	33.53	0.43	26.09
	S15	2.31	59.35	2.31	59.35	2.36	53.4
	S16	1.87	52.45	1.87	52.45	1.93	45.83
	S17	-0.27	36.95	1.09	44.71	1.16	38.3
	S18	0.24	42.82	1.49	50.3	1.55	43.94

Table 2 : apparent kinetic parameters obtained for each kinetic function and each heating rate.

Heating rates β_v (K/min)	Kinetic functions	Coats & Redfern		Ozawa		Ozawa with the Flynn algoritm	
		$\log(A_{jv})$ ($A : s^{-1}$)	E_{jv} (kJ/mol)	$\log(A_{jv})$ ($A : s^{-1}$)	E_{jv} (kJ/mol)	$\log(A_{jv})$ ($A : s^{-1}$)	E_{jv} (kJ/mol)
7	S1	-2.45	12.62	-0.27	21.92	-0.1	14.79
	S2	-1.65	20.3	0.2	29.22	0.33	21.48
	S3	-0.22	35.66	1.2	43.83	1.28	36.65
	S4	1.11	51.01	2.26	58.44	2.31	51.88
	S5	3.68	81.73	4.44	87.66	4.47	82.46
	S6	2.57	70.05	3.46	76.55	3.49	70.99
	S7	-0.82	29.82	0.74	38.27	0.83	31.02
	S8	-2.09	16.41	-0.09	25.52	0.04	18.75
	S9	8.95	150.51	9.2	153.1	9.21	151.01
	S10	9.32	157.84	9.54	160.08	9.54	158.21
	S11	1.16	50.65	0.97	48.18	1.04	41.27
	S12	-2.82	9.7	-0.47	19.14	-0.24	11.17
	S13	-2.09	16.41	-0.09	25.52	0.04	18.75
	S14	-0.82	29.82	0.74	38.27	0.83	31.02
	S15	2.9	66.73	2.9	66.73	2.94	60.74
	S16	2.33	58.14	2.33	58.14	2.38	51.61
	S17	0.35	43.23	1.62	51.03	1.68	44.58
	S18	0.91	49.93	2.08	57.41	2.13	50.97
10	S1	-2.43	11.6	-0.19	21.07	-0.02	14.21
	S2	-1.66	18.98	0.24	28.09	0.38	20.64
	S3	-0.29	33.74	1.19	42.13	1.26	35.23
	S4	0.99	48.5	2.18	56.18	2.24	49.08
	S5	3.43	78.03	4.24	84.26	4.27	78.73
	S6	2.36	66.63	3.3	73.42	3.33	67.5
	S7	-0.87	28.04	0.74	36.71	0.84	29.76
	S8	-2.09	15.18	-0.03	24.47	0.14	16.51
	S9	8.4	143.8	8.7	146.84	8.71	144.19
	S10	8.75	150.96	9.01	153.65	9.02	151.57
	S11	1.16	50.65	1.12	48.18	1.19	41.27
	S12	-2.8	8.75	-0.38	18.35	-0.15	10.71
	S13	-2.09	15.18	-0.03	24.47	0.14	16.51
	S14	-0.87	28.04	0.74	36.71	0.84	29.76
	S15	2.77	63.83	2.77	63.83	2.81	57.43
	S16	2.22	55.44	2.22	55.44	2.28	48.43
	S17	0.24	40.9	1.57	48.95	1.64	41.93
	S18	0.78	47.34	1.99	55.06	2.05	48.11

Table 2 : apparent kinetic parameters obtained for each kinetic function and each heating rate.

It is shown by plotting $\log A_{jv} = f(E_{jv})$ that straight lines are obtained for each heating rate and for each method used (**figure 2**) i.e. that the compensation effect is always observed.

The values of T_v and k_v are then calculated from the slopes and the intercepts of the above straight lines. The data obtained are presented in **table 3**.

For each method, the invariant kinetic parameters can be obtained by straight lines defined by the equation : $B_v = \log A_{inv} - E_{inv} I_v$. The results are presented in the table 4.

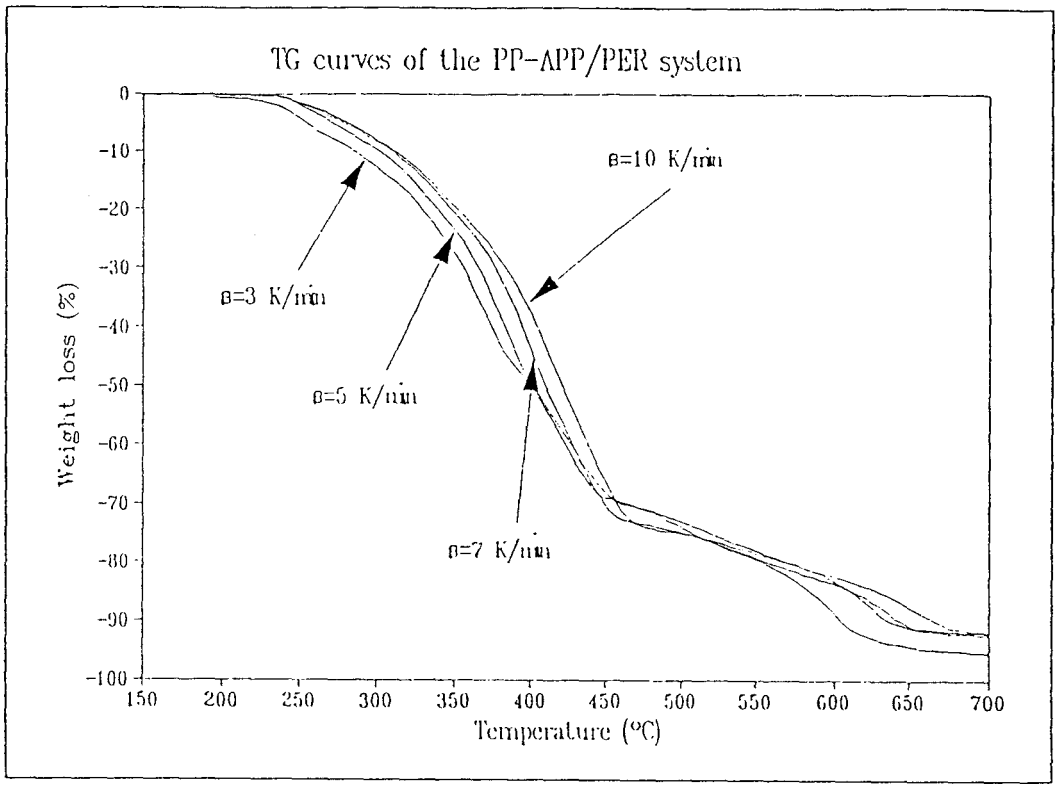

Figure 1 : TG curves of the PP-APP/PER system for all heating rates.

Methods used	β_v (K/min)	$B_v = \log(k_v)$ ($k_v : s^{-1}$)	T_v (K)
Ozawa	3	-2.34(± 0.21)	698.7(± 6)
	5	-2.07(± 0.23)	721.3(± 8)
	7	-1.99(± 0.26)	723.3(± 9)
	10	-1.81(± 0.25)	739.5(± 6)
Ozawa with the Flynn algorithm	3	-1.62(± 0.28)	738.5(± 6)
	5	-1.35(± 0.24)	763.4(± 7)
	7	-1.25(± 0.20)	764.9(± 5)
	10	-1.07(± 0.21)	783.5(± 6)
Coats & Redfern	3	-3.58(± 0.31)	609.8(± 5)
	5	-3.42(± 0.29)	615.1(± 6)
	7	-3.10(± 0.30)	633.1(± 5)
	10	-3.00(± 0.28)	639.2(± 5)

Table 3 : Invariant rate constants k_v at the temperatures T_v deduced from the compensation effects .

Method used	E_{inv} (kJ/mol)	$\log A_{inv}$ ($A_{inv} : s^{-1}$)	r*
Ozawa	128 (± 10)	7.4 (± 0,7)	0.99
Ozawa with the Flynn algorithm	137 (± 13)	8.1 (± 0,5)	0.99
Coats & Redfern	143 (± 8)	8.7 (± 0,7)	0.99

r : regression coefficient of the straight line :* $B_v = \log A_{inv} - E_{inv}/T_v$.

Table 4 : Invariant kinetic parameters obtained for each method used .

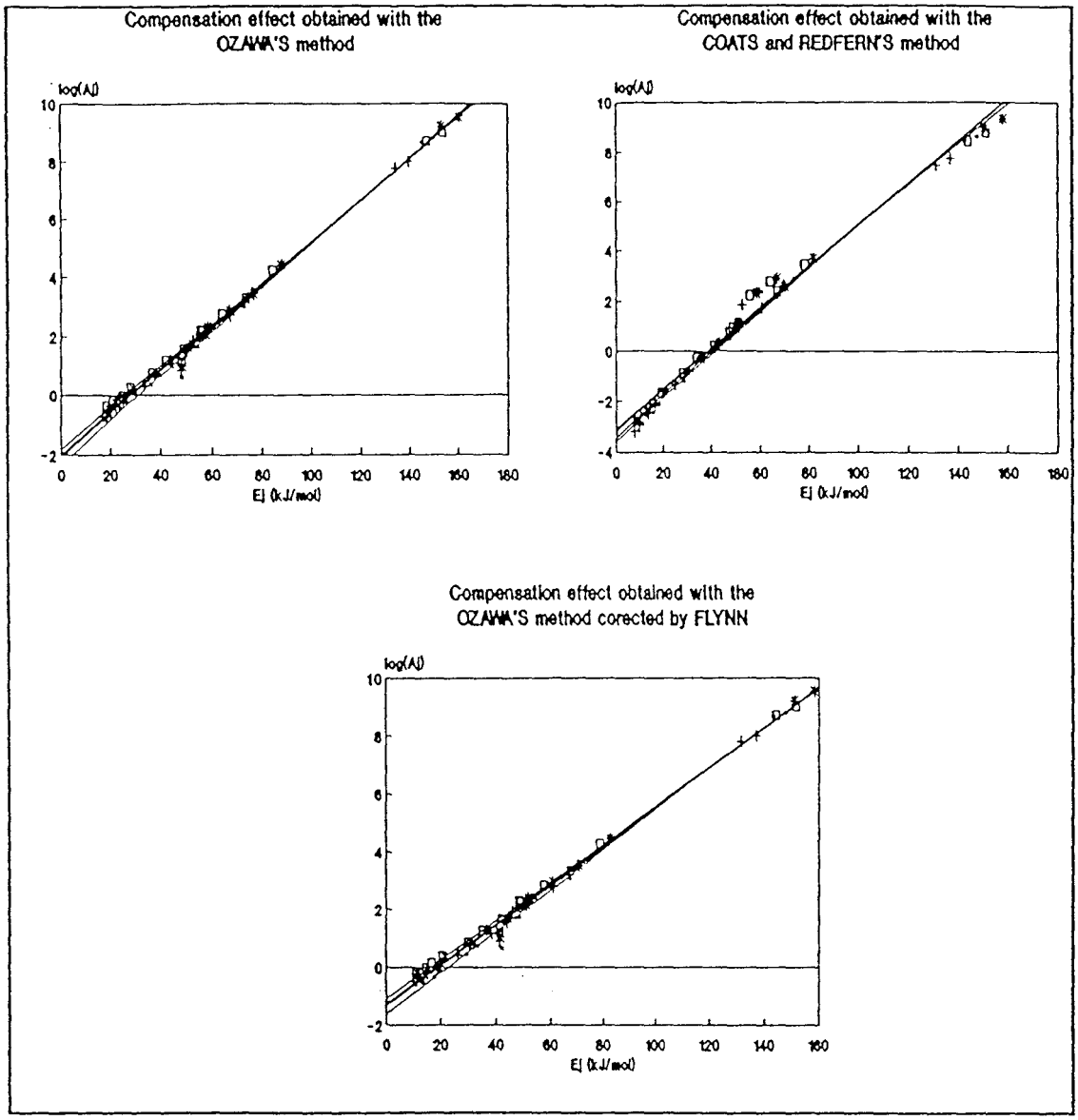

Figure 2 : Compensation effects of the PP–APP/PER system for each heating rates and for the three methods used.

The table 4 shows that the invariant kinetic parameters obtained are the same in the range of errors. Therefore it is demonstrated that these parameters are independent of the calculation method used. This result is consistent with the theoretical approach developed by Lesnikovich et al. [3]. Indeed the CE is a computational artefact which characterizes the method used rather than the experimental conditions.

The artefact can be eliminated by computing the invariant characteristics of the process, i.e., E_{inv} and A_{inv}. It is made by constructing a statistical model which is an adaptation of a more general approach to the description of multiparametric relations by polynomials [14]. So the model is independent of the method used and the kinetic parameters are real characteristics of the process. Therefore the study demonstrates for the first time that experimentally the IKP method is independent of the TG integral method used and that the mathematical treatment of Lesnikovich et al. is still verified in the case of an intumescent flame-retardant system.

The residual dispersions S^2_{jv} is calculated with 15 points (n=15) of the experimental TG-curves. The results with the average of the S^2_{jv} and the probabilities associated to each function are presented in the table 5 :

Type of the kinetic degradation functions	Ozawa		Ozawa with the Flynn algorithm		Coats & Redfern	
	$\bar{S}^{-2}_j$ ($\times 10^{-5}$)	P_j (%)	$\bar{S}^{-2}_j$ ($\times 10^{-5}$)	P_j (%)	$\bar{S}^{-2}_j$ ($\times 10^{-5}$)	P_j (%)
S1	0.9	5.8	1.8	1.3	4.7	0.0
S2	0.7	9.7	1.0	3.1	2.4	0.1
S3	0.8	8.0	0.7	9.9	1.1	4.0
S4	0.9	6.2	0.7	10.7	7.3	13.4
S5	0.9	5.9	0.6	12.4	4.7	31.7
S6	0.6	14.6	0.7	11.6	1.5	1.1
S7	0.7	10.6	0.5	16.8	7.2	13.6
S8	0.7	8.9	0.5	16.0	0.6	21.2
S9	7.1	0.0	14.6	0.0	33.8	0.0
S10	4.0	0.0	8.5	0.0	20.7	0.0
S11	181.6	0.0	269.6	0.0	46.8	0.0
S12	2.0	0.3	4.6	0.0	11.5	0.0
S13	2.5	0.1	5.9	0.0	15.1	0.0
S14	0.8	7.9	1.3	0.8	3.2	0.0
S15	0.9	5.5	0.8	6.5	1.2	3.3
S16	1.0	4.0	1.1	2.6	1.7	0.7
S17	0.7	10.2	0.9	4.4	2.2	0.2
S18	1.2	2.4	1.0	3.8	0.8	10.5

Table 5 : values of the average of the residual means of squares and of the probabilities for each calculation method used in the IKP method.

The histograms which show the distributions of the probabilities P_j obtained for each integral method, are compared **figure 3.**

It is observed that these distributions are different whereas the invariant kinetic parameters were pratically the same for the three methods. To explain this anomaly, it can be noted that the $\bar{S}^{-2}_j$ values computed by each method are quite similar but that the resulting values F_j are different enough to lead to three distinct distributions of probabilities. Indeed the approximation of the integral $\int_0^T \exp(-\frac{E}{Rx})dx$

changes with the integral method and so, may lead to different $\bar{S}^{-2}_j$. The Fisher distribution $q(F_j)$ (**figure** 4) has a sharp maximum at F_j near to one and for weak variation of F_j the area under the curve varies greatly and so, the values of P_j will be different. Another explanation is that the mathematical form of the kinetic function used is not adequate to describe the physical content of the real process and/or that this form has not yet been revealed either theoretically or experimentally.

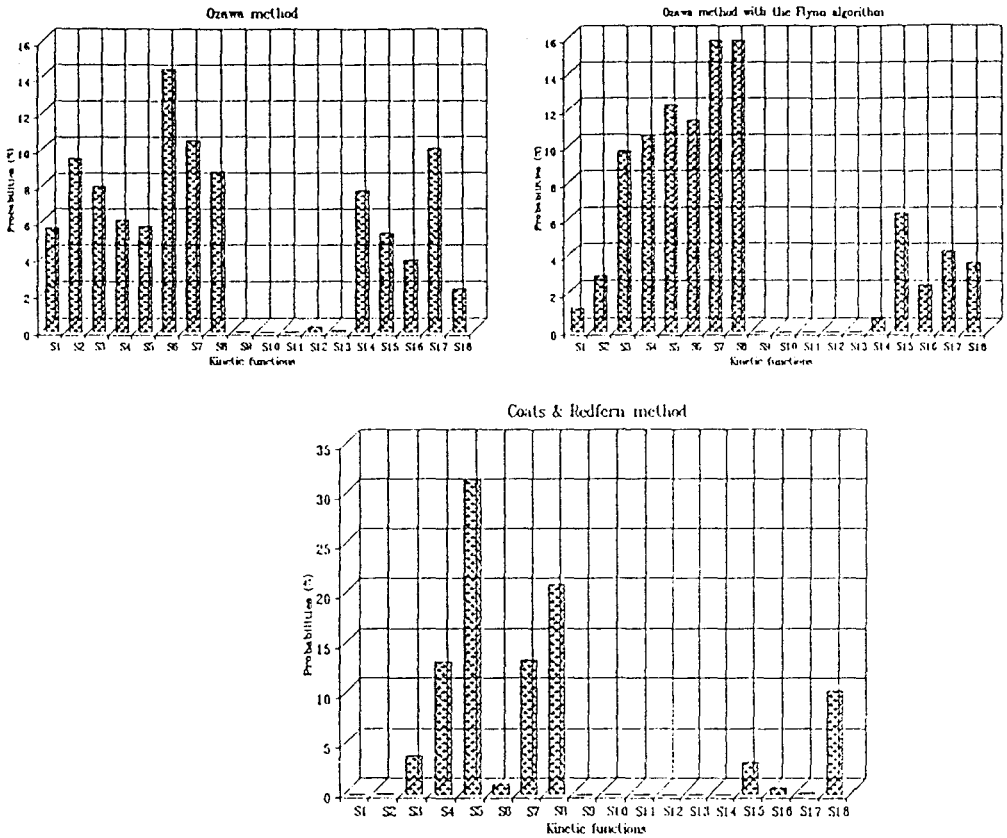

Figure 3 : distribution of the probabilities for the three methods used.

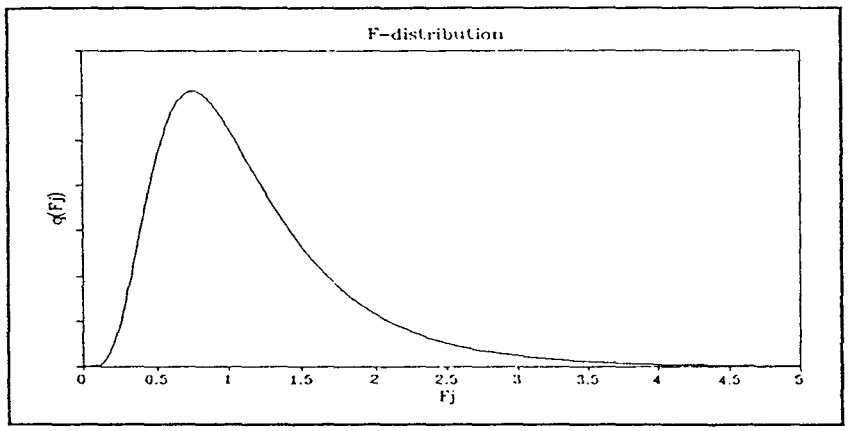

Figure 4 : F-distribution for the same degrees of freedom equalling 14.

To verify the accuracy of the method, the distribution of probabilities of the sole PP has been computed from the values obtain from our previous work [5]. The results are shown figure 5.

The distribution of probabilities shows that the classical function $1-\alpha$ is the most probable for the thermooxidative degradation of the PP. Indeed this function is generally admitted for the degradation of a polymer.It is therefore demonstrated that the method of probabilities computation may characterize the mode of degradation of a material. Moreover, this result shows that the degradation of the PP-APP/PER system changes compared with the sole PP and that therefore, there is an interaction between the additives and the polymeric matrix to form a new material.

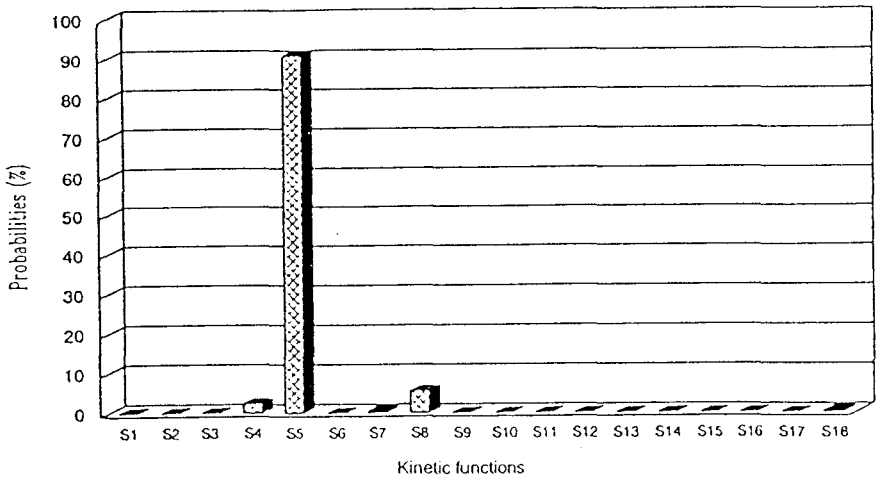

Figure 5 : distribution of probabilities of the sole PP computed with the Ozawa method.

The distribution of probabilities obtained with the PP-APP/PER system does not allow the discrimination of one function and it may appear more judicious to reason by considering the entire set of kinetic functions used as a space and by defining on this space several classes of functions. This study has been suggested for the first time by Vyazovkin et al. [16] who have demonstrated that the space formed by the kinetic functions may be subdivided into two-dimensional subspaces of four classes of functions. The authors have considered the kinetic function by analysing their mathematical form rather than elaborating their physical meaning. This approach is admissible because the kinetic functions are by essence mathematical descriptions of idealized chemical processes and because the possibility of combining any kinetic functions in a single system is an integral property of the unified approach, that is to say of the IKP method. Finally, the authors have shown that the entire space of kinetic functions may play the same role of an adjustable parameter as it is done with some function. The four classes of functions so obtained are resumed in **table 6**.

Classes	I	II	III	IV
Type of function	S9-S10-S11	S5-S7-S8-S15-S16	S1-S2-S3-S4	S6-S12-S13-S14-S17-S18

Table 6 : distribution of the kinetic degradation functions following the different classes.

The first class of functions includes all diffusion kinetic functions. The second class cover all the kinetic functions of the general form $(1-\alpha)^p$. Indeed the S5, S15 and S16 are only particulary cases of reaction order functions. The third class includes the functions of the Avrami-Erofeev type (nucleation and nucleus growing) instead of S5. The fourth class comprises the power law nuclear growth functions of the general form $m\alpha^n$ and S6 function which can be considered as a particularly case of potentiel function with m=1 and n=0.

The sum of the probabilities per class has been calculated and is presented **table 7**.

Classes	I	II	III	IV
Ozawa	0.2	34.8	29.7	35.3
Ozawa with the Flynn algorithm	0	54.2	24.9	20.9
Coats & Redfern	2.7	70.6	17.5	9.2

Table 7 : sum of the probabilities P_j in percent of kinetic degradation functions per class.

The analysis of the three diagrams of probabilities' distributions and of the **tables 6** and 7 shows that the functions' group belonging to class II seems to be the most probable, in particular when they are computed with the Coats & Redfern or Ozawa with the Flynn algorithm methods. It can be noted that the probabilities given by the Ozawa method do not allow to select certainly a class of functions, the classes II and IV presenting the same values. This loss of discrimination compared with the other methods may be due to the approximation of Doyle which gives values of activation energies with a great incertainly for the E/RT values near 20. As the E/RT values obtained are often near to 20, the Ozawa method corrected by the algorithm of Flynn or the Coats & Redfern method must be preferred to compute the distribution of probabilities. As an example for a value E/RT = 20, the approximation on the integral $\int_0^T \exp(-\frac{E}{Rx})dx$ is made with relative errors of 4%, 1.6% and 1.3% for respectively the Ozawa, Ozawa with Flynn and Coats & Redfern methods. Nevertheless, this latter gives the better discrimination of the degradation process. It shows that for a weak variation of the values of the couple (E_{inv}, A_{inv}), thus of F_j, the probabilities distribution changes greatly and that it must be preferred the Coats & Redfern method to computed the probabilities associated to each $f_j(\alpha)$. In the following, the discussion will be led by considering the results obtained with this method.

As seen in **table 7**, class I cannot be taken into account and so, a diffusion mechanism does not describe the degradation process of the material. The intumescence process develops via a mechanism in condensed phase [7] and so, the hypothesis of an additives' migration to create a protective shield had been proposed [7]. But as it is shown, it cannot occur (no diffusion mechanism). The values of the probabilities of the classes III and IV (17.5% and 9.2% respectively) are weak compared with this of the class II and they can be considered as negligible in the degradation process of the material.

Finally, it is observed that in the case of the intumescent system, the description per class may characterize the degradation process and that it may be proposed that the thermooxidative degradation of our material is principally governed by kinetic functions of class II (that is to say, by equations of the $(1-\alpha)^n$ type) which implies both nucleation, surface reactions and reactions of order 2 or 3 processes. Indeed the physicochemical processes as depolymerisation, ablation, surface and/or bulk oxidation may occur during the thermooxidative degradation of a polymer.

CONCLUSION :

In this work, we have shown that the IKP method was independent of the integral method used to compute the invariant activation energies and preexponential factors, but was sensitive to these methods, that is to say to invariant kinetic parameters obtained, to calculate the probabilities associated to each kinetic function. Nevertheless, it is proposed to select the Coats & Redfern method to compute the distribution of probabilities associated to kinetic functions in the IKP method.

Moreover, we have been demonstrated that in the case of an intumescent formulation, the degradation type of the system does not follow one single classical law but it is the contribution of a set of kinetic functions of the $(1-\alpha)^n$ type. This study has thus shown that it was preferable to reason with classes of kinetic functions rather than with the choice of one single law and that the degradation process could be characterized by the computation of the distribution of probabilities of different kinetic functions.

REFERENCES :

1 – **A. I. Lesnikovich**– Russ. J. Phys. Chem, 1981, 55(5), 652.

2 – **A. I. Lesnikovich and S. V. Levchik**– J. Therm. Anal., 1983, 27, 85.

3 – **A. I. Lesnikovich, S. V. Levchik and V. G. Guslev**– Thermochim., Acta, 1984, 77, 357.

4 – **S. V. Levchik, G. F. Levchik and A. J. Lesnikovich**– Thermochim. Acta, 1985, 92, 157.

5 – **S. Bourbigot, R. Delobel, M. Le Bras and Y. Schmidt**– J. Chim. Phys., 1992, 89, 1835.

6 – **R. Delobel, S. Bourbigot, M. Le Bras, Y. Schmidt and J. M. Leroy**– Makrom. Chem., 1992, under press.

7 – **R. Delobel, M. Le Bras, N. Ouassou and F. Alistiqsa**– J. Fire Sci., 1991, 8(2), 473.

8 – **A. V. Nikoalev, V. A. Logvimenko and V. M. Gorberchev**– J. Therm. Anal., 1974, 6, 473.

9 – **J. M. Criado and M. Gonzales**– Thermochim. Acta, 1981, 46, 201.

10 – **T. Ozawa**– Bull. Soc. Japn, 1965, 38(11), 1881.

11 – **J. H. Flynn**– J. Therm. Anal., 1983, 27, 95.

12 – **A. W. Coats and J. P. Redfern**– Nature, 1964, 201, 68.

13 – **C. D. Doyle**– J. Appl. Polym. Sci., 1961, 15, 285.

14 – **D. M. Himmelblau**– Process Analysis by statistical Methods, Wiley, New-York, 1970.

15 – P. G. Hoel– Statistique Mathématique, Armand Colin, Paris, 1991.

16– S. V. Vyazovkin and A. I. Lesnikovich– J. Therm. Anal., 1987, 32, 249.

GLOSSARY :

β_v : heating rates.

p : number of heating rates.

α_{iv} : degree of conversion of the i–th experimental point extracted of the thermogram plotted at β_v.

T_{iv} : temperature associated at α_{iv}.

$f_j(\alpha)$: j–th kinetic function among the 18 functions used.

E_{jv} : apparent activation energy calculated with $f_j(\alpha)$ and with the TG curve plotted at β_v.

A_{jv} : apparent preexponential factor calculated with $f_j(\alpha)$ and with the TG curve plotted at β_v.

B_v & l_v : parameter deduced of the linear relationship of the compensation effect at β_v.

k_v & T_v : invariant rate constant of the system at the temperature Tv (deduced of the compensation effect).

$(\frac{d\alpha}{dT})_{iv}$: value of the derivative curve at the point α_{iv}.

S^2_{jv} : residual sum of squares for each $f_j(\alpha)$.

$\bar{S}^2_j$: average on v of all S^2_{jv}.

$\bar{S}^2_{jmin}$: minimum average of $\bar{S}^2_j$.

F_j : $F_j = \frac{\bar{S}^2_j}{\bar{S}^2_{jmin}}$

$q(F_j)$: F–distribution.

ν : degree of freedom.

Γ : Gamma function.

P_j : probability associated with a given $f_j(\alpha)$.

Fire Degradation of an Intumescent Flame Retardant Polypropylene Using the Cone Calorimeter

S. BOURBIGOT, M. LE BRAS AND R. DELOBEL***
Laboratoire de Physicochimie des Solides, E. N. S. C. L.
Université des Sciences et Technologies de Lille
BP 108, F-59652 Villeneuve d'Ascq Cedex, France

(Received March 11, 1994)
(Revised August 19, 1994)

ABSTRACT: This work studies the fire degradation of an intumescent formulation Polypropylene (PP)–Ammonium Polyphosphate (APP)/Pentaerythritol (PER) using the cone calorimeter. An intumescence model is described which introduces the notion of degradation front. From the weight loss data recorded by the cone calorimeter and the results of the invariant kinetic parameters method (given in appendix) applied to the PP and to the PP-APP/PER system, the respective temperatures of the degradation fronts are measured. A stability zone is shown where the protection is effective. The intumescent coating degrades then by forming a carbonaceous residue which reduces the heat flux evolved.

KEY WORDS: cone calorimeter, flame retardant polypropylene, intumescence, degradation front, invariant kinetic parameters method.

INTRODUCTION

INTUMESCENT SYSTEMS IN thermoplastics give fire-proofing properties by developing a carbonaceous shield (char) which provides a protection

*Author to whom all correspondence should be sent.
**Also at Centre de Recherche et d'Etude sur les Procedés d'Ignifugation des Matériaux (CREPIM), BP 49, F-62160 Bully les Mines.

to the material [1]. The shield limits the heat transfer to the substrate. In this work, we use an intumescent formulation, which associates Ammonium Polyphosphate (APP) with Pentaerythritol (PER). This system in Polypropylene (PP) (additives' level equalling 30% (wt) leads to a Limiting Oxygen Index (LOI) of 32% and to a V-0 classification of the UL-94 test [2].

It seems interesting, therefore, to study the fire degradation of the PP-APP/PER. In the conditions of the fire, the system develops an intumescence phenomenon and forms a carbonaceous coating. This coating is constituted by stacks of polyaromatics the chemical composition of which has been extensively studied in the Laboratory [1,3]. We proposed that the mechanical properties of the shield are obtained by the phosphohydrocarbonated links bridging the polyaromatics which can accomodate the stresses due to the degradation of the material in the fire and so, hinder the creation and the propagation of cracks. The part played by the coating in the protection of the polymeric material, protective thermal shield and/or coating impermeable to the gases, resulting from the degradation of the material (fuel) or to the air (combustive agent), has to be examined.

The cone calorimeter [4] is an apparatus developed by NIST in the eighties. It allows the quantification of phenomena of fire development [5]. Virgin polymer or intumescent formulations can be tested under heat flux and the degradation of the materials is followed dynamically by recording the rate of heat release (RHR) and the weight loss.

In previous works [6–8], we studied the thermo-oxidative degradation of PP-APP/PER systems and showed that the invariant activation energies (see appendix) may be correlated to the fire-proofing properties (in the LOI sense) of the materials. The latter study led to propose the degradation kinetic laws for PP and PP-APP/PER. In the case of PP, the classical order law is put forward, whereas in the case of PP-APP/PER, a composite equation including terms belonging both to order and to diffusion kinetic laws is considered. These computed kinetic relations, including invariant paramaters, may be used whatever the temperature varies. Using TG results recorded by the cone calorimeter and the previously proposed kinetic laws, this paper examines the fire degradation of PP-APP/PER and of the sole PP using the rhr and the weight loss measured in order to put forward the thermal protective property of the intumescent coating.

EXPERIMENTAL

Material

Raw materials were PP (Polypropylene supplied by Elf-Atochem), PER (Aldrich R. P. grade) and APP $(NH_4PO_3)_n$, $n = 700$, Hoechst Exolit 422, soluble fraction in H_2O: < 1 wt%). The study has been carried out using the APP/PER mixture for the ratio APP/PER = 3 (wt/wt). In the particular case of polyethylenic materials, the fire-retardant properties are maximum for this ratio [1,8–9]. The additives were incorporated at 30% (wt/wt) in the polymer. Initial mixtures were first prepared by ballmilling after mechanical grinding and sifting (200 μm) of the raw materials. Sheets (100 × 100 × 3 mm^3) were then obtained using a Darragon press at $T = 190°C$ and at a pressure of 3 MPa.

Cone Calorimeter

Samples were exposed to a Stanton Redcroft Cone Calorimeter according to ASTM 1356-90 under a heat flux of 50 kW/m^2. This flux was chosen because it corresponds to the evolved heat during a fire [4]. The data were recorded with a computer connected to the cone calorimeter. One obtained conventional data (rhr, weight loss, weight loss rate . . .) using software provided by Polymer Laboratories. The rhr values were computed using the oxygen consumption principle [4]. Furthermore, the computation of the thermogravimetric data was carried out using the spreadsheet Quattro Pro 5 for Windows (Borland).

RESULTS AND DISCUSSION

Rate of Heat Release Profiles

Heat release has long been recognised as the major fire reaction parameter because it defines fire size [10]. Illustrative measurements are shown on the sole PP and the PP-APR/PER system (Figure 1).

The presence of APP/PER in the PP decreases strongly the rhr values compared to the sole polymer and the total heat evolved (the) of the flame-retardant PP is always less than PP. The additive implies, therefore, that the degradation reactions of the material are less exothermal than in the sole PP. This constitutes proof that the intumescent shield is efficient. Moreover, it is interesting to note that ignition appears earlier with the flame retardant PP (ignition time $t_i = 15$ s) than with the

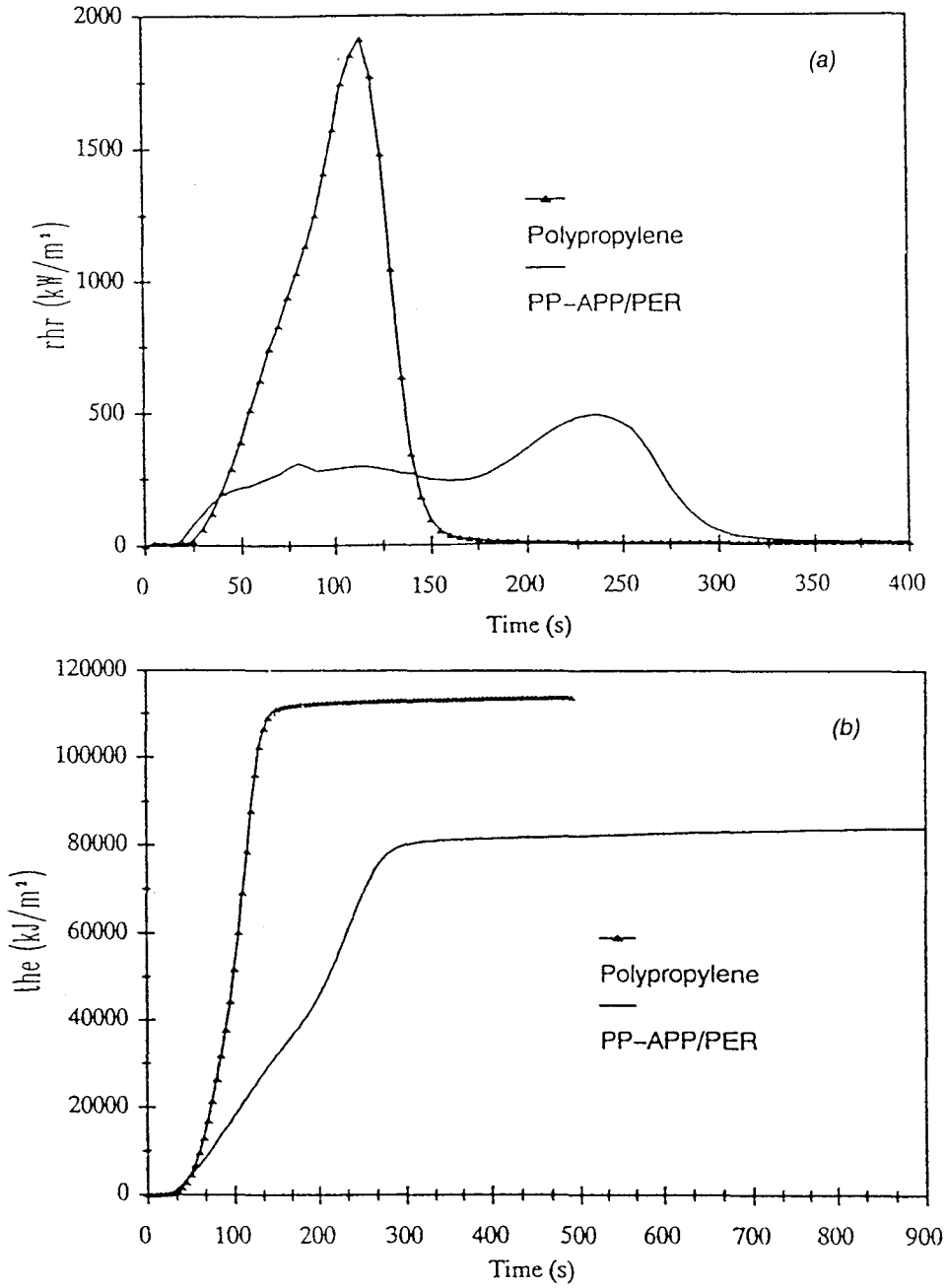

*Figure 1. rhr (a) and the (b) curve of PP and PP-APP/PER (*the $= \int_0^t$ rhr(t)dt*] under an irradiance of 50 kW/m².*

PP (t_i = 25 s). This observation agrees with previous work [6] which showed than an early decomposition of the intumescent system is necessary to increase the fire-proofing properties of the material.

The curves of rhr are directly in relation to the weight loss of the system. Indeed, superposition of the rhr curves and the weight loss rate (wlrate) curves show that the rhr maxima correspond to the maxima of the wlrates (Figure 2).

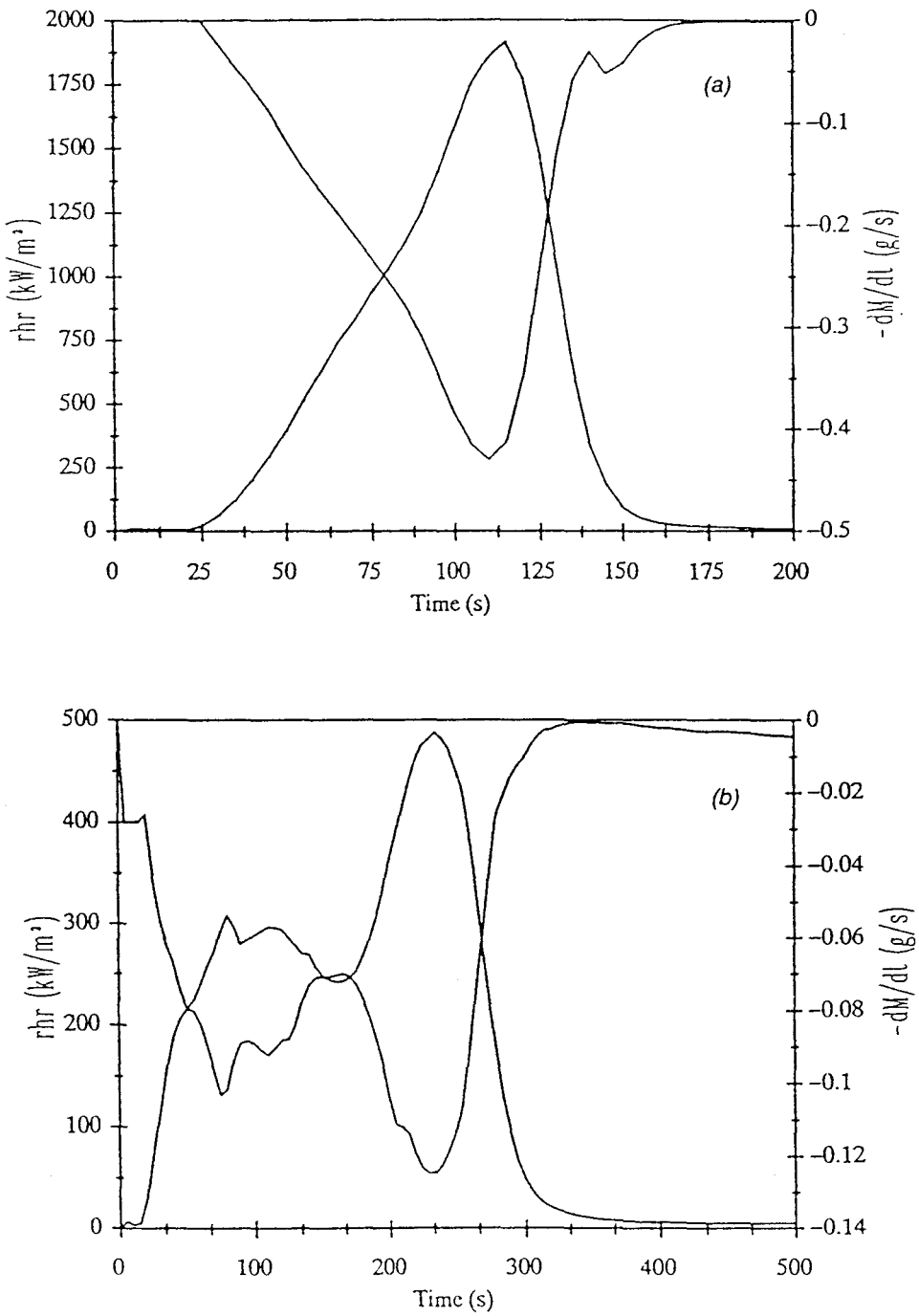

Figure 2. Curves of the rhr (a) and the wlrates (b) of PP and PP-APP/PER.

The rhr curve of the PP-APP/PER presents two broad bands (Figure 1). This behavior is generally observed with intumescent materials [11–13]. The first band may be interprated as ignition and flame propagation on the surface of the material and then, when the rhr values become constant, as protection by the intumescent coating. This time zone may be assigned to the protection of the polymer by the intumescent shield. The second peak could be explained by the destruction of the intumescent structure and the formation of a carbonaceous residue.

Weight Loss

The weight loss of a material tested with the cone calorimeter is generally not used by researchers, however it gives a lot of information about the degradation under the real conditions of inflamation and fire. Figure 3 compares the weight loss of PP and PP-APP/PER under these conditions.

After 150 s, PP degradation is achieved in an one step process. The PP-APP/PER degradation may be described by a two step process: the first step (up to 300 s) may be assigned to the formation of the intumescent shield and the degradation of PP; the second one to the degradation of the carbonaceous residue formed by reactions between the additives and the polymeric matrix or its degradation products [1]. This behavior leads us to consider that the degree of conversion α is 100% at

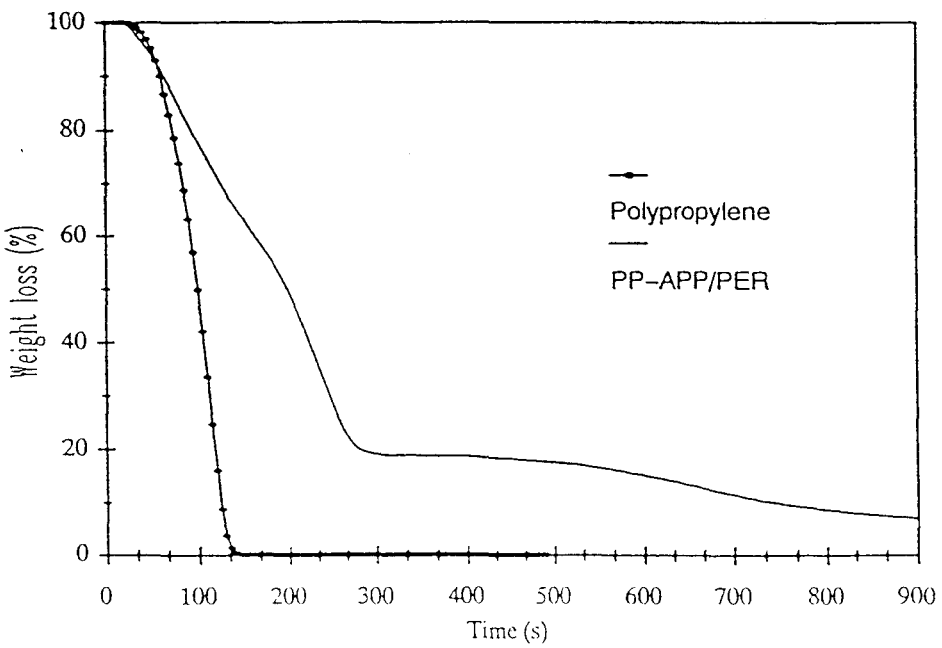

Figure 3. Curves of the weight loss of PP and PP-APP/PER under an irradiance of 50 kW/m².

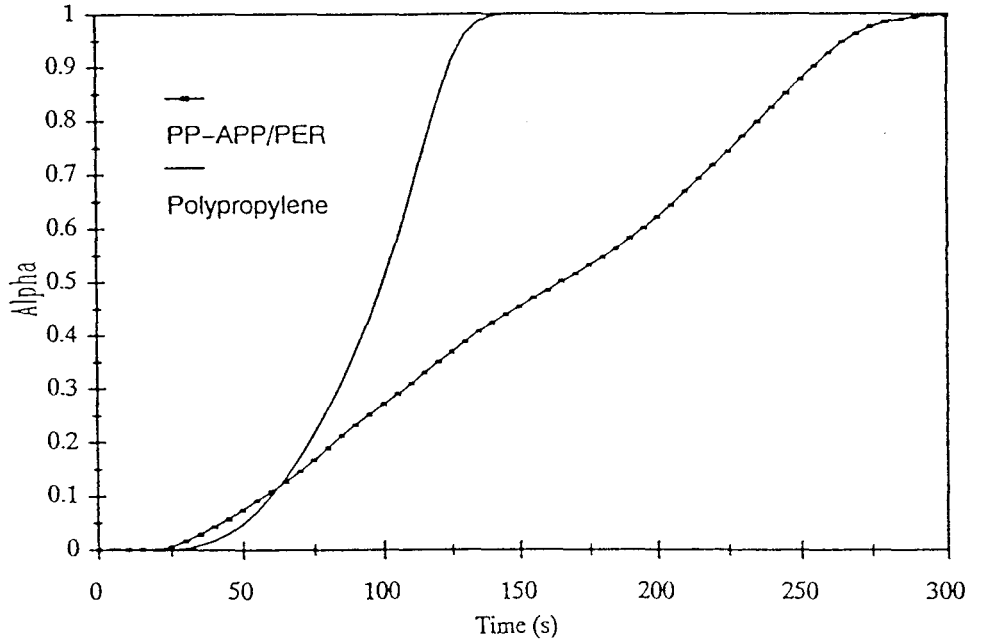

Figure 4. Curves of [α versus t] of PP and PP-APP/PER.

the end of the first step, PP being then completely degraded or chemically modified. α is defined by the relationship $\alpha = [m_i - m(t)]/(m_i - m_f)$ where m_i is the initial mass at the beginning of the degradation, m_f the mass at the end of the degradation and $m(t)$ is the mass at the time t. Figure 4 presents the curves [α versus t] then obtained.

Temperature of the Degradation Front

Intumescence Model

An intumescent formulation (polymer + additives) develops a carbonaceous shield under heat flux. The solid first begins to melt and dissipates thermal energy in the process. A state of a viscoelastic material is achieved which can trap the evolving gases. This material commences to expand and grow, i.e., to intumesce. The intumescent coating so formed no longer traps the evolving gases when the internal pressure increases and it degrades under the heat flux. The final state with PP-APP/PER consists of a carbonaceous residue consituted of polyaromatic and phosphorus oxides [3,9].

According to the work of Buckmaster et al. [14]. we may consider a one-dimensional configuration in order to define a degradation front (Figure 5). This front so defined corresponds to the place where the material degrades by evolving gases and, therefore, to the place where

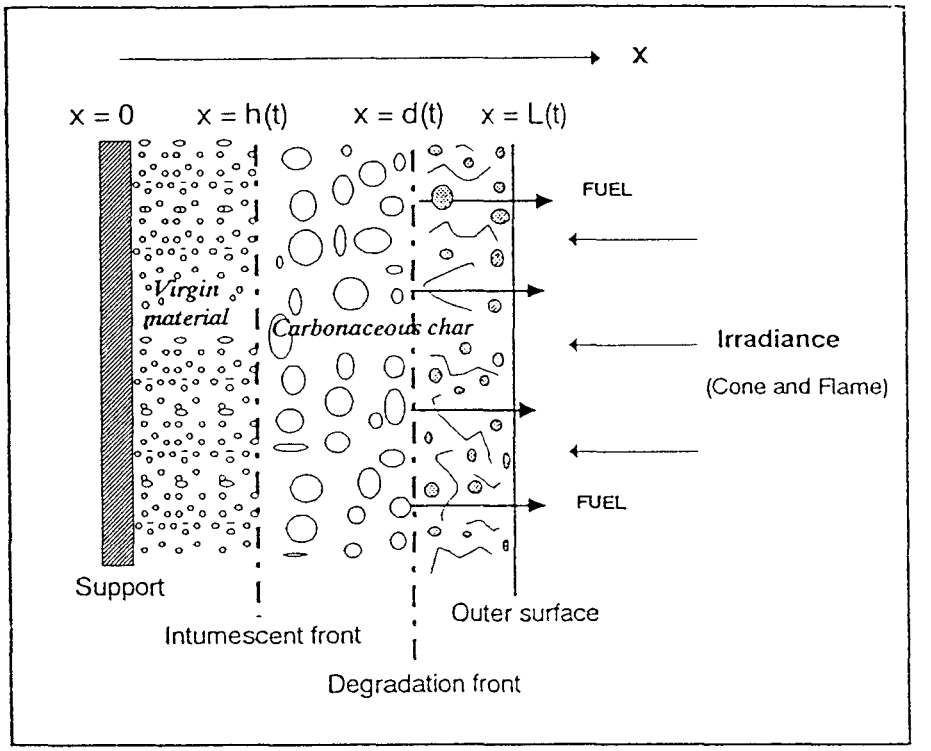

Figure 5. One dimensional intumescent model.

there is a real weight loss. It may be proposed that this front corresponds to the change of dynamic properties of the carbonaceous material. It is assumed that this change takes place over a particular temperature range. The calculation of these temperatures can be carried out using the invariant kinetic parameters (E_{inv}: invariant activation energy; A_{inv}: invariant preexponential factor) and the degradation functions [$f_i(\alpha)$].

Kinetic Consideration

The degradation modes of PP and PP-APP/PER are previously computed by thermogravimetry under air using the invariant parameters method (Appendix). The results so obtained are recalled in Tables 1 and 2.

Table 1. Invariant kinetic parameters of the PP and PP-APP/PER systems.

Systems	E_{inv} (kJ/mol)	log A_{inv} (A_{inv}:s^{-1})
PP	77 (±15)	4.2 (±0.1)
PP-APP/PER	143 (±8)	8.7 (±0.7)

Table 2. Probabilities P_j of the kinetic degradation functions of the PP and PP-APP/PER systems.

Type of the Kinetic Degradation Functions	P_j (%)	
	PP	PP-APP/PER
S1	0.0	0.0
S2	0.0	0.1
S3	0.0	4.0
S4	3.0	13.4
S5	90.0	31.7
S6	0.0	1.1
S7	0.0	13.6
S8	7.0	21.2
S9	0.0	0.0
S10	0.0	0.0
S11	0.0	0.0
S12	0.0	0.0
S13	0.0	0.0
S14	0.0	0.0
S15	0.0	3.3
S16	0.0	0.7
S17	0.0	0.2
S18	0.0	10.5

In order to compute the temperature of the degradation front T_d, we have considered the classical kinetic relationship making the hypothesis that the Arrhenius law is available:

$$\frac{d\alpha}{dt} = kf(\alpha) = A_{inv} \exp\left(-\frac{E_{inv}}{RT_d}\right) f(\alpha)$$

From the results presented above, the function $f(\alpha)$ can be written:

$$f(\alpha) = \sum_{j=1}^{j=18} P_j f_j(\alpha)$$

The temperature of the degradation front is therefore given:

$$T_d = \frac{E_{inv}}{R} \times \frac{1}{\ln\left(\frac{A_{inv} f(\alpha)}{d\alpha/dt}\right)}$$

This equation is verified for $\alpha > 0$ and for $\alpha < 1$ (If $\alpha = 0$ the degradation is not begun and if $\alpha = 1$ the degradation is finished. In these cases, $d\alpha/dt = 0$). Figure 6 compares the computed values of T_d of PP and PP-APP/PER.

The curves show that the initial temperature of degradation of PP is 100°C lower than that of PP-APP/PER. The PP-*Td* values increases sharply up to $\alpha = 0.1$ and then linearly versus α. They are lower than those of the flame retardant system up to $\alpha = 0.5$. Moreover, the PP-APP/PER-T_d values are constant between $\alpha = 0.1$ and $\alpha = 0.5$. From $\alpha = 0.5$ the T_d differences between the two systems become negligible.

Discussion

In a previous paper [1], we reported the measured temperature of PP-APP/PER under forced burning conditions using an LOI apparatus. The thermocouple placed below the initial [surface] allows measurement of the temperatures (T_s) in the intumescent shield under the conditions of a fire. These measurements are compared to the calculated T_d values in Figure 7.

The measured temperatures are in good agreement with the calculated T_d values in the sense that the two sets of temperatures are in the same range. It may be proof of the validy of our considerations. Moreover, the thermocouple is in the degradation front from $\alpha > 0.5$. It

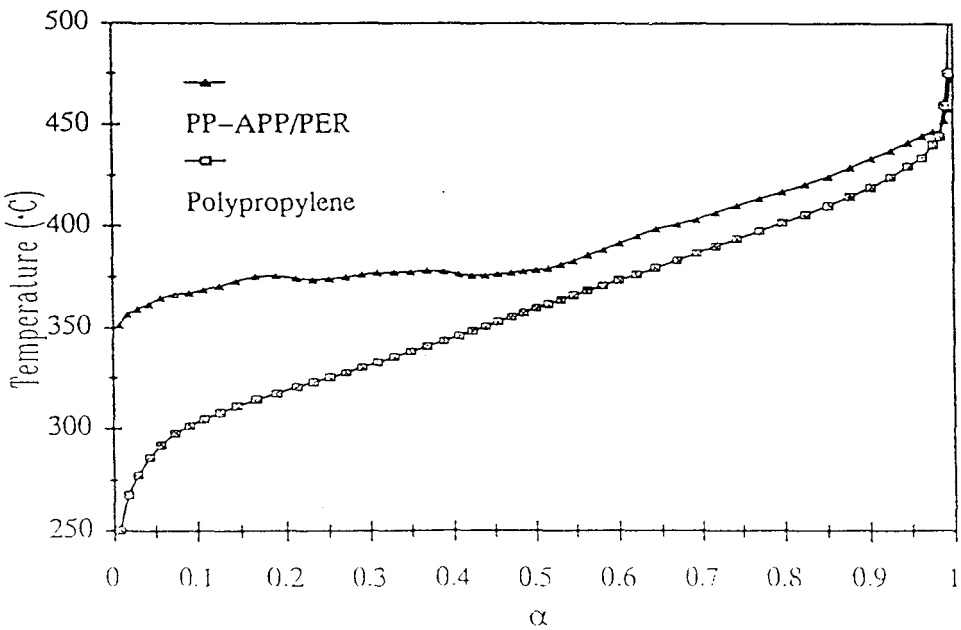

Figure 6. T_d values versus α for PP and PP-APP/PER.

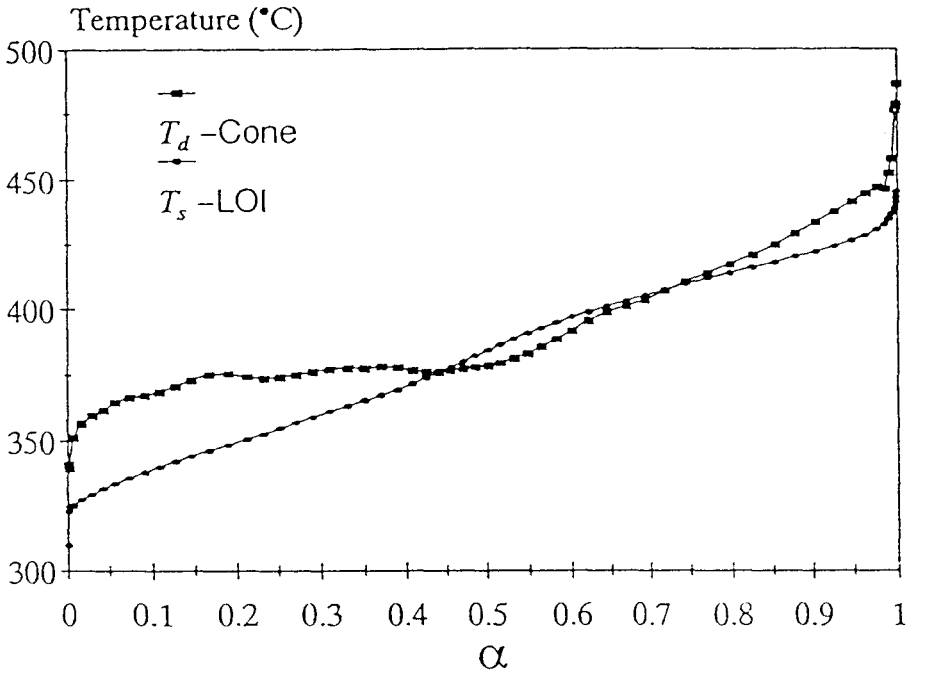

Figure 7. T_d *values and temperatures in a PP-APP/PER sheet measured under forced burning conditions versus* α.

is, therefore, verified that the polymer is protected for $\alpha < 0.5$, i.e., in the T_s temperature range 325–375°C.

The carbonization process of the flame retardant PP occurs via several steps [1]. From 190°C, there is a reaction between the additives, leading to a phosphate ester. Between 280°C and 350°C, development of intumescence occurs and between 350°C and 430°C, there is degradation of this intumescent coating. At higher temperatures, there are structural changes leading to the formation of a new carbonaceous species (established in the temperature range 430°C $< T <$ 550°C). These remarks allow us to assign the T_d values computed. These latter are in the temperature range 350–450°C, which corresponds to the degradation of the intumescent coating.

The computation of the T_d values shows that the degradation temperatures of the flame retardant PP are higher than the sole polymer in the first zone ($0 < \alpha < 0.5$). According to our previous work [1,9,11,15], it may be proposed that there is the creation of a new material which is thermally stable. This material is formed by polyaromatics which are bridged by phosphohydrocarbonated links. The polymer and/or fuel resulting from its degradation are therefore [blocked] in the coating and the fuel evolution is reduced. The sole PP degrades by chain scission which produces flammable (fuel flux) species feeding the fire. The temperature of the degradation front is, therefore, lower than that of

PP-APP/PER system because there is no possible formation of thermally stable intermediate products during the degradation process.

In the second zone ($0.5 < \alpha < 1$), the T_d values of PP and PP-APP/PER are nearly the same. It is, therefore, confirmed that the intumescent coating is no longer an effective thermal shield to protect the polymeric matrix. There is no longer the renewal of intumescent material and, therefore, the coating degrades by forming a residue. This residue is formed by stacks of very condensed polyaromatics making an anisotropic structure and containing phosphorus oxides. It has been previously reported that in this temperature range, acidic phosphate species do not exist. These species are responsible for the participation of the polymer to its protection. The present study suggests that the insulating properties of the coating may be related to the [trapping] of the PP chain by the phosphocarbonaceous material.

It seems interesting to compare the rhr curves and the T_d values against α (Figures 8, 9). In the case of the sole polymer, the temperature of the degradation front increases when the rhr increases. At the beginning, the temperature and the rhr increase strongly, corresponding to the inflammation of the material; the front of degradation is so defined. Then the T_d and rhr values increase linearly up to 450°C and 2000 kW/m², respectively. At $\alpha = 1$, there is no longer PP, therefore the rhr value becomes null and T_d is no longer defined.

In the case of the flame retardant PP, the rhr increases strongly for $0 < \alpha < 0.3$ due to the inflammation of the material, whereas the front of degradation reaches a constant temperature of 375°C almost

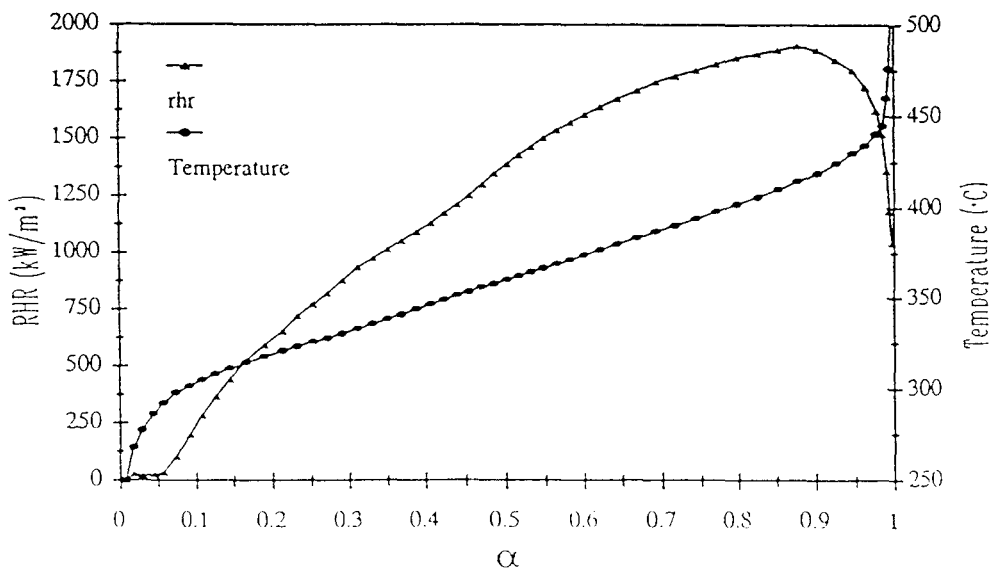

Figure 8. rhr and T_d values versus α of PP.

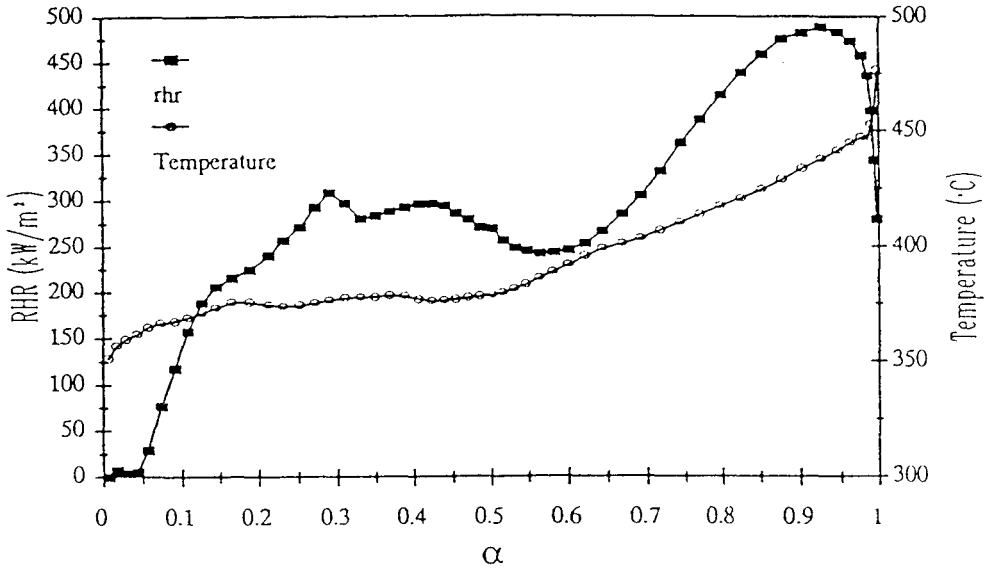

Figure 9. rhr and T_d values versus α of PP-APP/PER.

immediately. This temperature remains constant up to $\alpha = 0.5$ because the intumescent front is regenerated. The rhr reaches a stage for $0.3 < \alpha < 0.5$ indicating an equilibrium between the regeneration and the degradation of the protective shield. For $\alpha > 0.5$, T_d increases, implying a strong increase of the rhr values. The protective material is no longer regenerated and it degrades. Nevertheless, the rhr increases up to 500 kW/m², whereas that of PP increases five times greater. This signifies that the residue formed by the degradation of the intumescent coating limits the heat flux evolved and so participates in the protection of the material via an insulative action.

CONCLUSION AND SUMMARY

In this work, we have studied the fire degradation of the PP-APP/PER system using the cone calorimeter. The definition of a degradation front has allowed study of the thermal property of the intumescent coating. The measurements of the temperature of this degradation front show that the intumescent shield is only efficient in a region of degree of conversion ($0 < \alpha < 0.5$). Then ($\alpha > 0.5$) it is the formation of a carbonaceous char which reduces the heat flux involved. It implies, therefore in this case, that the char presents an effective insulative character.

From kinetic considerations using the invariant kinetic parameters method, we have proposed an original method to compute T_d. This method is in good agreement with the experimental results and with

the previous chemical considerations deduced from spectroscopic analyses. It may be a new tool to understand the thermal behavior of a material in the conditions of a fire.

REFERENCES

1. Delobel, R., M. Le Bras, N. Ouassou and F. Alistiqsa. 1990. "Thermal Behaviors of Ammonium Polyphosphate-Pentaerythritol Intumescent Additives in Polypropylene Formulations," *J. Fire Sc.,* 8(2):85.
2. "Standard Test Method for Measuring the Minimum Oxygen Concentration to Support Candle-Like Combustion of Plastics (Oxygen Index) ASTM D2863/77, American Society for Testing and Materials, Philadelphia," *Tests for Flammability of Plastic Materials for Part in Devices and Appliances (UL-94).* Underwriters Laboratories, Northbrook.
3. Bourbigot, S., M. Le Bras and R. Delobel. 1993. "Carbonization Mechanisms Resulting from Intumescence. Association with the Ammonium Polyphosphate-Penaerythritol Fire Retardant System," *Carbon,* 31(8):1219.
4. Babraukas, V. 1984. "Development of the Cone Calorimenter–A Bench Scale Heat Release Apparatus Based on Oxygen Consumption," *Fire and Materials,* 8(2):81.
5. Babraukas, V., J. R. Lawson, W. D. Walton and W. H. Twilley. 1982. "Upholstered Furniture Heat Release Rates Measured with a Furniture Calorimeter," *NBS-IR,* 82:2604.
6. Bourbigot, S., R. Delobel, M. Le Bras and Y. Schmidt. 1992. "Relation Between Limiting Oxygene Index and Invariant Activation Energy. Application to the Polypropylene–Ammonium Polyphosphate–Pentaerythritol System, *J. Chim. Phys.,* 89:1835.
7. Delobel, R., S. Bourbigot, M. Le Bras, Y. Schmidt and J. M. Leroy. 1993. "Invariant Values of Kinetic Parameters. Evaluation of Fire Retardancy. Application to the Polypropylene–Ammonium Polyphosphate–Pentaerythritol System," *Makromol. Chem., Macromol Symp.,* 74:59.
8. Bourbigot, S., R. Delobel, M. Le Bras and D. Normand. 1993. "Comparative Study of the Integral TG Methods Used in the Invariant Kinetic Parameters Method. Application to the Fire-Retardant Polyproylene, *J. Chim Phys.,* 90:1909
9. Alistiqsa, F. 1993. "Mise au Point de Nouvelles Formulations Intumescentes Polyphosphate d'Ammonium-Pentaérythritol. Application à l'Lgnifugation du Polypropylène", *Doctoral dissertation,* University of Lille, France.
10. Grayson, S. J. 1992. *Heat Release in Fire,* V. Babraukas and S. J. Grayson, ed., London: Elsevier Applied Science, pp. 1–5.
11. Bourbigot, S. 1993. " Nouveaux Agents de Synergie dans les Systèmes Intumescents. Comprhension des Mecanismes de Protection du Polyéthylène et de ses Copolymères," *Doctoral dissertation,* University of Lille, France.

12. Marshal, A., R. Delobel, M. Le Bras and J. M. Leroy. 1993. "Intumescence and Polymer Degradation," *Gordon Research Conf., "Analytical Pyrolysis and Oxidative Degradation of Materials,"* Polymouth (USA).
13. Marshal, A., R. Delobel, M. Le Bras, J. M. Leroy and D. Price. 1994. "Effect of Intumescence on Polymer Degradation," *Polym. Deg. & Stab.* 44:263.
14. Buckmaster, J., C. Anderson and A. Nachman. 1986. "A Model for Intumescent Paints," *Int. J. Engng. Sci.*, 24(3):263.
15. Bourbigot, S., M. Le Bras, R. Delobel, P. Bréant amd J. M. Trémillon. 1994. "Carbonization Mechanisms Resulting from Intumescence–Part II. Association with an Ethylene Terpolymer and the Ammonium Polyphosphate-Pentaerythritol Fire Retardant System, *Carbon,* paper no. 334, in press.

II-3-b Discussion synthétique

L'étude de la formulation EVA/APP/PER confirme les processus chimiques mis en jeu lors du développement du matériau intumescent. Elle montre que la teneur en radicaux libres piégés dans le matériau carboné est élevée (nsp $\geq 10^{20}$ spins/kg lorsque HTT $\geq$ 280°C). De telles teneurs sont toujours observées avec les formulations intumescentes [39, 104, 109, 130] et ont permis de proposer que la formation de la structure polyaromatique et sa dégradation impliquent un mécanisme radicalaire [33]. Cette discussion sera présentée dans le Chapitre III.

L'étude permet de préciser les profils de la température dans un matériau intumescent lors de son auto-combustion (proposés par Morice et al. [51]). La température du palier intermédiaire, à environ 350°C, correspond à la formation optimale du matériau expansé lors du traitement thermique de APP/PER. Cette observation confirme notre hypothèse préalable : le matériau issu des adjuvants seuls est, en fait, le matériau dont le rôle est primordial dans la protection.

Par ailleurs, l'étude des flux de chaleur dégagés lors de l'inflammation montre que l'inflammation de la formulation intumescente est plus rapide que celle du polymère seul ($t_{iEVA/APP/PER}$ = 30s et t_{iEVA} = 60s sous une irradiance de 50 kW/m^2). Ce résultat est universel pour ce type de formulations. Le mécanisme de formation des espèces polyaromatiques à partir du mélange des adjuvants est une réaction radicalaire. Les radicaux libres, présents dans la formulation à une température (280°C avec APP/PER) où le polymère seul ne se dégrade pas, sont des initiateurs

de la réaction de dégradation de la matrice polymère, où des scissions de chaînes conduisent à la libération de produits gazeux combustibles. La protection par intumescence est d'autant plus importante que le matériau isolant se forme à basse température. Il en résulte un paradoxe : **« la formulation est d'autant plus protégé que sa dégradation est aisée »**. Ce mode de protection est caractéristique d'un matériau ablatif qui « se sacrifie en partie » pour se protéger globalement.

Ce résultat pose un problème pour le classement des matériaux intumescents utilisés dans la construction et l'ameublement. En effet, le test français standard [131] considère « l'indice d'inflammation » i :

$$i = 1000/15\ t_1 + 1000/15\ t_2$$

(t_1 : temps d'inflammation de la surface supérieure, t_2 : temps d'inflammation de la surface au contact du support incliné (45°) soumis au flux de chaleur (30 kW/m^2))
qui pénalise les matériaux ablatifs et en particulier les intumescents.

Les études cinétiques de la dégradation de différents systèmes PP/APP/PER utilisant la méthode IKP vérifie l'invariance des paramètres calculés et que leurs valeurs ne dépendent pas de la méthode du calcul (Osawa, Osawa complété par l'algorithme de Flynn ou Coats et Redfern [132-134]). Les valeurs du facteur pré-exponentiel A et de l'énergie d'activation augmentent avec la teneur en adjuvant. L'examen des valeurs des constantes de vitesse en fonction de la température et de cette teneur confirme le caractère ablatif des systèmes intumescents : la vitesse de la dégradation thermo-oxydante de ces systèmes devient supérieure à celle de PP à une température d'autant plus basse que le taux de charge en adjuvants et, en conséquence, la propriété FR sont élevés.

L'étude propose une relation linéaire entre les valeurs des énergies d'activation et les valeurs du LOI. En illustration, la Figure II-12 montre que la relation linéaire est retrouvée avec différentes formulations du LRAM3,5. La pente des droites semble être une constante propre au polymère et indépendante du système d'adjuvants. Ce dernier résultat devra être vérifié avant d'affirmer que les valeurs des énergies permettent le classement comparatif des formulations intumescentes FR.

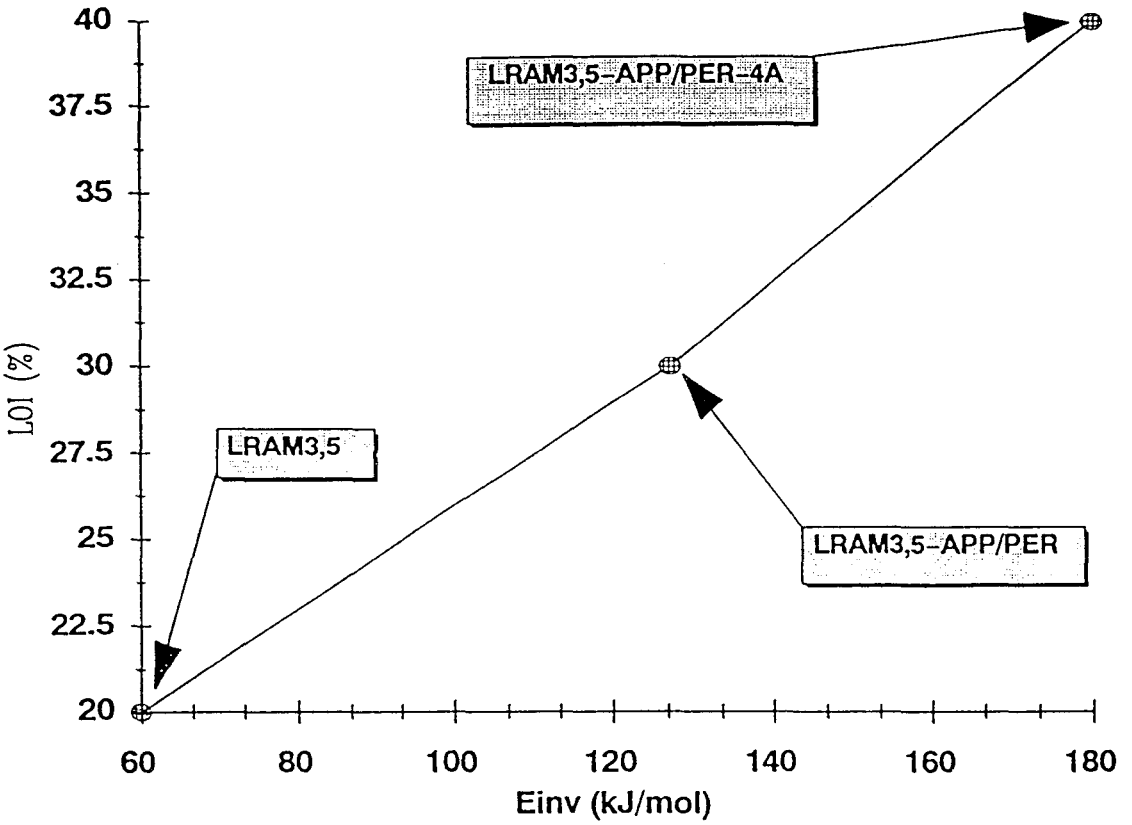

Figure II-12. Evolution comparée des valeurs des LOI et des énergies d'activation invariantes des dégradations thermo-oxydantes pour trois formulations du LRAM3,5.

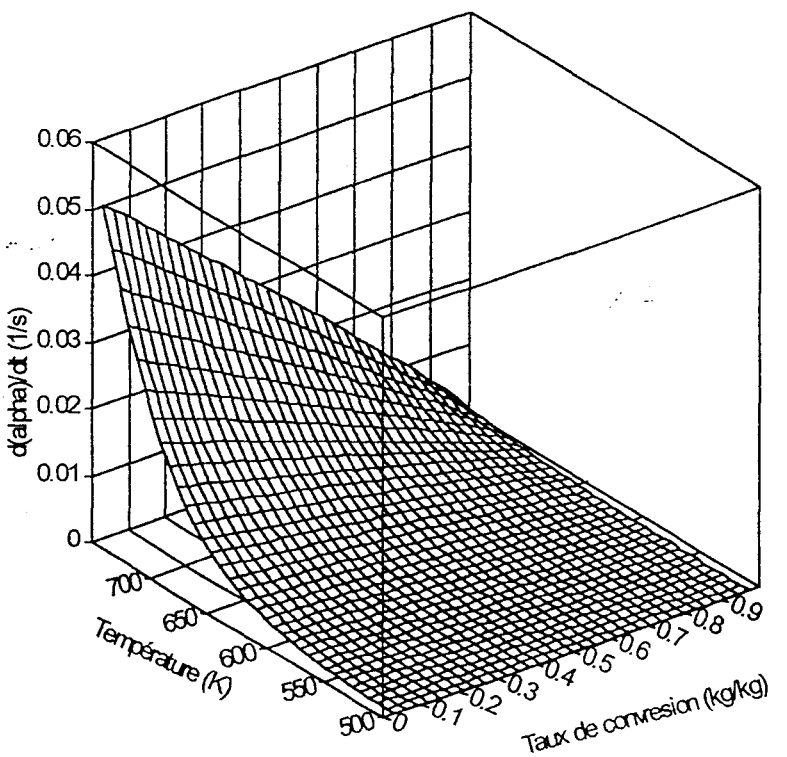

Figure II-13. Vitesse de la dégradation du PP sous air fonction de l'avancement de la réaction et de la température.

La dégradation thermique des polyoléfines est généralement décrite par un modèle cinétique d'ordre 1 [135] :

$$d\alpha/dt = A\, e^{-E/RT}(1-\alpha)$$

(α : taux de conversion pondéral)

Ce modèle ne s'applique pas à la dégradation du PP qui est principalement décrite par une loi de nucléation et de croissance de type Avrami-Arofeev. Cette dernière loi est, en fait, un cas particulier car son équation se résout comme une fonction à ordre de réaction. La figure II-13 présente les valeurs de la vitesse de dégradation qui admettent en isotherme une relation classique quasi linéaire avec (1 - α).

La répartition des fonctions de dégradation de PP/APP/PER dépend de la méthode du calcul. La méthode de Coats and Redfern est celle qui permet la meilleure approche du phénomène chimique global. Mais, dans ce cas, la répartition calculée ne permet pas une discussion des modes de dégradation. La représentation tridimensionnelle de la vitesse de la dégradation du système intumescent sous air (Figure II-14) révèle que dans le domaine de température 280-530°C, deux comportements existent en fonction du taux de conversion de la matrice PP :

- lorsque $0 < \alpha < 0.15$, la vitesse croît lorsque le taux de conversion augmente. Le comportement du type modèle potentiel peut s'expliquer par une réaction radicalaire en branches,
- pour des degrés de conversion $0,15 < \alpha < 1$, la vitesse en isotherme diminue avec l'avancement de la réaction,

Ces deux composantes peuvent être expliquées par la chimie du système. Le premier stade correspond à la formation du matériau protecteur par le processus ablatif. Les esters des acides phosphoriques se dégradent en espèces aromatiques et polyaromatiques, via une séquence réactions du type Diels-Alder puis via un mécanisme radicalaire de carbonisation. Lors de cette étape, la présence de radicaux libres dans le matériau favorise la dégradation du polymère par un mécanisme en chaînes radicalaires.

La deuxième étape est expliquée par la formation du matériau expansé protecteur cohérent. Les produits de la réaction résultent de la dégradation du polymère et de la dégradation du matériau carboné intumescent qui se régénère à

partir du matériau « protégé » inférieur. La vitesse de la dégradation est alors limitée par la diffusion des produits de la dégradation thermique des esters et du PP dans le revêtement superficiel et leurs réactions avec les constituants de ce revêtement.

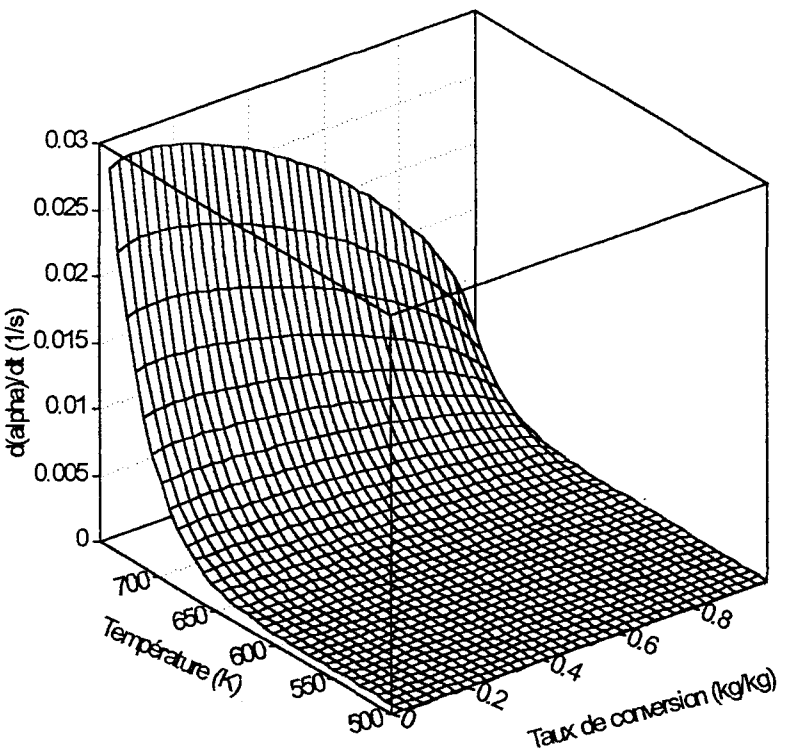

Figure II-14. Vitesse de la dégradation de la formulation PP/APP/PER sous air, fonction de l'avancement de la réaction et de la température.

Une comparaison des vitesses des dégradations de PP et de PP/APP/PER (Figure II-15), dans la gamme de températures ($295 < T < 355°C$) où la dégradation de PP se produit, montre que l'adjuvant augmente la stabilité thermique de la formulation. En effet, la vitesse de la dégradation thermo-oxydante de PP/APP/PER est toujours inférieure d'un ordre de magnitude à celle du PP seul.

La comparaison des courbes des rhr de PP et de la formulation intumescente montre que le comportement de cette dernière n'est pas celui d'un retardateur de flamme. En effet, le temps nécessaire à l'ignition du matériau intumescent est inférieur à celui du PP seul. Cette différence résulte des processus chimiques de l'ablation. **Attribuer un caractère retardateur de flamme à une formulation intumescente résulte donc d'un emploi abusif du qualitatif**. Les performances du matériau lors des classements par les tests classiques (LOI > 30 % volumique,

V0 (UL-94), M2 (AFNOR P 92-501), maxima du rhr < 500 kW/m^2) expliquent son utilisation. Cependant, l'étude comparative des t.h.e. montre que le qualificatif « **limiteur de flamme** » est plus approprié.

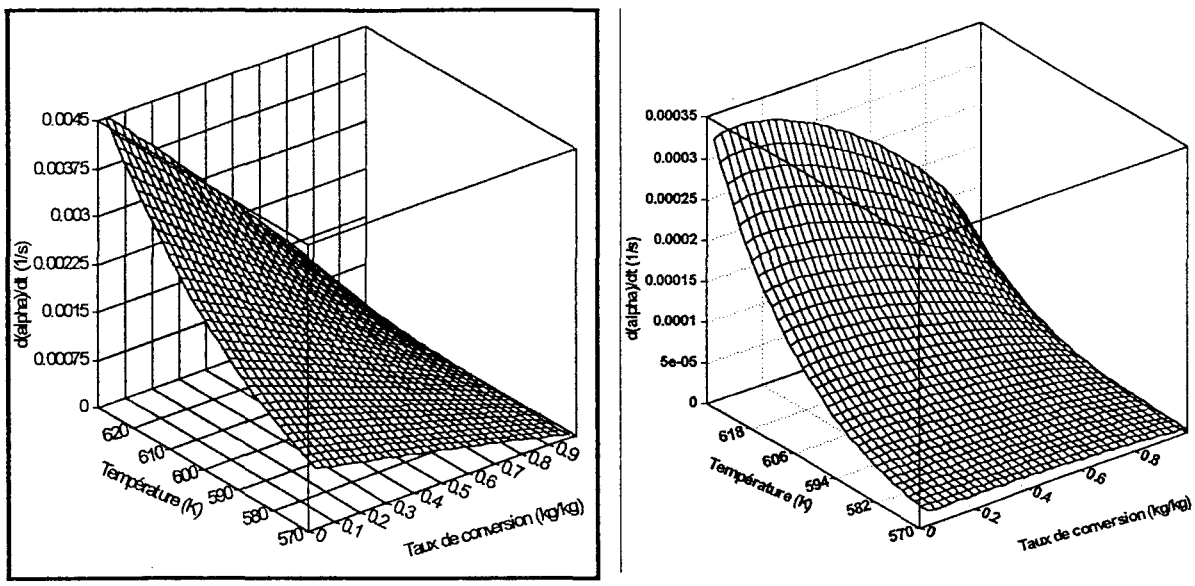

(a) (b)

Figure II-15. Comparaison des vitesses de dégradation de PP (a) et de PP/APP/PER (b) sous air dans le domaine de température où se produit la dégradation du PP dans les conditions opératoires de l'analyse thermogravimétrique.

Le PP présente un seul pic du rhr qui est relié à la vitesse de perte de masse du système. Le maximum de perte de masse observé à environ 120 s correspond à un taux de conversion de l'ordre de 90%. L'augmentation quasi constante de la vitesse de dégradation avec l'avancement de la réaction s'explique par l'augmentation de la température (calculée : de 290 à environ 400°C).

La présence des 2 maximums de la courbe de rhr de PP/APP/PER est expliquée par les deux maximums de la vitesse apparente de la dégradation. Le premier maximum correspond au processus ablatif qui permet le développement du matériau protecteur expansé. Lorsque ce revêtement est cohérent, la température du front de dégradation oscille autour d'une valeur moyenne : 375°C, qui permet la dégradation du matériau intumescent. Le matériau dégradé (amas de polyaromatiques supportant des espèces phosphates acides) est ensuite capable de se régénérer via la décomposition des esters des acides phosphoriques présents

dans le matériau résiduel « protégé » et/ou la fixation de chaînes polymères crées par la dégradation du PP. L'équilibre entre la dégradation et la reconstruction du matériau explique la valeur de la température constante. L'équation de la vitesse de dégradation implique que, lorsque α croît en isotherme, la vitesse de la dégradation et, en conséquence, le flux de gaz combustibles diminuent. Cette diminution explique alors celle de la consommation d'oxygène.

Lorsque la teneur en matériau susceptible de participer à la reconstruction du bouclier protecteur est faible, la troisième étape de la dégradation thermo-oxydante de PP/APP/PER (accélération du processus) est observée. Elle conduit à la dégradation du matériau intumescent lorsque la température devient supérieure à 430°C et à l'augmentation du flux de combustibles vers la flamme à laquelle correspondent les valeurs maximales du rhr.

Après l'extinction de la flamme, le rhr n'est jamais nul ; la consommation d'oxygène s'explique alors par le processus de post-incandescence. Ce processus est responsable des valeurs élevées de la température du front de dégradation lorsque α est supérieur à 98 % pondéral.

Pour conclure, l'utilisation des données TG, collectées conjointement par une ATG classique et dans les conditions d'un feu permet d'expliquer le comportement souvent complexe d'un matériau lors de son inflammation. Cette explication ne peut néanmoins être proposée qu'à la condition que la chimie du système soit connue. L'étude devra être complétée par les analyses qualitative et quantitative des produits de dégradation de PP et de PP/APP/PER qui doivent permettre de préciser les variations de la consommation d'oxygène en considérant les sélectivités relatives pour les différentes réactions d'oxydation (formation de CO, de CO_2, de cétones, d'aromatiques et des espèces polyaromatiques constituant les fumées ou les suies) qui se produisent lors de l'inflammation du matériau intumescent.

En conclusion, l'étude des systèmes intumescents modèles PP/APP/PER et LRAM3,5/APP/PER permet la compréhension du comportement chimique à la chaleur et au feu de matériaux polymères « retardateurs de flamme » (plus précisément « limiteurs de flamme ») par un processus ablatif de carbonisation.

L'étude spectroscopique montre que le matériau protecteur formé par réaction des adjuvants, dans les conditions d'un traitement thermo-oxydant ou d'un feu, est une structure carbonée polyaromatique. partiellement organisée qui « supporte » des espèces orthophosphates ou pyrophosphates acides. Ces espèces acides jouent le rôle de catalyseurs (elles sont retrouvées inchangées en fin des traitements) pour la formation des espèces polyaromatiques et la fixation de chaînes aliphatiques dans le matériau. Un résultat original est la mise en évidence la présence de l'hétéroatome N dans des groupements pyroles ou amides du matériau carboné.

La perte de la propriété protectrice est liée à la consommation des espèces acides. La matrice polymère permet la conservation de ces espèces à des températures supérieures à la température où se produit la dégradation du matériau intumescent.

Il est proposé que l'intumescence (« encapsulation » des produits gazeux de la réaction entre adjuvants et de la dégradation du polymère) est possible pour des propriétés dynamiques du matériau phosphocarboné particulière. Ces propriétés sont assurées par l'existence de pontages (chaînes phosphates et/ou chaînes aliphatiques) entre amas polyaromatiques.

L'étude illustre l'intérêt de la mesure des paramètres cinétiques invariants et de la répartition probable des fonctions de dégradation. Ces données permettent de discriminer les étapes de la dégradation des formulations intumescentes et de mettre en évidence le processus ablatif qui permet la formation du matériau protecteur. Il est proposé, par ailleurs, que les valeurs de l'énergie d'activation

invariante de la dégradation thermo-oxydante des formulations intumescentes d'un polymère conditionnent celles de l'indice limite d'oxygène de la formulation.

Finalement, le modèle du front de dégradation appliqué aux matériaux intumescents permet d'expliquer la consommation d'oxygène lors de l'inflammation. Il est montré que la protection du matériau est assuré par un revêtement dont la permanence est assurée par l'équilibre entre sa destruction thermique et sa formation via l'ablation du matériau « protégé » à une température constante.

Bibliographie

1- Fowell A.J., « *American Society for Testing and Materials - Fire and Flammability of Furnishings and Contents of Buildings* », ASTM STP 1233, Miami (USA) (Décembre 1992).

2 Gann R.G., « *Flame Retardants* » dans « *Kirk-Othmer Encyclopédia of Chemical Technology* » (4^{éme} édition), volume 10, John Wiley and Sons, New-York (1994) pp. 930-936.

3- Raufaste N.J., « *NIST Building and Fire Research Laboratory Projects Summaries, 1994* », NIST SP 838-5, Gaithersburg (USA) (,juin 1994).

4- Gay Lussac J.L., Annales. Chim., **18(2)** (1821) 211.

5- Rather L.O. et Russell C.K., « *The Market for Flame Retardants in the US - A Current Analysis* » dans « *Handbook of Flame Retardant Chemicals and Fire Testing Services* », Technomic Pub. Co., Lancaster (USA) (1988) pp.1-6.

6- « *Indices et Cotations* », l'Usine Nouvelle **2541** (1996) pp. 157-162.

7- Alakin M., Horrocks A.R. et Price D., J. Fire Sci, **6** (1988) 333.

8- Jin T. et Yamada T., J. Fire Sci., **8** (1990) 124.

9- Harland W.A. et Woolley W.D., « *Fire Fatality Study* » dans « *Building Research Establishment Information Paper* » **IP 18/79**, University of Glasgow (UK) (1979) ;
Woolley W.D., J. Macromol. Sci. A (Chemistry) **17(1)** (1982) 1.

10- Pal G. et Macskasy H., « *Studies in Polymer Science 6 - Plastics, their Behaviour in Fires* », Elsevier Sci. Pub. Co, New-York (USA) (1991) pp. 304-332 ;

11- Hommel G., « *Handbuch der Gefärlichen Güter* », Springer Verlag, Berlin (Allemagne) Volume I (1978), Volume II (1980), Volume III (1985).

12- Hilado C.J., « *Flammability Handbook for Plastics* », Technomic Pub. Co, Westport (USA) (1974).

13- Camino G., « *Combustion and Fire Retardants* » dans le recueil des Cours de « *The Postdoctoral Course on Degradation and Stabilisation of Polymeric Materials* », Clermont-Ferrand (24-28 octobre 1994), CNEP et ENSCCF, Clermont - Ferrand (1994)

14- 5th Draft Status Report « *OCDE Worhshop on the Risk Reduction of Brominated Flame Retardant* », Neufchâtel (Suisse) (26 mai 1992, 22-25 février 1993), OECD - Direction de l'Environnement (Avril 1993).

15- Preliminary 1st Draft report « *International Programme on Chemical Safety - Environmental Health Criteria for Brominated Diphenylethers* » (janvier 1993), 1st Draft report « *International Programme on Chemical Safety - Environmental Health Criteria for Tris(2,3-dibromopropyl) phosphate and Bis(2,3-dibromopropyl) phosphate* » (Janvier 1993), United Nations Environmental Programme, PCS/EHC/92.45, Rapports non édités.

16- van Krevelen D.W., Polymer, **16** (1975) 615-620;
Johnson P.R., J. Appl. Polym. Sci. **18** (1974) 491;
Kourtides D.A., Polym. Plast. Technol. Eng. 11 (1978) 159.

17- « *Standard Test Method for Measuring the Minimum Oxygen Concentration to Support Candle - like Combustion of Plastics* », ASTM D2863/77, Philadelphia (USA) (1977)

18- Nyden M.R. et Brown J.E., Actes du « *Safety 12th Joint Panel Meeting* », Tsukuba (Japon) (27 octobre-2 novembre 1992), Building Research Institute, Ibaraki (Japon) (1994) pp. 257-266 ;

19- Rose N., Costes B., Le Bras M. et Delobel R., Actes du Colloque « *Polymérisations: Mécanismes, Méthodes, Procédés* », Bordeaux (18-19-20 novembre 1991),.GFP (1991) *CA 27, p 73-74.*

20- Bente, M.P., « *Réactivité à l'état fondu des systèmes époxy-cyanamide - dicyanamide-mélamine.* », Thèse, Pau (1993).

21- Costes, B., « *Etude structurale du réticulat tétraglycidyle diaminodiphényle méthane - diaminodiphényle sulfone.* », Thèse, Le Mans (1989).

22- Bourbigot S., Le Bras M., Delobel R. et Normand D., J. Chim. Phys.,**90** (1993) 1909.

23- Bourbigot S., *« Nouveaux agents de synergie dans les systèmes intumescents. Compréhension des mécanismes de protection du polyéthylène et de ses copolymères. »*, Thèse, Lille (1993).

24- Butler K.M., Baum H.R. et Kashiwagi T., *« Three-dimensional Kinetic model for the swelling of intumescent materials »* dans *« Book of Abstracts - Annual Conference on Fire Research »*, NIST, Gaithersburg (USA) (1994) pp. 109-110.

25- Kroenke W.J., J. Mater. Sci., **21** (1986) 1123-1173.

26- Levchik G.F., Levchik S.V., Sachok P.D., Selevich A.S., Lyakhov A.S. et Lesnikovich A.I., Thermochim. Acta, **257** (1995) 117-125.

27- Levchik G.F., Levchik S.V., Camino G., Costa L. et Lesnikovich A.I., Fire & Materials, **20(4)** (1996) 183-190.

28- Camino G., Costa L. et Trossarelli L., Polym. Deg. & Stab. **7** (1984) 25.

29- Olsen J.W. et Bechle C. W., Brevet US 2,442,706 (Anaconda Wire & Cable) (1948).

30- Tramm H.L., Brevet US, 2,106,938 (Ruhrchemie Aktiengesellschaft) (1938).

31- Murray T.M., Liberti F. et Allen A.O., dans *« Advances in Chemistry (*Volume 9) »*, ACS (1953).

32- Vandersall H.L., J. Fire & Flammability **2** (1971) 97.

33- Le Bras M., Bourbigot S., Delporte C., Siat C. et Le Tallec Y., Fire & Materials **20(4)** (1996) 191-203.

34- Lauring E.A., Brevet US 2,594,937 ((Minnesota and Ontario Paper Company) (1952).

35- Jones G., Brevet US 2,628,946 (Albi Manufacturing Company) (1953).

36- Le Bras M., Bourbigot S., Le Tallec Y. et Laureyns J., Polym. Deg. & Stab. (1996) soumis pour publication.

37- Kishore K. et Mohandas K., Combustion & Flame **43** (1981) 145-153.

38- Camino, G., dans les Actes du *« Premier Colloque Francophone sur l'Ignifugation des Polymères »*, ed. Martel, J., Saint Denis (France) (1985) pp. 36.

39- Schmidt - Le Tallec, Y., « *Valorisation de Différents Polyols dans des Systèmes Retardants de Flamme : Application au Polyéthylène* », Thèse, Lille (1992).

40- Camino G., Costa L. et Martinasso, Polym. Deg. & Stab. **23** (1989) 359.

41- Zhu X., J. Fire Sci. (1996) soumis pour publication.

42- Le Bras M., Hermant M. et Leroy J.M., *« Recherche d'additifs du polypropylène apte au filage propre à conférer à ce polymère les propriétés d'ignifugation grâce à un phénomène d'intumescence »,* Rapport de fin d'étude pour la Société SOMMER S.A. (1993).

43- Bourbigot S. et Le Bras M., *« Développement de formulations intumescentes pour polyoléfines »,* Rapport de fin d'étude pour la Société TARAFLEX (1996).

44- Bourbigot S. et Le Bras M., « *Formulations du polypropylène retardateur de flamme apte au thermo-soudage* », Rapport de fin d'étude pour la C.E.A.C. (1996).

45- Le Bras M. et Leroy J.M., *« Optimisation de formulations du polypropylène aptes au filage et propres à conférer à ce polymère la propriété retard au feu grâce à un phénomène d'intumescence »,* Enveloppe Soleau n° 67043 (04 juin 1992), titulaire SOMMER SA.

46- Bourbigot S., Bréant P., Delobel R. et Le Bras M., *« Compositions ignifugeantes pour résines synthétiques contenant une zéolithe et résines synthétiques renfermant les dites compositions »,* Brevet français n° 93.07387 (18 juin 1993), Brevet européen n° 629677 A1 (21 décembre 1994), titulaire Elf-Atochem.

47- Bourbigot S. et Le Bras M., *« Association des polyamides et des phosphates d'ammonium dans des formulations ignifugeantes et des mélanges maîtres, additifs retardeurs de flamme utilisables dans des polymères et co-polymères de l'éthylène, du propylène et du styrène et dans des mélanges contenant les dits polymères »,*.Enveloppe Soleau n° 36972 (17 juillet 1995).

48- Le Bras M. et Bourbigot S., *« Formulations ignifugeantes et mélanges maîtres, additifs retardeurs de flamme utilisables dans des polymères et co-polymères de l'éthylène, du propylène et du styrène et dans des mélanges contenant lesdits polymères »,* Enveloppe Soleau n° 59305 (30 mai 1996).

49- Le Bras M. et Bourbigot S., Fire & Materials **20** (1996) 39-49.

50- Halpern Y., Mott D.M. et Niswander R.H., Ind Eng. Chem. Res. Dev. **23** (1984) 233.

51- Morice L., « *Etude et Modélisation des Transferts Thermiques dans un Bouclier Intumescent - Application au Polypropylène " Retard au Feu "* » Rapport du Diplôme d'Etudes Approfondies « Génie des Procédés », Compiègne (septembre 1996).

52- Beyler C., « *Thermal Decomposition of Polymers* » dans « *SFPE Handbook of Fire Protection* (Chapitre 1-12) », DiNenno P.J. ed., National Fire Protection Association pub., Quincy (USA) (Octobre 1992), pp. 165-178.

53- Fenimore C.P. et Jones G.W., Combustion & Flame **10** (1966) 295-301.

54- Lewis I.C. et Greinke R.A., J. Polym. Sci. **20** (1982) 1119-1132.

55- Lesnikovich A.I. et Levchik S.V, J. Thermal Anal. **27** (1983) 89.

56- Lesnikovich A.I., Levchik S.V. et Guslev V.G., Thermochimica Acta **77** (1984) 357.

57- Babrauskas V., Fire & Materials **13(1-2)** (1984) 3.

58- Babrauskas V., Lawson J.R., Walton W.D. et Twilley W.H., « *Unfoldered Furniture Heat Release Rates Measured with a Furniture Calorimeter.* » NBS-IR 82-2604 (1982)

59- Rose N., Le Bras M., Delobel R. et Leroy J.-M., « *Etude de la Thermodégradation de Résines Organiques Aéronautiques - Amélioration des Propriétés Retard au Feu* », Rapport de fin d'étude, Aide MRT - GIS Ignifugation (1994), (Collaboration avec la Société Aérospatiale et Jouany J.-M., Laboratoire de Toxicologie de l'Université de Pharmacie (Rouen)).

60- Wang X. et GillhamJ.K., J. Appl. Polym. Sci. **43** (1991) 2267-2277.

61- Rose N., « *Etude de la Dégradation Thermique et du Comportement au Feu de Résines Epoxydes Utilisées dans l'Aéronautique* », Thèse, Lille (France), 1995.

62- Draft Proposal ISO/DP 7111-1979, International Organization for Standardisation, Genève (Suisse) (1979).

63- Alger R.S., « *Electron Paramagnetic Resonance : Techniques and Applications* », Interscience, New-York (1968) pp. 42-60.

64- Hyde J.S., « *Experimental Techniques in EPR* », 6th Annual NMR-EPR Varian Workshop, Varian Associates Instrument Division, Palo Alto (1961).

65- Singer L.S. et Lewis I.C, Appl. Spectrosc. **36(1)** (1982) 52-57.

66- Thornton W., Philosophical Magazine & J. of Sci. **33(196)** (1917).

67- Hugget C., J. Fire & Flammability **12** (1980) ;
Hugget C., Fire & Materials **8(2)** (1980) 6.

68- Grayson S.J., « *Heat Release in Fire.* », Elsevier, Oxford (GB) (1992).

69- FAR part 25, Amendment 25-61, Federal Aviation Administration, Atlantic City, NJ (USA) (1986).

70- Conley R.T. et Dante M.F., « *Stability of Plastics* » Tech. Conf. Soc. Plastics Eng., Washington, DC (juin 1964).

71- Ackhammer B.G., Tyron M. et Kline G.M., « *Chemische Struktur und Beständigkeit der Polymeren* » dans « *Int. Symp. on Macromolecules* », IUPAC, Düsseldorf (Allemagne) (1959)

72- Lee J.H., J. Polym. Sci. A **3** (1965) 859.

73- Pal G. et Macskasy H., « *Studies in Polymer Science 6 - Plastics, their Behaviour in Fires* », Elsevier Sci. Pub. Co, New-York (USA) (1991) pp. 63-70.

74- Park W.R.R. et Blount J., Ind. Eng. Chem., **49** (1957) 1897.

75- Bellenger V. et Verdu J., J. Appl. Polym. Sci. **30** (1985) 363.

76- Calcraft A.M. et Maries K., Plast. Polym. **42** (1974) 162.

77- Calcraft A.M. et Maries K., Plast. Polym. **42** (1974) 247.

78- Hidalo C.J., Chem. Tech. **24** (1972),232;
Hidalo J.C., J. Cell. Plast. **7** (1971) 181.

79- Delobel R., Bourbigot S., Le Bras M., Schmidt Y. et Leroy J. M., Makromol. Chem., Macromol. Symp., **74** (1993) 59-69.

80- Richard-Campisi L., Bourbigot S., Le Bras M. et Delobel R., Thermochimica Acta **275** (1996) 37-49.

81- Bourbigot S., Richard-Campisi L., Le Bras M. et Delobel R., J. Textile Institute, 1996, papier 5-96, sous presse,

82- Nikoalev A.V., Logvimenko V.A. et Gorberchev V.M., J. Thermal Anal. **6** (1974) 473.

83- Criado J.M. et Gonzalés M., Thermochimica Acta **46** (1981) 201.

84- Koga N. et Sestak J., J. Thermal Anal. **37** (1991) 1103.

85- Koga N., Sestak J. et Malek J., Thermochimica Acta **182** (1991) 333.

86- Koga N et Sestak J., Thermochimica Acta **182** (1991) 201.

87- Bishop B.P. et Smith D.A., Ind. Eng. Chem. **59(8)** (1967) 32.

88- Venger A.E., Fraiman Y.E. et Yurevich F.B., J. Thermal Anal. **27** (1983) 325.

89- Coquillaud X., Le Tallec Y., Le Bras M. et Delobel R., *« European Seminar on Vibration Spectroscopy in Materials Science »* Louvain-la-Neuve (Belgique) (21-22 Avril 1994).

90- Le Bras M., Coquillaux X., Le Tallec Y. et Delobel R., *Actes* des *« Journées Francophones des Jeunes Physico-chimistes »*, Lille (16-18 juillet 1996), M. Martel et S. Obbade ed., U.S.T.Lille pub., Cession Posters P3 pp.43.

91- Mikroyannidis J.A. et Kourtides D.A., Polym. Mat. Sci. Eng. Proc. **49** (1983) 606.

92- Costes B., Henry Y., Buckingham M.R., Lindsay A.J., Stevenson D.E., Muller G., Morel E., Levchick S.V., Camino G., Luda, M.P., Costa L., Chambers P.L., Chambers C.M. et Kennedy A.C., *« Development of New Materials with Improved Fire Resistance, Reduced Smoke and Toxicity (Brite-Euram Progam 4412) »* dans *« Abstracts of Fire Retardant Polymers - 5th European Conference »*, Salford (GB) (septembre 1995).

93- FAR part 25, Amendment 25-853 grade al. (*« Test OSU »*), Federal Aviation Administration, Atlantic City, NJ (USA) (1990).

94- Duncan T.M. et Douglass D.C., Chem. Phys. **87** (1984) 339.

95- Littré E., *« Dictionnaire de la Langue Française »*, Gallimard et Hachette, Paris (1959).

96- Hugo V., dans *« L'homme qui rit »*, Lacroix ed., Paris (1869) ; *« Victor Hugo - Romans »*, les Editions du Seuil, Paris (1963).

97- Martel B., J. Appl. Polym. Sci. **35** (1988) 1213-1226 ;
Martel B., dans les *« Actes du 2ème Colloque Francophone sur l'Ignifugation des Polymères »*, Delfosse L. ed., USTL, Lille (1987) pp.13.

98- Tkac A., dans *« Developments in Polymer Stabilisation* (Volume 5) »,Scott G. ed., Applied Sci., Londres (1982) pp. 155.

99- Camino G., Costa L., Trossarelli L., Costanzi F. et Pagliari A., Polym. Deg. & Stab. **12** (1985) 213.

100- Delobel R., Le Bras M., Mouchel B. et Leroy J.-M., Annales des Composites, **1-2** (1990) 4-12.

101 Le Bras M., Delobel R., Descressain R. et Leroy J.-M., Bull. Soc. Chim. Belg., **98(9-10)** (1989) 735-740.

102- « *Test for Flammability of Plastic Materials in Devices and Appliances* », Underwriters Laboratories, Northbrook (USA) (1977) ANSI/ASTM D635-77.

103- Siat C., Bourbigot S. et Le Bras M., *« Recent Advances in FR of Polymeric Materials (Volume 7) »,* Lewin M. ed., Business Communications Co Inc., Norwall (USA) (1997), 318-326.

104- Alistiqsa F., *« Mise au Point de Nouvelles Formulations Intumescentes Polyphosphate d'ammonium - Pentaérythritol; Application à l'Ignifugation du Polypropylène. »,* Thèse, Lille (1993).

105- Delobel R., Le Bras M., Ouassou N. et Alistiqsa., J. Fire Sci., **8** (1990) 85-108.

106- Bourbigot S., Le Bras M., Delobel R., Bréant P. et. Trémillon J.-M., Polym. Deg. & Stab. **48** (1996) 275-287.

107- Camino G., Costa L. et Trossarelli L., Polym. Deg. & Stab. **12** (1985) 203-211.

108- Camino G., Martinasso G. et Costa L., Polym. Deg. & Stab. **27** (1990) 285-296.

109- Ouassou N., *« Etude d'un nouveau système intumescent « retard au feu » :pyrophosphate diammonique - pentaerythritol - Application au polypropylène* », Thèse Lille (1991).

110- Camino G., Costa L., Trossarelli L., Constanzi F. et Landoni G., Polym. Deg. & Stab.**8** (1984) 13.

111- Camino G., Martinasso G., Costa L. et Gobetto R., Polym. Deg. & Stab.**28** (1990) 17-38.

112- Delobel R., Le Bras M. et Ouassou N., Polym. Deg. & Stab.**30** (1990) 41-56.

113- Lewis I.C., J. Chim. Phys. **81(11-12)** (1984) 751.

114- Sternberg U., Prietrowski F. et Priess W., Z. Phys. Chem. **168** (1990) 115.

115- « *Studies in Inorganic Chemistry , Part 5 - Phosphorus, an Outline of ist Chemistry, Biochemistry and Technology* », Corbridge D.E.C. ed., Elsevier Sci., New-York (1985) pp. 157-221.

116- Sohma J., Colloid & Polym. Sci. **270** (1992) 1060-1065.

117- Butyagin P. et Abragjan G., Biophysics (traduction anglaise) **9** (1964) 161-171.

118- Sakaguchi M. et Sohma J., J. Polym. Sci. **13** (1975)1233-1245.

119- Sakaguchi M. et Sohma J., J. Appl. Polym. Sci. **22** (1978) 2915-2922.

120- Verdu J. dans les « *Proceedings of the 11th Bratislava IUPAC/FECS International Conference on Polymers - Thermal and Photo-induced Oxidation of Polymers and its Inhibition in the Upcoming 21th Century* », Stara Lesna (Slovaquie) (24-28 juin 1996) ML2 pp. 4-5.

121- Cullis C.F., Oxydation & Combustion Revs. **5** (1971) 83-133.

122- « *Chemical Kinetics of Degradation of Polymers* (Volume 14) », Bamford C.H. et Tipper C.F.H. ed., Elsevier Sci., New-York (1975) pp. 425-522.

123- Aseeva R.M. et Zaikov G.E. dans « *Combustion of Polymers Materials* », Nauka, Moscou (1981) pp. 280.

124- Mardorsky S.L. dans « *Thermal Degradation of Organic Polymers* », Interscience, New-York (1964).

125- Bourbigot S., Le Bras M., Delobel R., Revel B. et Trémillon J.-M. dans les « *Abstracts de la 6^{éme} Réunion de Travail sur la Résonance Magnétique dans les Solides - Méthodologie RMN : de la Théorie à l'Application* », Eveux (23-26 octobre 1994).

126- « *First International Fire Prevention Congress - The Official Congress Report* », British Fire Prevention Comittee, londres (1903).

127- « *Federal Trade Commission Complaint on the flammability of Plastic Products* », File 732-3040 (31 mai 1973).

128- Marchal A., Delobel R., Le Bras M. et Leroy J.-M. dans les « *Actes du XXII^{éme} Congrès National du GFP - Polymères et Civilisation* » Pau (22-24 novembre 1993), Grenier-Loustalot M.-F. ed., CNRS, Pau (1993), pp. 144-148.

129- Delobel R., Le Bras M., Schmidt Y. e-t Bourbigot S. dans les « *Actes du MOFFIS 91 - Mineral and Organic Functional Fillers in Polymers, International Symposium* », Le Mans (9-12 avril 1991) pp. 79-85.

130- Marchal A., Delobel R., Le Bras M. et Leroy J.-M., « *Gordon Research Conference on Analytical Pyrolysis and Oxidative Degradation of Materials* », Plymouth (USA) (13-18 juin 1993).

131- « *Test à l'épiradiateur* », AFNOR NF P 92-501 (1985).

132- Osawa T., Bull. Chem. Soc. Japn. **38(11)** (1965) 1881.

133- Flynn J.H., J. Thermal Anal. **27** (1983) 95.

134- Coats A.W. et Redfern J.P., Nature **201** (1964) 68.

135- Kotoyori T., Thermochimica Acta **5** (1972) 51-58.